

School of Doctoral Studies in Biological Sciences
University of South Bohemia in České Budějovice
Faculty of Science



**The involvement of the Hippo signalling pathway in the first two
cell-fate decisions of pre-implantation mouse embryo development**

Ph.D. Thesis

Aleksandar Mihajlović, MSc.

Supervisor: Alexander W. Bruce, Ph.D.

University of South Bohemia, Faculty of Science, Department of Molecular Biology and Genetics,
České Budějovice

České Budějovice 2017

This thesis should be cited as:

Mihajlović A.I. (2017) **The involvement of the Hippo signalling pathway in the first two cell-fate decisions of pre-implantation mouse embryo development.** Ph.D. Thesis in English, University of South Bohemia, Faculty of Science, School of Doctoral Studies in Biological Sciences, České Budějovice, Czech Republic, 188 pp.

Annotation

The first two cell-fate decisions of pre-implantation mouse embryo development have classically been described as a two-step process whereby a population of differentiating outer cells, called the trophectoderm (TE), first segregates from a population of pluripotent inner cells called the inner cell mass (ICM), that is subsequently followed by the segregation of pluripotent epiblast (EPI) and differentiating primitive endoderm (PrE) within the ICM. Recently, the Hippo signalling pathway that is tightly regulated by intra-cellular polarity, has been described as performing a pivotal role during the first cell-fate decision. Accordingly, it is responsible for the interpretation of relative inter-cellular positional cues and their translation, at molecular level, into adopting appropriate cell fate. To which extent these differentiating positional cues that guide the first cell-fate decision have an effect on the second cell fate has been a matter of intensive debate over the last few years. The first part of the thesis investigates the importance of cell history during the second cell-fate decision and demonstrates that the extent to which outer-residing ancestral cells of ICM cell progenitors are exposed to differentiative cues and the timing at which their internalised cell progeny are subject to Hippo signalling pathway activation during first cell-fate decision, has an important knock-on consequence for the second cell-fate decision. The second part of dissertation is focused on characterizing the molecular relationship between a recently described regulator of cell polarity, Rho-associated protein kinase, and Hippo signalling pathway components during the first cell-fate decision.

Declaration [in Czech]

Prohlašuji, že svoji disertační práci jsem vypracoval samostatně pouze s použitím pramenů a literatury uvedených v seznamu citované literatury. Prohlašuji, že v souladu s § 47b zákona č. 111/1998 Sb. v platném znění souhlasím se zveřejněním své disertační práce, v úpravě vzniklé vypuštěním vyznačených částí archivovaných Přírodovědeckou fakultou, elektronickou cestou ve veřejně přístupné části databáze STAG provozované Jihočeskou univerzitou v Českých Budějovicích na jejích internetových stránkách, a to se zachováním mého autorského práva k odevzdanému textu této kvalifikační práce. Souhlasím dále s tím, aby toutéž elektronickou cestou byly v souladu s uvedeným ustanovením zákona č. 111/1998 Sb. zveřejněny posudky školitele a oponentů práce i záznam o průběhu a výsledku obhajoby kvalifikační práce. Rovněž souhlasím s porovnáním textu mé kvalifikační práce s databází kvalifikačních prací Theses.cz provozovanou Národním registrem vysokoškolských kvalifikačních prací a systémem na odhalování plagiátů.

Declaration

I hereby declare that my Ph.D. thesis is my work alone and that I have used only those sources and literature detailed in the list of references. Further, I declare that, in accordance with Article 47b of Act No. 111/1998 Coll. in the valid wording, I agree to the publication of my Ph.D. thesis [in unabbreviated form – in the form arising from the omission of marked parts archived at the Faculty of Science] in electronic form in a publically accessible part of the STAG database operated by the University of South Bohemia in České Budějovice on its webpage, with the preservation of my rights of authorship to the submitted text of this thesis. Further, I agree to the publication, via the same electronic portal, in accordance with the detailed regulations of Act 111/1998 Coll., of the reviews of the supervisor and opponents of the thesis as well as the record of proceedings and result of the defence of the thesis. I also agree to the comparison of the text of my thesis with the Theses.cz database operated by the National Registry of Theses and the Plagiarism Tracing System.

Place and Date

Student's signature

České Budějovice, 18.01.2017.

.....

Aleksandar Mihajlović

This thesis originated from a partnership of the Faculty of Science, University of South Bohemia, and Institute of Entomology, Biology Centre of the ASCR, supporting doctoral studies in the Molecular and Cellular Biology and Genetics study programme.



Přírodovědecká
fakulta
Faculty
of Science

Jihočeská univerzita
v Českých Budějovicích
University of South Bohemia
in České Budějovice



BIOLOGY
CENTRE
ASCR

Financial support

This research was supported by a Marie Curie Career Integration Fellowship (IDNOVCEL FAT2011) within the 7th European Community Framework Programme and a Czech Science Foundation grant (13-03295S) awarded to Alexander W. Bruce Ph.D. Aleksandar Mihajlović was the recipient of a one-year Ph.D. student individual project grant (004/2015/P) funded by the Grant Agency of the University of South Bohemia.

List of original papers and author's contribution

The thesis is based on the following papers (listed chronologically):

- I Mihajlović A.I.,** Thamodaran V., Bruce A.W. (2015) The first two cell-fate decisions of preimplantation mouse embryo development are not functionally independent. *Scientific Reports*, 5: 15034. (IF₂₀₁₅=5.228)

Aleksandar Mihajlović has made substantial contributions to the conception and design of experiments, performed most of them and participated in manuscript preparation.

- II Mihajlović A.I.,** Bruce A.W. (2016) Rho-associated protein kinase regulates subcellular localization of Angiomotin and Hippo-signalling during preimplantation mouse embryo development. *Reproductive Biomedicine Online*, 33: 381-390. (IF₂₀₁₅=2.796)

Aleksandar Mihajlović has made substantial contributions to the conception and design of experiments, performed all of them and participated in manuscript preparation.

Acknowledgements

I would like to thank my supervisor Alexander W. Bruce for giving me the opportunity to enter the magical world of mouse embryology, for showing me the patience and understanding when I needed it the most, for all the guidance and help throughout these four years, for giving me enough freedom to think independently and finally helping me develop into a scientist. I want to express my gratitude to my dear colleague Vasanth Thamodaran for teaching me molecular cloning and basics of mouse embryo manipulation. Also, many thanks to other members of the Laboratory of Developmental Biology and Genomics as well as members of Alena Krejčí's lab who helped me in any kind of way during the course of my Ph.D. studies. I also thank Prof. Dr. Hiroshi Sasaki (Osaka University, Japan) for providing us the anti-Amot antibody and Dr. Marta Gajewska (Department of Genetics, Cancer Center and Institute of Oncology, Warsaw, Poland) for CBA/W mice.

I want to thank my parents and sister for supporting me throughout my entire education and for providing me the means to pursue my dreams.

Lastly, I thank Zorana, my eternal companion and my love, for making me persevere. I would have never finished my Ph.D. studies if it wasn't for you!

I wish to dedicate my Ph.D. thesis to my son who was my inspiration and motivation throughout the entire journey and to apologize for all those nights Daddy wasn't there to tuck him into bed and kiss him good night.

TABLE OF CONTENTS

List of Abbreviations	viii
List of Tables	xii
List of Figures	xiii
List of Appendix Tables	xv
List of Appendix Figures	xvii
1. INTRODUCTION	1
1.1 A BRIEF OVERVIEW OF MOUSE PRE-IMPLANTATION DEVELOPMENT	1
1.2 DEVELOPMENTAL BIAS OF EARLY BLASTOMERES IN MOUSE EMBRYO	9
1.2.1 Embryonic axes in the mouse pre-implantation embryo	10
1.2.2 Mosaic model	11
1.2.3 The first cell cleavage division	12
1.2.4 The second cell cleavage divisions	12
1.3 CELL POLARISATION AND COMPACTION	16
1.3.1 Compaction	16
1.3.2 Polarisation	18
1.3.2.1 Establishment of polarity in the mouse pre-implantation embryo	19
1.3.2.2 Planar cell polarity in mouse pre-implantation embryo	22
1.4 THE FIRST CELL-FATE DECISION	23
1.4.1 The establishment of two spatially distinct cell populations	24
1.4.2 The role of the Hippo signalling pathway in interpreting positional cues	25
1.4.3 Transcriptional factors involved in the first cell-fate decision	28
1.4.3.1 The role of Tead4 in the first cell-fate decision	29
1.4.3.2 The role of Cdx2 in the first cell-fate decision	31
1.4.3.3 The role of Gata3 in the first cell-fate decision	34
1.4.3.4 The role of Oct4 in the first cell-fate decision	34
1.4.3.5 The role of Sox2 in the first cell-fate decision	35
1.5 THE SECOND CELL-FATE DECISION	35
1.5.1 EPI and PrE transcriptional networks	36
1.5.2 Models proposed to explain segregation of EPI and PrE	37
1.5.3 Nanog and Gata6 mutual exclusion	41
1.5.4 Cell sorting within the ICM	43
1.5.5 The role of Oct4 in the second cell-fate decision	44
1.6 THE MODEL OF INTER-RELATED CELL-FATE DECISIONS	45
2. OBJECTIVES	48
2.1 OBJECTIVE 1	48
2.2 OBJECTIVE 2	48
3. MATERIAL AND METHODS	50

3.1 EMBRYO COLLECTION AND CULTURE	50
3.2 EMBRYO TREATMENT WITH CHEMICAL INHIBITORS.....	51
3.2.1 Y-27632 Rock1/2 inhibitor treatment	51
3.2.2 Cytochalasin D treatment	51
3.3 PREPARATION OF dsRNAs, mRNA AND MICROINJECTIONS	52
3.4 EMBRYO CHIMERAS	53
3.5 QUANTITATIVE REVERSE TRANSCRIPTION PCR (Q-RTPCR)	53
3.6 IMMUNO-FLUORESCENT STAINING	54
3.7 CONFOCAL MICROSCOPY AND IMAGE ANALYSIS.....	55
3.8 STATISTICAL ANALYSIS	57
4. RESULTS	58
4.1 PART I - INVESTIGATING THE IMPORTANCE OF THE HIPPO SIGNALLING PATHWAY AND CELL HISTORY DURING THE ACQUISITION OF THE SECOND CELL FATE	60
4.1.1 Functional down-regulation of <i>Tead4</i> expression within the developing pre-implantation mouse embryo	60
4.1.1.1 Global <i>Tead4</i> down-regulation using long dsRNA phenocopies the genetic zygotic <i>Tead4</i> ^{-/-} knock-out	61
4.1.1.2 Clonal down-regulation of <i>Tead4</i> expression allows blastocyst formation	63
4.1.2 Clonal down-regulation of <i>Tead4</i> expression biases cells towards EPI and away from PrE fate	65
4.1.2.1 Inhibition of TE-differentiation within half of the embryo biases internalised cells to EPI versus PrE fate	65
4.1.2.2 Inhibition of TE-differentiation within a quarter of the embryo also biases cells to EPI versus PrE fate.....	70
4.1.2.3 Inhibition of TE-differentiation within small chimeric ICM clones also biases against ultimate PrE cell fate	72
4.1.3 Molecular characterisation of attenuated PrE formation in TE-inhibited cell clones	75
4.1.3.1 Hippo signalling pathway inactivation within the ICM is unlikely to be required for appropriate PrE formation.....	76
4.1.3.2 Cell polarity establishment is largely unaffected in TE-inhibited cells.....	79
4.1.3.3 Inhibition of TE-differentiation is associated with unaltered expression of EPI and decreased expression of PrE lineage markers.....	82
4.1.4 A minor contribution of Dab2 to the importance of cell history during the second cell-fate decision (UNPUBLISHED RESULTS).....	85
4.1.4.1 Endogenous Dab2 protein is expressed in both the TE and PrE lineages	86
4.1.4.2 Dab2 protein expression is severely reduced in <i>Tead4</i> -KD cell clones	88
4.1.4.3 Down-regulation of Dab2 results in reduced contribution towards PrE.....	90
4.1.5 The allocation of <i>Tead4</i> -KD cell clone towards the ICM (UNPUBLISHED RESULTS)	93
4.1.5.1 The allocation of TE-inhibited cell clones towards the ICM commences after the 16-cell stage	93
4.1.5.2 Apical-abscission mediated internalisation of outer-residing TE-inhibited cells	96
4.2 PART II - THE INFLUENCE OF ROCK1/2 ON AMOT LOCALISATION AND THE HIPPO SIGNALLING PATHWAY DURING TROPHECTODERM AND INNER CELL MASS SEGREGATION	99
4.2.1 Rock1/2 inhibition prevents blastocoel formation in pre-implantation mouse embryo ...	100

4.2.2 Rock1/2 inhibition is associated with defective cell polarity establishment and improper tight junction formation.....	104
4.2.3 Rock1/2 inhibition effects on Hippo signalling pathway activation are mediated via Amot	107
4.2.3.1 Rock1/2 inhibition induces Amot mis-localisation in outer cells of late morula stage embryos and ectopic Hippo signalling pathway activation	108
4.2.3.2 Experimental down-regulation of Amot prevents Rock1/2 inhibitor from exerting an effect on Hippo signalling pathway.....	110
4.2.4 Rock1/2 inhibition effects on tight junction formation, cell polarity and Hippo signalling pathway are unlikely to be the consequence of aberrant actin polymerisation (UNPUBLISHED RESULTS)	112
4.2.5 Rock1/2 inhibition effects are already evident at the molecular level in 16-cell stage embryos	115
4.2.6 Rock1/2 activity is indispensable for the appropriate polarisation of 8-cell stage blastomeres (UNPUBLISHED RESULTS)	118
4.2.7 Rock1/2 activity is required for cell/ blastomere internalisation processes, possibly via regulation of myosin light chain-2 phosphorylation (UNPUBLISHED RESULTS)	120
5. DISCUSSION	123
5.1 DISCUSSION - PART I	123
5.2 DISCUSSION - PART II	132
6. CONCLUSIONS	140
REFERENCES.....	143
APPENDICES.....	158
APPENDIX A. SUPPLEMENTARY TABLES	158
APPENDIX B. SUPPLEMENTARY FIGURES.....	177
APPENDIX C. CURRICULUM VITAE.....	185

List of Abbreviations

AA	Amino acids
AJs	Adherens junctions
Amot	Angiomotin
ATPase	Adenosine triphosphate hydrolase
AV axis	Animal–vegetal axis
Bmi1	B lymphoma Mo-MLV insertion region homolog 1
Brg1	Brahma related protein 1
BSA	Bovine serum albumin
BSA-PBS-T	3% BSA in PBS-T
Carm1	Coactivator associated arginine methyltransferase 1
Cdh1	Cadherin 1
Cdh3	Cadherin 3
cDNA	Complementary deoxyribonucleic acid
Cdx2	Caudal type homeobox 2
CGFD	Cortical granule free domain
Ctnna1	Catenin alpha 1/Cadherin-associated protein alpha 1
Ctnnb1	Catenin beta 1/Cadherin-associated protein beta 1
Dab2	Disabled homolog 2
DAPI	4',6-diamidino-2-phenylindole
DMSO	Dimethyl sulfoxide
DNA	Deoxyribonucleic acid
DNaseI	Deoxyribonuclease I
dsRNA	Double-stranded RNA
Elf5	E74 like ETS transcription factor 5
Emk1/ Mark2	ELKL motif kinase 1/ Microtubule affinity regulating kinase 2
Eomes	Eomesodermin
EPI	Epiblast
Erk1/2	Extracellular signal-regulated kinases 1 and 2
ES cells	Embryonic stem cells
Ezr	Ezrin
F-actin	Filamentous actin
Fgf	Fibroblast growth factor
Fgf4	Fibroblast growth factor 4

Fgfr	Fibroblast growth factor receptor
Fgfr2	Fibroblast growth factor receptor 2
Gata3	GATA binding protein 3
Gata4	GATA binding protein 4
Gata6	GATA binding protein 6
GFP	Green fluorescent protein
Grb2	Growth factor receptor bound protein 2
GTPase	Guanosine triphosphate hydrolase
H2afz	H2A histone family member z
H3R26	Histone H3 arginine 26
Hand1	Heart and neural crest derivatives expressed 1
hCG	Human chorionic gonadotropin
HEK293 cells	Human embryonic kidney cells 293
ICM	Inner-cell mass
IQGAP1	IQ motif containing GTPase activating protein 1
Itga7	Integrin subunit alpha 7
Jnk	c-Jun amino-terminal kinase
KD	Knock-down
KSOM	Potassium simplex optimisation medium
Lats1/2	Large tumor suppressor kinase 1 and 2
Limk1/2	LIM-domain containing protein kinase 1 and 2
Lrp2	LDL receptor related protein 2
Mapk	Mitogen-activated protein kinase
Mek1/2	Mitogen-activated protein kinase kinases 1 and 2
MII oocyte	Metaphase II stage arrested oocyte
Mlc2	Myosin light chain 2
mRNAs	Messenger ribonucleic acids
Myh9	Myosin heavy chain 9
Nanog	Nanog homeobox
Nf2/ Merilin	Neurofibromin 2/ Moesin-Ezrin-Radixin-like protein
Oct4	Octamer-binding protein 4/ POU class 5 homeobox 1
OGDBs	Oregon-green-conjugated dextran beads
p38-Mapk	p38-mitogen activated protein kinase
p38-Mapk14/11	p38-mitogen activated protein kinases alpha and beta
PAK1	Human p21 activated kinase 1

PAK1-PBD-EYFP	p21 binding domain of PAK1 fused with enhanced yellow fluorescent protein
Pard3	Partitioning defective 3 homolog
Pard6	Partitioning defective 6 homolog
PB	Polar body
PBS	Phosphate-buffered saline
PBS-T	0.15% Tween-20 in PBS
PCP	Planar cell polarity
PCR	Polymerase chain reaction
Pdgfra	Platelet derived growth factor receptor alpha
pERM	phospho-Ezrin/Radixin/Moesin
pEzr	phospho-Ezrin
PFA	Paraformaldehyde
PHA	Phytohaemagglutinin
pMlc2	phospho(Ser19)-myosin light chain 2
PMSG	Pregnant mare's serum gonadotropin
ppMlc2	bi-phosphorylated (Thr18/Ser19) myosin light chain 2
PrE	Primitive endoderm
Prickle2	Prickle planar cell polarity protein 2
Prkci	Atypical protein kinase iota/lambda/ ι/λ
Prkcz	Atypical protein kinase zeta/ ζ
Prl3d	Prolactin family 3 subfamily d member 1
pYap1	phospho-Yes-associated protein 1
Q-RTPCR	Quantitative-reverse transcription polymerase chain reaction
Rac1	Ras-related C3 botulinum toxin substrate 1
RDBs	Rhodamine-conjugated dextran beads
RhoA	Ras homology family member A
RNAi	RNA interference
Rock1/2	Rho-associated protein kinase 1 and 2
Rpl23	60S ribosomal protein L23
Sall4	Spalt like transcription factor 4
Scrib	Scribbled homolog
shRNA	Short hairpin RNA
Sox17	SRY-Box 17
Sox2	SRY-Box 2
Sox21	SRY-Box 21

Sox7	SRY-Box 7
Tbp	TATA-Box binding protein
TE	Trophectoderm
Tead1	TEA domain transcription factor 1
Tead2	TEA domain transcription factor 2
Tead4	TEA domain transcription factor 4
Tjp1	Tight junction protein 1
Tjp2	Tight junction protein 2/ Zona occludens 2
TJs	Tight junctions
TS cells	Trophoblastic stem cells
UTR	Untranslated region
Wnt9A	Wnt family member 9A
Wwtr1	WW domain containing transcription regulator 1
Yap1	Yes-associated protein 1
ZGA	Zygotic genome activation
ZP	Zona pellucida

List of Tables

Table 3.1	Information on M2+BSA media composition	50
Table 3.2	Information on KSOM+AA media composition	51
Table 3.3	Information on the oligonucleotide primer sequences used to generate DNA template for dsRNA synthesis ..	52
Table 3.4	Information on oligonucleotide primers used in Q-RTPCR analysis	54
Table 3.5	Information on primary and secondary antibodies used in the immuno-fluorescent staining procedure	55

List of Figures

Figure 1.1	Development of the pre-implantation blastocyst in mice from embryonic day 0 (E0) through day 5 (E5.0).....	1
Figure 1.2	Morphological transformation of the mouse embryo from the zygote to the blastocyst stage.....	2
Figure 1.3	A schematic depiction of the mouse blastocyst at E4.5, comprising the three distinct cell lineages; TE, EPI and PrE.....	2
Figure 1.4	The developmental progress of half embryos and whole embryos.....	3
Figure 1.5	Transcriptional regulation and cell-fate decisions in pre-implantation development	4
Figure 1.6	Establishing the apical and basolateral membrane domains in the mouse pre-implantation embryo and generating the two different cell populations.....	5
Figure 1.7	A schematic diagram depicting two types of cleavage patterns	6
Figure 1.8	Blastocoel formation during pre-implantation embryo development	8
Figure 1.9	A schematic representation of the animal-vegetal axis	10
Figure 1.10	The embryonic-abembryonic axis in relation to animal vegetal axis in pre-implantation mouse embryo	11
Figure 1.11	The relationships between the second cleavage patterns at the 2-cell stage and later development as proposed by Zernicka-Goetz and colleagues.....	13
Figure 1.12	The difference in developmental success between chimeras made of the entirely equatorially derived blastomeres and meridionally derived blastomeres of 4-cell stage mouse embryos	14
Figure 1.13	Polarity proteins of the PAR, Crumbs and Scribble complexes	18
Figure 1.14	Scheme showing the cellular localisation of the PAR proteins and Prkcz/i during compaction and blastocyst morphogenesis in pre-implantation mouse embryos	20
Figure 1.15	Mechanisms that establish position-dependent Hippo signalling at the 32-cell stage	26
Figure 1.16	Integration of three hypotheses for the emergence of inside and outside cell differences	28
Figure 1.17	Molecular mechanisms for the ICM/TE segregation	29
Figure 1.18	Apical localisation of Cdx2 mRNA after the cell polarisation contributes to symmetry-breaking events in pre-implantation stage mouse embryo development	32
Figure 1.19	Establishment of two transcriptional networks responsible for segregation of EPI and PrE cells	36
Figure 1.20	Two competing models of how EPI and PE (primitive endoderm) progenitor cells become internalised to the ICM of mouse embryos	39
Figure 1.21	Molecular events underlying the second cell-fate decision	42
Figure 1.22	Model for the cooperative action of Oct4 and Sox-family transcription factors during lineage fate choice	45
Figure 1.23	A schematic representation of the inter-related cell-fate decisions model.....	46
Figure 4.1	Long dsRNA mediated <i>Tead4</i> down-regulation phenocopies the zygotic <i>Tead4</i> ^{-/-} null TE-deficit phenotype	62
Figure 4.2	Clonal down-regulation of <i>Tead4</i> expression and TE-differentiation inhibition	64
Figure 4.3	Inhibition of TE-differentiation within half of the embryo preferentially biases cells to EPI versus PrE fate.....	68
Figure 4.4	Inhibition of TE-differentiation within a quarter of the embryo also biases cells to EPI versus PrE fate	71
Figure 4.5	Inhibition of TE-differentiation within small chimeric ICM clones also biases against ultimate PrE cell fate	74
Figure 4.6	Cytoplasmic Yap1 localisation within the ICM is indicative of an active Hippo signalling pathway	78
Figure 4.7	Clonal down-regulation of <i>Tead4</i> expression is not associated with reduced expression nor mis-localisation of cell polarity markers	80

Figure 4.8	Global and clonal TE-inhibition; no enhanced <i>Nanog</i> expression prior to 32-cell stage but attenuated PrE-specific marker expression	84
Figure 4.9	The endogenous expression pattern of Dab2 during mouse pre-implantation embryo development reveals its presence in both TE and PrE lineages.....	87
Figure 4.10	Tead4 is responsible for initial Dab2 protein expression in the pre-implantation mouse embryo.....	89
Figure 4.11	Clonal down-regulation of Dab2 in half of the embryo results in mildly attenuated PrE formation	91
Figure 4.12	The allocation of TE-inhibited cell clones towards the ICM commences after 16-cell stage	95
Figure 4.13	Time-lapse confocal microscopy reveals the apical-abscission mediated internalisation of outer-residing TE-inhibited cells from 32-cell/ late morula (E3.5) stage.....	98
Figure 4.14	Determining an effective working concentration of Y-27632/ Rock1/2 inhibitor	101
Figure 4.15	Rock1/2-inhibited embryos equivalently develop in pace with controls until the 32-cell (E3.5)/ late morula stage but subsequently fail to cavitate.....	102
Figure 4.16	Averaged total embryo cell number in Rock1/2-inhibited (Y-27632 treated) and control (DMSO treated) groups, <i>in vitro</i> cultured from the 2-cell (E1.5) stage to the 8- (E2.5), 16- (E3.0) or 32-cell (E3.5) stages	104
Figure 4.17	Rock1/2-inhibition is associated with defective apical-basolateral polarity and tight-junction formation	106
Figure 4.18	Enhanced and mis-localised outer-cell Amot expression in Rock1/2-inhibited embryos is related to activation of the Hippo signalling pathway	109
Figure 4.19	The Rock1/2-inhibition induced ectopic activation of Hippo signalling in outer-cells is mediated by Amot	111
Figure 4.20	Cytochalasin D treatment disrupts adherens junctions and consequently prevents Hippo signalling pathway activation	114
Figure 4.21	Rock1/2-inhibition (from the 2-cell stage) is also associated with atypical cytoskeleton, apical-basolateral polarity and Hippo signalling related protein localisation at the 16-cell stage embryos	116
Figure 4.22	Rock1/2 inhibition effects on cell polarity establishment are observable as early as the late-8-cell stage (the developmental stage at which cellular polarisation ordinarily occurs).....	119
Figure 4.23	Rock1/2 inhibition is accompanied by a reduction in myosin light chain-2 phosphorylation (pMlc2) and decreased cell internalisation.....	121

List of Appendix Tables

Supplementary table ST1.	Quantified cell lineage segregation in individual late blastocyst stage (E4.5) embryos <i>in vitro</i> cultured from the 2-cell stage (E1.5).....	158
Supplementary tables ST2.	Quantified cell lineage segregation in individual late blastocyst stage (E4.5) embryos <i>in vitro</i> cultured from the 2-cell stage (E1.5) after microinjection in a single cell with fluorescent RDB ± Tead4-dsRNA (immuno-stained for Cdx2 and Gata4)	159
Supplementary tables ST3.	Quantified cell lineage segregation in individual late blastocyst stage (E4.5) embryos <i>in vitro</i> cultured from the 2-cell stage (E1.5) after microinjection in a single cell with fluorescent RDB ± Tead4-dsRNA (immuno-stained for Cdx2 and Sox17)	160
Supplementary tables ST4.	Quantified cell lineage segregation in individual late blastocyst stage (E4.5) embryos <i>in vitro</i> cultured from the 2-cell stage (E1.5) after microinjection in a single cell with fluorescent RDB ± Tead4-dsRNA (immuno-stained for Gata4 and Nanog).....	161
Supplementary tables ST5.	Incidence of apoptotic cells within individual late blastocyst stage (E4.5) embryos <i>in vitro</i> cultured from the 2-cell stage (E1.5) after microinjection in a single cell with fluorescent RDB ± Tead4-dsRNA (immuno-stained for Cdx2 and Gata4)	162
Supplementary tables ST6.	Incidence of apoptotic cells within individual late blastocyst stage (E4.5) embryos <i>in vitro</i> cultured from the 2-cell stage (E1.5) after microinjection in a single cell with fluorescent RDB ± Tead4-dsRNA (immuno-stained for Cdx2 and Sox17)	163
Supplementary tables ST7.	Incidence of apoptotic cells within individual late blastocyst stage (E4.5) embryos <i>in vitro</i> cultured from the 2-cell stage (E1.5) after microinjection in a single cell with fluorescent RDB ± Tead4-dsRNA (immuno-stained for Gata4 and Nanog).....	164
Supplementary tables ST8.	Quantified cell lineage segregation in individual late blastocyst stage (E4.5) embryos <i>in vitro</i> cultured from the 2-cell stage (E1.5) after microinjection in a single cell with fluorescent RDB tracer alone or RDB and GFP-dsRNA (immuno-stained for Cdx2 and Gata4).....	165
Supplementary tables ST9.	Incidence of apoptotic cells within individual late blastocyst stage (E4.5) embryos <i>in vitro</i> cultured from the 2-cell stage (E1.5) after microinjection in a single cell with fluorescent RDB tracer alone or RDB and GFP-dsRNA (immuno-stained for Cdx2 and Gata4).....	166
Supplementary tables ST10.	Quantified cell lineage segregation in individual late blastocyst stage (E4.5) embryos <i>in vitro</i> from the 4-cell stage (E2.0) after microinjection in a single cell with fluorescent RDB tracer alone or RDB and GFP-dsRNA (immuno-stained for Cdx2 and Gata4)	167
Supplementary tables ST11.	Incidence of apoptotic cells within individual late blastocyst stage (E4.5) embryos <i>in vitro</i> cultured from the 4-cell stage (E2.0) after microinjection in a single cell, with fluorescent RDB tracer alone or RDB and GFP-dsRNA (immuno-stained for Cdx2 and Gata4).....	168
Supplementary tables ST12.	Quantified cell lineage segregation in individual late blastocyst stage (E4.5) embryos derived from 8-cell stage (E2.5) chimeric embryos consisting of a single control (fluorescent RDB tracer alone) or <i>Tead4</i> -KD (fluorescent RDB tracer plus Tead4-dsRNA) cell (immuno-stained for Cdx2 and Gata4)	169
Supplementary tables ST13.	Incidence of apoptotic cells within individual late blastocyst stage (E4.5) embryos derived from 8-cell stage (E2.5) chimeric embryos consisting of a single control (fluorescent RDB tracer alone) or <i>Tead4</i> -KD (fluorescent RDB tracer plus Tead4-dsRNA) cell (immuno-stained for Cdx2 and Gata4)	170

Supplementary tables ST14. Quantified cell lineage segregation in individual late blastocyst stage (E4.5) embryos <i>in vitro</i> cultured from the 2-cell stage (E1.5) after microinjection in a single cell with fluorescent RDB \pm Dab2-dsRNA (immuno-stained for Gata4 and Nanog)	171
Supplementary tables ST15. Quantification of spatial cell lineage segregation in individual 16-cell stage (E3.1) embryos <i>in vitro</i> cultured from the 2-cell stage (E1.5) after microinjection in a single cell with fluorescent RDB \pm Tead4-dsRNA.....	172
Supplementary tables ST16. Quantification of spatial cell lineage segregation in individual 32-cell stage (E3.6) embryos <i>in vitro</i> cultured from the 2-cell stage (E1.5) after microinjection in a single cell with fluorescent RDB \pm Tead4-dsRNA.....	173
Supplementary table ST17. Total number of cells in control (DMSO treated) and Rock1/2-inhibited (Y-27632 treated) embryos <i>in vitro</i> cultured from the 2-cell (E1.5) stage until the 8-cell (E2.5), 16-cell (E3.0) or 32-cell (E3.5) stages.	174
Supplementary tables ST18. Quantified subcellular Yap1 localization in control (DMSO treated) and Rock1/2-inhibited (Y-27632 treated) embryos <i>in vitro</i> cultured from the 2-cell (E1.5) stage until the 32-cell (E3.5) stage.	175
Supplementary tables ST19. Total, outer and inner cell number in 16-cell (E3.0) and 32-cell (E3.5) stage, control (DMSO treated) and Rock1/2-inhibited (Y-27632 treated) embryos <i>in vitro</i> cultured from the 2-cell (E1.5) stage.	176

List of Appendix Figures

Supplementary figure S1.	Relative cell lineage segregation in unperturbed pre-implantation mouse embryos in vitro cultured from the 2-cell (E1.5) stage until the late blastocyst stage (E4.5); establishing an experimental baseline	177
Supplementary figure S2.	Average percentage rates of apoptosis in control and Tead4-dsRNA microinjected and chimeric embryos	178
Supplementary figure S3.	No statistically significant difference in blastocyst lineage derivation between two groups of control embryos microinjected with either RDBs alone or RDBs + GFP-dsRNA in one cell at the 2-cell stage.....	180
Supplementary figure S4.	Yap1, phospho-Yap1 and phospho-ezrin (pERM) expression and intracellular localisation within non-perturbed and Tead4-specific dsRNA microinjected (in one cell at the 2-cell stage) embryos at the mid-16-cell (E3.1) stage.....	182
Supplementary figure S5.	Rock1/2-inhibition causes apical mis-localisation of the basolateral polarity factor Scrib (Scribble) to the apical pole of outer cells at the 32-cell stage (+ quantitation)	184

1. INTRODUCTION

1.1 A BRIEF OVERVIEW OF MOUSE PRE-IMPLANTATION DEVELOPMENT

Mouse pre-implantation embryo development is defined as the period that begins with the fertilisation of the mouse egg and ends with the implantation of the so-called blastocyst embryo into the uterus after approximately 4.5 days (Fig. 1.1).

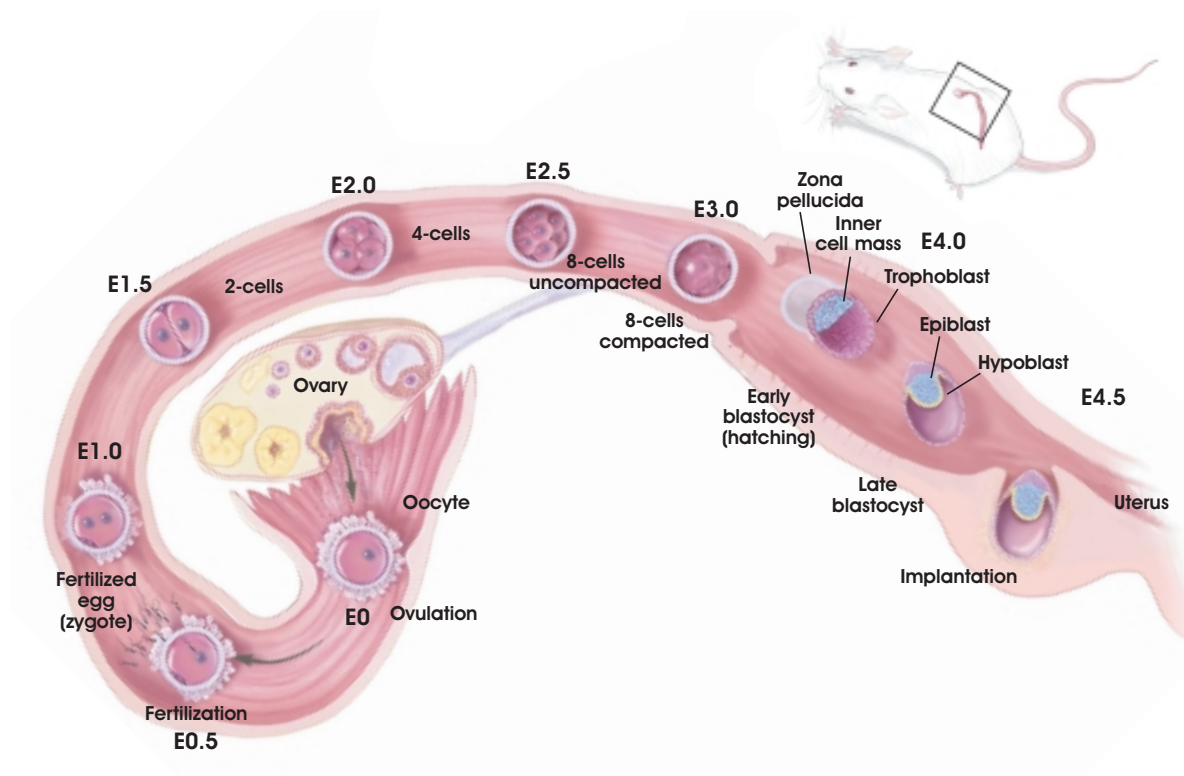


Figure 1.1 Development of the pre-implantation blastocyst in mice from embryonic day 0 (E0) through day 5 (E5.0) (taken from Kirschstein and Skirboll, 2001)

The fertilisation of the mouse egg initially leads to the formation of a zygote that undergoes a series of asynchronous cleavage divisions without any increase of cytoplasmic volume, thereby producing an increasing number of progressively smaller cells (known as blastomeres) without changing the overall size of the embryo. After a series of cleavages/cell divisions, the pre-implantation blastocyst stage embryo emerges as a morphologically recognised and distinct structure (Fig. 1.2).

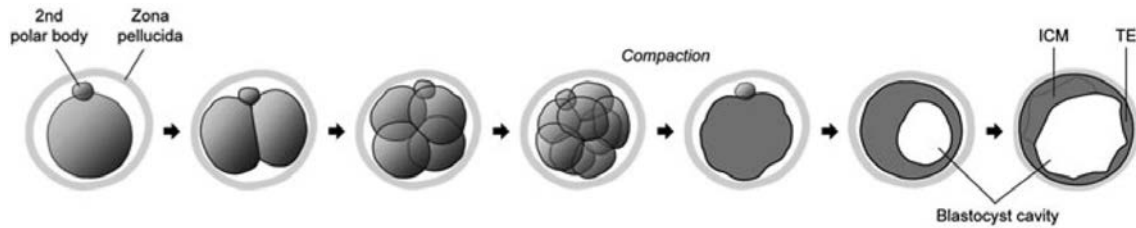


Figure 1.2 Morphological transformation of the mouse embryo from the zygote to the blastocyst stage (taken from Marikawa and Alarcon, 2012)

The pre-implantation period is devoted to the formation of extra-embryonic tissues that are not only essential for implantation and the subsequent support of the embryo but are also required for the germane and appropriate specification/ patterning of the developing embryo/ foetus. As a result, at the end of the mouse pre-implantation embryo development period, three distinct cell lineages are set aside: the trophoblast (TE), that will form the foetal part of the placenta, the

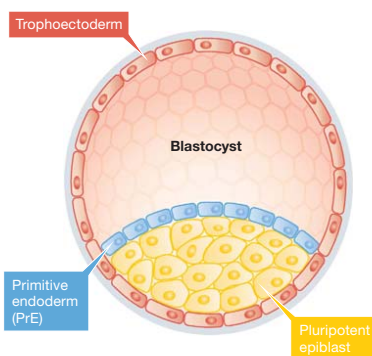


Figure 1.3 A schematic depiction of the mouse blastocyst at E4.5, comprising the three distinct cell lineages; TE, EPI and PrE (taken from Mansour and Hanna, 2013)

primitive endoderm (PrE), that will become the parietal and visceral endoderm and later contribute to the yolk sac and the epiblast (EPI), that will give rise to the embryo proper (Fig. 1.3). These three lineages arise as a result of two cell-fate decisions, the first one in which TE progenitor cells become segregated from encapsulated cells called the inner cell mass (ICM) and the second one in which EPI and PrE are specified and segregated within ICM. Proper formation of these three lineages is essential for the survival and normal development of the embryo. The presence of a functional TE, for example, is required for the complex molecular interactions that occur between the embryo and uterus during implantation (reviewed

in Cockburn and Rossant, 2010). It is the formation of these three pre-implantation lineages, and the underpinning molecular mechanisms associated with it, that remains a fertile field of developmentally related research.

Since the fusion of the sperm and egg initiates a developmental process that leads to the formation of both the placenta and the embryo and as the embryo is not an immediate product of fertilisation, but emerges subsequently in a process of “embryo-genesis” it has been suggested that the appropriate name for the product of fertilisation should be the conceptus or embryogen and not the embryo (Johnson and McConnell, 2004).

Mouse pre-implantation embryo development is driven by an as of yet unidentified endogenous clock, that assures specific developmental events are associated with particular developmental cell cycles (Johnson, 2009). This is best exemplified by the fact that when one blastomere of 2-cell stage embryo is removed (Fig. 1.4), the embryo still follows the same strict clock of developmental transitions as intact embryos (Morris *et al.*, 2012).

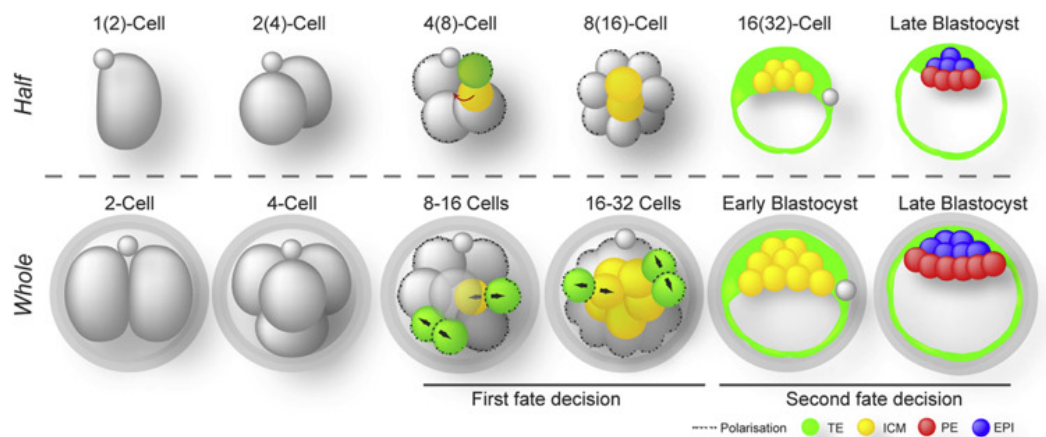


Figure 1.4 The developmental progress of half embryos and whole embryos (taken from Morris *et al.*, 2012)

The first two cell cycles in mouse pre-implantation development are significantly longer than subsequent ones and last approximately 20 hours versus the 12 hours of the later divisions (Artus and Cohen-Tannoudji, 2008). Although the zygote initially relies upon maternal stores of proteins and messenger RNAs (mRNAs), at the end of the 1-cell stage the zygotic genome becomes transcriptionally activated, initially by a minor burst but then followed by a major burst at the end of the 2-cell stage (Fig. 1.5b). This transition from reliance on maternal to zygotically derived transcripts is known as zygotic genome activation (ZGA). In parallel to the major burst of ZGA, the maternal mRNAs begin to be degraded, however, proteins that have been synthesised from maternal transcripts during oogenesis can, and often do, persist; some of them even until very late in development (reviewed in Zernicka-Goetz *et al.*, 2009).

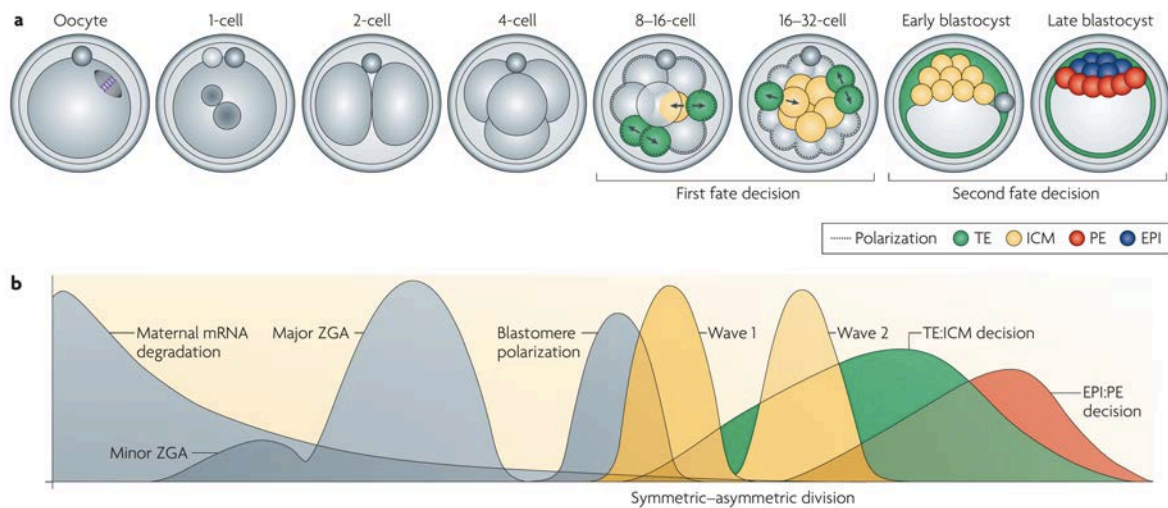


Figure 1.5 Transcriptional regulation and cell-fate decisions in pre-implantation development. a) The stages of pre-implantation development. Inner cell mass (ICM) progenitor cells are set aside from outer cells in two successive waves of possible asymmetric cell division commencing at the 8–16-cell and 16–32-cell stage transitions; the outer cells becoming trophoblast (TE) as a result of the first cell-fate decision. The second cell-fate decision involves the formation of primitive endoderm (PE) at the surface of the ICM facing the fluid filled blastocoel/ cavity and the formation of the epiblast (EPI) in the deeper encapsulated layers. **b)** A representation of the major events during pre-implantation development aligned with and in relation to the developmental/ cell division stages shown in part **a)**. Maternal mRNA degradation, the minor and major phases of zygotic genome activation (ZGA), cell polarisation and the two successive waves of possible asymmetric cell divisions (that give rise to inner residing cells) and the temporal onset of gene expression patterns associated with the first and second cell-fate decisions (taken from Zernicka-Goetz et al., 2009).

During the first three rounds of cell cleavage, early mouse embryos are highly adaptable and can withstand changes such as experimental removal, addition, and rearrangement of blastomeres. For example, if one cell of a 2-cell stage embryo is experimentally destroyed (Fig. 1.4), the remaining cell can often compensate for the loss of the other cell and support development to term (Morris *et al.*, 2012; Tarkowski, 1959). Although individual cells separated from the 4- or 8-cell mouse embryo cannot independently develop beyond implantation (Rossant, 1976; Tarkowski and Wroblewska, 1967), they can contribute to all tissues when combined with other blastomeres in chimeras, indicating that they still retain their full developmental potential (Kelly, 1977; Piotrowska-Nitche and Zernicka-Goetz, 2005). This is not to say that such cells have not already begun the process of differing from each other but does suggest that their potential have not been irreversibly restricted. Chimeras generated by the aggregation of two pre-implantation embryos together are also able to regulate their development to generate a single viable individual (Tarkowski, 1961). Thus, the observed plasticity with which mouse embryos are able to adapt to such experimental perturbations as those described, is one of the most distinguishing features of mammalian development and is a consequence of a process known as regulative development. This early flexibility greatly diminishes

as the three lineages of the blastocyst, first the TE and then the EPI and PrE, become established. At the present time, the exact timing when segregation of first two different cell populations that will form TE and ICM begins is somewhat controversial.

Notwithstanding the exact origin and timing of the generation of inter-blastomere variability, such differences remain a prerequisite of successful pre-implantation development and functional blastocyst formation. Up until the 8-cell stage, blastomeres of early cleavage embryos are morphologically identical. However, whether some initial molecular and functionally important differences between the blastomeres are already present is the matter of a long-lasting debate. Although evidence suggests that some degree of developmental bias toward one or another lineage,

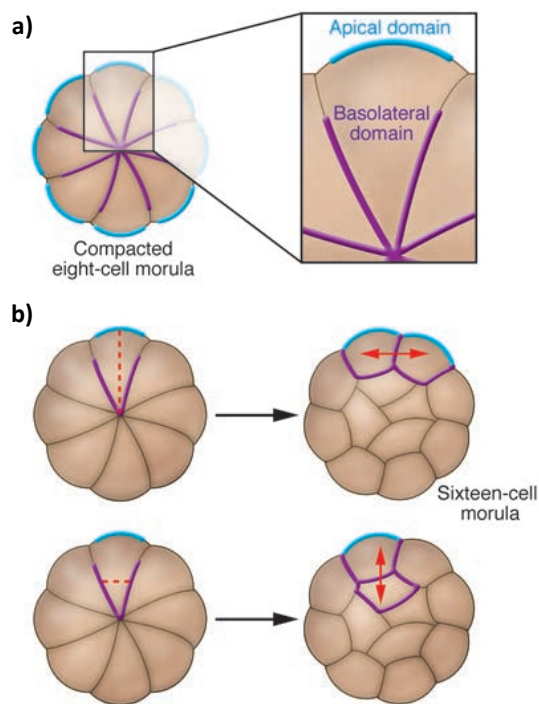


Figure 1.6 Establishing the apical and basolateral membrane domains in the mouse pre-implantation embryo and generating the two different cell populations. a) At the eight-cell stage, all blastomeres polarize along the axis of cell contact via the specific localisation of protein factors to either the outward and exposed apical (blue) cell surfaces or to the inwardly facing basal regions in cell-cell contact (purple). **b)** As the embryo transits from eight to 16 cells, blastomeres that divide parallel to the inside-outside axis produce two outside and polar daughter cells. Conversely, blastomeres that divide perpendicular to the inside-outside axis produce only one outer and polar daughter cell plus an inside and non-polar daughter cell. This creates two populations of cells: polarized outer cells and, nonpolar inner cells (taken from Cockburn and Rossant, 2010).

arising from such observed heterogeneity, might be present in early cleavage stage embryo blastomeres (reviewed in Zernicka-Goetz, 2004), it is clear that such cells are developmentally plastic and highly influenced by cell-cell interaction. During the 8-cell stage, blastomeres undergo a process of intracellular polarisation resulting in the asymmetric distribution of particular cellular components and the establishment of an apico-basal axis within each blastomere. The establishment of cell polarisation is then followed by the first morphogenetic event in pre-implantation embryo development, known as compaction. During compaction, the intercellular contact between cells is maximised and results in the flattening of blastomeres along their apico-basal axis and the formation of two different membrane domains, an adhesive and contact-engaged basolateral domain and contact-free apical domain. Compaction is then followed by the initiation of tight junction formation between neighbouring cells and their subsequent maturation in the outer-residing cells of later developmental stages. The successful conclusion of these two events, polarisation and compaction,

is absolutely essential for the generation of the two morphologically different populations of blastomeres (Fig. 1.6), that arise during the transition from the 8-cell to the 16-cell stage (and again during the 16- to 32-cell stage transition), when cells will become allocated to either inside or outside positions, as embryo enters morula stage (reviewed in Dard *et al.*, 2008; Zernicka-Goetz *et al.*, 2009; Bruce and Zernicka-Goetz, 2010; Cockburn and Rossant, 2010; Schrode *et al.*, 2013).

Once the 8-cell stage embryo has polarised and maximised its cell-cell contact during compaction, it next undergoes a cell cleavage division that will, based on the orientation of the mitotic spindle, result in the generation of two distinct cell populations. In cases when the mitotic spindle becomes oriented parallel to apico-basal axis, the resulting cleavage plane is perpendicular to the same axis and results in the generation of two different daughter cells (Fig. 1.7). As such, one cell retains the apical surface of the ancestral cell, remains polarised and is positioned on the outside of the embryo. Conversely the other cell inherits the basolateral region of the parental cell and

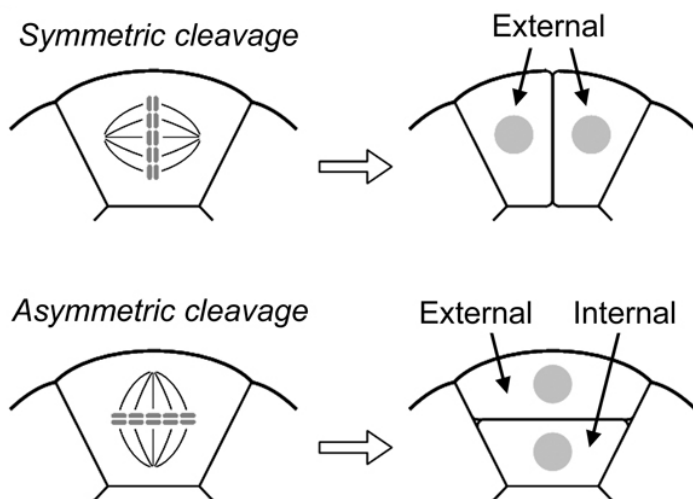


Figure 1.7 A schematic diagram depicting two types of cleavage patterns. Symmetric cleavage divides a blastomere along the apico-basal axis to generate two external blastomeres, whereas asymmetric cleavage divides perpendicular to the axis to generate one external and one internal blastomere. (taken from Marikawa and Alarcon, 2009)

becomes positioned to the inside compartment of the embryo and is non-polar. This type of division, in which two different daughter cells are generated, is called a 'differentiative' or 'asymmetric' division. Alternatively, if the mitotic spindle is oriented perpendicular to the apico-basal axis, the resulting cleavage plane is parallel to it and generates two daughter cells that each inherits apically and basolaterally distributed components. Such 'conservative' or 'symmetric' cell division results in the generation of

two seemingly identical daughter cells that will in most cases retain polarised intracellular organisation and occupy the outer positions of the 16-cell stage embryo. However, initially positioned outer cells can become internalised, as a result of increased cortical tension, in cases when they are incapable of establishing apical-basolateral polarity (Anani *et al.*, 2014); potentially arising from relatively oblique angles of cell division. The two described types of cell division (*i.e.* symmetric and asymmetric, or perhaps more appropriately the opportunity for cells to spatially segregate) also occurs during the 16- to 32-cell transition. Therefore, in this way, two separate populations of cells are successively generated in the pre-implantation embryo from an originating

population of conceptually uniform 8-cell stage blastomeres (reviewed in Dard *et al.*, 2008; Zernicka-Goetz *et al.*, 2009; Bruce and Zernicka-Goetz, 2010; Cockburn and Rossant, 2010; Schrode *et al.*, 2013).

Based on these initial differences in their position (inner/outer) and intracellular organisation (polarised/non-polarised) resultant cells gradually segregate into two different cell lineages; trophectoderm (TE) and inner cell mass (ICM). Outer polarised blastomeres will give rise to TE while non-polarised inner blastomeres will become the ICM. However, such initial spatial segregation and differential polarisation status is not immediately conveyed into the irreversible establishment of the TE and ICM lineages. This is perhaps best illustrated by the fact that both inner and outer cells that are experimentally removed from their original position at 16-cell stage and placed in the opposing spatial position in embryo chimeras, can still reprogram their route of differentiation in accordance to their new position and to give rise to both TE and ICM. This means that in the 16-cell embryo both inner and outer blastomeres remain pluripotent. Indeed, when uniform populations of such cells are re-aggregated into 16-cell clusters, they can subsequently, after uterine transfer, develop into normal and fertile mice. However, at 32-cell stage of mouse embryo development, it appears that these two populations of cells become irreversibly committed to one or another lineage, utilising similar chimera experimentation, thus marking the point at which the first cell-fate decision can be argued to be finalised (Suwinska *et al.*, 2008).

At the 32-cell stage and following the formation of an outer epithelium of TE cells, an osmotic gradient created by Na^+ influx through apically localised Na^+/H^+ exchangers and efflux via Na^+/K^+ ATPases on the basolateral side of the TE results in the formation of a fluid-filled cavity known as the blastocoel (Fig. 1.8) (Eckert *et al.*, 2004). It is the parallel maturation of tight junction assembly initiated during compaction that seems to maintain the blastocoels integrity as it grows. Accordingly, at around E3.5 after the blastocoel has been formed, the mouse embryo is considered a blastocyst.

The presence of a blastocoel is essential for appropriate further development of the ICM. This is because the blastocoel will be positioned asymmetrically to the one side of the embryo thereby restricting the ICM to the opposite pole and thus defining the orientation of the embryonic-abembryonic axis. The pole of the blastocyst where the ICM resides will be called the embryonic pole and the opposite side with the blastocoel is the abembryonic pole. Additionally, the part of the TE that is in contact with the cavity (in the abembryonic region) is called the mural trophectoderm while the portion opposite to it, covering the ICM, is called the polar trophectoderm.

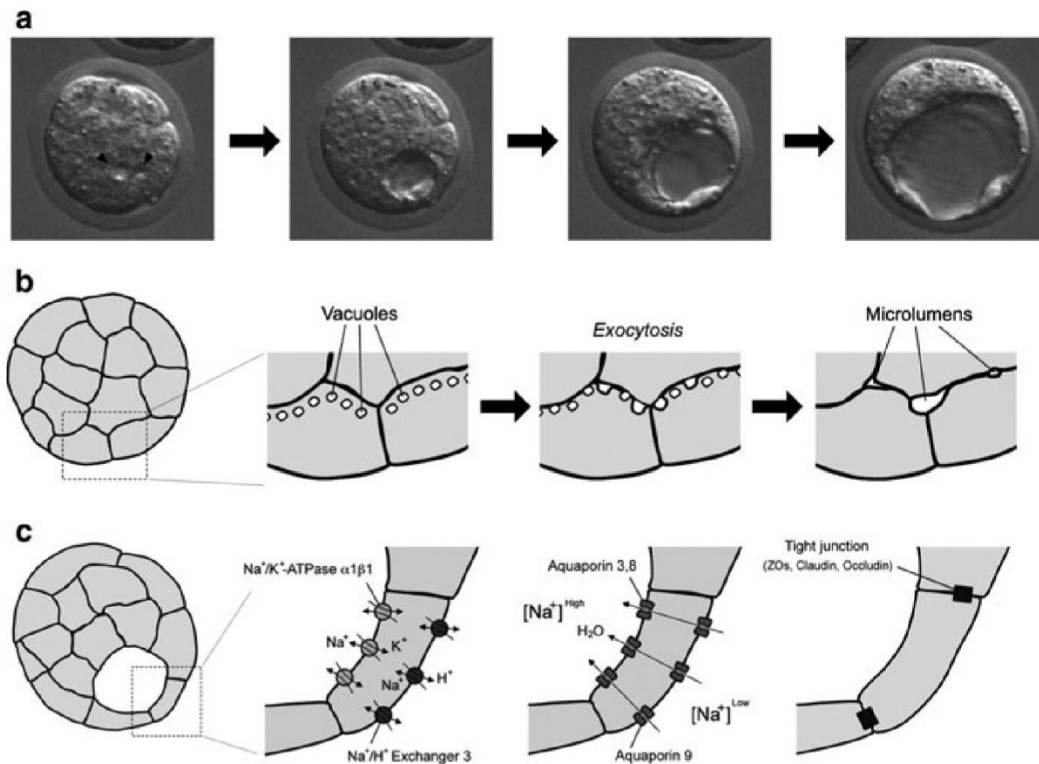


Figure 1.8 Blastocoel formation during pre-implantation embryo development. **a)** Snapshot images taken by time-lapse cinematography of a developing mouse embryo, showing the initial formation of microlumens and their expansion to generate the blastocyst cavity. **b)** Schematic diagrams, depicting microlumen formation by exocytosis of vacuoles at the basal membrane in the outer cells. **c)** Schematic diagrams, portraying three critical steps to expand and maintain the blastocyst cavity, namely, directional sodium ion transport, water influx, and paracellular sealing (taken from Marikawa and Alarcon, 2012).

After the specification of the TE and the formation of the blastocyst cavity, the ICM will further segregate into two lineages, the EPI and the PrE. PrE cells will constitute a single cell monolayer that is in contact with the blastocoel, while the EPI will remain as a mass of cells residing between the PrE and the overlying polar TE. Precursors of these two cell lineages are initially distributed through the ICM of the early blastocyst in a so-called ‘salt-and-pepper’ distribution and gradually segregate into the EPI and PrE compartments via processes of active cell movement, positional induction and programmed cell death, so that by day E4.5 of pre-implantation development, when the embryo will hatch and seek to implant into the uterus, these two distinct cell lineages will be formed (reviewed in Dard *et al.*, 2008; Zernicka-Goetz *et al.*, 2009; Bruce and Zernicka-Goetz, 2010; Cockburn and Rossant, 2010; Schrode *et al.*, 2013).

1.2 DEVELOPMENTAL BIAS OF EARLY BLASTOMERES IN MOUSE EMBRYO

Although cell fates are not fixed until the around 32-cell stage (Suwinska *et al.*, 2008), there is evidence that developmental potentials are unequal among blastomeres at much earlier stages and that these affect the ultimate cell fate of progeny cells later in pre-implantation development; therefore prompting a fundamental question as to when the first differences between blastomeres start to appear.

In this context, two models have been put forward to explain early mouse development. One defines the early mouse embryo as an entirely symmetric structure comprised of identical cells that are dividing in random orientations with no underlying pattern at the beginning of development (Alarcon and Marikawa, 2003; Hiiragi and Solter, 2004; Motosugi *et al.*, 2005). The initial differences between blastomeres appear only after the two distinct cell populations, inner and outer, are established (starting from the 8- to 16-cell stages). According to this model the blastocoel forms at a random site and therefore eliminates the possibility that the embryonic-abembryonic axis is related to any of the earlier events in embryogenesis or oogenesis (Motosugi *et al.*, 2005).

Another model proposes that some differences between cells exist well before blastomeres acquire inner or outer positions in the embryo and that these differences reveal themselves during the early cleavage stages of embryo development. Cited evidence in support of this claim are provided by observations that blastomeres of the 4-cell or even 2-cell stage embryo may already be biased to preferentially give rise to a particular type of cells or to contribute to a specific region in the blastocyst, although such bias may be erased or modified by experimental manipulations (Piotrowska *et al.*, 2001; Piotrowska-Nitsche *et al.*, 2005). In addition, a stronger piece of evidence in favour of this model came from the study of Tabansky and colleagues, whereby the authors induced randomised recombination events in so-called 'Rainbow' transgenic mice during the early cleavage stages, to indelibly label cells and their progeny. This approach allowed the retrospective ancestral tracing of the developmental origin of cells from later developmental stages (even beyond implantation) and showed, in a subset of embryos, the existence of a significant bias in the contribution of labelled cell clones towards either TE or ICM (Tabansky *et al.*, 2013). Hence such a model suggests that early inter-blastomere heterogeneity can ultimately bias subsequent progeny cell fate, albeit to a questionable extent.

The highly regulative nature of mouse pre-implantation embryo development often serves as an argument against the existence of any early pre-patterning/ developmental bias in the pre-implantation embryo, however subtle this may or may not be. Regardless of whether early patterning is present in the embryo it is important to emphasise that its existence would not be

mutually exclusive with the embryo's regulative nature and therefore this fact does not exclude the possibility that a "preferred" pattern of development under which embryos will tend to follow under unperturbed developmental conditions, may exist. Therefore, even though the early mouse embryo retains flexibility in responding to perturbations, its patterning may be initiated, to some degree, at the earliest developmental stages (reviewed in Zernicka-Goetz, 2004).

1.2.1 Embryonic axes in the mouse pre-implantation embryo

The mouse pre-implantation embryo has three axes of symmetry: the animal-vegetal axis, the embryonic-abembryonic axis and the axis of bilateral symmetry (Lu *et al.*, 2001). The animal-vegetal (AV) axis in the mouse embryo (Fig. 1.9) is defined by the position of the second polar body, which is extruded upon completion of the second meiotic division just after fertilisation, and marks the animal pole, whilst the diametrically opposed portion of zygote is designated as the vegetal pole (Lu *et al.*, 2001). The first meiotic polar body, which is extruded before fertilisation in the unfertilised egg, does not typically persist during development and its location does not seem to be strictly correlated with that of the second polar body. However the second polar body persists in most embryos and remains tethered to the embryo throughout pre-implantation development without changing original position and could therefore serve as a reliable and persistent marker of the AV axis (Gardner, 1997).

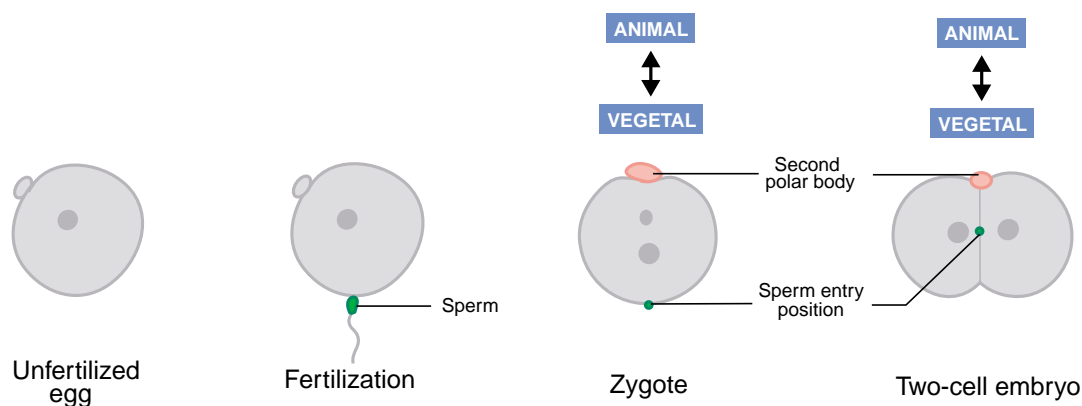


Figure 1.9 A schematic representation of the animal-vegetal axis (taken from Lu *et al.*, 2001)

Although, the early cavitating blastocyst had originally been considered spherical, it has since been shown that as early as the zygote stage, the embryo obtains an oblate spheroid shape and possesses bilateral symmetry (Gardner, 1997). Moreover, the axis of bilateral symmetry of the early blastocyst is normally aligned with the animal-vegetal axis of the zygote and correlates with the anterior-posterior axis of the later developing embryo/foetus (reviewed in Lu *et al.*, 2001).

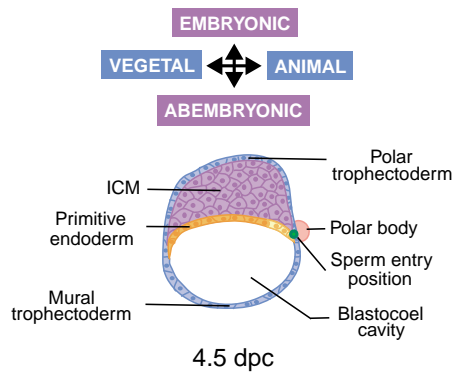


Figure 1.10 The embryonic-abembryonic axis in relation to animal-vegetal axis in pre-implantation mouse embryo (taken from Lu *et al.*, 2001)

The embryonic-abembryonic axis in the blastocyst is orthogonal to the animal-vegetal axis (Fig. 1.10) and is defined by the location of the ICM, with the embryonic pole on the side of the blastocyst containing the ICM and the abembryonic pole on the side with the blastocoel (Lu *et al.*, 2001). The observation that the boundary between the embryonic and abembryonic halves of the early blastocyst tends to align with the plane of the first cleavage, estimated by the localisation of the second polar body or traced by marking the zona pellucida (ZP) (Gardner, 2001) has led to the question whether the specification of the axes of the blastocyst depends on the patterned distribution of cytoplasmic or plasma membrane determinants within the egg or the zygote.

1.2.2 Mosaic model

The mouse metaphase II stage arrested oocyte (MII oocyte) is approximately 80µm in diameter and is a highly polarised cell. This polarisation is manifested in the presence of the polar bodies (extruded during oocyte maturation) that remain tethered at the presumptive animal pole (reviewed in Lu *et al.*, 2001), the subcortically positioned metaphase arrested spindle from the second meiotic cell cycle and a cortical granule free domain (CGFD) at the presumptive animal pole. Whether such characterised polarity or the existence of other unknown molecular polarities within the mouse oocyte reflects informative potential that could direct or influence the early stages of embryo development has been a matter of continuing speculation and debate. Although in many species the organisation of the egg itself does carry information that will instructively direct early embryo development, mammalian embryos are considered to be an exception in this regard because when any observed oocyte polarity is experimentally disturbed, viable embryos and subsequent adult animals are still able to develop (reviewed in Gardner, 1999).

Findings that the cytokine leptin and the signalling molecule Stat3 are asymmetrically distributed to the animal pole of the mouse MII oocyte (Antczak and van Blerkom, 1997) initially led to the proposal of a mosaic model in which oocyte polarity is a key determinant in the spatial patterning of the blastocyst and its constituent cells. It was postulated that the orientation of the cell cleavage planes later in development could lead to the differential inheritance of these two proteins between blastomeres thus affecting the balance of TE versus ICM cell fate (Johnson and McConnell, 2004). However, when the significance of the egg polarity on later development was experimentally

tested by removing either animal or vegetal pole of the zygote, the conclusion was reached that there could be no determinants uniquely localised to either the animal or the vegetal pole of the fertilised mouse egg essential for development, because zygotes were still able to develop not just to the blastocyst stage but also into adult animals; thus proving this model incorrect or at least demonstrating that the presence of any localised determinants that could be asymmetrically distributed amongst cells, according to the mosaic model, is not critical for successful development (Zernicka-Goetz, 1998).

1.2.3 The first cell cleavage division

The origin of potential spatial patterning in the mouse embryo can be traced back through the earliest developmental events to the first cell cleavage. Namely, it appears that the orientation of the first cleavage plane is not random but is almost exclusively parallel to AV axis and therefore passes through the animal pole and its opposite counterpart, the vegetal pole (Gardner, 2001; Gray *et al.*, 2004). It can be argued that the blastomeres of the 2-cell stage embryo can be considered already different from each other because one will give rise to progeny cells that will mainly contribute to embryonic half of the embryo while the other cell's progeny will contribute to the abembryonic part, although it does not mean that one blastomere contributes more cells to the TE and the other to the ICM lineage (Piotrowska *et al.*, 2001). Whilst this observation has only been proposed as a tendency and not as an absolute rule (it can be applied in 70–80% of the cases) it does demonstrate some potential for early spatial patterning in the embryo, that has yet to be substantiated with compelling molecular evidence.

It is noteworthy that the first cleavage plane aligns with the equatorial axis of bilateral symmetry, as observed in the blastocyst, and is orthogonal to the embryonic-abembryonic axis and that although the first cleavage plane defines the approximate orientation of the embryonic–abembryonic axis, it does not set up embryonic/ blastocyst morphological polarity *per se* (Plusa, Hadjantonakis, *et al.*, 2005).

1.2.4 The second cell cleavage divisions

In the majority of embryos the orientation of the cell divisions during the second cleavage are non-random with respect to the position of second polar body (*i.e.* the AV axis), because almost 80% of 2-cell stage mouse embryos are characterised by one meridional (M) (parallel to the animal-vegetal axis) and one equatorial (E) (perpendicular to the animal-vegetal axis) plane of cell division. The remaining 20% of embryos constitute those in which both divisions are either meridional or

equatorial. Therefore there exists a natural bias in terms of forming two distinct division orientations per 2-cell stage embryo. In addition, the second cell cleavage is also asynchronous because one blastomere divides earlier than its sister, thereby allowing the distinction of 4 different types of embryos that could be generated based on the order in which the cleavages happen and in respect to the orientation of the cleavage plane in relation to AV axis. In cases where the M cleavage precede the E cleavage embryos are designated as ME embryos. In contrast, embryos in which an E division precedes an M division are described as EM embryos. In cases when both divisions exhibit the same cell division plane the embryos are designated as either MM or EE (Fig. 1.11) (Piotrowska-Nitsche and Zernicka-Goetz, 2005).

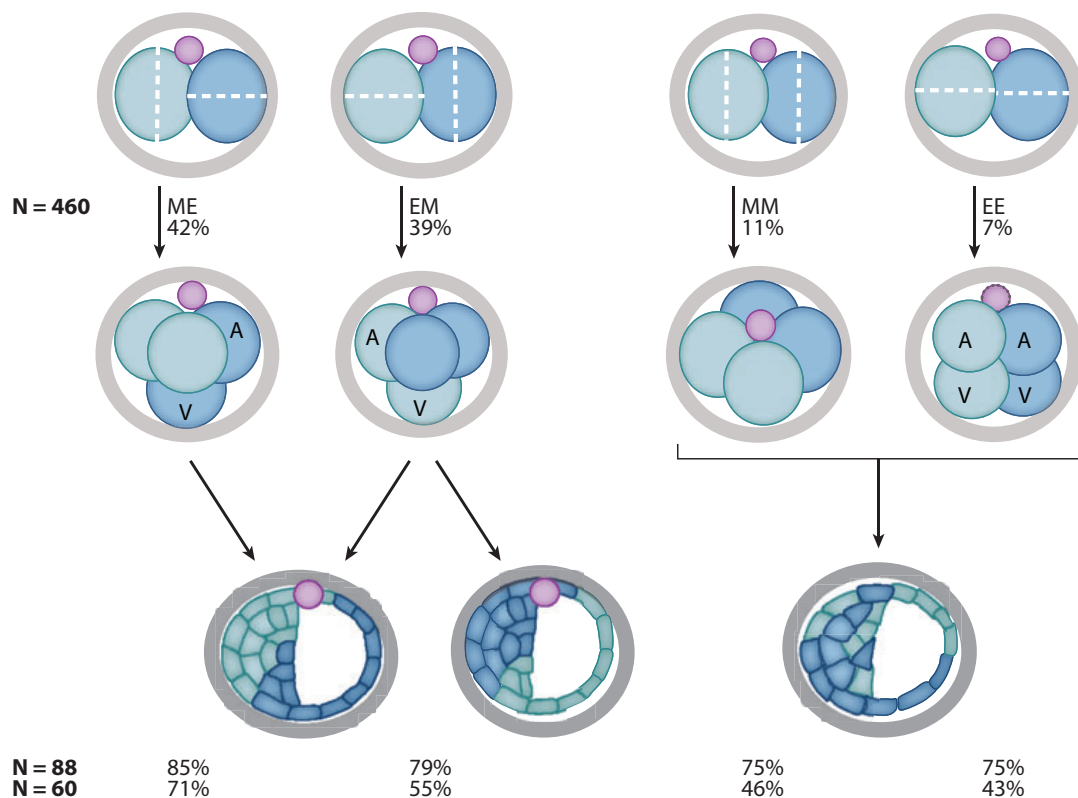


Figure 1.11 The relationships between the second cleavage patterns at the 2-cell stage and later development as proposed by Zernicka-Goetz and colleagues. Four-cell stage embryos are classified according to the cleavage pattern by which they formed, where both the orientation of the plane of cleavage (E, equatorial; M, meridional with respect to the second PB) and the sequence (ME or EM) are recorded. For equatorial divisions, the two E blastomeres can be further classified as primarily from the animal end (A) or the vegetal pole (V) (taken from Johnson, 2009).

The order in which blastomeres of 2-cell stage embryos divide and orientation of these divisions seems to harbour developmental relevance (Fig. 1.11). In embryos in which the earlier of the two cell divisions occurs meridionally (ME embryos), it is possible to predict that the progeny of the meridionally dividing cell will predominantly populate the embryonic part of the blastocyst.

Alternatively, in EM embryos this is not the case but instead the earlier equatorially dividing cell has an equal chance to develop into either the embryonic or the abembryonic part of the blastocyst (with the later meridionally dividing cell occupying the opposing pole). However, in the comparatively infrequent cases in which both the 2-cell stage blastomeres undergo either EE or MM divisions, the contribution of progeny cells appears random in relation to the embryonic-abembryonic axis of the blastocyst. In addition, the developmental competence of MM and EE embryos is severely compromised, in comparison to ME and EM embryo types, thus further emphasizing the potential importance of the cell cleavage planes divisions at the 2- to 4-cell stage transition (Piotrowska-Nitsche and Zernicka-Goetz, 2005).

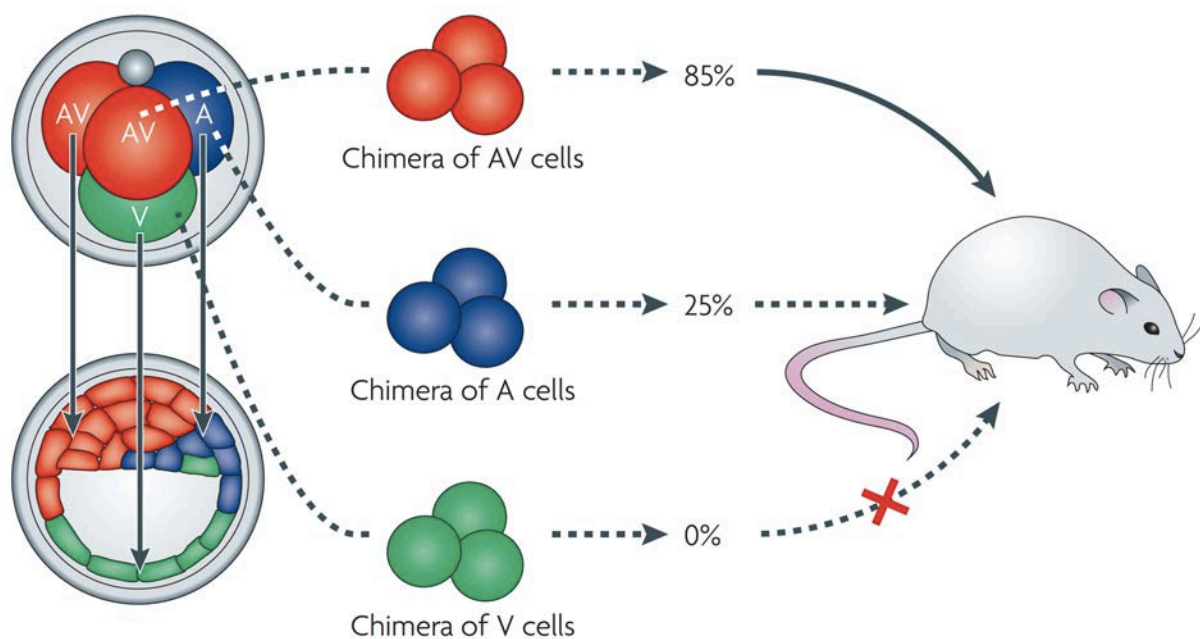


Figure 1.12 The difference in developmental success between chimeras made of the entirely equatorially derived blastomeres and meridionally derived blastomeres of 4-cell stage mouse embryos (taken from Zernicka-Goetz et al., 2009)

The importance of the timing and orientation of the cell division plane, during 2- to 4-cell stage transition, is further reinforced by the observation that the vegetal-most blastomere (*i.e.* the one which was generated by E division and is furthest away from the second polar body) in ME-pattern embryos, already possesses a distinct developmental potential to give rise to the abembryonic pole of the blastocyst, or specifically to the mural TE (Piotrowska-Nitsche *et al.*, 2005). Moreover, chimeras made exclusively of vegetal-most blastomeres that were isolated from ME embryos are unable to develop into viable mice once transferred to the uterus of foster mothers (Fig. 1.12) thus, indicating that the developmental potential of vegetal-most blastomeres is limited (Piotrowska-Nitsche *et al.*, 2005).

At the molecular level, individual blastomeres of 4-cell stage ME embryos exhibit heterogeneity in histone H3 arginine 26 (H3R26) methylation post-translationally modified chromatin levels. The vegetal-most blastomere of ME embryos is characterised by reduced overall levels of H3R26 methylation in comparison to other blastomeres of the same embryo (Torres-Padilla *et al.*, 2007). This epigenetic modification is known to be under the regulation of the H3-specific arginine methyltransferase, Carm1 (Co-activator associated arginine methyltransferase 1) (Torres-Padilla *et al.*, 2007; Goolam *et al.*, 2016; White *et al.*, 2016), as experimentally induced down-regulation of Carm1 results in the reduction of H3R26 methylation levels (White *et al.*, 2016), and the pharmacological inhibition of Carm1 activity abolishes them (Goolam *et al.*, 2016) in the early pre-implantation mouse embryo. In contrast, the overexpression of Carm1 causes an increase in H3R26 methylation and concomitant up-regulation of the pluripotency associated transcription factors Sox2 (SRY-Box 2) and Nanog (Nanog homeobox), thus ultimately directing cells to allocate towards the ICM lineage (Torres-Padilla *et al.*, 2007). In addition, it has recently been demonstrated that the extent of H3R26 methylation also affects the dynamics of Sox2 binding to DNA (Deoxyribonucleic acid); as exemplified by experiments showing that a reduction in H3R26 methylation levels in cells of the early embryo, caused by clonal Carm1 down-regulation, was associated with a reduction in the long-lived chromatin bound fraction of Sox2 and was also associated with a decrease in expression of Sox2 targets genes that would ultimately bias cells towards allocating to the TE cell lineage (White *et al.*, 2016). It is possible that one of these potential Sox2 targets genes might be the transcription factor Sox21 (SRY-Box 21), given that the expression of Sox21 mRNA correlates well with that of Sox2 and another pluripotency transcription factor Oct4 (Octamer-binding protein 4/ POU class 5 homeobox 1, also known as Oct3/4 and Pou5f1) and is dependent on H3R26 methylation. Indeed, pharmacological inhibition of Carm1 from the 2-cell stage, and the associated abolition of detectable H3R26 methylation levels, results in the absence of Sox21 expression. Moreover, endogenous Sox21 expression is heterogenous between the blastomeres of 4-cell stage ME embryos, being lowest in the vegetal blastomere. In addition, experimentally directed Sox21 depletion results in premature up-regulation of Cdx2 (Caudal type homeobox 2) mRNA, a transcription factor that serves as a TE lineage marker, as well as in decreased frequency of inner-cell generating asymmetric cell divisions and the direction of cells towards the TE lineage (Goolam *et al.*, 2016). This is in agreement with the observation that the progeny of the vegetal-most blastomere tends to express more Cdx2 mRNA (Jedrusik *et al.*, 2008). Consistently, it has been shown that the progeny of the vegetal-most blastomere are biased to undergo symmetric divisions at 8- to 16-cell and 16-32 cell transitions that will result in the generation of more outer cells (Bischoff *et al.*, 2008).

Therefore the orientation and the order of the second cleavages may affect cell fate by affecting the asymmetric distribution of certain proteins or factors that bias cells towards one or another lineage. It is important to note that although developmental bias at this stage is still insufficient to direct the ICM/TE lineage commitment (Chen *et al.*, 2010), even the smallest bias during the early cell cleavage events could be gradually amplified (via feedback mechanisms) to help determine embryo patterning in respect to cell fate (Zernicka-Goetz, 2004).

1.3 CELL POLARISATION AND COMPACTION

Blastomere polarisation and embryo compaction are two hallmark events of the 8-cell stage of embryo development. In undisturbed uncompact 8-cell stage embryos, cells are not yet polarised and are characterised by a round morphology having microvilli distributed throughout their entire cell surface. During compaction cells change their morphology, become flattened, maximise their contact and polarise along their apico-basal axis, with microvilli being excluded from the cell-to-cell contact regions and present only on the apical membrane. Although closely temporally linked, these two events, polarisation reflecting the organisation of the individual cell, and compaction, referring to intercellular organisation of the embryo, can be dissociated from one another. The mechanisms that drive polarisation and compaction of blastomeres during the 8-cell-stage mouse embryo are still largely unknown, but changes in the phosphorylation status of membrane associated proteins, such as Cdh1 (Cadherin 1, also known as epithelial cadherin/E-cadherin/uvomorulin), Ctnna1 (Catenin alpha 1/Cadherin-associated protein alpha 1, also known as α -catenin), Ctnnb1 (Catenin beta 1/Cadherin-associated protein beta 1, also known as β -catenin) and Ezr (Ezrin, the FERM domain containing protein also known as Villin 2/Cytovillin) suggest the integral involvement of kinases and phosphatases (reviewed in Johnson and McConnell, 2004).

1.3.1 Compaction

Compaction of the 8-cell stage embryo occurs as a consequence of increased flattening of blastomeres along their apico-basal axis during which cell-cell contacts become maximised; this is paralleled by the formation of adherens and tight junctions between cells. Arguably, the most important protein involved in process of compaction is Cdh1, the cell-cell adhesion molecule that is the major component of adherens junctions. Prior to compaction Cdh1 is present evenly on the entire plasma membrane of all 8-cell stage blastomeres. After compaction Cdh1 is localised to the cell-cell contact regions, becoming restricted to the basolateral cell surfaces (Vestweber *et al.*, 1987). The addition of specific antibodies that recognise Cdh1 antigens or the removal from the embryo

growth media of Ca^{2+} ions (that prevent Cdh1 homophilic binding) ablates compaction at the 8-cell stage (Ducibella *et al.*, 1977; Hyafil *et al.*, 1980; Vestweber and Kemler, 1984). Embryos in which Cdh1 has been zygotically removed using a genetic knock-out approach are still able to compact normally due to maternally provided stores of the protein, however they fail to form functional adherens junctions later in development at the blastocyst stage (Larue *et al.*, 1994; Riethmacher *et al.*, 1995). The full importance of the role of Cdh1 during compaction has only been demonstrated after the additional removal of the maternal pool of protein demonstrated that such embryos were unable to compact (De Vries *et al.*, 2004).

Experimental evidence suggests that all the protein components that are necessary for the initiation of compaction are already present in the blastomeres of 4-cell stage embryos (determined by the observation that 4-cell stage embryos in which transcription and translation have been chemically inhibited are able to appropriately compact at the would-be 8-cell stage) therefore suggesting all the changes required for the onset of compaction are post-translationally regulated (Kidder and McLachlin, 1985; Levy *et al.*, 1986). This is supported by the fact that at the time of compaction both Cdh1 and Ctnnb1 proteins become phosphorylated (Clayton *et al.*, 1993; Pauken and Capco, 1999). Another important protein implicated in compaction is Ezr, the role of which in the pre-implantation embryo is to prevent microvilli breakdown and inhibit the formation of cell-cell contacts mediated by Cdh1. During compaction Ezr is also phosphorylated, leading to its removal from basolateral membranes and thus allowing the formation of Cdh1-mediated cell-cell contacts (Dard *et al.*, 2004). There is some evidence to suggest that aPKC ζ/λ (atypical protein kinase C, represented by two isoforms zeta/ ζ and iota/lambda/ ι/λ , hereinafter commonly referred to as Prkcz/i or when necessary individually as Prkcz or Prkci), itself regulated by the small GTPase RhoA (Ras homology family member A, guanosine triphosphate hydrolase), might be responsible for this phosphorylation event (Liu *et al.*, 2013). Indeed, an important role for RhoA in compaction has been previously demonstrated via chemical inhibition, and shown to be associated with the prevention of inter-cellular flattening and intra-cellular polarisation of blastomeres (Clayton *et al.*, 1999). Additionally, the subcellular distribution of another small GTPase, Rac1 (Ras-related C3 botulinum toxin substrate 1, guanosine triphosphate hydrolase) and the Rac1-related protein, IQGAP1 (IQ motif containing GTPase activating protein 1), has been shown to change during compaction (Natale and Watson, 2002) and it has been proposed that IQGAP1 might be involved in preventing premature compaction until the appropriate eight-cell stage (Watson *et al.*, 2004).

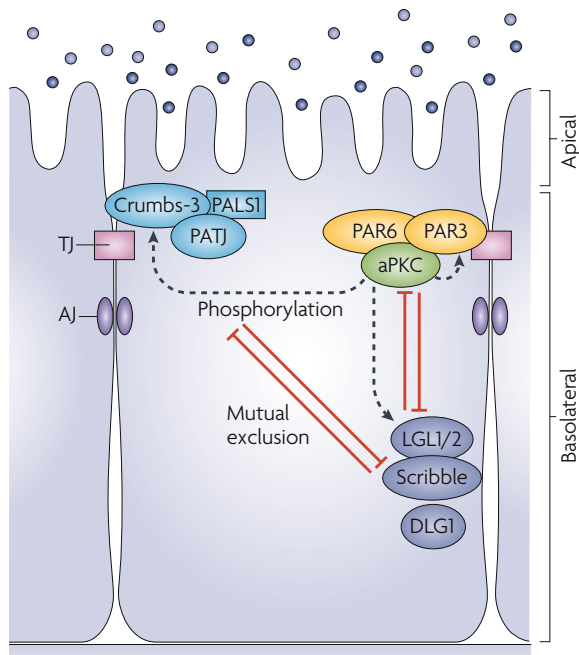


Figure 1.13 Polarity proteins of the PAR, Crumbs and Scribble complexes. The interplay of the three major polarity protein complexes - PAR, Crumbs and Scribble, at the plasma membrane is necessary to control and maintain the identity of apical and basolateral membrane domains. The PAR complex consists of PDZ domain-containing proteins partitioning defective-3 (PAR-3), PAR-6 and atypical protein kinase C (aPKC). The Crumbs complex comprises the transmembrane protein Crumbs and PDZ-domain-containing cytoplasmic scaffolding proteins PALS1 (protein associated with LIN-7)-1 and PATJ (PALS1-associated tight-junction protein). The third polarity protein complex Scribble is composed of Lethal Giant Larvae (LGL), Discs Large (DLG) and Scribble (SCRB). These polarity complexes become distributed asymmetrically between apical and basolateral membrane domain and will promote the expansion of the membrane domain that they associate with. PAR and Crumbs complexes will become localized apically reinforcing each others activity and localization whereas the Scribble complex will become restricted to the basolateral membrane domain. Polarity complexes are able to mutually antagonize each other and these basic steps will allow individual cells to become asymmetrically polarized (taken from Iden and Collard, 2008).

1.3.2 Polarisation

Cell polarity can be defined as a structurally and functionally asymmetric organisation of cellular components that contribute to cell asymmetry and are preserved and transmitted through cell divisions (Bornens, 2008). The establishment and maintenance of cellular polarity requires the integration of extrinsic and intrinsic polarity cues. A combination of intrinsic cues (provided by differential intra-cellular sorting and trafficking of proteins), as well as specification of plasma membrane domains and extrinsic cues (cell-to-cell contact sites, that provide positional information to the polarising/ polarised cell and instruct the cell to orientate its polarity) create the driving forces for members of the PAR (partitioning defective), Scribble and Crumbs polarity protein complexes to become asymmetrically distributed (Fig. 1.13). Such distribution permits the establishment of an axis of asymmetry that leads to the definition and stabilisation of membrane domains and finally results in the establishment of cellular polarity. Therefore as a result of polarisation, two distinct plasma membrane domains, apical and basolateral are established. The basal and lateral surfaces of a polarised cell are similar in their

composition and hence are referred together as a basolateral surface whilst the apical surface differs significantly. Strong cell-cell adhesions which are established at the apical-most part of lateral surfaces, defined by tight junctions, separate these membrane domains that are otherwise part of a continuous lipid bilayer and form a diffusion barrier which serves to prevent the free diffusion of proteins from one membrane domain to the other (Mellman and Nelson, 2008) as well as to limit

paracellular permeability *i.e.* passage of molecules through the intercellular space of neighboring epithelial cells (Bryant and Mostov, 2008).

1.3.2.1 Establishment of polarity in the mouse pre-implantation embryo

The establishment of cell polarity in the mouse pre-implantation embryo is initiated *de novo* at the 8-cell stage, however it still remains unclear exactly how this happens. The entire process of polarisation takes between 3-5 hours from induction until the apico-basal axis is established. All the necessary components for establishing cell polarity are already present in the 2-cell stage embryo (the earliest stage at which polarity in blastomeres could be experimentally induced) (Johnson and Ziomek, 1981a). Thus, it is a mechanism that seems to rely on cell-to cell contact to provide the information as to how and when the apical and basolateral domains should become established (reviewed in Johnson and McConnell, 2004). The orientation of the axis of polarity is highly dependent upon the asymmetric inter-cellular contact patterns of individual blastomeres at the early 8-cell stage (Johnson and Ziomek, 1981a). Numerous studies emphasise the importance of cellular interactions in setting up the orientation of this axis, based on the observation that the apical pole has a tendency to form as far away as possible from the sites of cell-cell contact. Although polarisation can be initiated in blastomeres that have been isolated from cell-cell contact or prevented from compacting, it is not possible to experimentally induce polarity in cells that are completely surrounded (reviewed in Johnson and McConnell, 2004). Therefore by changing the contact pattern of individual blastomeres of the early 8-cell stage embryo it is experimentally possible to change the axis of polarity of each cell, however this ability is lost 4–5 hours after 8-cell stage entry (Johnson and Ziomek, 1981a). Regardless of how it is initiated experimental evidence suggests that maintenance of polarity involves the activity of polarity protein/ factor complexes.

One of the earliest studies to investigate the presence of polarity factors demonstrated that the components of PAR polarity protein complex, Pard3 (Partitioning defective 3 homolog), Pard6 (Partitioning defective 6 homolog) and Prkcz/i, as well as basolateral domain marker of cell polarity, Emk1 (ELKL motif kinase 1, also known as Microtubule affinity regulating kinase 2 - Mark2; the mammalian homologue of PAR-1 in *Drosophila*), are all expressed in the pre-implantation mouse embryo (Fig. 1.14). *Prkcz* mRNA has been detected from the 2-cell stage and persists throughout the entire pre-implantation development (Vinot *et al.*, 2005) while the protein is first detectable from the 4-cell stage (Ralston and Rossant, 2008). Pard3 is expressed from the 2-cell to the 16-cell stage, in the form of a 150-kDa protein, whilst another 100-kDa isoform of Pard3 is present in blastocysts. In mouse, Pard6 is encoded by three different genes: *Pard6a*, *Pard6b* and *Pard6g*. In the pre-implantation stage embryo, *Pard6g* transcripts are completely absent, *Pard6a* mRNA is only present

at the 2-cell stage and Pard6b transcripts are present at all developmental stages. At the protein level both Pard6b and Emk1, are present from the 2-cell stage and persist throughout the entire pre-implantation development period. Interestingly, the mRNA encoding the Emk1 protein has only been detected in oocytes, suggesting the protein detected in subsequent pre-implantation embryo stages is actually maternally derived (Vinot *et al.*, 2005). In addition, many recent reports demonstrate the presence of components of the Scribble polarity complex in the blastomeres of pre-implantation mouse embryos and their localisation to basolateral membrane domains (Hirate *et al.*, 2013; Hirate *et al.*, 2015; Kono *et al.*, 2014; Tao *et al.*, 2012; Mihajlovic *et al.*, 2015; Mihajlovic and Bruce, 2016).

The localisation of all polarity proteins is highly dynamic and changes as development proceeds. At the 4-cell stage, Prkcz/i localisation is cytoplasmic, however at the 8-cell stage it becomes accumulated to the apical membrane (Ralston and Rossant, 2008). Similarly, from the 2-cell stage until the early 8-cell stage, Pard6b and Emk1 are mainly nuclear and only present at very low levels in the cytoplasm. After compaction, Pard6b becomes accumulated at the apical membrane while Emk1 becomes complementary localised to the basolateral part of the cell membrane (Vinot *et al.*, 2005) alongside the members of Scribble polarity complex (Hirate *et al.*, 2013; Hirate *et al.*, 2015; Kono *et al.*, 2014; Tao *et al.*, 2012).

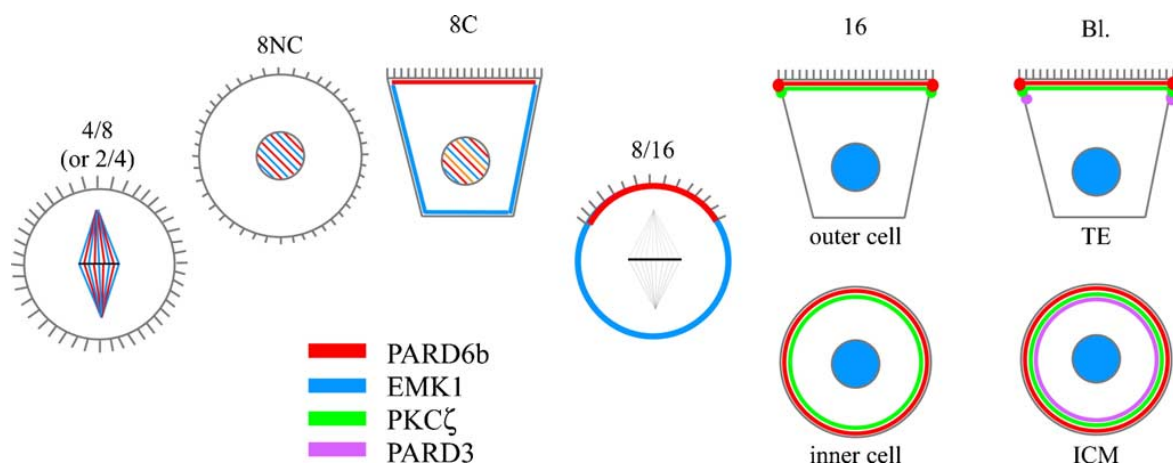


Figure 1.14 Scheme showing the cellular localisation of the PAR proteins and Prkcz/i during compaction and blastocyst morphogenesis in pre-implantation mouse embryos. 8NC: non-compacted 8-cell stage embryos, 8C: compacted 8-cell stage embryos, Bl: blastocyst, TE: trophectoderm, ICM: inner cell mass (taken from Vinot *et al.*, 2005).

The involvement of the small GTPase RhoA and its downstream effector Rock1/2 (Rho-associated protein kinase, represented by two isoforms Rock1 and Rock2) in pre-implantation mouse embryo development has been known for some time (Clayton *et al.*, 1999; Kawagishi *et al.*, 2004). However, it is only recently that they have been identified as being functionally upstream of cell polarity (Kono *et al.*, 2014). It has previously been demonstrated that RhoA activity is indispensable

for appropriate compaction and polarisation (Clayton *et al.*, 1999), while Rock1/2 activity has been shown to be absolutely required for blastocoel formation (Kawagishi *et al.*, 2004). Indeed, two recent independent studies have attempted to characterise this phenotype at molecular level, presenting somewhat contrasting results and conclusions (Duan *et al.*, 2014; Kono *et al.*, 2014). Kono and colleagues have reported that chemical inhibition of Rock1/2 activity, from the 2-cell stage, results in the mis-localisation of both apical and basolateral polarity factors and is associated with a developmental arrest at morula stage due to the inability of treated embryos to form blastocoels. The described polarity defects after Rock1/2 inhibition, were exemplified by atypically uniform distribution of ordinarily apically localised Pard6b and Prkcz/i proteins throughout the entire cell membrane (Kono *et al.*, 2014). In contrast, Duan and colleagues observed a much more severe phenotype comprising compaction defects and 8-cell stage developmental arrest, after Rock1/2 inhibition (Duan *et al.*, 2014).

The functional significance of appropriate polarity establishment during pre-implantation mouse embryo development is reflected in the fact that defects in cell polarity result in tight junction formation failure. Indeed, the apical polarity proteins themselves have been shown to be directly involved in the process of forming tight junctions. Specifically, Pard6b and Prkcz/i proteins are known to be targeted to tight junction regions as soon as they become established at the 8-cell stage and both are required for appropriate tight junction formation; as the observed distribution of Tjp1 (Tight junction protein 1, a cytoplasmic component of tight junctions) becomes severely impaired after either Pard6b or Prkcz/i experimentally induced down-regulation (Alarcon, 2010; Dard, Le, *et al.*, 2009). In addition, Pard3 is also targeted to the tight junctions, but only after the blastocoel has been formed indicating that Pard3 function may be responsible for the maintenance of tight junctions rather than their establishment. It is also possible that the observed eventual co-localisation of Pard6b, Prkcz/i and Pard3 at junctional complexes is indicative of the formation of a functional Par complex, as observed in other systems exhibiting cellular polarity (Vinot *et al.*, 2005). By means of contrast, it has been reported that experimentally induced disruption of cell polarity has no impact on embryo compaction or the formation of adherens junctions (Alarcon, 2010).

In addition to being indispensable for tight junction and cavity formation, disruption of cell polarity has a severe impact on relative cell positioning (*i.e.* inside or outside) and hence cell fate. The experimentally induced overexpression of a dominant negative (catalytically dead) form of Prkci and the down-regulation of *Pard3*, both result in biasing cells towards acquiring ICM cell fate. This observation has raised the possibility that mitotic spindle orientation might be regulated by cell polarity during 8- to 16-cell and 16- to 32-cell transitions, when the progenitor populations of inner cells are being generated (as a result of differentiative/ asymmetric cell divisions). Indeed, time-lapse

microscopy has revealed that overexpression of a dominant-negative form of Prkci instructs blastomeres to take more differentiative/ asymmetric divisions (hence favouring the formation of inner cells) or to become more frequently internalised by neighboring cell engulfment, thus decreasing the probability such cells could retain an outside position that would lead to eventual TE differentiation (Plusa, Frankenberg, *et al.*, 2005). However, this view has been somewhat contested by the observation that the number of inner cells observed in embryos at 16-cell stage is highly variable, suggesting that spindle orientation is not tightly regulated during 8- to 16-cell stage transition. Indeed, careful examination of spindle orientation during this transition has revealed that the cell cleavage patterns in the compacted 8-cell stage mouse embryo are not predetermined and that neither the relative timing of division nor the distance of a dividing cell from the centre of the embryo are able to influence it. Alternatively, it has been proposed that differential intercellular adhesion and cortical tension may be the major factors that enable some cells to almost completely protrude from the embryo and divide more frequently in a differentiative/ asymmetrical manner, while those cells retaining a large apical domain are more likely to divide more conservatively/ symmetrically. Taken together, the conclusion from this study was that regulated orientation of the spindle is not used as a mechanism to modulate the number of asymmetric divisions during the 8- to 16-cell stage transition (Dard, Louvet-Valee, and Maro, 2009).

Interestingly, another recent study has demonstrated that nuclear positioning might play an important role in predicting the orientation of cell division. This is because of the observation that at the early 8-cell stage, most cell nuclei are located in proximity to the apical domain yet as development progresses a certain portion are repositioned to the basolateral domain. As the nuclei that remain at the apical surface are statistically more likely to undergo conservative/ symmetric cell division (rather than differentiative/ asymmetric ones) and their counterparts repositioned to a more basolateral region do not exhibit any bias in the orientation of their division (Ajduk *et al.*, 2014), it can be argued that the orientation of cell division at the 8- to 16-cell stage is not a completely randomised process either.

1.3.2.2 Planar cell polarity in mouse pre-implantation embryo

Planar cell polarity (PCP) is manifested as the coordinated polarised orientation of cells within epithelial sheets. Recently, evidence for the involvement of the PCP-related protein Prickle2 (Prickle planar cell polarity protein 2) during mouse pre-implantation embryo development has been reported. This is primarily exemplified by the fact that Prickle2-deficient embryos have been shown to die between E3.0–3.5 (*i.e.* at the so-called late morula stage) as a consequence of being unable to form a functional blastocyst cavity. Accordingly, Prickle2 deficiency has been shown to be associated

with numerous apical-basolateral polarity defects, typified by an inappropriate and dispersed microtubule network, a complete absence of Pard6b and phosphorylated-Prkcz protein from the apical membranes and significantly reduced levels of Emk1 and dispersed Scrib (Scribbled homolog) protein from basolateral cell-to-cell contact regions. Nevertheless, Cdh1 localisation to the adherens junctions remained unaffected in Prickle2-deficient embryos. Prickle2 has also been shown to be important for the specification and development of the TE, as gene expression analysis of Prickle2-deficient embryos (at the late morula stage) have revealed the absence of TE critical transcripts for the transcriptional co-factor *Yap1* (Yes-associated protein 1) and transcriptional factor *Cdx2*, in addition to abnormally elevated expression levels of pluripotency-related transcription factor *Nanog*. However, although these data reveal an important role of Prickle2 in the establishment of transcriptional network required for TE specification, Prickle2 is not considered to be required for the initiation of *Yap1* and *Cdx2* gene transcription but rather their maintenance (Tao *et al.*, 2012).

1.4 THE FIRST CELL-FATE DECISION

During the first cell-fate decision two populations of cells that will ultimately become the TE and ICM are segregated from each other. These cells will become irreversibly committed to their respective lineages during the 32-cell stage (Suwinska *et al.*, 2008), at around E3.5, marking the time point at which the first cell-fate choice is irreversibly made. A fundamental question in mouse pre-implantation embryo development is how this is achieved.

Historically, two models have been proposed to explain how the first cell-fate decision is taken. The polarity model (Johnson and Ziomek, 1981b) proposes that upon the polarisation of a blastomere, cell-fate determinants become asymmetrically localised between the apical and basolateral poles, so that after asymmetric cell divisions the daughter cells inherit differing amounts of these determinants that will later decide their fate. The second model termed, the positional or inside-outside model (Tarkowski and Wroblewska, 1967), proposes that based on their position (*i.e.* on the inside or outside of the embryo) blastomeres will become exposed to different microenvironments (perhaps reflected in differential cell contacts) that will later become translated into different cell fates. Although historically the two models were in conflict it is important to emphasise that current thinking considers these two hypotheses as complementary rather than mutually exclusive.

1.4.1 The establishment of two spatially distinct cell populations

As previously mentioned, during the 8- to 16-cell stage transition the first two spatially distinct populations of cells are formed: a population of outer cells that will become TE and the other population of inner cells that will become the ICM. These two populations of cells were originally considered to originate mainly as a result of asymmetric divisions, however several recent studies, suggest this might not entirely be the case (Anani *et al.*, 2014; Samarage *et al.*, 2015; Watanabe *et al.*, 2014). Although asymmetric divisions can play an important role in allocating cells to the inner positions, it seems that very few inside cells are produced directly as a result of truly asymmetric cell divisions at this stage (*i.e.* cells that are allocated to the inside compartment as a direct consequence of cytokinesis). Rather, most inner cells seem to be generated by a process of cell internalisation/ engulfment that is subsequent to cell division and appears to correlate with the production of apolar cells that initially occupy an outer position (Anani *et al.*, 2014; Samarage *et al.*, 2015). Such cells that initially reside on the outside of the embryo before becoming internalised, appear to arise due to the fact that in reality cell division orientations are oblique rather than being exactly perpendicular or parallel to the apico-basal axis. As a consequence, it is possible that the asymmetric segregation of the apical domain between the two outer daughter cells arising from such oblique divisions (and in the size of the apical domains of blastomeres generated by distinct cell division events) is responsible for generating inter-blastomere heterogeneity in the relative 'strength' of apical-basolateral polarity, that is then interpreted and responsible for the subsequent internalisation of less polarised cells (Maitre *et al.*, 2016). Two recent studies have demonstrated that the driving force for this internalisation comes from the differences in actomyosin contractility between the neighbouring blastomeres and have highlighted the importance of Myh9 (Myosin heavy chain 9, also known as non-muscle myosin heavy chain IIa) in this process (Samarage *et al.*, 2015; Maitre *et al.*, 2016). Therefore, owing to the heterogeneity between blastomeres in the relative size of the apical domains generated (that has knock-on consequence on the extent of intra-cellular apical-basolateral polarisation), less polar cells are characterised by increased contractility in comparison to their neighboring polar cells and as a result become internalised (Samarage *et al.*, 2015; Maitre *et al.*, 2016). Therefore, the ultimate position of a blastomere in pre-implantation mouse embryo is highly dependent on the extent of its intra-cellular polarisation.

As embryonic development progresses it becomes an imperative that the position of a blastomere within the spatial context of the whole embryo and its extent of polarisation are subject to regulation, otherwise cells become incapable of appropriately sensing their surrounding environment and are unable to adjust their fates accordingly. The appropriate interpretation of the

positional cues provided by cell-to-cell contact and cellular polarity at molecular level is possible during pre-implantation mouse embryo development, due to the existence of a functioning Hippo signalling pathway.

1.4.2 The role of the Hippo signalling pathway in interpreting positional cues

The first clues about the molecular mechanism that acts upstream of TE/ICM lineage segregation came from the study of Nishioka and colleagues that demonstrated the involvement of the Hippo signalling pathway in the first cell-fate decision (Nishioka *et al.*, 2009). This study initially discovered that differential cell-to-cell contacts between the inner and outer blastomeres, mediated via Hippo signalling, instruct the first cell-fate decision via a mechanism of differential activation of the serine/threonine protein kinase Lats1/2 (Large tumor suppressor kinase 1 and 2). In turn, the differential activation status of Lats1/2 (active in inner cells, inactive in outer cells) was shown to result in the differential subcellular localisation of the Yap1 protein (a transcriptional co-activator of Tead4/ TEA domain transcription factor 4 – a transcription factor required to activate transcription of TE-related genes), whereby unphosphorylated Yap1 was nuclear in outer cells, but the phosphorylated form was cytoplasmic in inner cells, thus providing a mechanism by which outer cells can express required TE genes and inner cells cannot. Subsequently, several other studies have demonstrated the involvement and importance of other Hippo signalling pathway components during the first cell-fate decision (Cockburn *et al.*, 2013; Hirate *et al.*, 2013; Leung and Zernicka-Goetz, 2013; Lorthongpanich *et al.*, 2013).

Two independent studies have recently highlighted the importance of the Amot (Angiomotin) protein in Hippo signalling pathway activation (Hirate *et al.*, 2013; Leung and Zernicka-Goetz, 2013). The Amot protein first becomes expressed from the late 8-cell stage and is weakly detected on the apical domain of the plasma membrane. However, from the 16-cell stage, Amot protein is differentially localised in inner versus outer cells, being present throughout the entire plasma membrane of inner cells and restricted to the apical membrane of outer cells. In addition, cytoplasmic Amot level in inner cells are slightly higher when compared to the levels in outer cells (Hirate *et al.*, 2013; Leung and Zernicka-Goetz, 2013). This pattern of Amot protein distribution in embryo is of paramount importance and appropriately reflects the nature of its function.

In outer cells, owing to the presence of the contact-free apical domain, Amot is sequestered away from adherens junctions (Hirate *et al.*, 2013). As a consequence, Hippo signalling is inhibited in outer cells resulting in low levels of Lats1/2 activity and consequently insufficient Yap1 phosphorylation to prevent its translocation to the nucleus (Fig. 1.15). Accumulation of nuclear Yap1

in outer cells enables Tead4 to activate the transcriptional expression of TE lineage-specific genes and transcription factors, such as *Cdx2*, reinforcing TE cell fate in outer cells (Nishioka *et al.*, 2009).

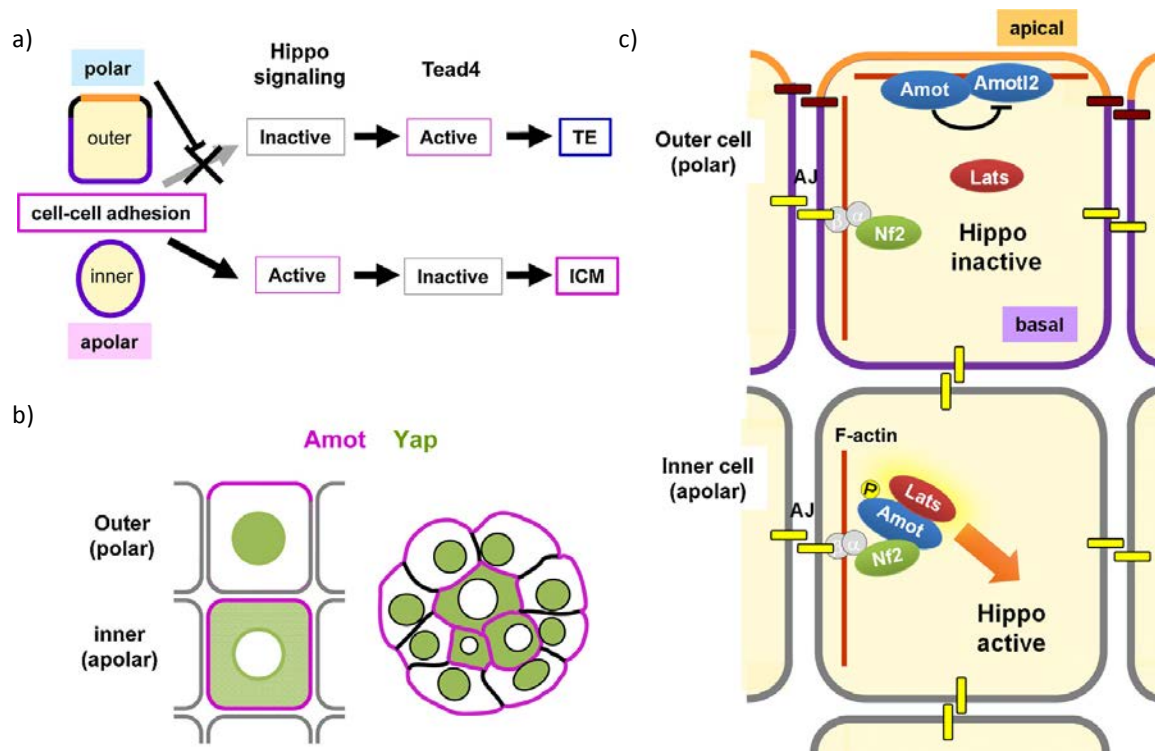


Figure 1.15 Mechanisms that establish position-dependent Hippo signalling at the 32-cell stage. **a)** A combination of cell-cell adhesion and cell polarisation establishes position-dependent Hippo signalling. **b)** Position-dependent distribution of Amot and its relationship with the distribution of Yap1. **c)** A model of position- and polarity-dependent Hippo signalling in mouse embryos (taken from Sasaki, 2015).

The appropriate establishment of apical-basolateral cell polarity in outer cells is an absolute prerequisite for proper localisation of Amot and its sequestration to the contact-free membrane of the apical domain. Indeed, experimental disruption of either apical or basolateral polarity proteins, results in the ectopic mis-localisation of Amot to adherens junctions and the aberrant activation of Hippo signalling pathway, as evidenced by cytoplasmically localised and phosphorylated Yap1 (Hirate *et al.*, 2013). Furthermore, the fact that it has been observed that Yap1 is also phosphorylated, as a result of Hippo signalling pathway activation, in naturally occurring outer cells with impaired apical-basolateral polarity (that still possess a contactless apical domain), highlights the importance of a polarised and functional apical domain in the regulation of Hippo signalling pathway activity (Anani *et al.*, 2014). It is noteworthy that due to the fact that the effects on Yap1 localisation and *Cdx2* expression after disrupting the apical polarity complex at the 16-cell stage are comparatively weak (compared to later stages), it was recently proposed that there might be another molecular

mechanism operating at this stage that works in parallel with the apical cell polarity protein complex(es) to regulate the Hippo signalling pathway (Hirate *et al.*, 2015).

In apolar inner cells, the absence of the contact-free apical domain allows the association of Amot with components of adherens junctions and results in Hippo signalling pathway activation (Hirate *et al.*, 2013). An elegant study recently demonstrated the requirement of the Nf2/Merlin (Neurofibromin 2/ Moesin-Ezrin-Radixin-like protein), in Amot mediated and Lats1/2-dependent phosphorylation of Yap1. Specifically, that in the experimentally induced absence of Nf2, embryos are unable to activate Hippo signalling and hence ectopically localise Yap1 to the nuclei of the ICM cells (Cockburn *et al.*, 2013). Thus, it has been proposed that Nf2, which itself is capable of binding to the adherens junction component Ctnna1, is required to mediate the interaction between Amot and adherens junctions. Moreover, once Amot binds to Nf2 and associates with adherens junctions, the interaction is stabilised by Lats1/2 dependent phosphorylation of Amot, resulting in a reduced affinity of Amot for cortical filamentous actin (F-actin), that ultimately results in robust Hippo signalling activation (Hirate *et al.*, 2013). This robust activation of Lats1/2 is then subsequently responsible for the phosphorylation of Yap1 (at S112) that promotes its cytoplasmic localisation (via an interaction with the cytoplasmic scaffold protein 14-3-3). Therefore the physical sequestration of Yap1 to the cytoplasm prevents the formation of any active transcriptional complexes with nuclear Tead4 and thus inappropriate expression of TE lineage-specific transcription factors (Nishioka *et al.*, 2009). It is interesting that Yap1-deficient embryos exhibit normal TE development (Morin-Kesincki *et al.*, 2006), however this could be easily explained by a functional redundancy of Yap1 and the Yap1-related protein Wwtr1 (WW domain containing transcription regulator 1, also known as Taz). Accordingly, the double genetic knock-out of both the *Yap1* and *Taz* genes results in pre-implantation lethality before the morula stage and prior to the establishment of inner and outer cell populations (Nishioka *et al.*, 2009).

Taken together these observations demonstrate that Tead4 and Yap1/Taz, interpret positional information along the inside/outside axis of the embryo, in a manner dependent upon cellular polarisation, to restrict expression of TE specific genes to the outside cells of the embryo (Nishioka *et al.*, 2009). The fact that the subcellular localisation of Yap1/Taz affects cell-fate decisions in the pre-implantation embryo (coupling the apical polarity complex and Hippo signalling pathway in regulation of Yap1/Taz phosphorylation and subsequently localisation), emphasises the fact that the “inside-outside” and “polarity” models of pre-implantation embryo cell-fate choice are not mutually exclusive. Moreover, it supports the view that they are actually interconnected/ mutually dependent. Thus, a combined model that integrates all three existing original models: the early asymmetry,

polarisation and inside-outside models, has been proposed to explain how the first cell-fate decision is made (Fig. 1.16).

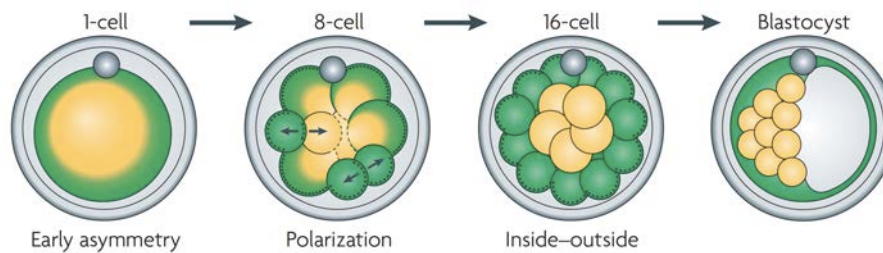


Figure 1.16 Integration of three hypotheses for the emergence of inside and outside cell differences. The combined model that suggests that the early asymmetry, polarisation and inside–outside models proposed to explain the first cell-fate decision are not exclusive. Asymmetry of the mouse oocyte leads to heterogeneity between the cells, the extent to which depends on when the cleavage divisions separate animal and vegetal parts of the embryo. Heterogeneity is revealed through asymmetry in epigenetic modifications at the 4-cell stage and through the expression levels of transcription factors such as *Cdx2* at the 8-cell stage. Such heterogeneity could generate differences in the timing or extent of blastomere polarisation along the apico-basal axis that, in turn, would affect whether a cell divides symmetrically or asymmetrically (or internalise following division). Asymmetric divisions generate inherently different inside and outside cells that will occupy different positions in the embryo. Cell position further reinforces cell fate, possibly owing to the different environment of inside (yellow) and outside (green) cells. This combined model proposes that the development of polarity to affect cell fate occurs progressively. Feedback loops reinforcing cell-fate decisions ensure that even a small initial bias is sufficient to break the symmetry (taken from Zernicka-Goetz, 2009).

This model proposes that an early asymmetry existing within the mouse egg drives heterogeneity between blastomeres of early cleavage stage embryo. The extent of the heterogeneity would be dependent upon the orientation of division planes during early cleavage. Such heterogeneity results in differences in the timing and extent of polarisation, that could be instructive of spindle orientation and/or the plane of cell division and/or cell internalisation, that in turn is responsible for generating two spatially distinct populations of cells. Such cells are then exposed to different microenvironments (not least the presence or absence of cellular polarity) that thereby enable them to acquire an appropriate cell fate (Zernicka-Goetz *et al.*, 2009).

1.4.3 Transcriptional factors involved in the first cell-fate decision

Transcription factors are required to transduce emerging molecular inter-cellular heterogeneities and differences into appropriate and distinct cell fates. For example when inner and outer cells are set apart, distinct transcriptional networks result in specific gene expression patterns required for differential cell fate. In inner cells, a network consisting of *Oct4*, *Sox2*, *Nanog* and *Sall4* (Spalt like transcription factor 4) promote pluripotency and resist differentiation whilst in outer cells

Tead4, Cdx2, Gata3 (GATA binding protein 3), Eomes (Eomesodermin), Elf5 (E74 like ETS transcription factor 5) transcription factors will lead to cell differentiation and eventual acquisition of TE cell fate (Fig. 1.17). The reciprocal repression between the members of these two networks assures that these two lineages remain segregated (reviewed in Chen *et al.*, 2010). The following sections will describe the roles of some critical transcription factors acting during the first cell-fate decision.

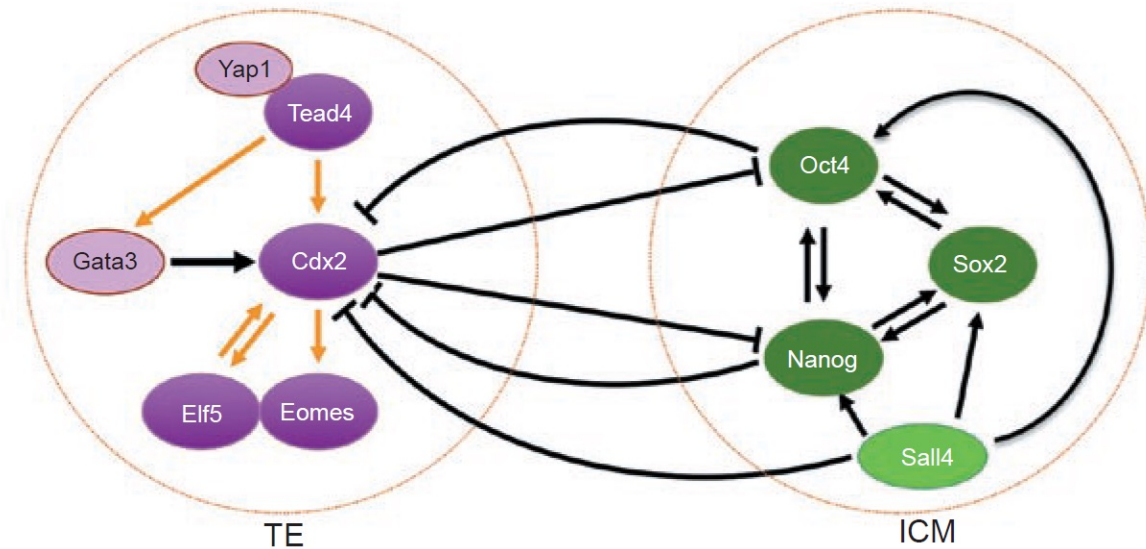


Figure 1.17 Molecular mechanisms for the ICM/TE segregation. The regulatory network of key transcription factors in ICM/TE specification. Cdx2, Tead4, Eomes, and Elf5 are the major TE-specific transcription factors. Tead4 cooperates with Yap1 to activate Cdx2, which in turn up-regulates Eomes and Elf5. Conversely, Elf5 is able to enhance Cdx2 expression. In addition, Gata3 directly binds to the intron 1 region of the Cdx2 locus and activates Cdx2 expression. In contrast, Oct4, Nanog, and Sox2 form a core regulatory circuitry to promote ICM cell fate. Sall4 not only activates Oct4, Nanog, and Sox2 but also suppresses Cdx2 expression, and this is critical to the segregation of the ICM and the TE. Furthermore, cross-regulation between the ICM-specific factors and the TE-specific factors secures the appropriate cell fate in individual blastomeres. So far, no biochemical evidence demonstrates that Cdx2, Tead4, Eomes, and Elf5 bind to each other's promoters. To distinguish from other interactions with direct promoter binding, the genetic interactions among these four factors are marked with orange arrows (taken from Chen *et al.*, 2010).

1.4.3.1 The role of Tead4 in the first cell-fate decision

The significance of the *Tead4* gene in mouse pre-implantation embryo development is demonstrated by the pre-implantation lethality of embryos deficient for this gene (Yagi *et al.*, 2007; Nishioka *et al.*, 2008). Moreover its importance has been further emphasised by its pattern of expression during the pre-implantation period. *Tead4* mRNA level is very low in oocytes and zygotes but rapidly increases from the 2-cell stage and persists through until the blastocyst stage, reaching a peak at 8-cell and morula stage (the developmental window in which TE and ICM progenitors begin

their specification) and becoming slightly lower by the late blastocyst stage (Yagi *et al.*, 2007). *Tead4* deficient embryos are able to compact and are morphologically indistinguishable from wild-type embryos up to the late morula stage, however they die at the pre-implantation stage without forming the blastocoel (Yagi *et al.*, 2007; Nishioka *et al.*, 2008). Although *Tead4*-deficient embryos fail to form a blastocoel, the mechanisms required for successful blastocoel development such as formation of adherens junctions, initiation of cell polarity, and activation of the Jnk (c-Jun amino-terminal kinase) and p38-Mapk (p38-mitogen activated protein kinase) signalling pathways, appear to be unaffected by deletion of the *Tead4* gene (Nishioka *et al.*, 2008).

The inability of *Tead4*^{-/-} embryos to implant stems from the fact that *Tead4* is necessary to activate genes required for the establishment of the trophectoderm lineage (that include those required for blastocoel expansion and hatching from the proteinaceous encapsulating *zona pellucida* shell). The role of *Tead4* in specifying the trophectoderm lineage appears to be unique among the *Tead*-related gene family of transcription factors, as the other members that are expressed during the pre-implantation mouse embryo developmental period (represented by TEA domain transcription factors 1 and 2, *Tead1* and *Tead2*, respectively), are unable to compensate for the absence of *Tead4* (Yagi *et al.*, 2007; Nishioka *et al.*, 2008). Gene expression analyses have shown that *Tead4* deficient embryos do not express most of the classified trophectoderm-specific genes, such as the transcription factors *Cdx2* and *Eomes*, the cell surface receptor *Fgfr2* (*Fibroblast growth factor receptor 2*), the integrin *Itga7* (*Integrin subunit alpha 7*), the placental *Cdh3* (*Cadherin 3*), nor the respective giant cell (trophoblastic cell derivatives of the TE) specific transcription factor or prolactin-related genes, *Hand1* (*Heart and neural crest derivatives expressed 1*) or *Prl3d1* (*Prolactin family 3 subfamily d member 1*) (Nishioka *et al.*, 2008). Although the majority of abnormalities observed in *Tead4*-deficient embryos have been attributed to the down-regulation of *Cdx2* expression, it is important to note that *Tead4* must also play other roles in TE cell lineage specification based on the fact that the phenotypes of *Tead4* and *Cdx2* deficient embryos are distinct (Strumpf *et al.*, 2005; Yagi *et al.*, 2007; Nishioka *et al.*, 2008). It should be further noted that very weak *Cdx2* expression between the 8- and 18-cell stages have been observed in *Tead4*-deficient embryos, suggesting that whilst *Tead4* is required for the maintenance of *Cdx2* expression, it is probably not required for its initial expression (Nishioka *et al.*, 2008). This basal level of *Cdx2* expression in the absence of *Tead4* has recently been suggested to be associated with the activity of a TE enhancer element, in the *Cdx2* locus, that is under the regulation of Notch signalling pathway (Rayon *et al.*, 2014).

1.4.3.2 The role of Cdx2 in the first cell-fate decision

The expression of Cdx2 protein is first detected at the 8-cell stage and is initially ubiquitously expressed at the 16-cell stage (irrespective of a cell relative position in relation to the inner/outer cell axis of the embryo) before becoming progressively restricted to the outer TE cells by the 32-cell stage (Ralston and Rossant, 2008). Genetically *Cdx2*-null embryos are able to initiate cavitation and expansion of the blastocoel, however the cavity cannot be maintained resulting in structural collapse and an inability of such embryos to hatch from the *zona pelucida*, suggestive of improper TE differentiation and epithelialisation (Strumpf *et al.*, 2005).

Although, the involvement of *Cdx2* in the appropriate establishment and maturation of TE cells had previously been implied on the physiological level, unequivocal confirmation of its molecular importance in TE differentiation came from the study of Niwa and colleagues (Niwa *et al.*, 2005) that demonstrated *Cdx2* is required to mediate transcriptional repression of the *Oct4* gene. The transcription factor *Oct4* has been shown to play a central role in the derivation of the pluripotent cell lineage because embryos lacking the *Oct4* gene fail to form an ICM (Nichols *et al.*, 1998). *Cdx2* inhibits the activity of *Oct4* by repressing the transcription of its gene while in turn *Oct4* protein can block the transcription of the *Cdx2* gene, thus establishing a reciprocal mechanism of transcriptional repression that both promotes and simultaneously antagonises the acquisition of either one of the TE or ICM cell lineage fates. *Cdx2* is also known to auto-regulate transcription of its own gene (Niwa *et al.*, 2005). Further insights into the molecular mechanism of *Cdx2* mediated transcriptional regulation have come from the study of Wang and colleagues that demonstrated that the chromatin remodelling protein Brg1 (Brahma related protein 1) is required for *Cdx2*-mediated repression of the *Oct4* gene in the mouse blastocyst. As such, Brg1 represents an essential co-repressor required for *Cdx2*-mediated gene silencing of *Oct4* expression/ transcription in the trophectoderm (Wang *et al.*, 2010).

Prior to embryo compaction, *in situ* hybridisation experiments show that *Cdx2* mRNA is evenly distributed within each individual blastomere (Skamagi *et al.*, 2013). However, concomitant with compaction, *Cdx2* mRNA has been shown to be preferentially localised in an asymmetrically manner towards the apical region of 8-cell stage blastomeres (Fig. 1.18) where it remains polarised in the outer blastomeres of the 16-cell stage embryo (Jedrusik *et al.*, 2008). This localisation has been shown to be dependent on a 97 nucleotide *cis*-localisation element at 3' end of the *Cdx2* open reading frame, that is not only important to mediate *Cdx2* mRNA apical localisation but is also required for anchorage and stability of the transcript at the apical cortex. Interestingly, experimentally induced compaction is unable to induce premature asymmetrical localisation of *Cdx2*

transcripts, indicating that it is the process of cellular polarisation at 8-cell stage, and not compaction itself, that is the main prerequisite for the observed localisation. Moreover, the process also requires the proper localisation of active Prkcz/i to the apical pole, plus an intact microtubule and actin cytoskeletal network and is dependent upon a motor protein of kinesin superfamily (Skamagi *et al.*, 2013).

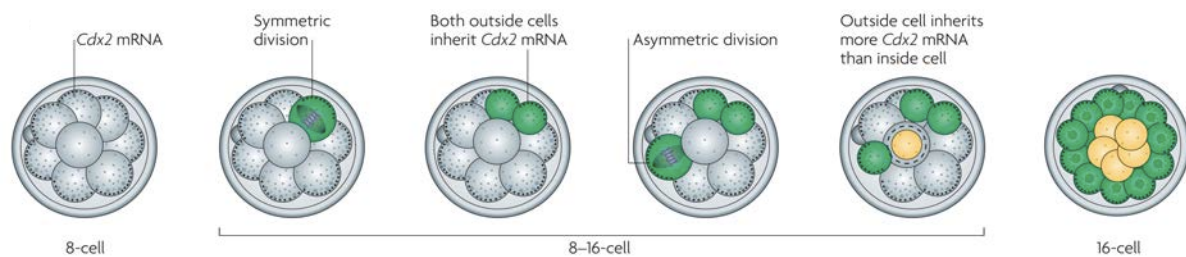


Figure 1.18 Apical localisation of Cdx2 mRNA after the cell polarisation contributes to symmetry-breaking events in pre-implantation stage mouse embryo development. mRNA for the Cdx2 transcription factor (small grey dots) becomes asymmetrically localised at the cortex of polarised blastomeres at the 8-cell stage. Thus, when these cells divide conservatively/ symmetrically the mRNA is equally partitioned between the daughter cells, but when the division is differentiative/ asymmetric, outer daughters inherit more Cdx2 mRNA than inner daughters, thus contributing to cell fate. When, after differentiative/ asymmetric divisions, cells reach their inside (yellow) or outside (green) position, molecular mechanisms that sense cell position can further influence transcription from the Cdx2 locus (taken from Zernicka-Goetz *et al.*, 2009).

As a consequence of the asymmetrical localisation of Cdx2 mRNA at the 8-cell stage, conservative/ symmetric divisions (defined here for simplicity – see above) provide both derived outer daughter cells with roughly equivalent amounts of Cdx2 mRNA. Conversely, differentiative/ asymmetric divisions furnish the outer daughter cell with relatively more Cdx2 mRNA than the inside residing sister cell (Jedrusik *et al.*, 2008; Skamagi *et al.*, 2013). The asymmetric localisation of Cdx2 mRNA therefore results in outside cells (TE progenitors) acquiring more Cdx2 in comparison to inside (ICM progenitor) cells, thus providing confirmation that the differentiative/ asymmetric divisions of pre-implantation mouse embryo development are truly asymmetric as they lead to the asymmetric segregation of at least one factor that is critical for cell differentiation (*i.e.* Cdx2 mRNA). Interestingly, in cases where such apical localisation of Cdx2 mRNA is experimentally prevented, ICM cells become positive for ectopically expressed Cdx2 protein, resulting in increased levels apoptotic cell death. Therefore, it is possible that the apical localisation of Cdx2 mRNA, in addition to contributing to the provision of appropriate outer cells fate identity, might also serve to ensure that inside cells do not inherit debilitatingly elevated levels of Cdx2 transcript that could impede their pluripotency (Skamagi *et al.*, 2013). It is also interesting to note that embryo cell clones that express experimentally elevated levels of Cdx2, significantly and more frequently undergo symmetric divisions that lead to

the generation of more outer TE progenitor cells, by the blastocyst stage. In contrast, clonal cells in which Cdx2 is experimentally depleted, more often divide asymmetrically thereby contributing more progenitor cells to the ICM (Jedrusik *et al.*, 2008). Accordingly, Jedrusik and colleagues claim that during the 8-cell stage, differential levels of endogenous Cdx2 are responsible for promoting the up-regulation of Prkcz/i in some blastomeres thereby increasing the degree of their polarisation and the frequency with which they will divide symmetrically (contributing more to TE progenitors). In return, they argue that cell polarity potentiates asymmetrical distribution of Cdx2 mRNA therefore ensuring that during differentiative divisions outer blastomeres will preferentially inherit Cdx2 mRNA (Jedrusik *et al.*, 2008). Conversely, observations that the apical localisation of Prkcz/i is unaffected in Cdx2-deficient embryos and precedes the nuclear localisation of Cdx2 in wild-type embryo dispute the above view. Moreover, the fact that cells lacking Cdx2 are still able to contribute the outside part of the embryo in chimeras and in parallel show apical localisation of Prkcz/i, indicate that Cdx2 acts temporally and functionally after the onset of cellular polarisation (Ralston and Rossant, 2008). Notwithstanding these observations it has not been conclusively demonstrated that Cdx2 does not have a polarisation related role or impact during unperturbed development. An explanation for the above described discrepancies has been offered by Saiz and Plusa in 2013, based on the potential existence of a positive feedback loop characterised by the presence of conserved Cdx2 transcription factor binding sequence motifs in the promoter region of the mouse *aPKC* gene (although exactly which has not been specified by Jedrusik *et al.*, 2008). Accordingly, it has been suggested that by overexpressing Cdx2 mRNA at the 2-cell and 4-cell stages (that represents premature expression of Cdx2 when compared to the endogenous gene expression) the experimental interventions of Jedrusik and colleagues resulted in the premature elevation of Cdx2 protein levels that in turn prematurely activated the transcriptional induction of Prkcz/i genes. The resultant premature induction of Prkcz/i proteins in the experimentally manipulated cell clones (potentially resulting in increased apical polarisation when compared to the non-manipulated clones of the same embryos) ultimately resulted in increasing their probability of becoming TE (Saiz and Plusa, 2013). Indeed, it seems most probable that this explanation is valid, given that Cdx2 overexpression, phenocopies Prkci overexpression (allocating cells preferentially to the TE), suggesting that Cdx2 does not play any functionally important role in initiating cellular polarisation under unperturbed developmental conditions but could well be important in maintaining polarity once established. Consistent with this interpretation is the observation that RNAi (RNA interference) mediated loss of Cdx2 function is also associated with a tendency to promote asymmetric divisions, in a manner that represents a convincing phenocopy of direct experimental down-regulating the polarity (Jedrusik *et al.*, 2008; Plusa, Frankenberg, *et al.*, 2005). Therefore it is most probable that Cdx2 lies functionally downstream of the initiation of cell polarity (Ralston and Rossant, 2008).

1.4.3.3 The role of Gata3 in the first cell-fate decision

Another transcription factor that has been shown to have a role in the establishment of the trophoblast cell lineage is Gata3. During the pre-implantation embryo developmental period, Gata3 specific mRNA is present from the 4-cell stage onwards (Home *et al.*, 2009) while Gata3 protein expression is detectable from the 8-cell stage, becoming exclusively restricted to the nuclei of trophoblast cells by the blastocyst stage. Although *Gata3* is co-expressed with *Cdx2*, its expression is unaffected by the experimentally induced loss of the *Cdx2* gene (Ralston *et al.*, 2010). Conversely, Gata3 is able to directly regulate *Cdx2* transcription (down-regulation of *Gata3* expression results in reduced *Cdx2* expression) and is associated with developmental defects during morula to blastocyst transition (Home *et al.*, 2009). Gata3 and *Cdx2* are known to induce the transcriptional expression of both common (224 genes) and independent target genes (225 and 102 genes, respectively) that are expressed in the trophoblast lineage; thus Gata3 and *Cdx2* have both shared and distinct roles during trophoblast development. In addition, nuclear levels of detectable Gata3 protein are significantly reduced in *Tead4*-deficient embryos supporting the proposal that *Cdx2* and Gata3 act in parallel and functionally downstream of *Tead4* (Ralston *et al.*, 2010). Although, it is interesting to note that the genetic ablation of the *Gata3* gene in mice, only leads to embryonic lethality at the midgestation stage (E11.5) without any apparent defects in early, peri- or post-implantation development possibly reflecting functional redundancy provided by other expressed Gata factors.

1.4.3.4 The role of Oct4 in the first cell-fate decision

At present, it remains strongly debated how and when early cells in the mammalian embryo acquire the first developmental differences that are functionally/ developmentally relevant and can predict specific lineage patterning and cell fate. However, it has been shown that as early as the 4-cell stage, inter-blastomere differences in the nuclear localisation kinetics of the pluripotency-associated transcription factor Oct4 exist prior to any morphologically distinguishable differences between the blastomeres. These are manifested by two sub-populations, whereby some cells contain a large and predominantly immobile nuclear fraction of Oct4 (defined by increased accessibility to Oct4 transcription factor binding sites in chromatin) as opposed to others that contain a highly mobile fraction that is in flux with the cytoplasm (observable by utilising photo-activatable-GFP/ Green fluorescent protein-Oct4 fusion constructs). Interestingly, cell lineage tracing experiments of cells belonging to each sub-population have shown that these differences in Oct4 kinetic rates are important, as they are indicative of future cell lineage commitments (with blastomere nuclei

exhibiting lower levels of highly mobile Oct4 protein giving rise to more TE cells and *vice-versa*) (Plachta *et al.*, 2011). Hence, this data suggest earlier than previously appreciated mechanism of differential Oct4 dependent gene transcription that could underpin the pluripotent potential of cells and their progeny in later development.

1.4.3.5 The role of Sox2 in the first cell-fate decision

Similarly to Oct4, it has recently been demonstrated that the differential dynamics in the DNA binding of the pluripotency-associated transcriptional factor Sox2 during early mouse embryo development can have an impact on the first cell-fate decision (White *et al.*, 2016). Namely, a live-cell tracking study using a photo-activatable Sox2-GFP tagged construct has revealed the existence of heterogeneity between the 4-cell stage blastomeres in the nature of Sox2-GFP binding to DNA (*i.e.* classified as the existence of short- and long-lived Sox2-DNA interactions). These differences in the nature of Sox2-DNA binding are likely to reflect differential epigenetics status between individual 4-cell stage blastomeres, as a reduction in H3R26 methylation levels after *Carm1* down-regulation leads to reduced observance of the long-lived Sox2-GFP bound fraction and a significant decrease in the mRNA and protein expression of Sox2 target genes. Consistently, the progeny of the 4-cell stage blastomeres that contained larger fractions of long-lived bound Sox2-GFP, contributed significantly more towards the inner cell population at 16-cell stage. In support of the general notion that Sox2 is required for the pluripotent lineage formation, single-cell mRNA and protein expression analyses have revealed that *Sox2* expression already becomes restricted to the inner cell population at 16-cell stage; thus making it the earliest reported marker of the ICM (Guo *et al.*, 2010; Wicklow *et al.*, 2014). Furthermore, it has recently been demonstrated that the inactivation of the Hippo signalling pathway in outer cells is required to keep the expression of *Sox2* restricted to the inner cell mass (Wicklow *et al.*, 2014), suggesting that potential ectopic *Sox2* expression might otherwise be able to prevent TE differentiation. Taken altogether, these reports suggest that the *Sox2* gene has important role during the first cell-fate decision in establishing the pluripotent inner cell lineage. Nevertheless, it is of note that the endogenous pattern of Sox2 protein expression prior to 16-cell stage has not been examined in any of the above referenced studies.

1.5 THE SECOND CELL-FATE DECISION

During the second cell-fate decision, cells within the ICM segregate into the EPI and PrE lineages. The PrE becomes morphologically apparent at the late blastocyst stage, as a monolayer of epithelial cells positioned on the surface of the ICM adjacent to the blastocyst cavity while the

deeper ICM cells that escape differentiation and thus maintain their pluripotency, become the EPI. Commitment to either the EPI or PrE lineage cell fate is completed by the time of implantation at the late blastocyst stage (E4.5), as demonstrated by the observation individual cells dissociated at this stage are no longer capable of contributing to any lineage other than their own, when injected into blastocysts (Gardner and Rossant, 1979).

1.5.1 EPI and PrE transcriptional networks

By the late blastocyst stage (E4.5) stage, two different transcriptional networks responsible for maintaining the identity of the PrE and EPI cell lineages are established (Fig. 1.19). PrE cells express the transcriptional factors Gata6 (GATA binding protein 6), Gata4 (GATA binding protein 4), Sox17 (SRY-Box 17) and Sox7 (SRY-Box 7) that work in concert to establish a transcriptional regulatory network responsible for proper PrE differentiation (Chazaud *et al.*, 2006; Morris *et al.*, 2010; Niakan *et al.*, 2010; Artus *et al.*, 2010). Conversely, the core of the pluripotency transcription network in EPI cells consists of Nanog, Oct4 and Sox2 transcription factors that are responsible for maintenance of EPI cell identity.

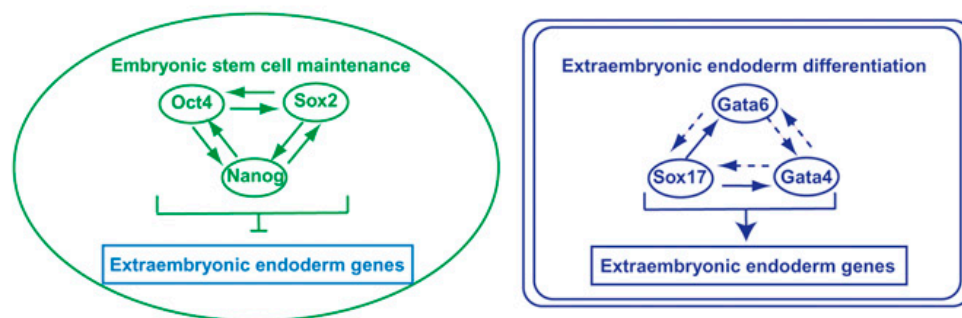


Figure 1.19 Establishment of two transcriptional networks responsible for segregation of EPI and PrE cells. The Oct4, Sox2, and Nanog transcription factor network is a feed-forward loop maintaining cell pluripotency while inhibiting genes involved in differentiation in EPI cells. In PrE cells, Gata6 functions upstream of Gata4 and Sox17 in the differentiation cascade (depicted as dashed lines, indicating no evidence to date that these interactions are direct), lies at the head of the PrE determining transcription factor hierarchy. Sox17 that lies downstream from Gata6 directly regulates the expression of Gata6 and Gata4 (solid lines). Sox17 and Gata4 are responsible for directing PrE differentiation (taken from Niakan *et al.*, 2010).

Nanog is an epiblast marker required for the formation of both the epiblast (cell autonomously) and PrE (non-cell autonomously) lineages. Accordingly, Nanog directly represses *Gata6* gene expression in pluripotent EPI cells, thereby cell autonomously suppressing the PrE

identity and promoting EPI cell fate. However, *Nanog* is also required for proper PrE differentiation, within the ICM, in a non-cell autonomous manner, because in its absence initiated PrE differentiation (as marked by *Gata6* expression) cannot be maintained and the subsequent expression of later PrE markers, indicative of continued PrE differentiation, such as *Sox17* and *Gata4* does not occur (Frankenberg *et al.*, 2011).

In terms of developmental time, *Gata6* is the earliest known transcription factor that has been shown to be indispensable for PrE formation (Cai *et al.*, 2008), with its expression beginning at the 8-cell stage (Plusa *et al.*, 2008). The expression of *Sox17* and *Gata4* are both initiated during later development, becoming detectable at the protein level during the early- to mid- blastocyst stages (Artus *et al.*, 2011; Plusa *et al.*, 2008). Initially *Gata4* and *Sox17* expression within the ICM is not interdependent, however once activated they are able to up-regulate each other expression. In addition, the *Sox17* protein is known to compete for the same DNA-binding sites as those also targeted by the pluripotency-related transcription factors, *Sox2*, *Nanog*, and *Oct4*; thereby promoting differentiation at the expense of pluripotency and self-renewal. Additionally, *Gata6*, *Sox17* and *Gata4* are all required for the appropriate down-regulation of *Nanog* expression during PrE differentiation (Niakan *et al.*, 2010). Importantly, the expression of *Sox7* can be used as a reliable marker of cells that are fully committed to the PrE lineage, as it only becomes expressed once PrE cells have attained their final position within the future PrE layer (Artus *et al.*, 2011). A further marker of PrE cells is the *Pdgfra* (Platelet derived growth factor receptor alpha) that is required for PrE lineage expansion and maintenance (Plusa *et al.*, 2008). Initiation of *Pdgfra* expression requires *Gata6*, while its maintenance requires both *Gata4* and *Gata6* (Artus *et al.*, 2010). According to the temporal expression pattern of PrE markers during mouse blastocyst maturation, a model of sequential *Gata6* → *Pdgfra* → *Sox17* → *Gata4* → *Sox7* activation within the emerging PrE lineage has been proposed (Artus *et al.*, 2011).

1.5.2 Models proposed to explain segregation of EPI and PrE

The mechanisms that govern PrE and EPI lineage segregation within the ICM are still not completely elucidated but involve the progressive emergence of differential gene expression in their respective precursors followed by a combination of cell sorting and cell death. Several models have been proposed to explain how this might occur.

One of the early models proposed to explain the second cell-fate decision is the “positional induction” model that is conceptually very similar to the inside-outside model proposed for the segregation of the ICM and TE lineages. According to this model, initially identical ICM cells

differentiate based upon their differential relative position so that cells that are in contact with the blastocyst cavity acquire PrE fate while deeper-lying ICM cells adopt an EPI fate (Enders *et al.*, 1978). A principle flaw of this model stems from the fact that it postulates the existence of an initially homogenous population of ICM cells. However, this seems not to be the case as progenitor cells of the EPI and PrE are a heterogeneous population of cells randomly distributed within ICM in “salt and pepper” pattern as judged by the expression of lineage specific marker genes (Chazaud *et al.*, 2006). Nevertheless, this is not to say that positional cues do not, or could not, play some role during the second cell-fate decision.

Another explanation of how second cell-fate decision is acquired has been offered in the form of the three-step model of PrE lineage specification. The three-step model proposes that: 1) initial co-expression of EPI and PrE lineage markers, Nanog and Gata6, at 32-cell stage is driven by stochastic processes; 2) at around 64-cell stage, after the establishment and maturation of inhibitory regulatory pathways, mutual exclusion of Nanog and Gata6 expression results in the formation of a heterogeneous population of ICM cells expressing either Nanog or Gata6 and the generation of the “salt and pepper” pattern distribution of EPI and PrE progenitor cells; 3) cell sorting within ICM driven by active and/or passive cell movements leads to the final spatial segregation of the EPI and PrE cell lineages at around 128-cell stage (Plusa *et al.*, 2008). However, a recent mathematical model indicates that stochastic processes are unlikely to be the driving force for the induction of the “salt and pepper” distribution of Gata6 and Nanog proteins throughout the ICM (Bessonard *et al.*, 2014).

Whether the emergence of the “salt and pepper” pattern of distribution of EPI and PrE progenitor cells happens at random, driven by stochastic process, or could be related to cell history is a matter of serious debate. Two opposing models have been proposed to explain how this salt-and-pepper distribution of PrE and EPI progenitor cells is initially generated (Fig. 1.20). The “time inside-time outside” model proposes that the origin of EPI and PrE progenitor cells in the ICM is not random but dependent upon the developmental timing of ancestral cell internalisation. Cells that become internalised in the first wave of possible asymmetric/symmetric (differentiative/conservative) cell divisions during 4th cleavage (at 8- to 16-cell division) are biased towards forming the pluripotent EPI, whereas ones internalised in the second wave during 5th cleavage (*i.e.* derived from the outer 16-cell stage blastomere at the 16- to 32-cell stage transition) are biased towards becoming PrE. Progeny of the cells internalised in an atypical and rare third wave, during 6th cleavage (at 32- to 64-cell transition) exclusively contribute to the PrE. According to this model, the more time blastomeres spend on the outside of the embryo, the more exposed to the differentiative factors they become and as such are biased to providing progenitor cells for differentiating PrE cells rather than pluripotent EPI cells. Accordingly, the opposite applies, whereby cells internalised temporally earlier

are protected from differentiating cell environments and thus more able to retain their pluripotency and ultimately populate the EPI (Morris *et al.*, 2010).

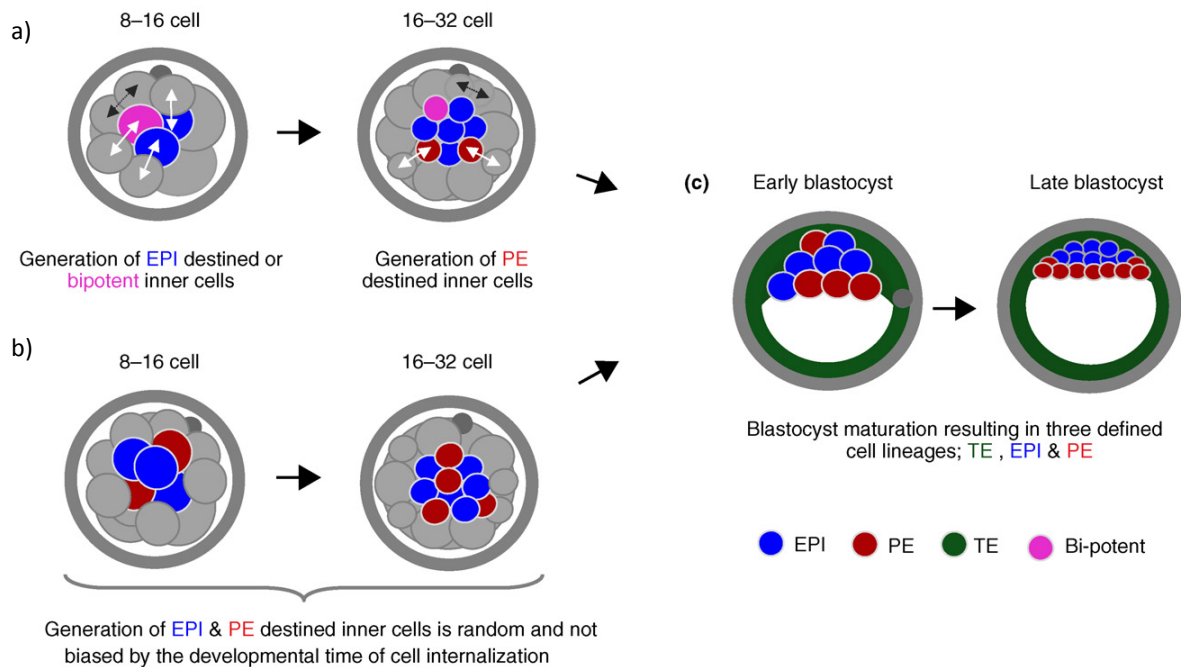


Figure 1.20 Two competing models of how EPI and PE (primitive endoderm) progenitor cells become internalised to the ICM of mouse embryos. a) The “Time Outside-Time Inside” model suggests that cells internalised first, in the ‘first wave of differentiative/asymmetric cell division’ during the 8–16 cell transition (represented in blue) give rise to more pluripotent cells, biased to generate EPI, and that cells internalised later, in the ‘second wave of differentiative/asymmetric cell division’ during the transition between the 16-cell and 32-cell stages, are strongly biased to provide inner cells that are PE progenitors (shown in red); **b)** The “Unbiased/Random” model suggests that the time of cell internalisation does not affect cell fate and that generation of EPI and PE progenitors occurs at random; **c)** Both models converge with the appearance of the ‘salt and pepper’ pattern of EPI and PE marker gene expression by the early/ mid blastocyst stage and its subsequent resolution by the late blastocyst stage (taken from Bruce and Zernicka-Goetz, 2010).

Evidence in support of this model comes from the findings that cells internalised in the first wave have been reported to inherit less *Fgfr2* mRNA (Krupa *et al.*, 2014) than those internalised in the second wave, thus making them also less responsive to the *Fgf4* (Fibroblast growth factor 4) signalling, known to be required to promote PrE differentiation (Yamanaka *et al.*, 2010) and subsequently biasing their progeny into adopting EPI cell fate. Accordingly, in support of this mechanism, clonal overexpression of *Fgfr2* results in a bias contribution of ICM residing cell clone descendants towards the PrE lineage (Morris *et al.*, 2013). Moreover, the expression levels of both *Sox17* and *Gata6* have been shown to be upregulated in cells internalised from the second but not from the first wave of asymmetric cell division (Morris *et al.*, 2010). An alternative, and as yet not necessarily competing explanation, that is nevertheless still in accordance with “time inside-time

outside” model, is that by internalizing earlier, newly derived inner cells are afforded the opportunity to initiate the pluripotency transcriptional program sooner, perhaps by initiating the expression of the *Sox2* gene. Consistent with this hypothesis is the fact that inner cells of the 16-cell stage embryo (internalised in the 1st wave) do indeed up-regulate *Sox2* expression (Guo *et al.*, 2010; Krupa *et al.*, 2014). Moreover, the recent discovery that the differential activity of the Hippo signalling pathway in derived inner and outer cell populations restricts the expression of *Sox2* to ICM cells further supports this hypothesis (Wicklow *et al.*, 2014). As a consequence, it is possible that the induced levels of *Sox2* expression in cells internalised comparatively earlier, may result in the induction of *Fgf4* mRNA production, particularly given that the *Fgf4* gene is known to be a direct target of the pluripotency-related transcription factors Oct4 and Sox2 (Yuan *et al.*, 1995). This would in turn explain the observation that cells internalised in the first wave are characterised by the higher levels of the *Fgf4* mRNA expression (Krupa *et al.*, 2014). In contrast, cells internalised later would potentially have been exposed to *Fgf4* for a comparatively longer period of time without having the opportunity to activate *Sox2* expression and initiate the pluripotency transcriptional programme that would have directed them towards an EPI cell fate, hence directing them towards the PrE (reviewed in Bergsmedh *et al.*, 2011).

Although appearing theoretically appealing, the “time inside-time outside” model has been challenged. For example, Yamanaka and colleagues put forward an opposing model, after being unable to observe an association between a cell’s developmental history and its final fate, using a permanent cell lineage marking protocol that investigated clonal cell contributions through to the post-implantation stages, and suggested that the salt-and-pepper distribution of EPI and PrE progenitors in the blastocyst ICM arises as a consequence of stochastic processes unrelated to a cell’s developmental origin of a particular cell (Yamanaka *et al.*, 2010). Recent single cell whole transcriptome analysis has revealed that the gene expression profiles of individual ICM cells, of the early blastocyst appear to be initially indistinguishable, thus supporting such a stochastic model (Ohnishi *et al.*, 2014); although the extent to which functionally important heterogeneity in the transcriptome responsible for biasing ICM cell fate, is open to interpretation (as is the number of assayed individual cells from different embryos used in the cited study).

In an attempt to reconcile these contrasting observations it has been suggested that the experimental design of the study of Yamanaka and colleagues may have resulted in the generation of an atypically increased ICM cell number, derived from the first wave of cell internalisation (associated with the potential disruption of cellular polarisation at the apical pole, caused by the microinjection strategy employed, leading to internalisation of the manipulated cell by neighbouring cell ‘engulfment’) and thus may account for the discrepancies (Morris, 2011). Indeed, it seems that

the extent of the originally observed EPI specific bias of cells internalised during the first wave, upon which the “time inside-time outside” model is founded, might also be dependent on the number of initial inner cells produced. Accordingly, it has been shown that in instances when up to three inner cells are produced in the first wave of asymmetric division, a significant EPI-specific bias is observable, however, after the generation of four or five inner cells the contribution of first wave ICM progeny cells to the PrE becomes more substantial, hence weakening the observed EPI bias (Morris *et al.*, 2013). Therefore, it appears that the number of initially generated inner cells is an important regulating factor for the simplest interpretation of the “time inside-time outside” model. In support of this notion, the results of experiments in which 16-cell stage embryos were reconstituted from disaggregated single 16-cell stage blastomeres with varying numbers of inner-cells, showed that when up to three inner cells were present, the inner cell EPI associated bias was observable in derived blastocysts, however this bias was lost in aggregates made out of four or five inner cells (Krupa *et al.*, 2014).

1.5.3 Nanog and Gata6 mutual exclusion

Regardless of how the salt-and-pepper distribution of EPI and PrE progenitor cells within the ICM is generated, the key role of the Fgf (Fibroblast growth factor) signalling pathway in establishing the mutual exclusion of *Nanog* and *Gata6* gene expression within the emerging PrE and EPI populations is beyond any doubt (Fig. 1.21). The first indication of the importance of Fgf signalling in the segregation of the two ICM lineages came from the studies of embryos containing genetic mutations in the *Grb2* (Growth factor receptor bound protein 2, an adaptor protein involved in the receptor tyrosine kinases signalling), *Fgf4* and *Fgfr2* genes (Feldman *et al.*, 1995; Arman *et al.*, 1998; Cheng *et al.*, 1998; Chazaud *et al.*, 2006). These embryos were all characterised by peri-implantation lethality due to an inability to form PrE. In addition, the observation that culturing mouse embryos from the 8-cell to the late blastocyst stage in the presence of Fgfr (Fibroblast growth factor receptor) and Mek1/2 (Mitogen-activated protein kinase kinases 1 and 2) inhibitors results in a complete absence of *Gata6* expressing PrE cells (Nichols *et al.*, 2009; Yamanaka *et al.*, 2010) also strengthened the view that the Fgf signalling pathway plays an important role during the second cell-fate decision (reviewed in Lanner and Rossant, 2010). Indeed, it has been shown that by modulating Fgf signalling levels, the cell fate of ICM cells could be shifted to either EPI or PrE. Specifically, that the inhibition of Fgf signalling, utilising a pharmacological inhibitor of the Mapk (Mitogen-activated protein kinase) pathway genes, Mek1/2, themselves activators of the Erk1/2 (Extracellular signal-regulated kinases 1 and 2), that act functionally downstream of liganded and activated Fgfrs directed all ICM cells to acquire an EPI cell fate, whilst in contrast, high levels of Fgf/MAPK signalling, induced by an

exogenous dose of recombinant Fgf4, instructed all ICM cells to acquire PrE fate (Yamanaka *et al.*, 2010). Indeed, it has been demonstrated that exogenously administered Fgf4 can control the relative proportion of PrE and EPI cells within ICM in a dosage dependent manner (Krawchuk *et al.*, 2013).

Even though, PrE lineage restriction absolutely requires Fgf4 signalling, the initiation of the PrE program does not. By utilising genetic knock-out embryos in which both zygotic and maternal Fgf4 protein has been removed, Kang and colleagues have shown that in the absence of Fgf4, EPI and PrE markers initially show widespread co-expression indicating Fgf4 signalling is not required in the initial onset of *Gata6*, *Sox17*, *Pdgfra* and *Nanog* expression; furthermore, suggesting other mechanisms are at work. However, notwithstanding this fact the derived PrE precursors fail to become committed and instead ultimately adopt an EPI fate within the ICM. It was reported that the reason underlying this failure of ICM cells to restrict to the PrE lineage was their inability to maintain the expression of *Gata6* after the 64-cell stage thus resulting in the subsequent absence of later PrE marker gene expression (*e.g.* *Gata4* and *Sox7*) (Kang *et al.*, 2013).

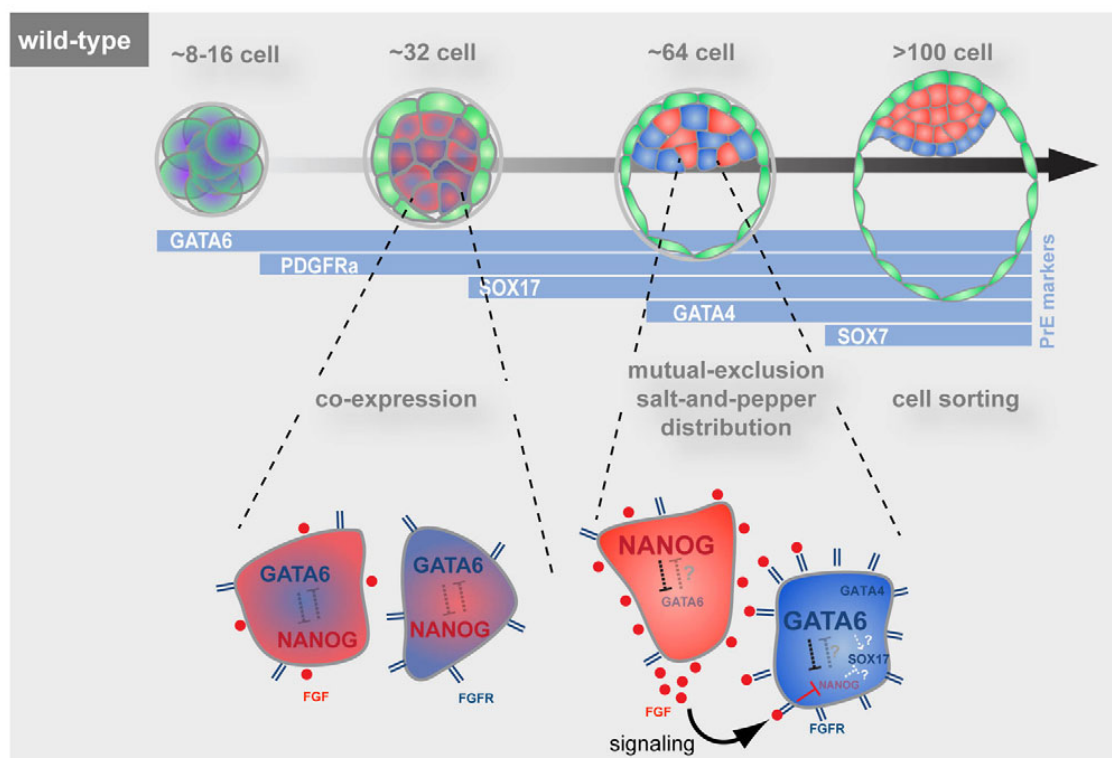


Figure 1.21 Molecular events underlying the second cell-fate decision. Differential expression levels of Fgf4 and Fgfr2 establish lineage biases within the ICM at the 32-cell stage. At the 64-cell stage, embryos exhibit a salt-and-pepper distribution of Nanog and Gata6 that represents the two lineages of Nanog expressing epiblast (EPI) and Gata6- expressing primitive endoderm (PrE) lineage-biased cells. Continuous Fgf4 signalling ensures lineage bias by (1) maintaining expression of the early PrE-specific factors Gata6, Pdgfra and Sox17, (2) activating the later PrE-specific factors Gata4 and Sox7, and (3) inhibiting EPI-specific factors such as Nanog (taken from Kang *et al.*, 2013).

An additional mechanism responsible for the reinforcement of mutually exclusive *Nanog* and *Gata6* gene expression has also been described, whereby Bmi1 (B lymphoma Mo-MLV insertion region homolog 1), a polycomb gene group member, controls Gata6 protein stability by preventing Gata6 ubiquitination and protecting it from subsequent proteasome-dependent degradation. An increase in Gata6 stability is able to shift the balance between Gata6 and Nanog protein levels in individual blastomeres and bias cells toward becoming PrE. It has been suggested that this could be an early event in PrE differentiation (Lavial *et al.*, 2012). Additionally, it is possible that the activity of p38-Mapk14/11 (p38 mitogen-activated protein kinases alpha and beta) is required during a narrow developmental window during early blastocyst formation (between E3.5 and E3.75) to allow complete segregation of mutually exclusive Nanog and Gata6 expression pattern within the ICM cells as recently proposed (Thamodaran and Bruce, 2016). Consistent with this notion is the fact that embryos cultured in the presence of p38-Mapk14/11 inhibitor from E3.5 fail to resolve the co-expression of *Nanog* and *Gata6* by E4.5 but nonetheless do induce *Sox17* expression at the mid blastocyst stage, that is then lost during the remaining half of blastocyst ICM maturation (Thamodaran and Bruce, 2016).

1.5.4 Cell sorting within the ICM

At the time of blastocyst cavity formation the majority of cells within the ICM occupy a position that corresponds to their subsequent fate; the prospective PrE cells being positioned at the surface of the ICM and the prospective EPI cells residing in the deeper layers. Cells that are inappropriately positioned in respect to their presumptive fate will either undergo apoptosis or sort, via active or passive movement, to the correct cell compartment. In this context, the action of Gata6 is required for PrE destined cells to retain their surface position, as demonstrated by an inability of such cells expressing a dominant negative Gata6 construct to do so. However, Gata6 alone is insufficient to drive the movement of an incorrectly positioned cell from the deeper layers of ICM to the surface and it has accordingly been shown that such repositioning also requires the action of Wnt9A (Wnt family member 9A) (Meilhac *et al.*, 2009).

In addition, the involvement of Prkcz/i in the overall ICM cell sorting process and PrE maturation has been revealed. Namely, Prkcz/i becomes enriched in prospective PrE cells at the time when the salt and pepper pattern is established (*i.e.* just before the point at which cell sorting commences) and appears to be highly dependent on Fgf/Erk1/2 signalling, since blocking Erk1/2 pathway activation (using chemical inhibitors of Mek1/2) results in homogeneously low levels of Prkcz/i throughout the ICM. The contact of such PrE progenitor cells with the blastocyst cavity has been shown to trigger a polarised localisation of Prkcz/i, thus supporting the formation of a mature

epithelium and its importance during cell sorting was first indicated by the observation that mosaic down-regulation of *Prkcz/i* results in a significantly decreased number of cells residing at the ICM surface. However, the exact role of *Prkcz/i* in the cell sorting mechanism was only demonstrated after showing that although PrE precursor cells are able to migrate through the ICM and come into the contact with the blastocyst cavity, the inhibition of *Prkcz/i* activity prevents them from maintaining their position at the ICM surface. Instead, they migrate deeper and become scattered throughout the ICM consequently leading to improper segregation of EPI and PrE lineages (Saiz *et al.*, 2013). Hence, *Prkcz/i* appears to play a role by which sorting PrE progenitors rely on its activity to sense when they have appropriately found the surface of the ICM and ensures that they remain there.

1.5.5 The role of Oct4 in the second cell-fate decision

As previously stated, Oct4 is a component of the transcription factor network (together with Sox2 and Nanog) responsible for repressing genes that promote differentiation and activates genes required to maintain a state of self-renewing pluripotency (Yamanaka *et al.*, 2006; Hanna *et al.*, 2010).

Apart from being indispensable for the maintenance of the EPI pluripotent state, Oct4 has recently been described as an important factor during PrE specification. In EPI progenitor cells, Oct4, in concert with Sox2, is responsible for activating the expression of the *Fgf4* gene (Yuan *et al.*, 1995). The derived Fgf4 protein ligand is then thought to act upon PrE progenitors, through a non-cell autonomous mechanism, to sustain PrE differentiation. Indeed, in genetically deficient *Oct4* embryos the expression of the later PrE marker, Sox17 is not detectable above the background levels. However, although this defect could simply be attributed to the absence of Fgf4, the exogenous provision of Fgf4 to Oct4-deficient embryos, during blastocyst maturation, is not able to rescue Sox17 expression. It has therefore been proposed that Oct4 might be required to induce PrE cell fate via an additional and uncharacterised cell-autonomous mechanism (Frum *et al.*, 2013) that has more recently been discredited by the observation that after temporally refined removal of *Oct4* from the morula or early blastocyst stage, administration of exogenous Fgf4 was able to rescue Sox17 expression levels (Le Bin *et al.*, 2014); an observation that also strongly illustrates the potential inter-dependence of the first and second cell-fate decisions.

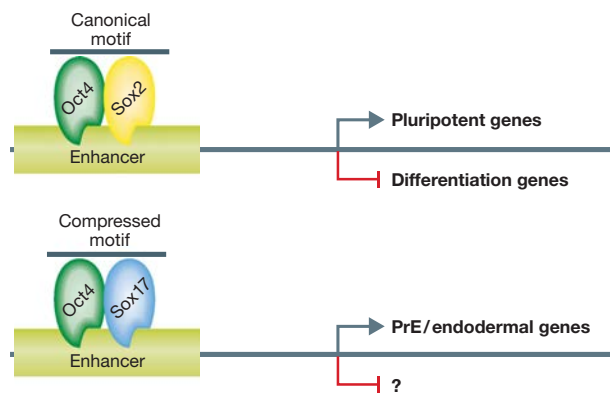


Figure 1.22 Model for the cooperative action of Oct4 and Sox-family transcription factors during lineage fate choice. In the epiblast, the cooperative binding of the Oct4/Sox2 complex to canonical motif-containing enhancers facilitates pluripotency maintenance by the up- and down-regulation of pro-pluripotent and differentiation factors, respectively. Upon induction of PrE differentiation, Sox17 levels increase and directly recruit Oct4 to compressed sequence motif-containing enhancers, that positively regulates a set of PrE specification genes and likely negatively regulates other yet to be defined genes (taken from Mansour and Hanna, 2013).

such as Sox17, to promote and reinforce the PrE specification. Under such a proposed mechanism, it is possible that the differential expression of *Sox2* and *Sox17* between EPI and PrE progenitor ICM cells, acts as a cell-fate switch that fine tunes the preference of Oct4 to bind to enhancers that either promote the expression of pluripotency or differentiation related genes, thus contributing to germane lineage specification (Aksoy *et al.*, 2013).

1.6 THE MODEL OF INTER-RELATED CELL-FATE DECISIONS

Based on the existing evidence, the model that perhaps most faithfully describes the mechanism(s) underpinning pre-implantation mouse embryo development is the model of “inter-related cell-fate decisions” (Fig. 1.23). According to this model, the first and second cell-fate decisions are not made separately but are instead closely inter-linked, since changes that lead a blastomere to take the first fate choice inevitably influence the second one.

However, an explanation of how Oct4 might still be able to act in a cell autonomous manner to reinforce PrE cell fate, may come from the finding that Oct4 is able to directly interact with Sox17. The interaction of Oct4 and Sox17 results in their binding to enhancer motifs that are known to be enriched in the transcriptional regulatory regions of genes involved in PrE differentiation (Fig. 1.22). Therefore it is possible that in EPI destined cells, Oct4 directly interacts with its pluripotency related partner Sox2, to cooperatively bind canonical gene-regulatory enhancers that activate pluripotency-related genes. Conversely, in PrE progenitor cells it is perhaps not surprising that Oct4 could interact with a related Sox family member,

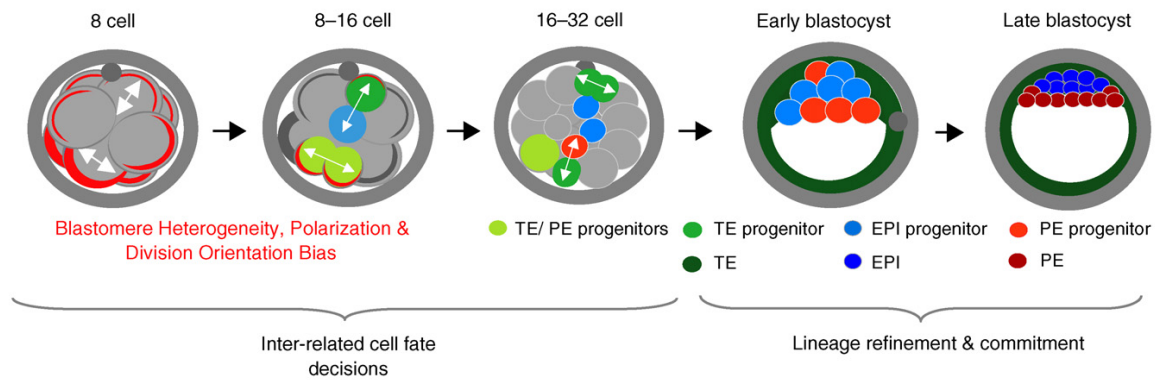


Figure 1.23 A schematic representation of the inter-related cell-fate decisions model. Inter-blastomere heterogeneities, revealed at the 8-cell stage, but related to the division orientation at the 4-cell stage, potentially biases the degree of apical-basolateral polarity (indicated by the thickness of red lines in 8-cell representation). This in turn influences whether 8-cell blastomeres divide differentially/asymmetrically to generate inner EPI progenitors and outer TE progenitors or conservatively/symmetrically, providing two outer TE/PE progenitors (also potentially influencing cell internalisation via post-cell division mechanisms related to extend of inherited cellular polarity and contractility). During the 16–32-cell transition TE/PE progenitors most often divide asymmetrically, possibly due to down-regulation in polarisation caused by the partitioning of the apical pole in the previous cell division, to provide inner PE progenitors and outer TE destined cells. Conversely outer cells derived from the asymmetric divisions of the previous 8–16-cell transition divide in a symmetric manner, potentially caused by accumulative apicalisation achieved by this time in these cells, and generate two further TE progenitors. Further refinement of the EPI and PE allocation within the ICM proceeds during blastocyst maturation (taken from Bruce and Zernicka-Goetz, 2010).

Specifically, the first heterogeneity among blastomeres that is detected at the 4-cell stage, and is reflected in the molecular differences in epigenetic modifications of histone proteins, the nuclear localisation kinetics of Oct4/ Sox2 protein and *Cdx2* mRNA levels (Jedrusik *et al.*, 2008; Plachta *et al.*, 2011; Torres-Padilla *et al.*, 2007; White *et al.*, 2016), potentially leads (by as yet unappreciated mechanisms) to blastomeres of the 8-cell stage embryo inheriting differing amounts of cellular polarity determinants. Such heterogeneity thus differentially effects the degree of intra-blastomere apical-basolateral polarity, thus contributing to an unequal population of cells that differ in their capacity to affect the orientation of the division plane of ensuing divisions (leading to spatial segregation of daughter cells via the adoption of either conservative/symmetric or differentiative/asymmetric cell divisions or subsequent internalisation of less polarised cells, thus, underpinning the first cell-fate decision). As such, cells that inherited comparatively/relatively less cellular polarity will divide in a differentiative/asymmetric way, to give rise to one outer TE progenitor and one inner EPI progenitor cell; and the resulting outer cell will more probably divide conservatively/ symmetrically at the subsequent 16- to 32-cell transition, due to the accumulation of polarity determinants consequent to it inheriting the entire apical domain in the previous division, thereby giving rise to still more TE progenitor cells. Conversely, 8-cell stage blastomeres with an

ancestry that favoured relatively enhanced cellular polarity are more likely to divide conservatively/symmetrically, yielding two outer cells progenitors with the capacity to contribute to both TE and PrE. This is because they are more likely to divide in a differentiative/asymmetric manner, in the 16- to 32-cell cleavage, as a consequence of the reduced degree of cellular polarisation they exhibit after the partitioning of the apical pole caused by the preceding cell division. Hence the net result would be the generation of outer, progenitor cells of TE and inner, progenitor cells of PrE (Bruce and Zernicka-Goetz, 2010).

Thus based on this model, initial heterogeneities (potentially resulting in the uneven segregation of initial polarity determinants/ initiation factors, but potentially also involving other unrecognised mechanisms) among early cleavage stage blastomeres and the relative timing of cell internalisation are the driving force in directing cell-fate decision, resulting in the formation of progenitors of the three blastocyst lineages in an integrated mechanism. However active cell movements as a response to positional cues and further cell sorting, as observed and discussed above, are still required to ensure the correct segregation and final commitment of the pre-implantation mouse embryo cell lineages.

2. OBJECTIVES

2.1 OBJECTIVE 1

The origin of the first observable cell-fate heterogeneities within the maturing mouse blastocyst ICM cell population has been the subject of intense research and serious debate over the last few years. The stochastic model proposes that the tiny differences in transcriptional noise among founding ICM progenitor cells become progressively amplified, during the atypically long cell cycles of early mouse embryo development, eventually leading to the mutually exclusive expression pattern of EPI and PrE lineage markers. The opposing “time-inside time-outside” model emphasises the importance of cell history in generating the initial differences that ultimately drive the segregation of these two ICM lineages. Accordingly, this model postulates that the extent of differentiating cues an outer-residing ICM ancestor blastomere is exposed to during the first cell-fate decision (defined by the timing of progeny cell internalisation, either as relatively short if it occurs at the 8- to 16-cell transition or long at the following or 16- to 32-cell cleavage division) is responsible for creating such differences in the spatially internalised ICM progenitor cells of the blastocyst. Moreover, given that newly internalised cells invoke an activated Hippo signalling pathway activity responsible for preventing the execution of the same differentiating cues that induce differentiation in their outer-residing sister cells, the model can equally be conceptualised as reflecting the relative importance/temporal history of Hippo signalling pathway activation in derived ICM cell progenitors.

Therefore, the original goal of this Ph.D. thesis was to assess the importance of ancestral cell history on the acquisition of second cell-fate choice (*i.e.* EPI versus PrE in the ICM); a functional investigation of the validity of the “time-inside time-outside” model. Specifically, to ascertain if the extent of the exposure to differentiating cues, caused by experimentally mimicking Hippo signalling activation in defined clones of cells, could effect the cell-fate derivation of ICM progenitors to either EPI or PrE. In addition, experiments designed to precisely identify the molecular components involved in uncovered phenotypes were undertaken.

2.2 OBJECTIVE 2

Rock1/2 activity has been demonstrated to be indispensable for successful pre-implantation mouse embryo development and specifically for the germane execution of the first cell-fate decision. However, two recent studies have reported completely different phenotypes after chemical inhibition of Rock1/2 activity.

Therefore, in order to clarify these conflicting results it was firstly decided to re-examine the effects of Rock1/2 inhibition on pre-implantation mouse embryo development, cytoskeleton dynamics, cell polarity establishment, plus adherens and tight junction formation. However, the main goal was to determine whether the reported and observed (herein) Rock1/2 inhibition effects on the Hippo signalling pathway are mediated through the Amot protein, as this represented a crucial gap in the reported literature. In addition, a further aim was to more thoroughly and comprehensively characterise the observed Rock1/2 inhibition associated phenotype, to determine the developmental timing of the onset of Rock1/2 activity and to assay for the first time if it would have an effect on relative cell positioning and hence fate, prior to blastocyst formation.

3. MATERIAL AND METHODS

All described experimental procedures on mice and mouse embryos were ethically approved by the local relevant committees of the University of South Bohemia and Biology Centre of the Czech Academy of Sciences and approved and ratified by the regulatory national authority within the government of the Czech Republic.

3.1 EMBRYO COLLECTION AND CULTURE

Embryos were recovered into M2 medium containing 4mg/ml BSA (M2+BSA; detailed information on M2+BSA media composition is provided in the table 3.1) from the dissected oviducts of 10 weeks old F1 hybrid (C57Bl6 x CBA/W) super-ovulated female mice that had been mated with F1 stud males. Superovulation was performed by peritoneal injections of 7.5 IU of pregnant mare's serum gonadotropin (PMSG; Sigma), followed by injection of 7.5 IU human chorionic gonadotropin (hCG; Sigma) 48 hours later. Mating pairs were immediately established and successful mating confirmed the following day by inspection of vaginal sperm plugs. Both 2- and 4-cell stage embryos were recovered from freshly dissected oviducts 44 and 53 hours post-hCG administration. Unless microinjected immediately, recovered embryos were washed through a series of 10 KSOM (Potassium simplex optimisation medium) media drops (EmbryoMax, Millipore) and cultured in a final KSOM drop under mineral oil in a 5% CO₂ containing atmosphere at 37°C (15 embryos/ 20µl drop).

Table 3.1 Information on M2+BSA media composition

M2+BSA MEDIUM						
	Component	Concentration			Cat. No.	Supplier
		(g/l)	(mM)	(ml/l)		
A	Sodium chloride	5,552	95.00		S7653	Sigma-Aldrich
B	Potassium chloride	0.356	5.00		P5405	Sigma-Aldrich
C	Potassium dihydrogen phosphate	0.162	1.20		P5655	Sigma-Aldrich
D	Magnesium sulfate heptahydrate	0.293	1.20		M1880	Sigma-Aldrich
E	Sodium DL-lactate solution	2,521	22.50	3.20	L7900	Sigma-Aldrich
F	D-(+)-Glucose	1,000	5.50		G7021	Sigma-Aldrich
G	Penicillin G sodium salt	0.060	0.17		P3032	Sigma-Aldrich
H	Streptomycin sulfate salt	0.050	0.07		S1277	Sigma-Aldrich
I	Sodium bicarbonate	0.336	4.00		S5761	Sigma-Aldrich
J	Sodium pyruvate	0.036	0.33		P4562	Sigma-Aldrich
K	Calcium chloride dihydrate	0.252	1.71		C7902	Sigma-Aldrich
L	HEPES	5,004	21.0		H4034	Sigma-Aldrich
M	Bovine serum albumin (BSA)	4,000			A3311	Sigma-Aldrich

* pH was adjusted to 7.2-7.4 and medium was subsequently filter-sterilised

** M2+BSA components D and K are excluded from Ca²⁺/Mg²⁺ ion free M2+BSA media that is otherwise identical

3.2 EMBRYO TREATMENT WITH CHEMICAL INHIBITORS

3.2.1 Y-27632 Rock1/2 inhibitor treatment

To determine the effective working concentration of Rock1/2 inhibitor, embryos were recovered at the 2-cell (E1.5) stage and *in vitro* cultured until the late blastocyst (E4.5) stage in KSOM supplemented with amino acids (KSOM+AA; detailed information on KSOM+AA media composition is provided in the table 3.2) and 20 μ M, 50 μ M or 100 μ M Rock1/2 inhibitor (Y-27632, Enzo Life Sciences; previously described in Narumiya *et al.*, 2000) or appropriate volumes of DMSO (Dimethyl sulfoxide) vehicle control. In all subsequent experiments embryos were cultivated from 2-cell (E1.5) stage until 8-cell (E2.5/ E2.75), 16-cell (E3.0), or 32-cell (E3.5/ E3.75) stage in KSOM+AA in the presence of 50 μ M Y-27632/ Rock1/2 inhibitor.

Table 3.2 Information on KSOM+AA media composition

KSOM+AA MEDIUM					
Component	Concentration			Cat. No.	Supplier
	(g/l)	(mM)	(ml/l)		
A Sodium chloride	5,552	95.00		S7653	Sigma-Aldrich
B Potassium chloride	0.186	2.50		P5405	Sigma-Aldrich
C Potassium dihydrogen phosphate	0.048	0.35		P5655	Sigma-Aldrich
D Magnesium sulfate heptahydrate	0.049	0.20		M1880	Sigma-Aldrich
E Sodium DL-lactate solution	1,120	10.00	1.42	L7900	Sigma-Aldrich
F D-(+)-Glucose	1,000	5.50		G7021	Sigma-Aldrich
G Sodium bicarbonate	2,101	25.00		S5761	Sigma-Aldrich
H Sodium pyruvate	0.022	0.20		P4562	Sigma-Aldrich
I Calcium chloride dihydrate	0.252	1.71		C7902	Sigma-Aldrich
J Ethylenediaminetetraacetic acid disodium salt dihydrate	0.004	0.01		E5134	Sigma-Aldrich
K L-Glutamine	0.146	1.0		G8540	Sigma-Aldrich
L MEM Essential amino acids solution (50x)			10.00	11130	Gibco
M MEM Non-essential amino acids solution (100x)			5.00	11140	Gibco
N Bovine serum albumin (BSA)	4,000			A3311	Sigma-Aldrich

* pH was adjusted to 7.2-7.4 and medium was subsequently filter-sterilised

3.2.2 Cytochalasin D treatment

Embryos were collected at the 2-cell (E1.5) stage and *in vitro* cultured in KSOM+AA medium up until two hours prior to reaching the 32-cell (E3.5) stage, at which point they were transferred into pre-warmed and CO₂ equilibrated KSOM+AA containing 0.5 μ g/ml cytochalasin D (sc-201442, Santa Cruz) or fresh KSOM+AA medium alone and further cultured to reach the 32-cell (E3.5) stage.

3.3 PREPARATION OF dsRNAs, mRNA AND MICROINJECTIONS

Tead4 and Dab2 specific long double-stranded RNAs (dsRNAs) were designed (using the E-RNAi web application) to specifically target the coding region sequences of the relevant mRNAs. Amot-dsRNA was designed to target the 3' untranslated region (UTR) sequence of Amot mRNA as previously described (Leung and Zernicka-Goetz, 2013). In addition, GFP-dsRNA was synthesized to serve as a control lacking an endogenous target. DNA templates for *in vitro* dsRNA synthesis were generated in PCR (Polymerase chain reaction) using bacteriophage T7-promoter linked oligonucleotide primers specific for each targeted mRNA (the exact primer sequences are provided in table 3.3). Tead4, Dab2 and Amot-targeting dsRNA DNA templates were amplified from mouse embryonic stem (ES) cell complementary DNA (cDNA) (HMI ES cells; Wu *et al.*, 2009) while GFP-targeting dsRNA DNA template was amplified using pRN3P:EGFP plasmid DNA (Morris *et al.*, 2010) as initial template. All dsRNAs were synthesized using MEGAscript T7 Transcription Kit (Ambion) according to manufacturer's protocol and the integrity of each was confirmed on non-denaturing agarose gels.

Table 3.3 Information on the oligonucleotide primer sequences used to generate DNA template for dsRNA synthesis

T7-promoter linked oligonucleotide primers list			
#	Targeted mRNA	Forward primer (5'-3')	Reverse primer (5'-3')
1	Amot	<u>TAATACGACTCACTATAGGG</u> TGTGTTGGGGAGAAAAGGA	TAATACGACTCACTATAGGGGAAGTCCAGGAAAAGGCCTGA
2	Dab2	TAATACGACTCACTATAGGGCCTGGACGCTGTTGTCTAC	TAATACGACTCACTATAGGGGAAGTGGGGTTGCAATG
3	GFP	TAATACGACTCACTATAGGGAGAGTACAAATTTCTGTGAGTGGAGAGG	TAATACGACTCACTATAGGGAGATGTATAGTTCATCCATGCCATGTGTA
4	Tead4	TAATACGACTCACTATAGGGTGTGGAGTTCTCGGCTTTC	TAATACGACTCACTATAGGGTCGGTAGATGTGGTGCTGAG

*Note that T₇-promoter sequence is underlined.

The reporter of Rac1 activity used in a time-lapse experiment, PAK1-PBD-EYFP encoding mRNA (containing amino acid residues 65-150 of human PAK1 (p21 activated kinase 1)/ p21 binding domain fused with enhanced yellow fluorescent protein), has previously been described elsewhere (Halet and Carroll, 2007). PAK1-PBD-EYFP insert was amplified in a PCR reaction using pcDNA3-PBD-EYFP plasmid as a template (from addgene; ID: 13723) and the following pair of oligonucleotide primers: F:5'-GACTATGGATCCGCCACCATGAATAAAAAGAAAGAGAAAGAGCGG-3'; R:5'-GACTATTCTAGATCACTTGTACAGCTCGTCCATGCCGAGAGTGA-3'. The insert was subsequently digested with the combination of BamHI and XbaI restriction enzymes and subcloned into pRN3p vector downstream of the T3 bacteriophage-derived RNA polymerase promoter and flanked with 5' and 3' UTR sequences from the frog β -globin gene (Zernicka-Goetz *et al.*, 1996). Sfil linearised pRN3p-PAK1-PBD-EYFP plasmid served as a template for *in vitro* transcription. The synthesis of PAK1-PBD-EYFP encoding mRNA was performed using the mMESSEGEEmMACHINE T3 kit (Ambion) according to

manufacturer's protocol. A poly(A) tail of approximately 200 nucleotides in length was added to the synthesised mRNA using a proprietary poly(A) tailing kit (Ambion). The size and integrity of PAK1-PBD-EYFP mRNA was then confirmed on a denaturing agarose gel.

Single blastomere microinjections were performed on 2- or 4-cell stage embryos in suspended M2+BSA media drops according to defined protocols (Zernicka-Goetz *et al.*, 1997) using IX71 inverted microscope (Olympus), micromanipulators (Leica) and FemtoJet microinjection system (Eppendorf). *Tead4*-dsRNA (100 ng/ μ l) was co-microinjected with Rhodamine-/ Oregon-Green-conjugated Dextran Beads microinjection markers (RDBs/ OGDBs; 2 μ g/ μ l and 1 μ g/ μ l), with controls comprising either RDBs/ OGDBs microinjection alone or RDBs plus GFP-dsRNA (100ng/ μ l). *Dab2*-dsRNA (120ng/ μ l), *Amot*-dsRNA (200ng/ μ l) or control GFP-dsRNA (120ng/ μ l or 200ng/ μ l) was co-microinjected with RDBs (2 μ g/ μ l). Non-microinjected embryos (1-3 per experiment) served as sentinels for appropriate *in vitro* development.

3.4 EMBRYO CHIMERAS

Fluorescent microinjected (both blastomeres at 2-cell/ E1.5 stage) donor non-compacted 8-cell stage (E2.5), *zona*-less (following acid tyrodes treatment), embryos were transferred into Ca²⁺/Mg²⁺ ion free M2+BSA media and disaggregated into single blastomeres. Per chimera, single fluorescently-labelled control or *Tead4*-KD blastomeres were placed in contact with non-compacted *zona*-less 8-cell stage (E2.5) embryos in PHA (phytohaemagglutinin – 300 μ g/ml; Sigma) containing M2+BSA media and incubated for 10 minutes (37°C and 5% CO₂). Following confirmation of aggregation, chimeras were returned to conventional KSOM culture until the late blastocyst (E4.5) stage. All manipulations were performed in pre-warmed (37°C) media under mineral oil on heated stereo-dissecting microscope stages.

3.5 QUANTITATIVE REVERSE TRANSCRIPTION PCR (Q-RTPCR)

Total RNA was prepared from: i) 16-cell (E3.1) or 32-cell (E3.6) stage *Tead4*-KD or control embryos previously microinjected at the 2-cell stage (E1.5) in both blastomeres; ii) 32-cell (E3.5) stage embryos treated from the 2-cell stage with 50 μ M Y-27632 Rock1/2 inhibitor or the appropriate amount of DMSO vehicle as a control. Typically, 30 embryos for each condition were used as starting material and RNA was extracted according to manufacturer's provided instructions (Arcturus Biosciences; 'PicoPure RNA isolation kit'). The entire amount of purified total RNA (eluted into 10 μ l of nuclease free water) was DNaseI (Deoxyribonuclease I) treated as instructed (Ambion; 'DNA-free' kit) to remove potential genomic DNA contamination and subsequently used to derive cDNA using

oligodT priming in 30µl reactions (Invitrogen; 'Superscript III Reverse Transcriptase'). Synthesised cDNA was diluted with nuclease free water (1:3) and used as template (0.5µl per reaction) in 10µl real-time PCR reactions (Qiagen: 'SYBR Green PCR kit') to detect the presence and abundance of gene specific transcripts (BioRad, 'CFX96 Real Time System') - see table 3.4 for details of gene specific oligonucleotide primer pair sequences (used at a final reaction conc. 400nM). All gene specific transcript levels in i), were internally normalised against *Rpl23* (60S ribosomal protein L23) and/ or *H2afz* (H2A histone family member z) levels, while in ii), the expression level of *Amot* was normalised to the composite of both the *H2afz* and *Tbp* (TATA-Box binding protein) expression levels. The internally normalised expression fold changes (plus s.e.m.) were derived using the $\Delta\Delta C_t$ method (Livak and Schmittgen, 2001) and a minimum of 2 biological replicates consisting of at least three technical replicates were employed.

Table 3.4 Information on oligonucleotide primers used in Q-RTPCR analysis

Q-RTPCR oligonucleotide primers list			
#	Gene name	Forward primer (5'-3')	Reverse primer (5'-3')
1	<i>Amot</i>	GACAGAAATCCAACGGGTCT	CTTCTAATCTCGCCCTCCAG
2	<i>Cdx2</i>	TCAAGAAGAAGCAGCAGCAG	GCAAGGAGGTCACAGGACTC
3	<i>Dab2</i>	GTCGGGGATTGGCTGGTATC	GGCCATTGGTTGTGCTTGTT
4	<i>Fgfr2</i>	AAGAGGGACACAGGATGGAC	TGTGGGTCTCTGTGAGGGTA
5	<i>Gata3</i>	CCGAAACCGGAAGATGTCTA	AGATGTGGCTCAGGGATGAC
6	<i>H2afz</i>	GCGCAGCCATCCTGGAGTA	CCGATCAGCGATTGTGGA
7	<i>Lrp2</i>	TGGTCAGTGTGTTCCCATCG	CGTGTATAGCAGGCTCCGT
8	<i>Nanog</i>	GGTTGAAGACTAGCAATGGTCTGA	TGCAATGGATGCTGGGATACTC
9	<i>Rpl23</i>	CCAGCAGTGGTAATTCGACA	GCAAGCCTTTTCATCTCTCC
10	<i>Tbp</i>	GAAGAACAATCCAGACTAGCAGCA	CCTTATAGGGAACTTCACATCACAG
11	<i>Tead4</i>	GAGCCCGGAGAACATGATTA	CCAAATGAGCAGACCTTCGT

3.6 IMMUNO-FLUORESCENT STAINING

Embryos were fixed in 4% PFA (paraformaldehyde) dissolved in PBS (phosphate-buffered saline) for 20 minutes at 37°C and prepared for confocal-based immuno-fluorescence microscopy as follows (all steps were performed at room temperature in a volume of 150µl, unless stated otherwise): i) three 5 minute washes in PBS, ii) 20 minutes permeabilisation in 0.5% Triton X-100 diluted in PBS (for *Fgfr2* immuno-staining 0.1% Triton X-100 was used), iii) three 10 minute washes in PBS-Tween 20 (0.15%; PBS-T), iv) one 10 minute wash in NH₄Cl (50mM) diluted in PBS, v) one 4 hour blocking step in 3% BSA diluted in PBS-T (BSA-PBS-T) at 4°C, vi) overnight incubation in primary antibody diluted in BSA-PBS-T at 4°C, vii) three 10 minute washes in PBS-T, viii) a second 4 hour blocking step at 4°C in BSA-PBS-T, ix) 1 hour incubation in fluorescently labelled secondary antibody diluted in BSA-PBS-T at 4°C, x) three 10 minute PBS-T washes, xi) 20 minutes fluorescently conjugated

phalloidin staining (1:200 diluted in PBS; an additional/ optional step in cases when F-actin was to be visualised) xii) terminal 30 minutes wash in PBS, and xiii) mounting (Vectashield plus DAPI (4',6-diamidino-2-phenylindole), Vector Labs) on glass-bottomed, poly-L-lysine coated culture dishes. In case of phospho-Yap1 (pYap1) immuno-staining, embryos were pre-treated with 1000 units of λ -phosphatase (sc-200312, Santa Cruz Biotech) in 50 μ l of provided buffer for 1 hour at 30°C prior to the first blocking step, according to manufacturers protocol. F-actin was visualised by Texas-Red-conjugated phalloidin staining (T7471, Invitrogen). The information about the primary and secondary antibodies and dilutions used is provided in table 3.5. Note, that for embryos double immuno-stained for Nanog and Gata4, the mouse monoclonal version of the anti-Nanog antibody was used.

Table 3.5 Information on primary and secondary antibodies used in the immuno-fluorescent staining procedure

Primary antibodies list						
#	Antigen	Cat. no.	Supplier	Species raised in and clonicity	Dilution used	Secondary antibody used (refer to below table)
1	Amot	<i>a generous gift from Hiroshi Sasaki (see Hirate et al., 2013)</i>		rabbit, polyclonal	1 in 100	E,G
2	Cdh1	3195	Cell Signalling	rabbit, polyclonal	1 in 500	E
3	Cdx2	MU392A-UC	BioGenex	mouse, monoclonal	1 in 200	B,C
4	Ctnnb1	sc-7963	Santa Cruz	mouse, monoclonal	1 in 200	D
5	Dab2	610464	BD BioScience	mouse, monoclonal	1 in 400	C
6	Fgfr2	sc-122	Santa Cruz	rabbit, polyclonal	1 in 200	F
7	Gata4	sc-9053	Santa Cruz	rabbit, polyclonal	1 in 100	E,G
8	Nanog	14-5761	Affymetrix/eBioscience	rat, monoclonal	1 in 100	H
9	Nanog	ab80892	Abcam	rabbit, polyclonal	1 in 200	E
10	Pard6b	sc-67393	Santa Cruz	rabbit, polyclonal	1 in 100	E,G
11	phospho-ezrin (Thr567)/pERM	3149	Cell Signalling	rabbit, monoclonal	1 in 500	E,G
12	phospho-myosin light chain 2 (Ser19)/pMlc2	3671	Cell Signalling	rabbit, polyclonal	1 in 50	E
13	phospho-Yap1 (Ser127)/pYap1	4911	Cell Signalling	rabbit, polyclonal	1 in 200	E
14	Prkcz/i	sc-216	Santa Cruz	rabbit, polyclonal	1 in 200	E,G
15	Scrib	sc-28737	Santa Cruz	rabbit, polyclonal	1 in 100	E,G
16	Sox17	AF1924	R&D Systems	goat, polyclonal	1 in 100	A
17	Tead4	ab58310	Abcam	mouse, monoclonal	1 in 200	C
18	Tjp1	61-7300	Invitrogen	rabbit, polyclonal	1 in 200	G
19	Tjp2	sc-11448	Santa Cruz	rabbit, polyclonal	1 in 200	E
20	Yap1	sc101199	Santa Cruz	mouse, monoclonal	1 in 100	B,C,D
21	α -Tubulin	A11126	Invitrogen	mouse, monoclonal	1 in 200	D
Secondary fluorescent conjugated antibodies list						
	Species of antibody targeted	Cat. no.	Supplier	Species raised in and fluorophore	Dilution used	Used in combination with primary antibody (refer to above table)
A	goat	A-21222	Life Technologies	rabbit, Alexa488	1 in 500	16
B	mouse	715-605-150	Jackson Immuno Research Inc.	donkey, Alexa647	1 in 500	3, 20
C	mouse	A-11029	Life Technologies	goat, Alexa488	1 in 500	3, 5, 17, 20
D	mouse	A-21424	Life Technologies	goat, Alexa555	1 in 500	4, 20, 21
E	rabbit	A-21206	Life Technologies	donkey, Alexa488	1 in 500	1, 2, 7, 9-15, 19
F	rabbit	A-21429	Life Technologies	goat, Alexa555	1 in 500	6
G	rabbit	A-31573	Life Technologies	donkey, Alexa647	1 in 500	1, 7, 10, 11, 14, 15, 18
H	rat	712-096-150	Jackson Immuno Research Inc.	donkey, FITC	1 in 400	8

3.7 CONFOCAL MICROSCOPY AND IMAGE ANALYSIS

An Olympus IX71 inverted microscope was used to make group snapshot images of live embryos at all examined stages. Fixed and immuno-fluorescently stained embryos were imaged using either Fluoview Fv10i or IX81 inverted confocal microscopes (both from Olympus). Exemplar reproduced embryo figure micrographs (depicted in the results and published manuscripts) were representative of at least n=5 embryos.

The average number of cells per embryo was calculated by counting DAPI-stained cell nuclei in individual fixed embryo confocal microscopy z-stacks in each experimental condition (at the appropriate developmental stage). The contribution of individual cells of E4.5 stage blastocysts within and outwith the injected clone (in both directly microinjected 2- and 4-cell embryos and 1+8 chimeric embryos), or within either inner or outer cell populations, or within cell lineage marker protein positive or negative cells (after specific immuno-staining), plus the incidence of cells with fragmented/ apoptotic nuclei, were determined in both experimental and control embryos by serial inspection of confocal z-sections using Fluoview ver 1.7. (Olympus) and Imaris 6.2.1 (BitPlane) software. The above contribution criteria were initially assessed in an undisturbed/ culture control group of embryos that had been collected at the 2-cell stage (E1.5) and *in vitro* cultured to the late blastocyst (E4.5) stage (details of this analysis are provided in supplementary figure S1 and supplementary table ST1) in order to establish a baseline for the appropriate development of individual control and experimental embryos subject to some level of experimental perturbation (*e.g.* microinjection). This baseline was subsequently used to eliminate embryos with compromised development owing to excessive manipulation (especially in the case of chimeras). Accordingly, embryos with fewer than 64, or less than four Gata4 positive cells (minimum we observed in the reference data) were excluded from the analysis.

To quantify the extent of Scrib protein apical mis-localisation in Rock1/2-inhibited embryos the image intensity tool in the Olympus Fluoview ver.1.7. software was used. The pixel intensity (of derived confocal z-stack micrographs, in the anti-Scrib channel) was quantified along the apico-basal axes of a random selection of outer cells from control and Rock1/2-inhibited embryos (note that all derived micrographs were imaged with the same confocal laser power and gain settings). Graphical plots of the data were prepared in Microsoft Excel and individual points were normalised and expressed as percentage of the maximum/ saturated pixel intensity, to permit inter-embryo/ inter-treatment/ inter-measurement comparison.

Time-lapse imaging was performed using Fluoview FV10i inverted confocal microscope (Olympus). Microinjected embryos were *in vitro* cultured in the already described manner until they reached the 32-cell (E3.5) stage, at which point they were transferred into the pre-equilibrated drops of KSOM/ EmbryoMax media under mineral oil on glass-bottom dishes (MatTek Corporation). They were then subjected to the stated imaging regime during the following time period of 12 hours. Images were acquired using Olympus UPlanSApo 60x/1.2 W water immersion objective, with an optical section thickness of 2.0 μm and an interval of 20 minutes between acquired z-stacks. Data was analysed and a series of individual optical z-sections images prepared using Olympus Fluoview ver.1.7. software.

3.8 STATISTICAL ANALYSIS

The mean numbers and the standard error of the means (mean \pm s.e.m.) of cells within defined embryonic cell populations at the various developmental stages assayed were calculated, and the statistical significance between the stated means determined by calculating the probability/p-value using a 2-tailed Student's t-test.

4. RESULTS

The results section of this Ph.D. thesis is divided into two parts, each consisting of published data followed by unpublished work that is based upon or related to the previously described findings. **Part I** of the results investigates the importance of the Hippo signalling pathway and cell developmental history during the acquisition of the second cell fate and describes an attempt made to decipher the underlying molecular mechanisms responsible for the observed phenotype. Part I of the results is based upon the following publication:

Mihajlović A.I., Thamodaran V., Bruce A.W. (2015) The first two cell-fate decisions of preimplantation mouse embryo development are not functionally independent. *Scientific Reports*, 5: 15034.

Abstract

During mouse pre-implantation embryo development, three distinct cell lineages are formed, represented by the differentiating trophectoderm (TE), primitive endoderm (PrE) and the pluripotent epiblast (EPI). Classically, lineage derivation has been presented as a two-step process whereby outer TE cells are first segregated from inner-cell mass (ICM), followed by ICM refinement into either the PrE or EPI. As ICM founders can be produced following the fourth or fifth cleavage divisions, their potential to equally contribute to EPI and PrE is contested. Thus, modelling the early sequestration of ICM founders from TE-differentiation after the fourth cleavage division, we examined ICM lineage contribution of varying sized cell clones unable to initiate TE-differentiation. Such TE-inhibited ICM cells do not equally contribute to EPI and PrE and are significantly biased to form EPI. This bias is not caused by enhanced expression of the EPI marker *Nanog*, nor correlated with reduced apical polarity but associated with reduced expression of PrE-related gene transcripts (*Dab2* and *Lrp2*) and down-regulation of plasma membrane associated *Fgfr2*. Our results favour a unifying model where the three cell lineages are guided in an integrated, yet flexible, fate decision centred on relative exposure of founder cells to TE-differentiative cues.

Part II of the results highlights the role of the Hippo signalling pathway component Amot in mediating Rho-associated protein kinase (Rock1/2) regulation of what is classically termed the first cell-fate decision. In addition, particular aspects of the observed Rock1/2 inhibition associated phenotype have been re-examined and the phenotype more thoroughly characterised. Part II of the results is based upon the following publication:

Mihajlović A.I., Bruce A.W. (2016) Rho-associated protein kinase regulates subcellular localisation of Angiomotin and Hippo-signalling during preimplantation mouse embryo development. *Reproductive Biomedicine Online*, 33: 381-390.

Abstract

The differential activity of the Hippo signalling pathway between the outer- and inner-cell populations of the developing pre-implantation mouse embryo directs the appropriate formation of trophectoderm (TE) and inner cell mass lineages (ICM). Such distinct signalling activity is under the control of intra-cellular polarisation, whereby Hippo signalling is either suppressed in polarised outer-cells or activated in apolar inner-cells. The central role of apical-basolateral polarisation to such differential Hippo signalling regulation prompted us to re-investigate the role of potential upstream molecular regulators affecting apical-basolateral polarity. Here we report, that the chemical inhibition of Rho-associated kinase (Rock1/2) is associated with failure to form morphologically distinct blastocysts, indicative of compromised TE-differentiation, and defects in the localisation of both apical and basolateral polarity factors associated with malformation of tight-junctions. Moreover, Rock1/2-inhibition mediates mis-localisation of the Hippo signalling activator Amot, to the basolateral regions of outer-cells and is concomitant with aberrant activation of the pathway. The Rock1/2-inhibition phenotype is mediated by Amot, as RNAi-based *Amot* knockdown totally rescues the normal suppression of Hippo signalling in outer-cells. We conclude that Rock1/2, via regulating appropriate apical-basolateral polarisation in outer-cells, regulates the appropriate activity of the Hippo signalling pathway, by ensuring the correct sub-cellular localisation of the Amot protein in outer-cells.

4.1 PART I - INVESTIGATING THE IMPORTANCE OF THE HIPPO SIGNALLING PATHWAY AND CELL HISTORY DURING THE ACQUISITION OF THE SECOND CELL FATE

As previously described, during pre-implantation mouse embryo development ICM founder cells are typically generated during or shortly after the fourth (the 8- to 16-cell transition) and fifth cleavage (the 16- to 32-cell transition) divisions (Anani *et al.*, 2014; Johnson and Ziomek, 1981b). The elapsed developmental time between the completion of these divisions is approximately 12 hours (Artus and Cohen-Tannoudji, 2008), during which outer-residing 16-cell stage blastomeres remain polarised along their apico-basal axis and exposed to TE-differentiative cues, such as a suppressed Hippo signalling pathway, whilst apolar inner-cells are protected from TE-differentiation by an active Hippo signalling pathway (Cockburn *et al.*, 2013; Hirate *et al.*, 2013; Leung and Zernicka-Goetz, 2013; Nishioka *et al.*, 2009; Plusa, Frankenberg, *et al.*, 2005; Ziomek and Johnson, 1980). Given that such outer-residing 16-cell stage blastomeres can also generate further ICM founders after the fifth cleavage, it is questionable whether ICM progenitors produced by the fourth and fifth cleavage divisions have equal potential to contribute progeny to both the late blastocyst ICM lineages, the EPI and PrE (Krupa *et al.*, 2014; Morris, 2011; Yamanaka *et al.*, 2010).

4.1.1 Functional down-regulation of *Tead4* expression within the developing pre-implantation mouse embryo

Therefore, in order to test if ICM cells are generated with an equal potential, irrespective of the extent of TE induction their parental cells received, an RNAi microinjection based strategy was designed to target the *Tead4* gene, thus blocking the initiation of TE-differentiation within defined cell clones and enabling an assay of their ultimate cell fate contribution within the ICM. As *Tead4* is the earliest known transcription-factor to function in TE specification (Yagi *et al.*, 2007; Nishioka *et al.*, 2008) and its transcriptional activating properties are known to be regulated by the Hippo signalling pathway, thereby confining its regulatory output to polarised outer-cells (Nishioka *et al.*, 2009; Hirate *et al.*, 2013), it was reasoned that down-regulation of *Tead4* would prevent cells from sensing TE-differentiative cues thus mimicking the naturally occurring removal of cells from *Tead4* regulation that occurs during their internalisation after the fourth cleavage division. Accordingly, it was hypothesised that if the extent of TE induction had been unimportant for PrE differentiation in the ICM, internalised TE-inhibited clones would not have been impaired in their potential to contribute to PrE. Conversely, if being able to initiate TE-differentiation facilitates PrE differentiation,

such clones would be disadvantaged in populating the PrE, therefore supporting the integrated cell-fate model.

4.1.1.1 Global *Tead4* down-regulation using long dsRNA phenocopies the genetic zygotic *Tead4*^{-/-} knock-out

Accordingly, a *Tead4* specific long double-stranded RNA (*Tead4*-dsRNA) was designed and *in vitro* synthesised for use in single cell microinjection experiments, in order to induce a clonal TE-differentiation block in the pre-implantation mouse embryo. It was first decided to confirm the efficacy of the construct and validate the RNAi based approach. Therefore, both blastomeres of 2-cell stage (E1.5) embryos were microinjected with the *Tead4*-dsRNA plus RDBs (Rhodamine dextran conjugated beads, as an injection marker and lineage tracer) or RDBs alone (microinjected controls), cultured to the mid-16-cell (E3.1) or 32-cell (E3.6) stages and processed for Q-RTPCR or confocal immuno-fluorescence based microscopic analysis.

As shown in figure 4.1b, a >95% reduction in *Tead4* mRNA expression was observed in *Tead4*-dsRNA injected embryos (*Tead4*-KD embryos) compared to microinjection controls, at both mid-16- and 32-cell stages. More importantly, nuclear localised *Tead4* protein, readily detectable in all cells of control microinjected embryos, was undetectable after *Tead4*-dsRNA microinjection at the same assayed stages (Fig. 4.1c), thus confirming the efficacy of the *Tead4*-dsRNA construct used. In addition, robust reductions in the mRNA expression of two essential TE-specific transcription factor genes (Fig. 4.1b) known to function downstream of *Tead4*, *Cdx2* (Strumpf *et al.*, 2005) and *Gata3* (Home *et al.*, 2009; Ralston *et al.*, 2010), were also recorded. Accordingly, *Cdx2* protein was not detectable in *Tead4*-KD embryos (Fig. 4.1c), demonstrating a successful block in TE-specification. Moreover, it was observed that when such *Tead4*-KD embryos were *in vitro* cultured, their morphological developmental progression was indistinguishable from that of microinjected control embryos until the 32-cell (E3.5) stage, after which they subsequently failed to initiate blastocoel formation and displayed considerable cell-death by the late blastocyst stage (E4.5) (Fig. 4.1d); therefore, recapitulating the phenotype exhibited in genetically null zygotic *Tead4*^{-/-} knock-out embryos (Yagi *et al.*, 2007; Nishioka *et al.*, 2008) and validating the RNAi mediated approach adopted.

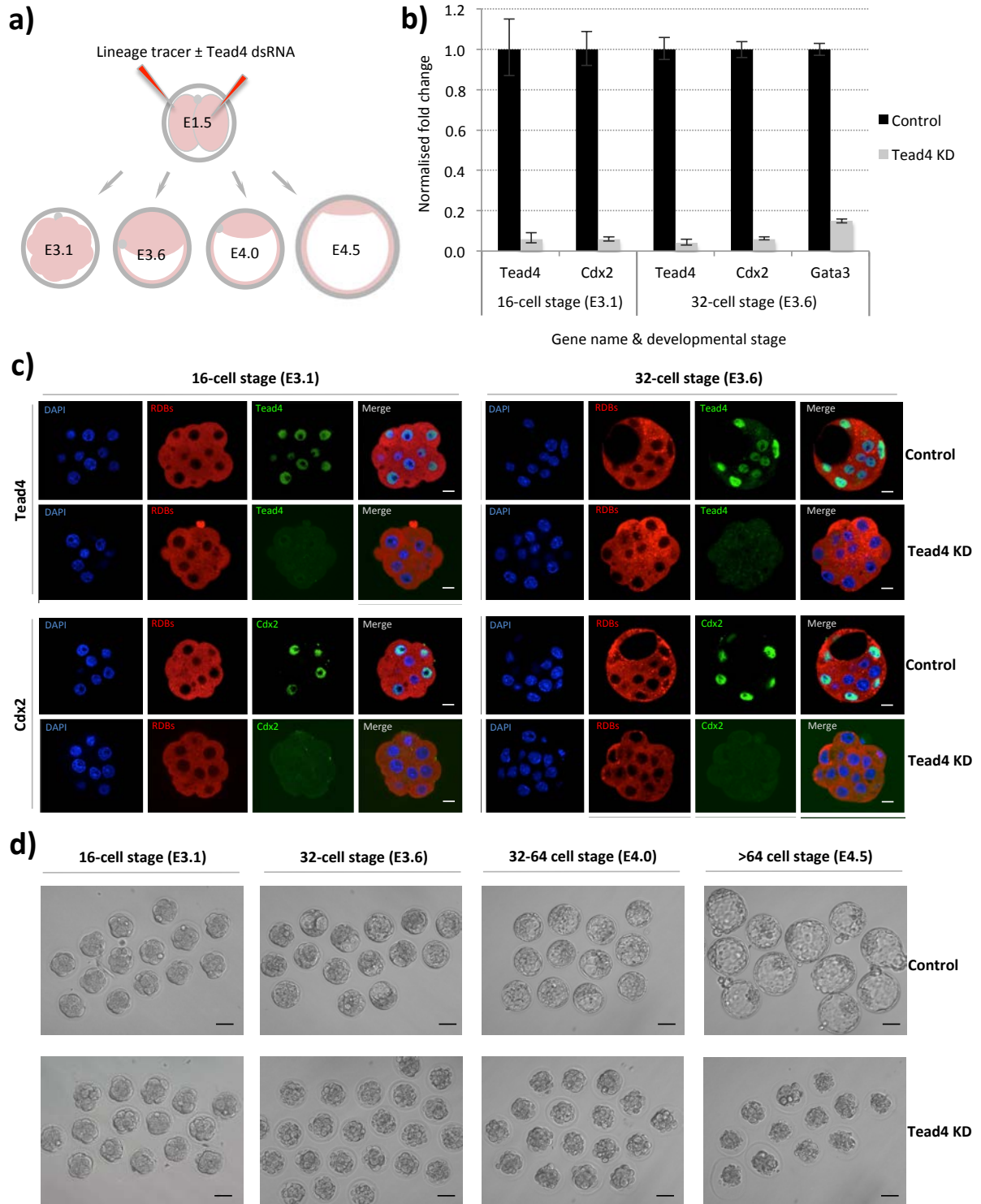


Figure 4.1 (legend overleaf)

Figure 4.1 Long dsRNA mediated *Tead4* down-regulation phenocopies the zygotic *Tead4*^{-/-} null TE-deficit phenotype. a) Schematic representation of experimental strategy. Embryos were microinjected with RDB injection marker (red) ± *Tead4*-dsRNA in both cells at the 2-cell stage (E1.5) and *in vitro* cultured until the mid-16-cell (E3.1), 32-cell (E3.6), 32-64-cell (E4.0) or >64-cell (E4.5) stages, prior to Q-RTPCR/ microscopic analyses. **b)** Q-RTPCR data detailing normalised average fold changes in mRNA expression of *Tead4*, *Cdx2* and *Gata3* in embryos microinjected with *Tead4*-dsRNA, relative to microinjection control embryos. Individual gene mRNA levels were normalised against *Rpl23* and/ or *H2afz* within control and experimental knockdown conditions and the fold change associated with *Tead4*-KD calculated. Errors are given as s.e.m. n = at least 2 for biological replicates and 3 for technical replicates. **c)** Representative single confocal immunofluorescence microscopy sections of embryos microinjected with RDB injection marker ± *Tead4*-dsRNA immuno-stained for *Tead4* or *Cdx2* protein (green) and DNA co-stained with DAPI (blue). RDB microinjection marker is visible (red). Scale bars = 10µm. **d)** Bright-field micrographs of control and *Tead4*-dsRNA microinjected embryos at various pre-implantation stage developmental time-points of *in vitro* culture. Note that the *Tead4*-KD embryos fail to initiate blastocoel formation and starting from the E4.0 time-point exhibit cell death; a phenotype consistent with that observed in zygotic genetic *Tead4*^{-/-} null pre-implantation embryos. Scale bars = 50µm.

4.1.1.2 Clonal down-regulation of *Tead4* expression allows blastocyst formation

As shown above, *Tead4* down-regulation in the whole embryo caused developmental arrest at the late morula/ early non-cavitated blastocyst stage thus preventing the examination of the effects of TE-inhibition on later development; *i.e.* during the segregation of EPI and PrE lineages in blastocyst ICM maturation. Therefore, it was decided to assay if the clonal inhibition of TE-differentiation would permit blastocyst formation and thus enable the contribution of internalised TE-inhibited clones to the two ICM cell lineages to be determined.

Accordingly, 2-cell (E1.5) stage embryos were microinjected in one blastomere with RDBs ± *Tead4*-dsRNA, to elicit a fluorescently marked and TE-inhibited clone of cells comprising half the embryo, cultured to the mid-16-cell (E3.1), 32-cell (E3.6) and >64-cell (E4.5) stages, fixed and processed for confocal immunofluorescence based microscopic analysis. As shown in figure 4.2, such embryos exhibited a complete down-regulation of both *Tead4* and *Cdx2* protein only within the cell clone derived from the *Tead4*-dsRNA microinjected blastomere at all examined stages of development (although from the 32-cell stage onwards, the *Cdx2* expression domain of the non-microinjected clone had become restricted to outer cells as normal). No such clonal down-regulation of either *Tead4* or *Cdx2* protein expression was observed in microinjected control embryos, thus confirming that the approach to clonally inhibit TE-differentiation, using *Tead4*-dsRNA, was valid. Moreover and in contrast to the global down-regulation of *Tead4* (Fig. 4.1), clonal *Tead4*-KD embryos were able to initiate appropriate blastocoel formation, illustrating the regulative capacity of the pre-implantation mouse embryo, and permitting the contribution of cells from the internalised TE-inhibited clone to be assessed.

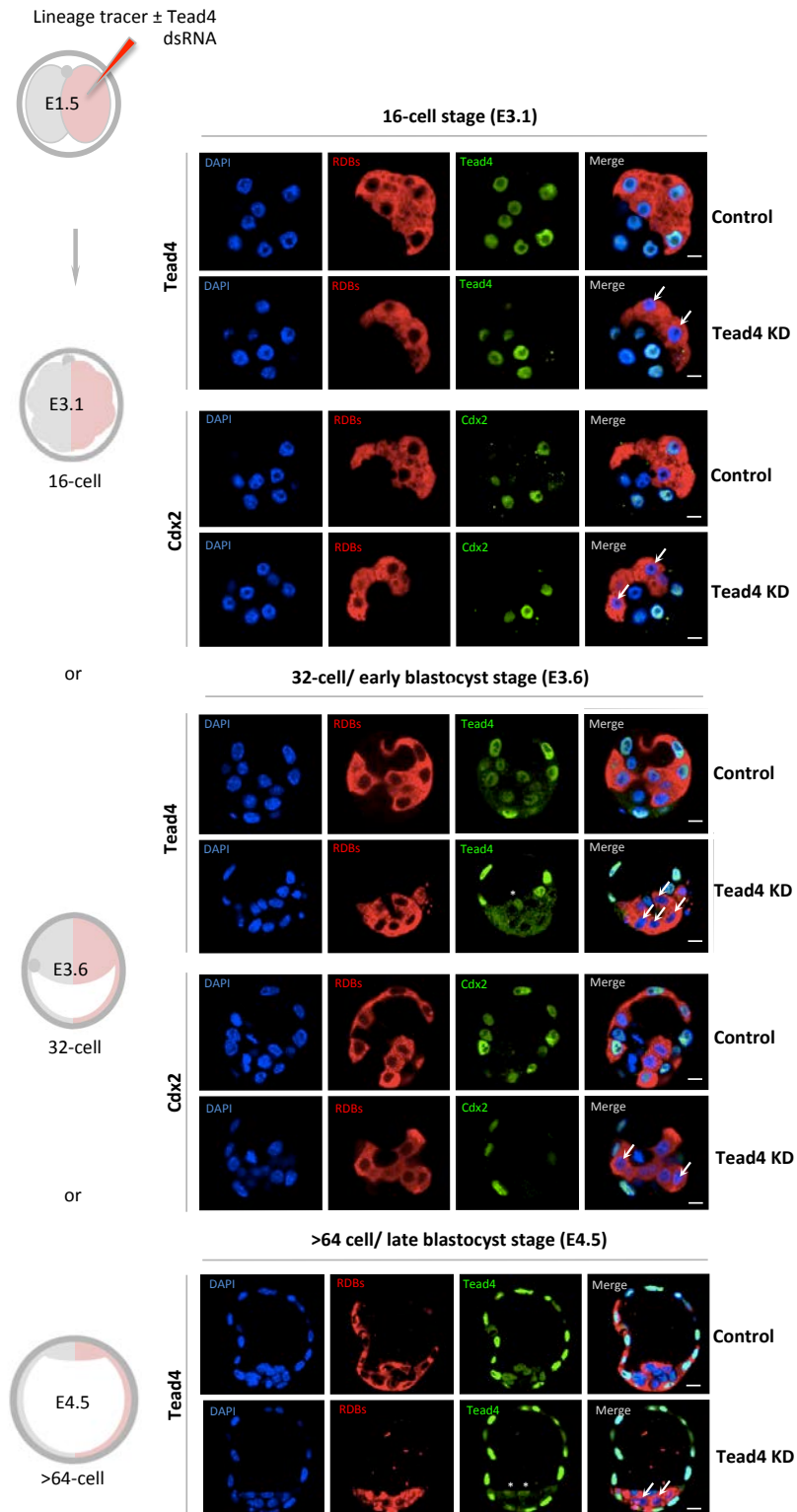


Figure 4.2 (legend overleaf)

Figure 4.2 Clonal down-regulation of *Tead4* expression and TE-differentiation inhibition. A schematic of the experimental strategy to effect clonal *Tead4* knock-down (KD) and TE-inhibition in one-half of the embryo using microinjected RDBs \pm *Tead4*-dsRNA (see materials and methods) is given on the left. Representative single z-plane confocal micrographs of control and *Tead4*-KD embryos at either the mid-16-cell (E3.1), 32-cell (E3.6) or >64-cell (E4.5) stages immuno-stained for *Tead4* or *Cdx2* (green) are given. Cells derived from the microinjected 2-cell stage clone are distinguishable by the co-injected RDB fluorescence (red). DNA counter-stain (blue) is also shown. In merged images the arrows denote cells exhibiting a lack of *Tead4* or *Cdx2* expression in the *Tead4*-KD microinjected cell clone, thus confirming the efficacy and the functional and clonal inhibition of TE-differentiation by *Tead4*-dsRNA until the late blastocyst stage (E4.5). ICM cells not from the microinjected clone, expressing *Tead4* protein are marked with asterisks (in *Tead4* alone micrographs). Note, in contrast to global *Tead4*-KD embryos (Fig. 4.1), such clonal *Tead4*-KD embryos initiate blastocoel formation in a manner indistinguishable from microinjected control embryos. Scale bars = 10 μ m.

4.1.2 Clonal down-regulation of *Tead4* expression biases cells towards EPI and away from PrE fate

Satisfied that the clonal *Tead4* knock-down strategy was technically valid, the next question to be addressed was to observe if the clonal down-regulation of *Tead4*, in internalised clones, would have a consequence on the derivation of the two ICM lineages in the developing mouse embryo. Thus, it was undertaken to assay the frequency at which ICM cells derived from a *Tead4*-dsRNA/*Tead4*-KD clone contributed to the EPI and PrE lineages when compared to both the non-injected clones within an experimental embryo group and the equivalent clones of control microinjected embryos.

4.1.2.1 Inhibition of TE-differentiation within half of the embryo biases internalised cells to EPI versus PrE fate

Accordingly, further experiments in which single blastomere microinjection of 2-cell (E1.5) stage embryos were repeated and then *in vitro* cultured to the late blastocyst (E4.5) stage, the developmental time-point at which PrE and EPI populations are known to become spatially distinct within the ICM (Gardner and Rossant, 1979), were conducted. The lineage contribution was then assayed in clonal RDB alone microinjected control and clonal *Tead4*-KD experimental embryo groups that had been double immuno-fluorescently stained for either i) *Gata4*, a definitive marker of the PrE (Plusa *et al.*, 2008), and *Cdx2*, a marker of TE cells (Strumpf *et al.*, 2005), or ii) *Sox17*, an early PrE marker expressed during PrE differentiation (Morris *et al.*, 2010; Niakan *et al.*, 2010), and *Cdx2* (under each immuno-fluorescent staining protocol, ICM cells devoid of either marker were classified as EPI), or, iii) *Gata4* and *Nanog*, a marker of the EPI, when not co-expressed with PrE marker genes (Mitsui *et al.*, 2003), (thus directly assaying both the ICM cell lineages, whilst simultaneously designating outer cells negative for either marker as TE). Further comprehensive analyses relating to

the relative spatial location of cell clones, ICM versus outer-TE location, and cells with fragmented nuclei typical of apoptosis were also undertaken and recorded. Note that each of the three respective immuno-staining regimes described above were associated with dedicated and matched control and experimental *Tead4*-KD embryo groups that were microinjected during the same experimental sessions. Accordingly, n=24, 13 and 25 for RDB alone microinjected control groups and n=24, 9 and 23 for clonal *Tead4*-KD embryo groups per respective immuno-staining regime (Fig. 4.3 summarises these data and supplementary tables ST2, ST3 and ST4 provide individual embryo data for each of immuno-staining method used; the information relating to apoptosis is provided in supplementary figure S2 and supplementary tables ST5, ST6 and ST7). In addition, the comparison of blastocyst lineage contribution and the incidence of apoptosis in RDBs alone microinjected control embryos with RDBs plus a GFP specific dsRNA (GFP-dsRNA; lacking an endogenous mouse mRNA target - supplementary figure S3 and supplementary tables ST8 and ST9) microinjected control embryo group is also presented, in which no statistically significant difference between the two control groups was observed; thus confirming the appropriateness of using the RDB alone microinjected control in all described assays.

This comprehensive analysis revealed that although the clonal *Tead4*-KD embryos are able to develop into morphologically normal late blastocysts (Fig. 4.3b) a striking cell lineage allocation phenotype was present. Namely, cells within the *Tead4*-KD clones preferentially and significantly contributed to the ICM over the TE, when compared to either their non-microinjected sister clones or the equivalent microinjected cell clones from control embryos (Fig. 4.3c). Moreover, there was also evidence of a partial compensation for this allocation, with the non-microinjected clone in *Tead4*-KD embryos contributing statistically more cells to the TE and fewer to the ICM. However, this regulation was not fully completed as clonal *Tead4*-KD embryos in general presented with significantly less TE and more ICM cells. In addition, cells derived from the *Tead4*-KD clone that remained in an outer TE position, did not express Cdx2 protein (with very few isolated exceptions detailing very weak anti-Cdx2 immuno-fluorescence signal) and were almost exclusively spatially restricted to the polar TE, overlying the ICM, rather than mural TE surrounding the expanding blastocoel. Although marked, such a preferential ICM allocation phenotype associated with clonal *Tead4*-KD is entirely consistent with its known and well-characterised role in TE differentiation (Nishioka *et al.*, 2009).

However, when it was determined to which lineage the extra ICM cells were segregated, it was discovered that they were not equally distributed between EPI and PrE. ICM cells derived from the *Tead4*-KD clone preferentially and significantly contributed to the EPI versus the PrE, when compared again to either their non-microinjected sister clones or the equivalent microinjected cell clones from control embryos. In fact, whilst the ICM of *Tead4*-dsRNA microinjected embryos were

significantly larger than those of control embryos, the number of cells within the PrE remained statistically equal in both groups with all the extra ICM cells, derived from the *Tead4*-dsRNA microinjected cell clone, contributing to an increased EPI cell number (Fig. 4.3c). More strikingly, the much smaller ICM component that consists of the non-microinjected cell clone in *Tead4*-dsRNA microinjected embryos (for example comprising 7.0 ± 0.8 cells versus 22.6 ± 1.1 cells for the microinjected clone in embryos immuno-stained with Gata4/ Cdx2), contributed a statistically equal number of PrE cells than the microinjected clone (equating, in the Gata4/ Cdx2 immuno-stained example but a trend repeated in the other staining groups, to 50.3% of its overall size, versus 19.0% in the microinjected *Tead4*-KD ICM clone – Fig. 4.3d), emphasising the bias within the microinjected *Tead4*-KD clone against contributing to the PrE, despite forming the majority of the total cell number of the ICM. By contrast, the percentage PrE contributions of the non-microinjected and microinjected ICM cell clones in RDB alone microinjected control embryos was statistically equal (in the Gata4/ Cdx2 immuno-stained example - 33.6% and 34.3%, respectively). Therefore, the smaller non-microinjected ICM cell clone, in *Tead4* KD embryos, contributes significantly more PrE cells, as a proportion of its total size, than the microinjected ICM cell clone. A significant reduction in total cell number in *Tead4*-KD embryos versus microinjected control embryos was also observed. However, this reduction can be accounted for by an increased incidence of apoptosis within outer-residing cells of the microinjected clone, presumably unable to adapt to a spatial location that requires them to differentiate towards TE.

Overall, it was found that individual ICM cells from either the non-microinjected and microinjected TE-inhibited clones of *Tead4*-KD embryos did not segregate between the EPI and PrE in a manner that would be consistent with them being generated with equal potential. Rather TE-inhibited ICM cells preferentially allocated to the EPI, with the non-microinjected cell clone contributing a greater proportion of its cells to the PrE. Importantly, this result was consistently observed irrespective of the combination of specific antibody markers used to assay the emerging late blastocyst cell lineages, thus validating the functional relevance of the ICM allocation phenotype observed. It has previously been reported that the ICMs of late blastocyst stage embryos can present with cells expressing neither an EPI or PrE marker (Frankenberg *et al.*, 2011; Plusa *et al.*, 2008). Consistent with these reports, such incidences, using the anti-Gata4/ Nanog antibody combination, of late blastocyst stage ICM cells that were either negative or positive for both ICM markers were observed, albeit at very low frequencies and in both the control and *Tead4*-KD embryo groups (on average less than one cell per embryo in both conditions – Fig. 4.3d).

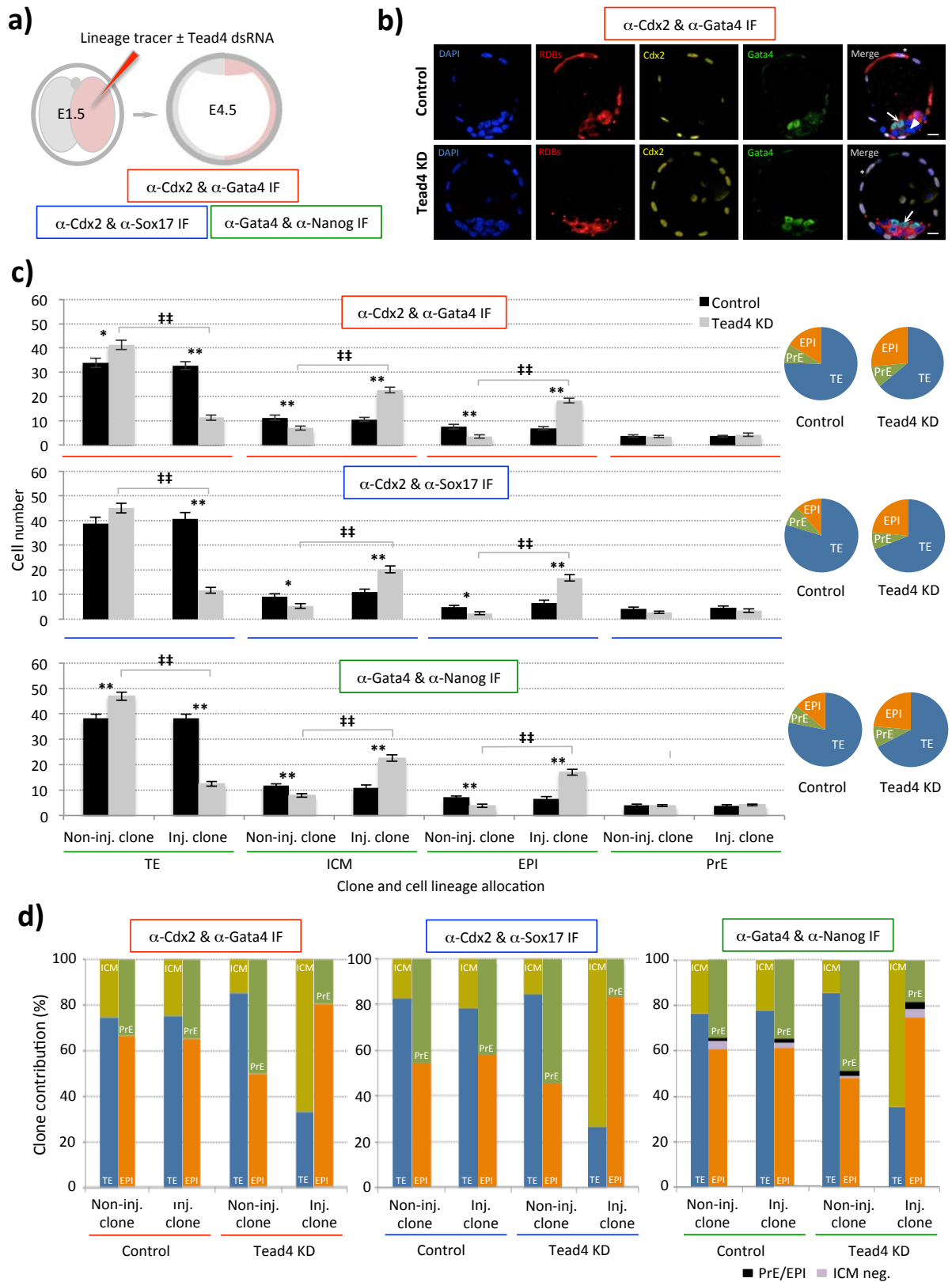


Figure 4.3 (legend overleaf)

Figure 4.3 Inhibition of TE-differentiation within half of the embryo preferentially biases cells to EPI versus PrE fate. a) Experimental strategy to effect clonal *Tead4*-KD and TE-inhibition in one-half of the embryo and assess cell lineage allocation in late blastocysts (E4.5) via immuno-fluorescence detection of marker gene expression, using: i) Cdx2 (TE) & Gata4 (late PrE) - red, ii) Cdx2 & Sox17 (early PrE) – blue, and iii) Gata4 & Nanog (EPI) – green, (*n.b.* inner-cells devoid of either lineage marker in i) and ii) were classified as EPI and outer cells devoid of immuno-reactivity in iii) were designated as TE). **b)** Representative single z-plane confocal micrographs of microinjection control and clonal *Tead4*-KD late blastocyst (E4.5) embryos immuno-stained for Cdx2 (pseudo-coloured yellow) and Gata4 (green) protein expression. Progeny of the microinjected cell are distinguishable by co-injected RDB fluorescence (red). DNA is counterstained with DAPI (blue). Merged image asterisks represent exemplar cells classified in our analyses as TE, arrows as PrE cells and arrow-heads as EPI. Scale bars = 10µm. **c)** Average number of cells from either non-microinjected or microinjected cell clones contributing to late blastocyst (E4.5) lineages, in control and clonal *Tead4*-KD embryos, immuno-stained in each of the three regimes outlined in a). Error bars represent s.e.m.; * / ** and ‡ / †† denote statistically significant differences between equivalent cell clones of control and clonal *Tead4*-KD embryos, or between cell clones within control and clonal *Tead4*-KD embryo groups, respectively ($p < 0.05$ and $p < 0.005$, 2-tailed student t-tests). The relative average percentage contribution of total cell number to each late blastocyst lineage in both control- and *Tead4*-KD embryos is also provided as a pie-chart. **d)** Averaged percentage contribution of non-microinjected and microinjected cell clones, of control and clonal *Tead4*-KD embryos, immuno-stained according to the three regimes outlined in a), between the TE (blue) & ICM (yellow) and the PrE (green) & EPI (orange) of analysed late blastocysts (E4.5). In the anti-Gata4/ Nanog immuno-stained embryo groups, the contribution of ICM cells either positive or negative for both PrE and EPI marker gene expression are shown in black and violet, respectively. Overall, for control embryos $n = 24, 13$ & 25 and for clonal *Tead4*-KD embryos $n = 24, 9$ & 23 in each of the three immuno-staining regimes outlined in a), respectively.

Although there was a statistically significant increased frequency of cells exhibiting negative immuno-fluorescence for each marker in the microinjected clone of *Tead4*-KD embryos, when compared with both the non-microinjected clone or the equivalent clone of control embryos, it was in overall numbers extremely modest (0.9 ± 0.2 cells per embryo versus 0.0 and 0.3 ± 0.1 , respectively). Moreover, it was insufficiently large to explain the increased contribution of cells classified as EPI in embryos that were assessed by immuno-fluorescent staining for either Gata4/ Cdx2 or Sox17/ Cdx2 (Fig. 4.3) as being derived from unspecified ICM cells.

Therefore the collective interpretation of these experimental datasets, demonstrates that the clonal inhibition of TE cell fate does bias internalised ICM progeny towards EPI rather than PrE formation, albeit with a very small number of ICM cells remaining uncommitted to either lineage. Moreover, this correlates with TE-differentiation potentiating later PrE differentiation, as suggested by the integrated cell-fate model. However, inhibition of TE-differentiation is not an impermeable block to future PrE formation, as cells derived from the TE-inhibited clone can populate the PrE but at much reduced frequency.

4.1.2.2 Inhibition of TE-differentiation within a quarter of the embryo also biases cells to EPI versus PrE fate

Despite the above approach of clonally down-regulating *Tead4* expression from the 2-cell stage being reproducibly associated with preferential EPI versus PrE fate in the ICM, a consciousness that the ICMs of such embryos (as a result of an excessive allocation of *Tead4*-KD cell clone to the ICM) were on average much larger than those of control microinjected embryos (e.g. 29.6 ± 1.5 cells in *Tead4*-KD versus 21.8 ± 1.0 cells in control microinjected embryos immuno-stained for Gata4 and Cdx2), was recognised. Coupled with the fact that average number of PrE cells in both conditions was statistically equal (e.g. 7.8 ± 0.8 cells in *Tead4*-KD and 7.4 ± 0.6 cells in control microinjected embryos immuno-stained for Gata4 and Cdx2), it was decided to test if the extra EPI cell contribution observed in TE-inhibited clones was not simply a function of embryos at the late blastocyst (E4.5) stage only being able to support a finite number of PrE cells; hence raising the possibility that the observed results were only consequent to excessive developmental regulation (*i.e.* that once a finite number of PrE cells had been specified, any extra ICM cells would be defaulted to form EPI). Thus, it was decided to create embryos that contained smaller sized TE-inhibited cell clones and to assay if the observed bias against PrE contribution persisted.

Accordingly, single individual blastomeres of mid-4-cell stage (E2.0) embryos were microinjected with *Tead4*-dsRNA plus RDBs (or RDBs alone, as a microinjection control group), causing *Tead4*-KD in one quarter of the embryo. Following microinjection, the embryos were cultured until the late blastocyst stage (E4.5), fixed and immuno-fluorescently stained for Gata4 and Cdx2 (Fig. 4.4 and supplementary tables ST10 and ST11 for individual embryo data; n=19 control microinjected and n=29 *Tead4*-KD embryos). This analysis revealed very similar results to that described above for the 2-cell stage microinjected embryos experiments. Namely, cells of *Tead4*-KD clone preferentially allocated towards the ICM and away from TE cell lineage, when compared to the equivalent microinjected cell clone of control embryos (Fig. 4.4e,e'). More importantly, the increase in the ICM cell number of *Tead4*-KD clone was solely due to greater EPI cell contribution, with the average PrE cell numbers remaining unchanged, again relative to control microinjected embryos (4.4e'). Consistently, the *Tead4*-dsRNA microinjected, ICM residing, cell clone contributed a significantly smaller percentage of its cells to the PrE than either its non-microinjected ICM residing sister cell clone or either of the two clones in control embryos (Fig. 4.4g). Therefore these data, again point to the TE-inhibited/ *Tead4*-dsRNA microinjected, cell clone being biased away from contributing to the differentiating PrE, in favour of populating the pluripotent EPI.

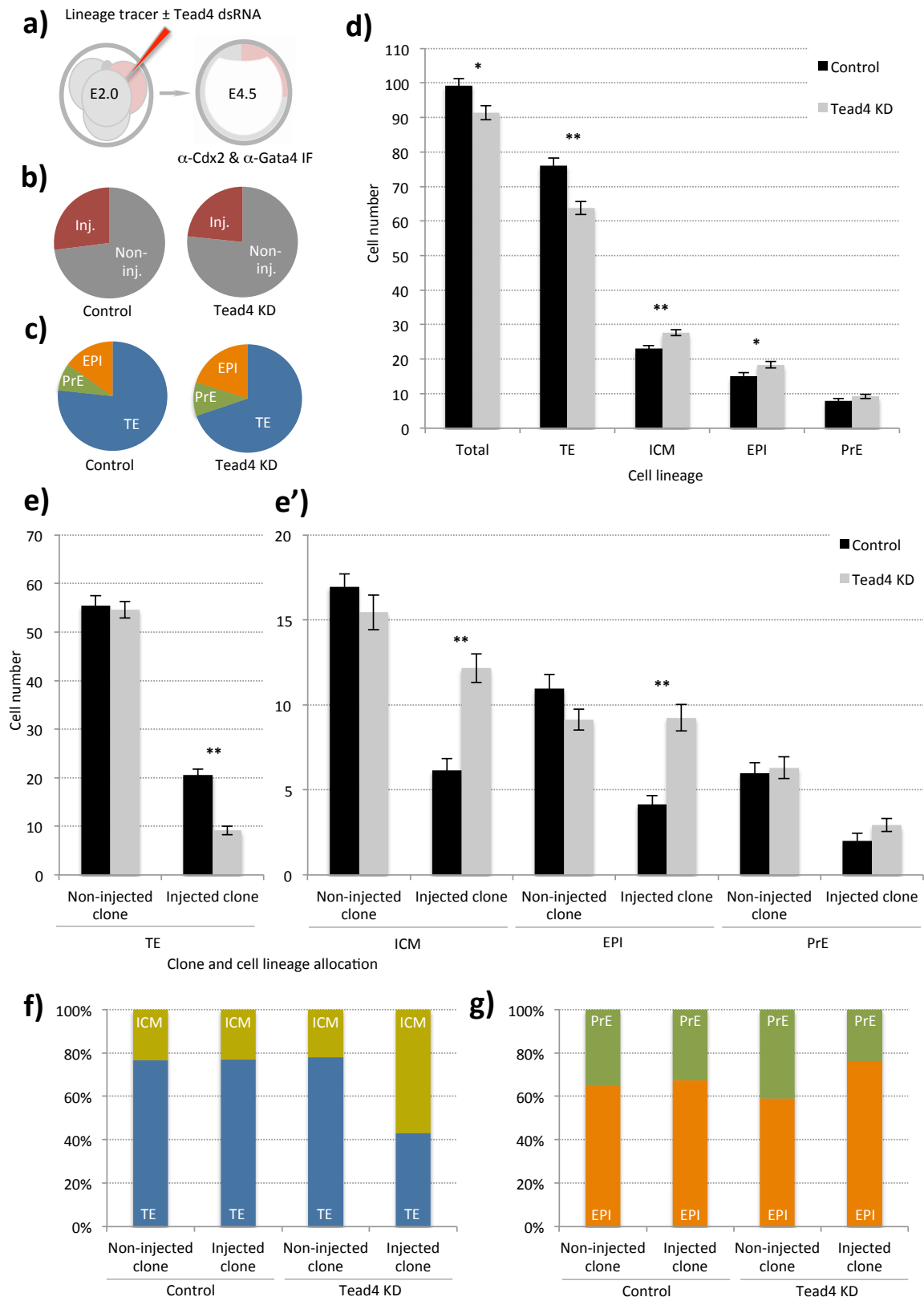


Figure 4.4 (legend overleaf)

Figure 4.4 Inhibition of TE-differentiation within a quarter of the embryo also biases cells to EPI versus PrE fate. **a)** Schematic of the experimental strategy to effect clonal *Tead4*-KD and TE-inhibition in one-quarter of the embryo and assess cell lineage in late blastocysts (E4.5) via *Cdx2* (TE marker) and *Gata4* (late PrE marker) immuno-fluorescence detection. **b)** Average total cell percentage contribution of microinjected and non-microinjected cell clones in control and *Tead4*-KD embryos. **c)** Relative percentage contribution of total cell number to the late blastocyst lineages (TE, PrE and EPI) in control and *Tead4*-KD embryos. **d)** Averaged total cell number for each late blastocyst lineage (ICM = EPI + PrE) in *Tead4*-KD and control embryos. **e)** Average number of cells from either non-microinjected or microinjected cell clones in TE lineage, in control and *Tead4*-KD embryos. **e')** As in e) but describing contribution to the other late blastocyst lineages. In d), e) and e') error bars represent s.e.m; */ ** denote statistically significant differences between equivalent cell clones of control and *Tead4*-KD embryos (confidence intervals of $p < 0.05$ and $p < 0.005$, 2-tailed student t-tests). **f)** Percentage contribution of non-microinjected and microinjected cell clones, of control and *Tead4*-KD embryos, to TE or ICM of late blastocysts. **g)** Percentage contribution of non-microinjected and microinjected ICM cell clones, in control and *Tead4*-KD embryos, to PrE or EPI lineages. Overall, control embryos $n = 19$ and *Tead4*-KD embryos $n = 29$.

However, unlike the situation documented after microinjecting *Tead4*-dsRNA into single blastomeres at the 2-cell stage (E1.5), the derived non-microinjected cell clone arising from these 4-cell stage (E2.0) microinjections did not display any statistically significant evidence of compensatory regulation. For example it did not contribute extra TE cells to compensate for the increased ICM/ EPI contribution of the *Tead4*-dsRNA injected clone, nor did it contribute fewer cells to the ICM/ EPI. These data suggest less of an overall requirement for such 4-cell stage (E2.0) microinjected embryos to regulate their development, most probably owing to the smaller size of the *Tead4* KD cell clone; although they did exhibit significantly fewer TE cells than the control microinjection embryos. Although, this reduced TE number could again be accounted for by increased incidence of apoptosis within the outer-residing cells of the *Tead4* KD cell clone as was the case for embryos microinjected at the 2-cell stage.

Overall the smaller *Tead4*-KD cell clone obtained by microinjecting single 4-cell stage (E2.0) embryos was biased against forming PrE within the ICM of embryos that exhibited evidence of less regulated development. However, despite this TE-inhibited clone being smaller on average than that derived after 2-cell stage (E1.5) microinjections, the average ICM size of such *Tead4*-KD embryos was still greater than the ICM size observed in control microinjected embryos (27.6 ± 0.9 cells in *Tead4*-KD embryos versus 23.1 ± 0.9 cells in control embryos).

4.1.2.3 Inhibition of TE-differentiation within small chimeric ICM clones also biases against ultimate PrE cell fate

Since the previous two experimental strategies used to clonally down-regulate *Tead4* yielded late blastocysts (E4.5) with larger averaged size ICMs than observed in control groups, an alternative

strategy was employed to create even smaller sized clone of TE-inhibited cells that involved the generation of chimeric embryos. Accordingly, the aggregation of non-compacted 8-cell stage (E2.5) embryos with a single developmental stage matched donor blastomere in which *Tead4* expression had previously been down-regulated was undertaken (Fig. 4.5a). The resulting embryo chimeras contained marked TE-inhibited clones (*Tead4*-KD-chimeras) equivalent to one-ninth of their initial total cell number and when *in vitro* cultured to the last blastocyst stage were morphologically indistinguishable from control-clone containing chimeras (referred to as control-chimeras; see supplementary tables ST12 and ST13 for individual embryo data). Importantly, when cell lineage segregation was assayed in such chimeric embryos, it was discovered that the total ICM cell number of *Tead4*-KD-chimeras was not statistically different from control-chimeras (20.9 ± 1.0 versus 19.0 ± 0.9 cells, respectively). Moreover and in accordance with both of the direct microinjection strategies described above, it was observed that the marked TE-inhibited clone of *Tead4*-KD-chimeras was not only biased to populate the ICM (Fig. 4.5h) but it was also biased, in a statistically significant manner, to contribute to the EPI rather than the PrE (Fig. 4.5i). Therefore, it was found that the inhibition of TE-differentiation within a discreet clone of small size, within ICMs of more physiological appropriate size, also biased cell fate against PrE formation. Overall these data argue that the anti-PrE biases observed in TE-inhibited ICM residing clones, derived from any of the three experimental strategies described, are not simply a function of generating unusually large ICMs.

Overall, the three experimental strategies employed to inhibit the initiation of TE-differentiation, mediated by *Tead4*-dsRNA, in cell clones of varying size in the developing pre-implantation mouse embryo have provided consistent results. Namely, cells of such clones predictably segregate away from the emerging TE cell lineage in favour of populating the ICM. Any cells that remain in inappropriate outer positions are more likely to undergo apoptosis than their inner residing sister cells. However, the enhanced ICM cell contribution of TE-inhibited cell clones is not associated with a subsequent unbiased segregation between EPI and PrE. Rather, the cells of such clones preferentially contribute, in a statistically significant manner, to the pluripotent EPI cell lineage. Expressed alternatively, the clonal inhibition of the initiation of TE cell fate also inhibits the ability of the progeny of that clone to differentiate towards a PrE cell fate, when competing with otherwise unperturbed cells outwith the clone.

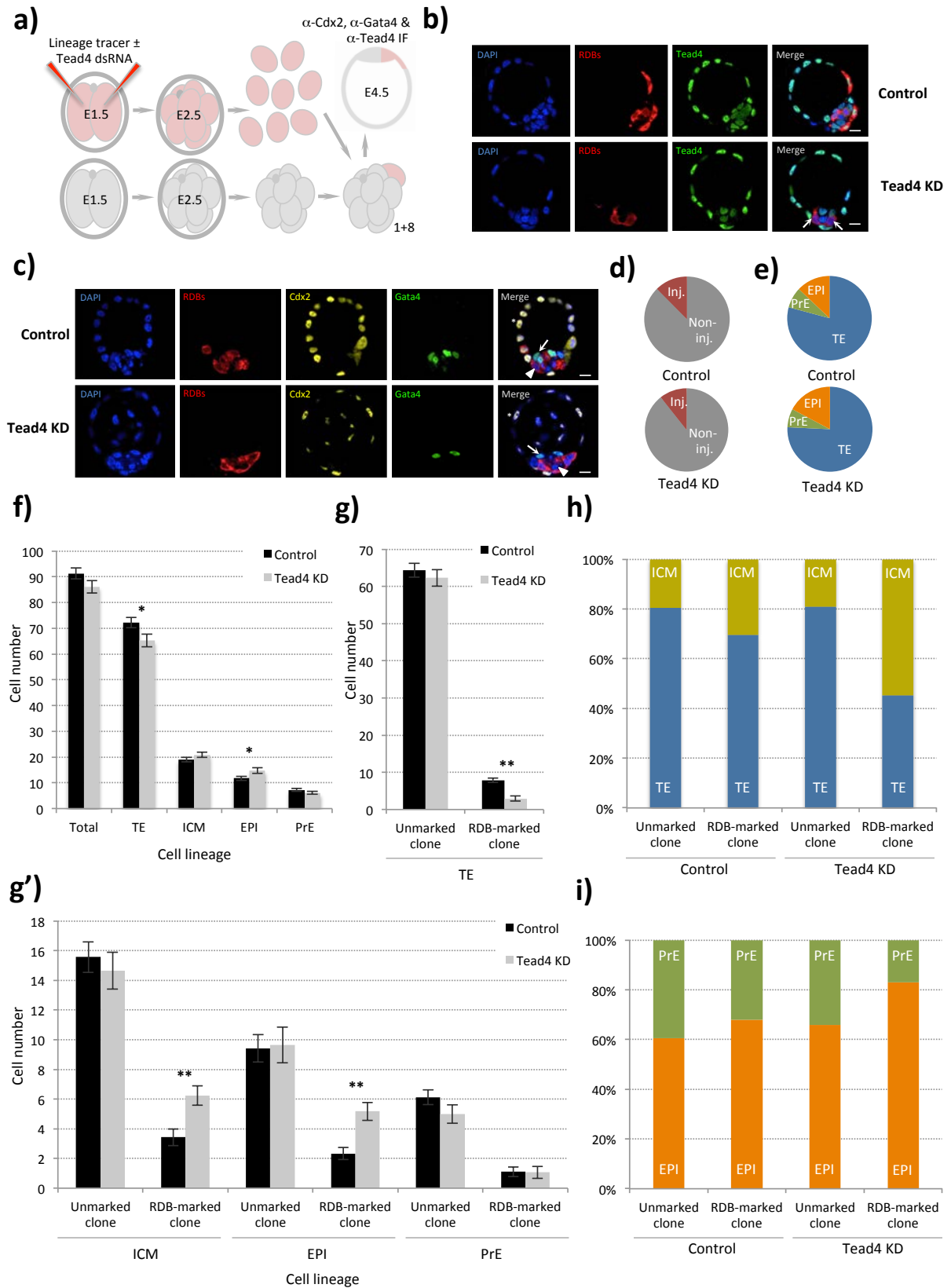


Figure 4.5 (legend overleaf)

Figure 4.5 Inhibition of TE-differentiation within small chimeric ICM clones also biases against ultimate PrE cell fate. a) The experimental strategy to generate embryo chimeras containing TE-inhibited cells equivalent to one ninth of the embryo and to assess late blastocysts (E4.5) lineages, via immuno-fluorescent staining for Cdx2 and Gata4. **b)** Representative single z-plane confocal micrographs of control and *Tead4*-KD clone containing chimeras immuno-stained for Tead4 (green) expression. In merged image arrows denote cells not expressing detectable levels of Tead4 derived from original *Tead4*-KD donor blastomere **c)** Further, representative single z-plane confocal micrographs of late blastocyst (E4.5) chimeras immuno-stained for Cdx2 (pseudo-coloured yellow) and Gata4 (green). Merged image asterisks represent exemplar cells classified in the analyses as belonging to the TE, arrows PrE and arrow-heads EPI. In b) and c), cells deriving from donor blastomeres, themselves originally derived from control or *Tead4*-dsRNA microinjected 2-cell (E1.5) stage embryos, within chimeras are distinguishable by co-injected RDBs (red). DNA is counterstained (DAPI, blue). Scale bars = 10µm. **d)** Average total cell percentage contribution of marked and non-marked cell clones. **e)** Relative average percentage contribution of total cell number to late blastocyst lineages in control- and *Tead4*-KD-chimeras. **f)** Averaged total cell number for each late blastocyst lineage (ICM = EPI + PrE) in control- and *Tead4*-KD-chimeras. **g)** Average number of cells from either RDB-marked or non-marked cell clones in TE lineage, in control and *Tead4*-KD-chimeras. **g')** As in g) but describing contribution to the other late blastocyst lineages. In f), g) and g') error bars represent s.e.m; */ ** denote statistically significant differences between equivalent cell clones of control- and *Tead4*-KD-chimeras ($p < 0.05$ and $p < 0.005$, 2-tailed student t-tests). **h)** Percentage contribution of RDB-marked and unmarked cell clones, in control- and *Tead4*-KD-embryos, to TE or ICM of late blastocysts. **i)** As in h) but describing PrE and EPI lineage contribution in ICM. Overall, control-chimeras $n = 30$ and *Tead4*-KD-chimeras $n = 17$.

4.1.3 Molecular characterisation of attenuated PrE formation in TE-inhibited cell clones

Next, the molecular mechanisms underlying the observed bias were experimentally addressed; as such three scenarios that could explain why *Tead4*-KD cell clone would be biased to contribute more towards EPI over PrE lineage were formulated and tested. The first possibility was that the inactivation of the Hippo signalling pathway/ *Tead4* activity (*n.b.* *Tead4* and *Yap1* represent the transcriptional effectors of inhibited Hippo signalling; Nishioka *et al.*, 2009) within the ICM might have a direct effect for the appropriate specification of PrE lineage. Alternatively, it was considered that cellular polarity establishment may have been affected after *Tead4* down-regulation and subsequently influenced the ability of PrE progenitor cells to mature. Lastly, the possibility that *Tead4* itself might be either directly or indirectly involved in regulation of EPI and PrE lineage marker gene expression. Therefore, in the following result section, the attempts to uncover the mechanism causing attenuated PrE formation in the internalised TE-inhibited cell clones will be described.

4.1.3.1 Hippo signalling pathway inactivation within the ICM is unlikely to be required for appropriate PrE formation

A simple explanation for the observed attenuated PrE formation in the internalised TE-inhibited cell clones, could be that Hippo signalling pathway inactivation, and hence Tead4 activity (in combination with nuclear localised Yap1) within the ICM might be directly required for appropriate PrE formation.

In order to examine this possibility, 2-cell (E1.5) stage embryos were recovered and *in vitro* cultured until the late blastocyst (E4.5) stage. Following fixation, the embryos were subject to confocal-based immuno-fluorescence microscopy to assay for the expression and subcellular localisation of Yap1 protein (using an anti-sera that does not discriminate between Yap1 phospho-forms) and the definitive PrE marker, Gata4. Under this regime, Yap1 protein localisation served as the readout of Hippo signalling activity, while the presence of Gata4 was an indicator of a proper PrE maturation. As presented in the figure 4.6b, the exclusion of Yap1 protein from the nuclei of all ICM cells indicates the Hippo signalling pathway is active (and therefore Tead4 is inactive) throughout the entire ICM at this stage. Furthermore, the obvious presence of nuclear Gata4 localisation in the surface cell layer of the ICM, adjacent to the blastocoel, clearly demonstrates appropriate spatial and temporal formation of the PrE lineage. Therefore, this observation strongly suggests that Tead4 activity and Hippo signalling pathway inactivation are not required, at least in a manner similar to that reported for TE derivation, for appropriate PrE formation.

Nevertheless, it was further decided to investigate Yap1 localisation and Hippo signalling pathway activity in both control microinjected and clonal *Tead4*-KD embryos, throughout the pre-implantation mouse embryo development period. Accordingly, 2-cell (E1.5) stage single blastomere microinjections were again employed to introduce RDBs \pm *Tead4*-dsRNA, and the microinjected embryos were cultured until the mid-16-cell (E3.1), 32-cell (E3.6) and >64-cell (E4.5) stages, fixed and assayed for Yap1 protein expression/ intra-cellular localisation alone or in combination with Gata4. The assay of Yap1 localisation in *Tead4*-KD embryos at mid-16-cell stage (E3.1) showed that apart from being present in the nuclei, Yap1 was unusually enriched in the cytoplasm of the outer-residing cells of the TE-inhibited clone (Fig. 4.6d). This was in contrast to the more typical nuclear localisation pattern observed in the outer-residing cells of the non-microinjected sister clone or within the outer cells of either clone in control embryos. By the 32-cell (E3.6) stage, such Yap1 mis-localisation to the cytoplasm of outer-residing TE-inhibited cells became more prominent. Using anti-sera previously reported (Nishioka *et al.*, 2009) to only recognise phosphorylated Yap1 (pYap1), it was determined that the mis-localised Yap1 was non-phosphorylated (see supplementary figure S4); thus confirming

the atypical cytoplasmic localisation was not because of the induction of activated Hippo signalling. Although not directly addressed here, it is possible that this observation may reflect the lack of a mechanism to retain Yap1 in the nucleus given its binding partner's (*i.e.* Tead4) absence, and thus reflects the existence of a speculative equilibrium between the active nuclear import and passive export of non-phosphorylated Yap1. Curiously, nuclear localisation of pYap1 in outer mid-16-cell stage blastomeres, both within and outside the Tead4-dsRNA microinjected clone, was also observed. The significance of this outer cell nuclear localised pYap1, at this developmental stage is unclear and unintuitive. However, it is important to note that pYap1 was predominantly cytoplasmic in the inner cells of the same assayed embryos, in a manner supportive of its characterised role in functional Hippo signalling in this spatial embryonic compartment. However, in agreement with the notion that the Hippo signalling pathway is retained in an active state in all ICM cells, Yap1 localisation was found to be consistently enriched in the cytoplasm of all inner cells at all examined stages, irrespective of the clonal origin (Fig. 4.6d). More importantly, at >64-cell (E4.5) stage, Gata4 positive cells exhibited cytoplasmic localisation of Yap1 in both *Tead4*-KD and control microinjected embryos.

Overall, these results demonstrate that Yap1 localisation is restricted to the cytoplasm of ICM cells, from when they are first generated and throughout the entire remaining period of pre-implantation mouse embryo development; thus, indicating that Hippo signalling is permanently active in inner cells during the segregation of the EPI and PrE lineages. This strongly suggests that the appropriate formation of PrE does not require Hippo signalling pathway inactivation and as a consequence Tead4 activity within the ICM (*i.e.* Tead4 becoming functionally enabled within the nuclei of ICM cells, by an association with its cognate binding partner Yap1). Interestingly, even though the absence of Tead4 does not result in ectopic Hippo signalling pathway activation, its presence is required for the appropriate nuclear localisation of Yap1 in outer-residing cells.

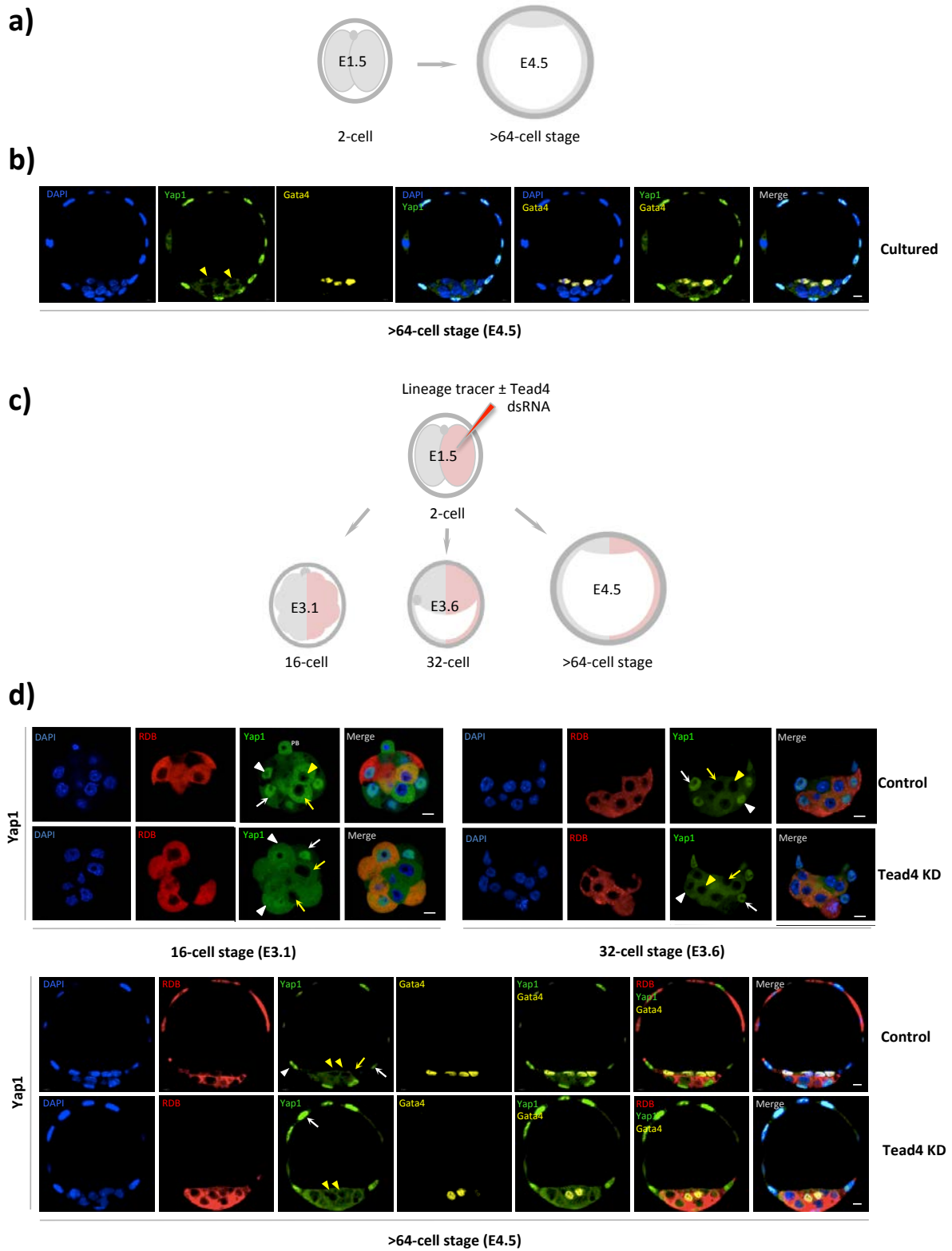


Figure 4.6 (legend overleaf)

Figure 4.6 Cytoplasmic Yap1 localisation within the ICM is indicative of an active Hippo signalling pathway. **a)** A schematic representation of the experimental strategy to assay, via confocal immuno-fluorescent staining, Yap1 localisation in undisturbed culture control embryos harvested at 2-cell stage and *in vitro* cultured until the late blastocyst (E4.5) stage. **b)** Representative single confocal z-plane micrographs of undisturbed culture control embryos immuno-fluorescently stained for Yap1 (green; note that anti-sera does not discriminate between phosphorylated or non-phosphorylated forms) and Gata4 (yellow) at late blastocyst (E4.5) stage. **c)** A schematic representation of the experimental strategy to assay, via confocal immuno-staining, Yap1 localisation in TE-inhibited clones (comprising half the embryos cells) at the mid-16-cell (E3.1), 32-cell (E3.6) or >64-cell (E4.5) stages. **d)** Representative single confocal z-plane micrographs of control and *Tead4*-KD embryos immuno-stained for Yap1 (green) at the mid-16-cell (E3.1), 32-cell (E3.6) or Yap1 (green) and Gata4 (yellow) at >64-cell (E4.5) stages. In **b)** and **d)**, DNA DAPI counter-stain (blue) and RDB marked microinjected clones (red) are also shown. Arrows and arrow-heads highlight exemplar Yap1 protein localisation within non-microinjected and microinjected clones respectively. White arrows or arrow-heads indicate staining in outer-cells and yellow variants in inner-cells (second polar body = 'PB'). Scale bars = 10µm.

4.1.3.2 Cell polarity establishment is largely unaffected in TE-inhibited cells

Under unperturbed *in vitro* culture developmental conditions, PrE progenitor cells that reach the ICM/blastocoel interface have to polarise in order to be able to maintain their position and participate in the formation of the maturing PrE epithelium. The enrichment of *Prkcz/i* protein in such PrE progenitor cells and its requirement for polarisation and subsequent appropriate PrE lineage maturation has recently been demonstrated (Saiz *et al.*, 2013). In addition, it has previously been proposed that *Cdx2* might be involved in the transcriptional regulation of *Prkcz/i* (Jedrusik *et al.*, 2008). Therefore, by preventing *Cdx2* expression after knocking-down *Tead4* expression it could be speculated that the appropriate establishment of cell polarity would be impaired, with the consequence that any generated ICM cells may have decreased potential to polarise. In turn, such a reduced capacity to polarise could lead to a reduced contribution of *Tead4*-KD cell clones contributing to the PrE lineage. Thus, it was decided to test if cell polarity was affected in the TE-inhibited cell clone generated. Accordingly, 2-cell (E1.5) stage single blastomere microinjections with RDBs ± *Tead4*-dsRNA were repeated and the embryos *in vitro* cultured until the mid-16-cell (E3.1) and 32-cell (E3.6) stages. Fixed embryos were then assayed for apical polarity (pERM, short for phospho-Ezrin/Radixin/Moesin; the anti-pERM antibody detects phosphorylated form of three closely related proteins of ERM-family, *Prkcz/i* and *Pard6b*), basolateral polarity (*Scrib*) and the adherens junction (*Cdh1*) marker protein expression and sub-cellular localisation by confocal immuno-fluorescence microscopy.

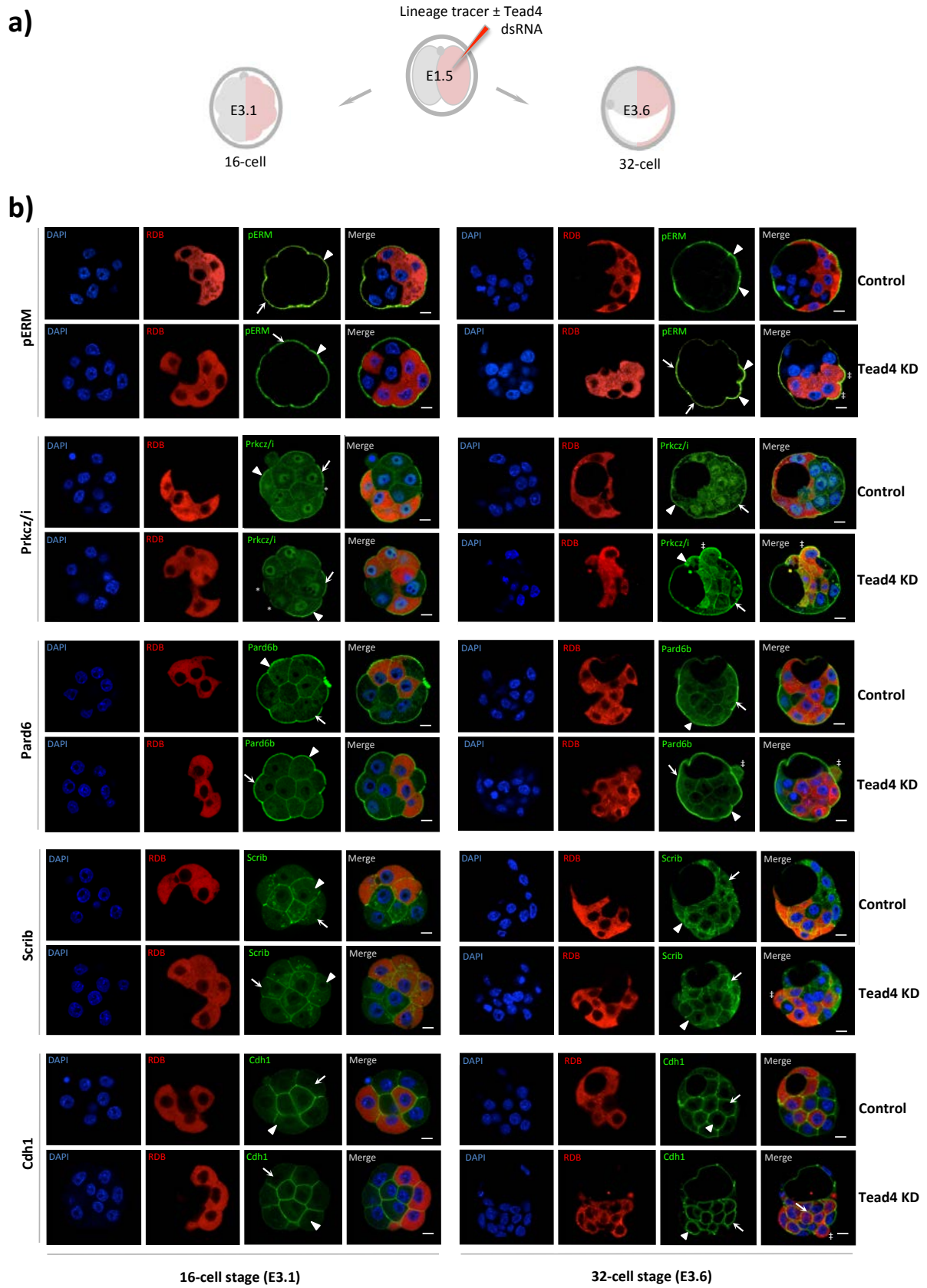


Figure 4.7 (legend overleaf)

Figure 4.7 Clonal down-regulation of *Tead4* expression is not associated with reduced expression nor mis-localisation of cell polarity markers. **a)** A schematic of the experimental strategy to assay, via confocal immuno-fluorescent staining, the apical polarity markers (pERM, also known as phospho-Ezrin/Radixin/Moesin, Prkcz/i and Pard6b), the basolateral polarity marker (Scrib) and the adherens junction marker (Cdh1) expression in TE-inhibited clones (comprising half the embryos cells) at the mid-16-cell (E3.1) or 32-cell (E3.6) stages. **b)** Representative single confocal z-plane micrographs of control and *Tead4*-KD embryos immuno-fluorescently stained for pERM, Prkcz/i, Pard6b, Scrib and Cdh1 expression (all in green) at the mid-16-cell and 32-cell stages. DNA DAPI counter-stain (blue) and RDB marked microinjected clones (red) are also shown. Arrows denote exemplar outer-cell apical domains immuno-fluorescently stained for either pERM, Prkcz/i or Pard6b or basolateral domains immuno-fluorescently stained for Scrib and Cdh1, derived from the non-microinjected cell clone of both control and *Tead4*-KD embryos, whereas, arrow-heads highlight the same within the microinjected cell clone. Asterisks denote outer 16-cell stage embryo cells exhibiting reduced apical immuno-fluorescent staining for either Prkcz/i or Pard6b that is not restricted to one or other clone in either control or *Tead4* KD experimental embryos. Double cross-hairs in merged images highlight outer-cells from the microinjected cell clone of *Tead4* KD embryos that exhibit atypical rounded morphology at the 32-cell stage (E3.6), irrespective of the primary antibody used in the immuno-staining procedure. However such cells are typically associated with enhanced apical pERM or Prkcz/i immuno-staining. Scale bars = 10µm.

The indicated analyses did not reveal any differences in the expression level or alterations in localisation of either the respective apical pERM/Prkcz/i/Pard6b or basolateral Scrib/Cdh1 marker proteins between the non-microinjected and microinjected cell clones of both control and *Tead4*-KD embryos at the 16-cell stage (Fig. 4.7b). It is noteworthy that some outer 16-cell stage blastomeres were observed to exhibit substantially reduced apical pERM or Prkcz/i immuno-fluorescence at frequencies similar to recent reports (Anani *et al.*, 2014); however such cells were present in both the TE-inhibited and microinjection control clone containing embryo groups (and in non-microinjected cells clones) to the same extent and therefore did not correlate with TE-inhibition. However at the 32-cell (E3.6) stage, enhanced apical polarity (evidenced by pERM and Prkcz/i immuno-staining) associated with atypical rounded non-TE like morphology was observed within outer-residing TE-inhibited cells at frequencies consistent with subsequent apoptosis. In contrast, there were no obvious defects in basolateral polarity or cell adhesion molecule localisation as determined by Scrib and Cdh1 immuno-staining at the 32-cell (E3.6) stage.

Taken altogether, apical polarisation deficits or intracellular mis-localisations within TE-inhibited clones that could have potentially led to the generation of ICM cells with the reduced capacity to polarise, were not observed. Therefore, it is unlikely that defective cell polarity establishment could be responsible for the reduced contribution of the internalised TE-inhibited clone towards the PrE lineage.

4.1.3.3 Inhibition of TE-differentiation is associated with unaltered expression of EPI and decreased expression of PrE lineage markers

Given that TE-inhibited cell clones within the ICM are biased away from the PrE lineage in favour of EPI, experiments designed to ascertain if this segregation towards EPI cell fate was associated with precocious and/ or increased expression of the EPI marker gene *Nanog* (Chazaud *et al.*, 2006; Mitsui *et al.*, 2003) or perhaps diminished expression of PrE markers, were conducted.

Accordingly, Q-RTPCR analyses on 16- (E3.1) and 32-cell (E3.6) stage embryos that had been microinjected in both blastomeres at 2-cell (E1.5) stage with RDB \pm *Tead4*-dsRNA, to exert TE-inhibition across whole embryo, were performed to examine the expression level of EPI and PrE lineage markers (Fig. 4.8a). The normalised mRNA expression levels of the following genes were assayed: *Nanog* (the pluripotency related transcription factor (Chambers *et al.*, 2003; Mitsui *et al.*, 2003) known to be a marker that distinguishes the EPI from the PrE cell lineage in mature (E4.5) blastocysts (Chazaud *et al.*, 2006), *Fgfr2* (known to integrate *Fgf4* signalling in the ICM to promote PrE cell differentiation and formation (Nichols *et al.*, 2009; Yamanaka *et al.*, 2010; Frankenberg *et al.*, 2011; Morris *et al.*, 2013)), *Dab2* (Disabled homolog 2; a characterised PrE marker, exhibiting detectable protein expression in E4.5 stage blastocysts, that is required for appropriate endodermal cell positioning (Yang *et al.*, 2002, 2007)) and *Lrp2* (LDL receptor related protein 2; a marker of progenitor PrE cells in the ICM that is detectable from E3.5 (Gerbe *et al.*, 2008)). It was discovered that *Nanog* transcript levels remained unchanged by *Tead4*-KD/ TE-inhibition at both stages assayed (Fig. 4.8a). Moreover, that an assay of *Nanog* protein expression, utilising the clonal down-regulation model by microinjecting one blastomere at the 2-cell (E1.5) stage (to permit side-by-side comparison of *Nanog* protein levels in non-microinjected and TE-inhibited microinjected clones by confocal immuno-fluorescent microscopy), similarly reported unchanged *Nanog* protein expression levels between TE-inhibited and non-microinjected clones and either of the clones of the control microinjected embryo group (Fig. 4.8b). Therefore, the increased number of ICM/ EPI cells observed in *Tead4*-KD embryos can not be accounted for by enhanced or precocious *Nanog* expression. Next, the expression of PrE related genes was investigated and it was found that both *Lrp2* and *Dab2* mRNA levels were down-regulated by >95%; indicating that the TE-inhibition causes deficits in the expression of genes required for appropriate PrE formation. In addition, a 40% reduction in *Fgfr2* mRNA expression was also detected (Fig. 4.8a). Given the centrally important role of the *Fgf4* signalling pathway within the maturing ICM in promoting successful derivation of the PrE (Frankenberg *et al.*, 2011), it was decided to assay the expression of *Fgfr2* at the protein level (Fig. 4.8c). To this end, 32-cell (E3.5) stage embryos derived from *in vitro* cultured 2-cell stage (E1.5)

embryos that had been microinjected in a single blastomere with fluorescent Oregon-green conjugated dextran beads (OGDBs) \pm Tead4-dsRNA, were fixed and immuno-fluorescently stained using an anti-Fgfr2 antibody. In control microinjected embryos, Fgfr2 protein was observed associated with the plasma membrane in regions demarking the approximate boundary between TE and ICM cells. At the resolution used it was not possible to ascertain if the signal was derived from either the outer or inner, or indeed both cells. However, it was also possible to observe similar Fgfr2-derived signals in regions of the ICM that were consistent with cell-to-cell contact regions between fellow ICM cells, thus confirming some Fgfr2 protein expression within cells of the ICM. Notably not all the potential ICM-to-ICM cell contact regions exhibited this anti-Fgfr2 derived signal, therefore indicating that there is heterogeneous inter-cell, membrane associated, Fgfr2 protein expression within the ICM of such microinjection control embryos. This is consistent with similar heterogeneous and reciprocal inter-cell expression pattern of EPI (Nanog) and early PrE (Gata6) marker protein expression, characterised as the 'salt and pepper' pattern (Chazaud *et al.*, 2006). When embryos containing Tead4-dsRNA mediated TE-inhibited clones were assayed, it was not possible to detect any membrane associated Fgfr2 protein in any ICM-to-ICM cell contact regions within the *Tead4*-KD clone; although membrane association at the boundary between ICM cells within the clone and outer-TE cells outwith the clone were detectable. Moreover, these inner cells also exhibited prominent levels of nuclear localised Fgfr2. Interestingly, nuclear localised Fgfr2 protein expression was seen in some, but not all, ICM cells of control embryos, with the suggestion that such cells also lacked plasma membrane associated Fgfr2 in their ICM-to-ICM cell contact regions, akin to the TE-inhibited clones (Fig. 4.8c). Thus, it is appealing to speculate that nuclear sequestration of Fgfr2 away from the plasma membrane, be it in a subset of ICM cells of control embryos or within the TE-inhibited clones of *Tead4* KD embryos, blunts their capacity to respond to Fgf4 signals at the plasma membrane, thus promoting the acquisition of EPI cell fate.

Taken together this data indicates that the biased contribution of internalised TE-inhibited cell clones towards EPI and away from PrE cell fate is unlikely to be driven by precocious or increased expression of the EPI marker Nanog but instead more likely to be caused by sequestration of Fgfr2 protein away from the plasma membrane of ICM cells and/ or decreased expression levels of PrE lineage markers, such as *Dab2* and *Lrp2*.

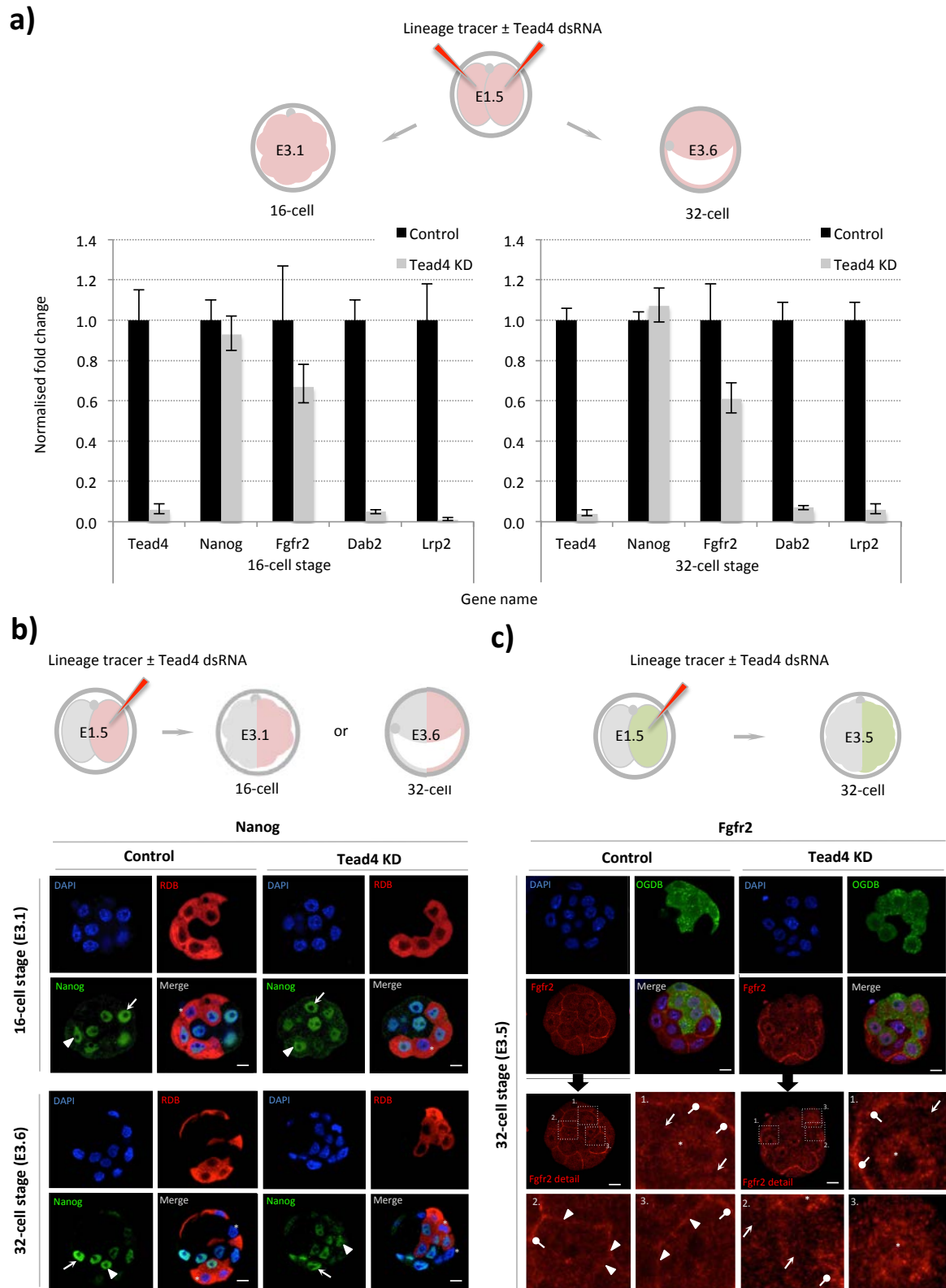


Figure 4.8 (legend overleaf)

Figure 4.8 Global and clonal TE-inhibition; no enhanced *Nanog* expression prior to 32-cell stage but attenuated PrE-specific marker expression. **a)** The experimental strategy to down-regulate *Tead4* expression and inhibit TE-differentiation throughout all cells of the embryo prior to Q-RTPCR analysis (upper). Normalised expression fold changes, resulting from *Tead4*-KD, of the stated transcripts at the mid-16-cell (E3.1) or 32-cell (E3.6) stages (lower panels). Individual gene mRNA levels were normalised against *Rpl23* and/ or *H2afz* transcript levels within control and experimental knockdown conditions prior to fold change calculation. Errors = s.e.m, n = at least 2 for biological and 3 for technical replicates (*n.b.* *Tead4* specific data is repeated from Fig. 4.1 as Q-RTPCR was performed from same cDNA preparations). **b)** Confocal microscopy analysis of *Nanog* (green) expression after clonal *Tead4*-KD at the mid-16-cell (E3.1) and 32-cell (E3.6) stages. Arrows and arrow-heads denote exemplar *Nanog* expression in non-microinjected and microinjected clones, respectively. Asterisks highlight TE cells without *Nanog* expression reflecting previously characterised inter-cell heterogeneity. **c)** Confocal microscopy analysis of *Fgfr2* (red) expression after clonal *Tead4*-KD at the 32-cell (E3.5) stage. Representative single z-plane confocal micrographs are shown (middle panels) with the lower 4 panels detailing magnified anti-*Fgfr2* immuno-stained images, according to numbered regions of interest. Arrow-heads highlight plasma membrane associated *Fgfr2* between neighbouring ICM cells (control embryos) and arrows approximate equivalent regions of other neighbouring ICM cells without anti-*Fgfr2* signal (illustrating heterogeneous *Fgfr2* expression within control embryo ICMs). Similarly, arrows show ICM cell boundaries between cells of the microinjected clone devoid of *Fgfr2* in *Tead4*-KD embryos. Asterisks and lollipop markers, in both control and *Tead4*-KD embryos, show nuclear *Fgfr2* protein (especially in *Tead4*-KD embryos) or expression at the interface of TE and ICM cells, respectively. In both b) and c) progeny cells of microinjected clones are distinguishable by co-injected RDBs (red) or OGDBs (Oregon-green dextran beads – green). DNA was counterstained with DAPI (blue). Scale bars = 10µm.

4.1.4 A minor contribution of *Dab2* to the importance of cell history during the second cell-fate decision (UNPUBLISHED RESULTS)

Dab2 is an adaptor protein involved in clathrin-mediated endocytosis and intra-cellular cargo trafficking. Previous genetic studies have demonstrated that the *Dab2* gene is indispensable during early mouse embryo development as embryos lacking it exhibit early embryonic lethality between E5.5 and E6.5 (Moore *et al.*, 2013; Yang *et al.*, 2002, 2007). The early lethality of *Dab2*-deficient mice has been attributed to the failure of appropriate PrE formation. Importantly, the removal of *Dab2* does not prevent PrE differentiation/ specification (as judged by the presence of *Gata4* positive cells in *Dab2*-deficient embryos) but is instead associated with the inadequate cell positioning within the ICM. Namely, in the absence of *Dab2*, PrE cells fail to position themselves to the ICM surface and appropriately organise to form an epithelium, suggesting that *Dab2* may influence ICM cell migration/ sorting (Yang *et al.*, 2007).

Collectively, these studies indicate that the reduction in *Dab2* transcript levels, observed after *Tead4* down-regulation as described above, may offer an explanation for the attenuated PrE formation within internalised TE-inhibited *Tead4*-KD embryo cell clones.

4.1.4.1 Endogenous Dab2 protein is expressed in both the TE and PrE lineages

To date, Dab2 protein has largely been described in the literature as a late PrE lineage marker, the expression of which was first observed at the late blastocyst (E4.5) stage (Yang *et al.*, 2002). Nevertheless, our Q-RT-PCR results demonstrated that Dab2 mRNA is already present at both mid-16-cell (E3.1) and 32-cell (E3.6) stages and was severely reduced after global *Tead4* down-regulation (Fig. 4.8a); indicating the functional involvement of this TE-lineage specification associated transcription factor (*Tead4*) in the transcriptional regulation of the *Dab2* gene itself. On the basis of this evidence, it was decided to re-examine, in greater detail, the expression pattern of endogenous Dab2 protein during the pre-implantation period of mouse embryo development. Accordingly, recovered 2-cell stage (E1.5) embryos that had been *in vitro* cultured until either the mid-16-cell (E3.1), 32-cell (E3.6) and late blastocyst (E4.5/ E4.75/ E5.0) stages were fixed and assayed by confocal immuno-fluorescent microscopy for Dab2 protein expression (either alone or in combination with *Gata4*). It was discovered that Dab2 protein levels were undetectable at the mid-16-cell stage (data not shown; despite mRNA being detected – see figure 4.8a), however by the 32-cell (E3.6) stage Dab2 protein expression was evident in all TE cells and interestingly exhibited heterogeneity in its level of expression between spatially dispersed cells of the ICM (Fig. 4.9b). Moreover, the expression levels of Dab2 protein in TE cells and Dab2-expressing ICM cells were almost equivalent at this stage. However, by the late blastocyst (E4.5) stage, Dab2 protein levels became significantly elevated in TE cells but remained unchanged between the subsets of ICM cells staining positive for Dab2 protein expression in each of the two examined developmental stages; thus strongly suggesting that Dab2 mRNA (known to be expressed at the 16-cell stage; Fig. 4.8a), inherited from the ancestral outer-residing cells could be entirely responsible for the observed Dab2 protein expression in the ICM at this later stage. Moreover, that functionally important Dab2 heterogeneity within the ICM, potentially relevant to the acquisition/ segregation of EPI and PrE cell fate, may arise from the different timing of ICM founder cell internalisation, and hence Dab2 mRNA inheritance, as proposed by the ‘time-inside/ time-outside’ or ‘combined’ models. As stated above, heterogeneity in Dab2 protein expression between cells of the late blastocyst (E4.5) stage ICM was also observed, but in contrast to the early blastocyst (E3.5) stage, Dab2 expressing cells were preferentially found to reside at the blastocoel facing surface of the ICM (*i.e.* the presumptive PrE layer) rather than being dispersed throughout the ICM. As the embryo progressed further in development, by the hatched blastocyst (E4.75/ E5.0) stage, Dab2 protein expression within the ICM was found to be elevated to a level matching that observed in the TE lineage and was completely restricted to the PrE (as marked by *Gata4* co-expressing cells). It is possible that this increase in Dab2 protein expression level in PrE cells, observed in the hatching blastocyst (E4.75) stage onwards, could be attributed to the activity of

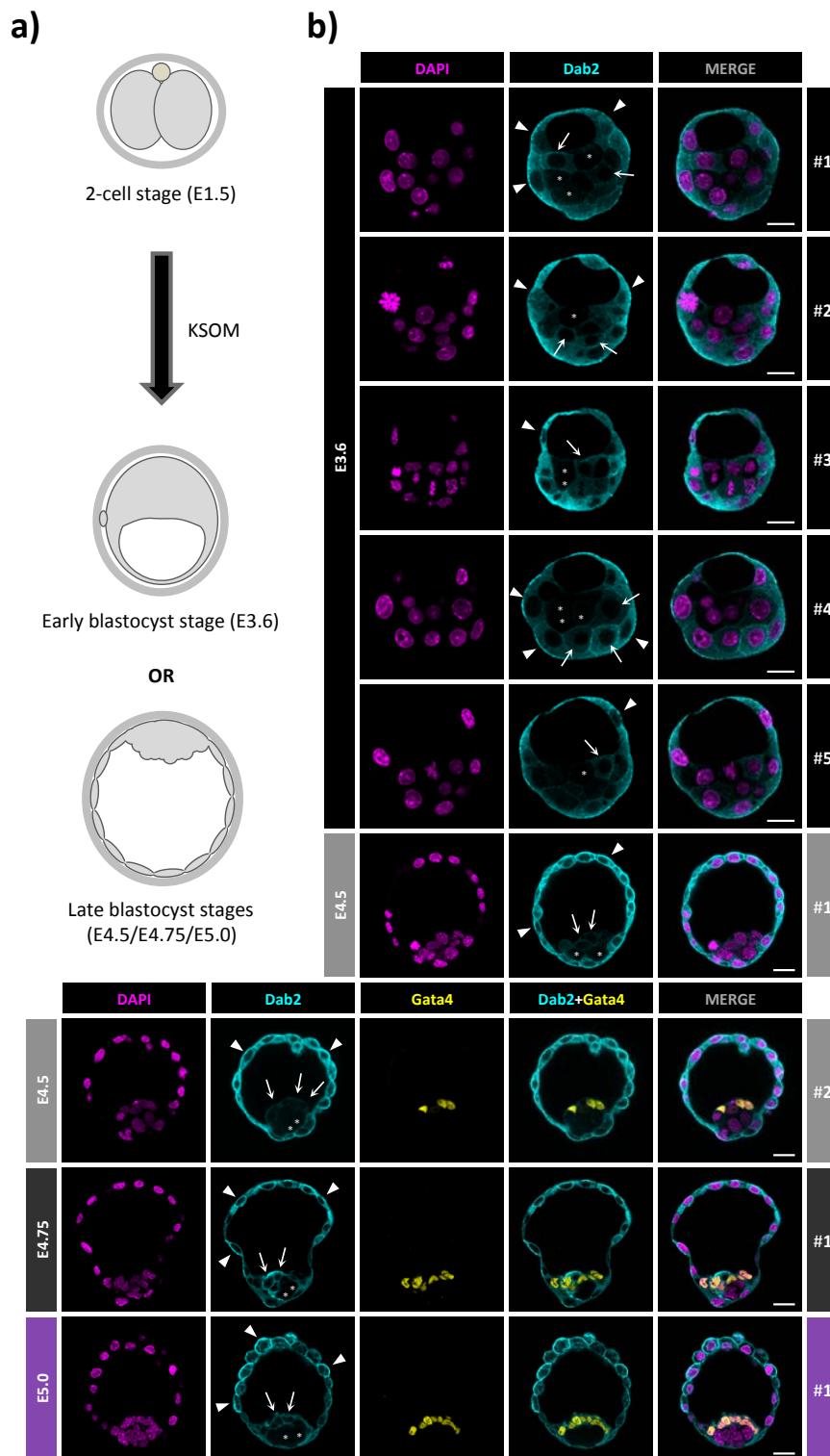


Figure 4.9 The endogenous expression pattern of Dab2 during mouse pre-implantation embryo development reveals its presence in both TE and PrE lineages. **a)** A schematic representation of the experimental strategy to assay the endogenous expression pattern of Dab2 protein from the E3.6-E5.0 stages of pre-implantation mouse embryo development **b)** Representative single z-plane confocal micrographs of *in vitro* cultured E3.6-E5.0 stage embryos immuno-fluorescently stained for Dab2 (cyan) alone or in combination with Gata4 (yellow). DNA is counterstained with DAPI (magenta). In Dab2 images, arrow-heads highlight Dab2 expression in TE cells, while arrows and asterisks denote Dab2-expressing and Dab2-non-expressing ICM cells, respectively. Scale bars = 20 μ m.

the PrE lineage associated transcription factors Gata6 and Gata4, previously reported to transcriptionally regulate *Dab2* gene expression (Morrisey *et al.*, 2000).

Overall, the re-examination of the endogenous Dab2 protein expression pattern throughout the latter stages of pre-implantation mouse embryo development have revealed that, in contrast to previously reported observations, Dab2 is present in both the TE and PrE lineages. Interestingly, at the 32-cell (E3.6) stage, a time-point when ICM founder cell generation is complete, ICM cells exhibit appreciable heterogeneity in Dab2 protein expression levels, possibly related to their developmental origin and history.

4.1.4.2 Dab2 protein expression is severely reduced in *Tea4*-KD cell clones

Since the Dab2 protein expression pattern during pre-implantation mouse embryo development was in agreement with the notion that *Tea4* might be responsible for the initial transcriptional regulation of the *Dab2* gene expression, it was next decided to confirm that this indeed was the case. Therefore, 2-cell (E1.5) stage single blastomere microinjections with RDBs \pm *Tea4*-dsRNA were performed and the resulting embryos cultured to the 32-cell (E3.6) stage, before being fixed and assayed for Dab2 protein expression, using confocal immuno-fluorescence microscopy. A significant reduction in Dab2 protein levels was observed in the *Tea4*-dsRNA microinjected cell clone, when compared to either the non-microinjected sister clones or the equivalent microinjected clones of control embryos (Fig. 4.10b). Normally abundantly present in all TE cells, Dab2 protein was barely detectable in outer-residing cells of the *Tea4*-KD clone. Meanwhile, Dab2 expression remained unaffected in outer cells of the non-microinjected sister clones and in both clones of control microinjected embryos. Importantly, heterogeneity in Dab2 protein expression within the cells of the ICM was preserved in both control and *Tea4*-KD embryos. However, Dab2-expressing cells within the ICM of *Tea4*-KD embryos originated exclusively from the non-microinjected clone, since the inner cells of *Tea4*-KD clone expressed no detectable levels of Dab2.

Overall, these results demonstrate that *Tea4* is indeed responsible and absolutely required for generating the initial heterogeneity in Dab2 protein expression observed between cells of the 32-cell (E3.6) stage mouse embryo ICM.

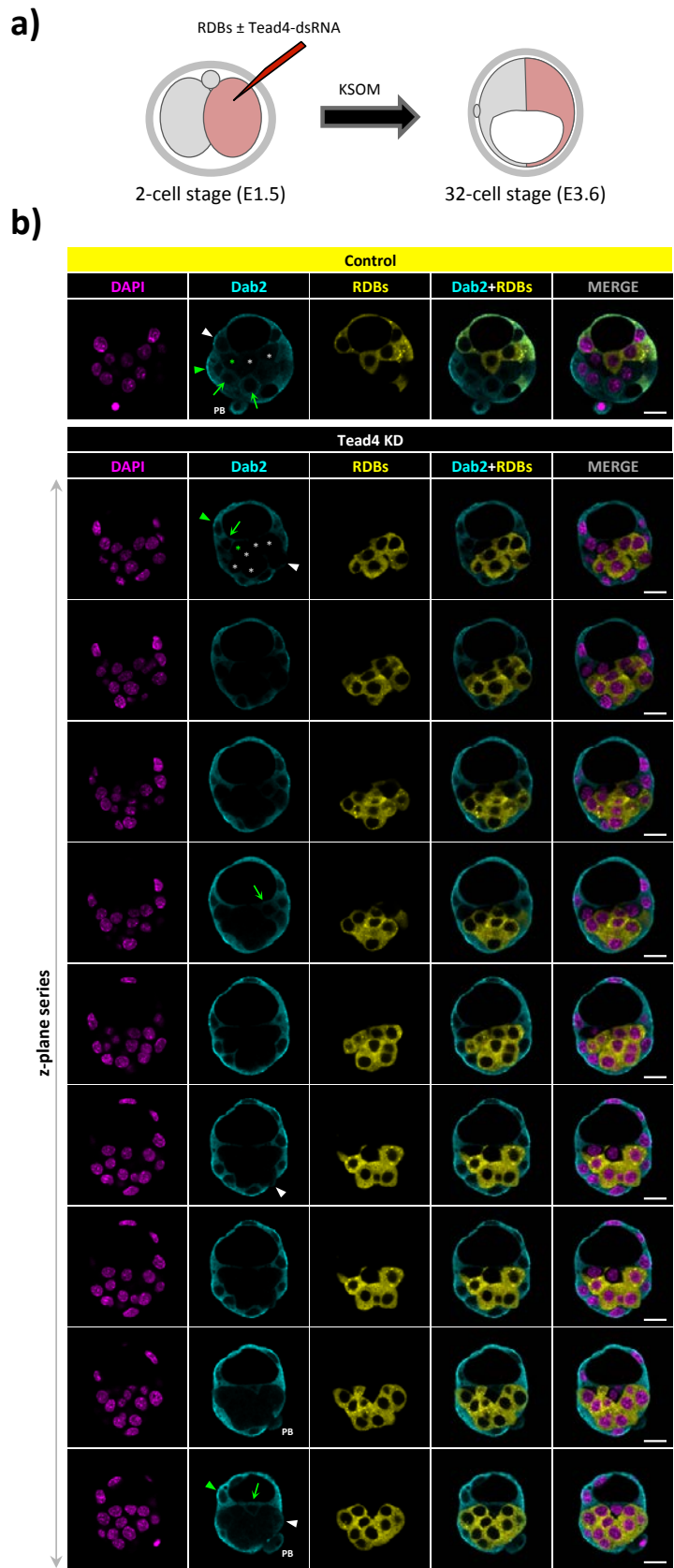


Figure 4.10 (legend overleaf)

Figure 4.10 *Tead4* is responsible for initial *Dab2* protein expression in the pre-implantation mouse embryo. **a)** A schematic representation of the experimental strategy to assay *Dab2* protein expression at the 32-cell (E3.6) stage after clonal *Tead4* knock-down in one-half of the embryo using microinjected RDBs \pm *Tead4*-dsRNA. **b)** Representative z-plane confocal micrographs of control and *Tead4*-KD embryos at the 32-cell (E3.6) stage immuno-fluorescently stained for *Dab2* (cyan). Cells derived from the microinjected clone are distinguishable by the co-injected RDBs (pseudo-coloured yellow). DNA counter-stained with DAPI (magenta) is also shown. In *Dab2* images, white and green arrow-heads denote outer cells of microinjected and non-microinjected clone, respectively. Note a severe reduction in *Dab2* protein levels in outer cells of *Tead4*-KD clone in comparison to the non-injected sister clone and both clones of control microinjected embryo. Green arrows highlight *Dab2*-expressing ICM cells of non-microinjected clone while white and green asterisks denote *Dab2*-non-expressing ICM cells of microinjected and non-microinjected clone, respectively. Note the absence of *Dab2* expression within ICM cells of *Tead4*-KD clone. 'PB' denotes second meiotic polar body. Scale bars = 20 μ m.

4.1.4.3 Down-regulation of *Dab2* results in reduced contribution towards PrE

Finally, it was decided to examine if the observed heterogeneity in *Dab2* protein expression level within the early blastocyst (E3.5) ICM was functionally relevant for the subsequent specification and segregation of the EPI and PrE cell lineages. Thus, *Dab2* expression was clonally down-regulated in half of the embryo, using a *Dab2* specific dsRNA (*Dab2*-dsRNA) RNAi mediated approach, and the frequency at which ICM cells derived from a *Dab2*-dsRNA/ *Dab2*-KD clone contributed to each of the ICM lineages at late blastocyst (E4.5) stage, when compared to both the non-injected clone and the equivalent clone of control microinjected embryos was subsequently assayed. Accordingly, single blastomere microinjections of 2-cell (E1.5) stage embryos with either *Dab2*-dsRNA+RDBs or GFP-dsRNA+RDBs (*i.e.* a microinjection control as GFPdsRNA does not have any specific nucleic acid targets in the mouse genome/ transcriptome) were performed and the resulting manipulated embryos *in vitro* cultured to the late blastocyst (E4.5) stage. The efficacy of the employed knock-down approach was first determined by assaying *Dab2* protein expression and ICM cell lineage contribution was subsequently examined in embryos that had been double immuno-fluorescently stained for *Nanog* and *Gata4* protein (as markers of the EPI and PrE, respectively) (Fig. 4.11 and supplemental tables ST14 for individual embryo data).

The analyses revealed a robust reduction in *Dab2* protein expression in clonal *Dab2*-KD embryos that was observed in all the cell progeny belonging to the *Dab2*-dsRNA microinjected blastomere, thus validating the employed RNAi-mediated knock-down approach (Fig. 4.11b). Nevertheless, clonal *Dab2*-KD embryos developed into morphologically normal late blastocysts by the E4.5 stage. When *Nanog* and *Gata4* immuno-fluorescently stained embryos, were analysed, no statistically significant differences in the total cell number between clonal *Dab2*-KD and control microinjected embryo groups was observed, further suggesting, in addition to their morphology, they were at equivalent stages of development.

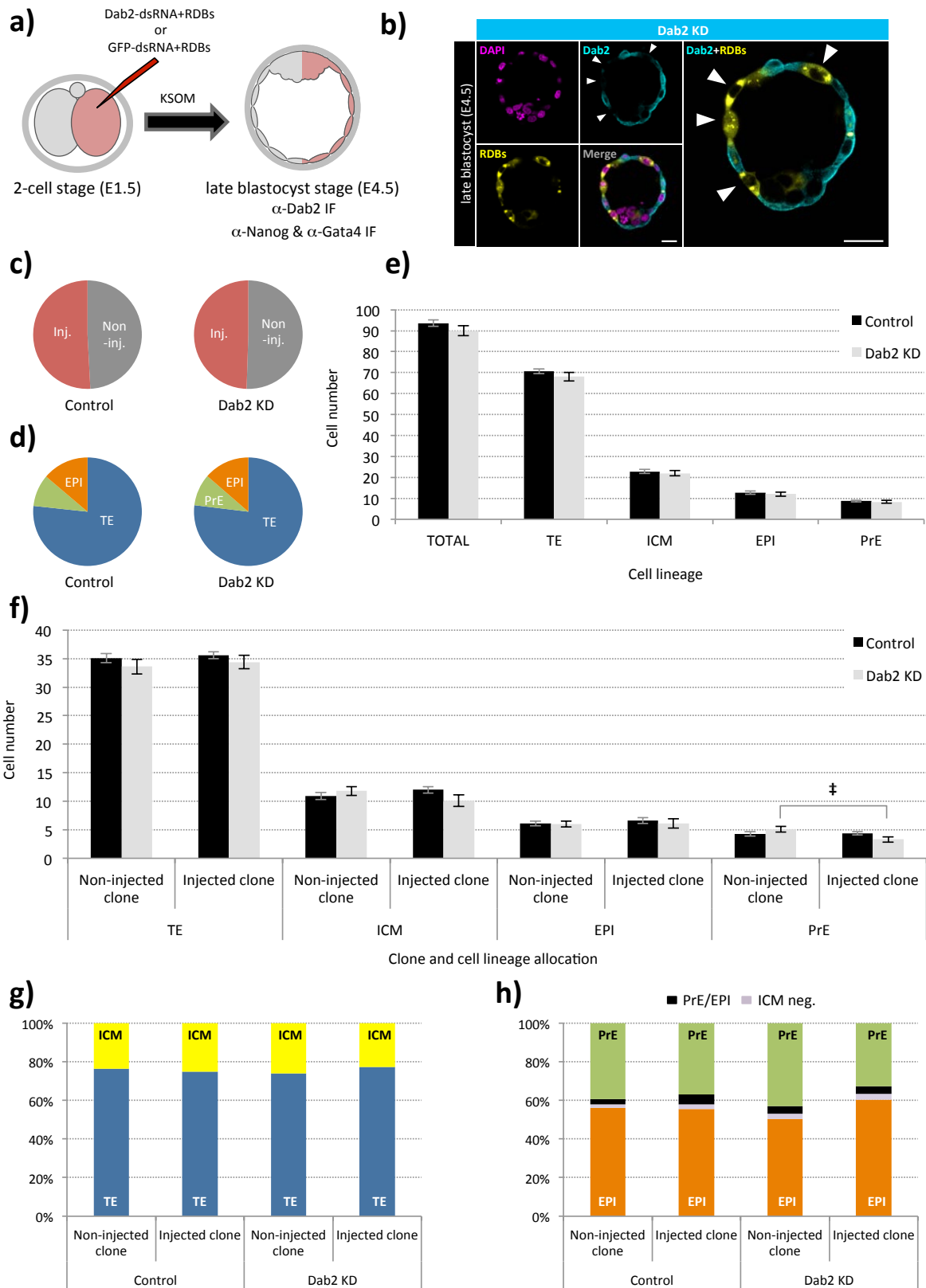


Figure 4.11 (legend overleaf)

Figure 4.11 Clonal down-regulation of *Dab2* in half of the embryo results in mildly attenuated PrE formation. **a)** A schematic representation of the experimental strategy to clonally down-regulate *Dab2* expression in half of the embryo, confirm the successfulness of the knock-down and assess cell lineage contribution in late blastocysts (E4.5) via Nanog (EPI marker) and Gata4 (late PrE marker) immuno-fluorescence detection (*n.b.* outer-residing cells were classified as TE, inner cells that were either double negative or double positive for Nanog and Gata4 were also recorded). **b)** Representative single z-plane confocal micrographs of a clonal *Dab2*-KD late blastocyst (E4.5) embryo immuno-fluorescently stained for Dab2 protein expression (cyan). Progeny of the microinjected cell are distinguishable by co-injected RDB (pseudo-coloured yellow). DNA is counterstained with DAPI (magenta). In Dab2 and Dab2+RDBs merged images, arrow-heads highlight reduced level of Dab2 protein expression in *Dab2*-dsRNA microinjected cell clone thus confirming the successfulness of the knock-down and antibody specificity. Scale bars = 20µm. **c)** Average total cell percentage contribution of microinjected and non-microinjected cell clones in control and clonal *Dab2*-KD late blastocyst stage embryos. **d)** Relative averaged percentage contribution to late blastocyst lineage cell numbers (TE, PrE and EPI) in control and clonal *Dab2*-KD embryos. **e)** Averaged total cell number for each late blastocyst lineage (ICM = EPI + PrE) in clonal *Dab2*-KD and control embryos. **f)** Average number of cells from either non-microinjected or microinjected cell clones contributing to late blastocyst lineages, in control and clonal *Dab2*-KD embryos. In e) and f), error bars represent s.e.m; ‡ denotes statistically significant difference between cell clones within clonal *Dab2*-KD embryo group ($p < 0.05$, 2-tailed student t-tests). **g)** Averaged percentage contribution of non-microinjected and microinjected cell clones, of control and clonal *Dab2*-KD embryos, to TE or ICM of late blastocysts. **h)** As in g) but describing PrE and EPI lineage contribution in ICM, in addition to the relatively infrequent incidence of cells positively immuno-stained for both ICM lineage markers (EPI/PrE-black) or non at all (ICM neg-violet). Overall, control embryos $n=34$ and clonal *Dab2*-KD embryos $n=24$.

Moreover, no statistically significant differences in the total cell number for any of the late blastocyst lineages was found between the clonal *Dab2*-KD and control embryo groups (Fig. 4.11e) and the averaged total cell percentage contribution of microinjected and non-microinjected cell clones was also equal; suggesting no adverse effect of either dsRNA on embryonic development, *per se* (Fig. 4.11c). However, a statistically significant reduction in the number of PrE cells in the microinjected clone of the clonal *Dab2*-KD embryo group, in comparison to the non-microinjected sister clone, was present (Fig. 4.11f). Consistently, when compared to the equivalent cell clones in the clonal control microinjected embryos, the PrE cell lineage contributions of the microinjected and non-microinjected cell clone of *Dab2*-KD embryos were respectively decreased and increased, however not to levels that achieved statistical significance. Nevertheless, these results reveal the existence of a very subtle compensatory effect in the PrE contribution between the two cell clones of *Dab2*-KD embryos and are also in accord with previous data that report PrE specification *per se* may not be so profoundly affected by genetic ablation of the *Dab2* gene, rather that it is the active cell sorting mechanism that are effected (Moore *et al.*, 2013; Yang *et al.*, 2002, 2007).

Therefore, it seems that the observed heterogeneity in *Dab2* protein expression levels observed in early blastocyst (E3.5) stage embryos, and consequent to presumed transcriptional activation by Tead4, might be functionally relevant for subsequent and appropriate formation of the

PrE cell lineage, in a manner supportive of the ‘time-outside-time-inside’ and ‘integrated’ cell-fate models. However, taking into consideration the fact that apart from *Dab2*, *Tead4* is highly likely to regulate other genes functionally important for PrE formation, the relatively mild ICM phenotype consequent to loss of functional *Dab2*, reported herein, might be explained by multiple and functionally converging *Tead4*-dependent mechanisms; hence potentially serving as a partial explanation for the attenuated PrE formation phenotype observed in clonal *Tead4*-KD embryos.

4.1.5 The allocation of *Tead4*-KD cell clone towards the ICM (UNPUBLISHED RESULTS)

As previously shown, owing to the highly regulative nature of the pre-implantation mouse embryo, cells within the TE-inhibited clone were found to preferentially allocate to the ICM of clonal *Tead4*-KD late blastocysts (E4.5). Consequently, the average ICM size of *Tead4*-KD blastocysts was significantly increased (despite the fact that the non-TE-inhibited part of the embryo also allocated but in the opposite direction in order to compensate for the excess in ICM cell number - see figure 4.3c). However, the exact developmental time-point when TE-inhibited cells begin to allocate toward the ICM had not been examined and therefore remained unknown. In addition, previous studies reporting the biased contribution of ICM founder cells that originate from the two successive waves of potential asymmetric cell division/ cell internalisation (*i.e.* towards EPI after the fourth cleavage division and PrE after the fifth) have also stressed the importance of the number of initially generated ICM progenitors (*i.e.* those resulting from the fourth cleavage) to the observed bias in ultimate ICM fate (with larger numbers masking the bias via an increased contribution of such cells to the PrE) (Krupa *et al.*, 2014; Morris *et al.*, 2010). It was therefore decided, against these context, to assay at which developmental point cells belonging to the *Tead4*-KD clone internalised.

4.1.5.1 The allocation of TE-inhibited cell clones towards the ICM commences after the 16-cell stage

Given previous reports regarding the importance of initial ICM size generated after the first wave of cell internalisation (during the fourth cleavage division/ 8-16-cell transition) for the integrated cell-fate decision model, the assessment of the number of inner cells produced at 16- and 32-cell stage in clonal *Tead4*-KD embryos was required. Accordingly, 2-cell (E1.5) stage embryos were microinjected in one blastomere with RDBs \pm *Tead4*-dsRNA, *in vitro* cultured to the 16-cell (E3.1) and 32-cell (E3.6) stage, fixed, stained with rhodamine conjugated phalloidin and with DAPI (to visualise the plasma-membrane associated cortical actin and to label the nuclei; in order to accurately assess cell position and cell number, respectively) and subsequently imaged by confocal microscopy. In

order to precisely determine the exact number of cells that have internalised in each of the first two waves, only the embryos with a total number of cells exactly matching the cell number of developmental stage examined were included in the analyses.

As shown in figure 4.12, the contribution of both non-microinjected and microinjected cell clones of control and *Tead4*-KD embryos to the total cell number was equal at both the examined developmental stages examined (each clone having either 8 or 16 cells at the 16- and 32-cell stages, respectively; see supplemental tables ST15 and ST16 for individual embryo data). This finding argues against the presence of any deleterious effect of either *Tead4*-dsRNA or the microinjecting procedure by the 32-cell stage, but more importantly allows an accurate assessment of the number of cells that internalise in the first and the second wave. Importantly, the analysis of the average number of inner cells at 16-cell (E3.1) stage (Fig. 4.12c,d) revealed no statistically significant differences between the initial ICM size of *Tead4*-KD embryos (2.4 ± 0.3 cells) and that of control microinjected embryos (2.8 ± 0.3 cells) suggesting that the previously published correlations describing biased ICM cell fate as a function of the relative timing of progenitor internalisation (Morris *et al.*, 2010) should not have been masked *per se*, by the generation of extra/ atypically numerous inner cells in clonal *Tead4*-KD embryos, as previously reported (Krupa *et al.*, 2014). Similarly, the number of outer cells between the two groups did not significantly differ either (13.6 ± 0.3 vs 13.2 ± 0.3 cells in *Tead4*-KD and control embryos, respectively). Surprisingly, the analysis of the averaged clonal contribution towards the outer and inner cell populations also revealed a complete absence of cell allocation in *Tead4*-KD embryos at 16-cell stage, suggesting that TE-inhibited cells do not begin to excessively internalise during the first wave of cell internalisation. Instead, they behave similarly to their non-microinjected counterpart sister clones as well as the equivalent cell clone of control microinjected embryos at this stage. In contrast, examination of the average number of inner and outer cells at the 32 cell (E3.6) stage, revealed a significant increase in the overall number of inner cells in *Tead4*-KD embryos (at the expense of an equally decreased average number of outer cells), when compared against the corresponding cell populations in stage stage microinjected control embryos (13.7 ± 0.4 vs 10.7 ± 0.4 inner cells and 18.3 ± 0.4 vs 21.3 ± 0.4 outer cells in *Tead4*-KD and control embryos, respectively; Fig.4.12c',d'). Analysis of the clonal contribution of cells showed that the observed increase in the inner cell number (as well as the decrease in the number of outer cells) in 32-cell (E3.6) stage *Tead4*-KD embryos is entirely accounted for by the significantly increased tendency of *Tead4*-KD cell clone to internalise (or by the lack of its ability to retain outside position in the embryo; Fig. 4.12e'). The behaviour of the *Tead4*-KD cell clone was mirrored by the non-microinjected cell clone counterpart that increasingly populated outside positions of the embryo, however was not able to fully compensate for the lack of outer-residing TE-inhibited cells.

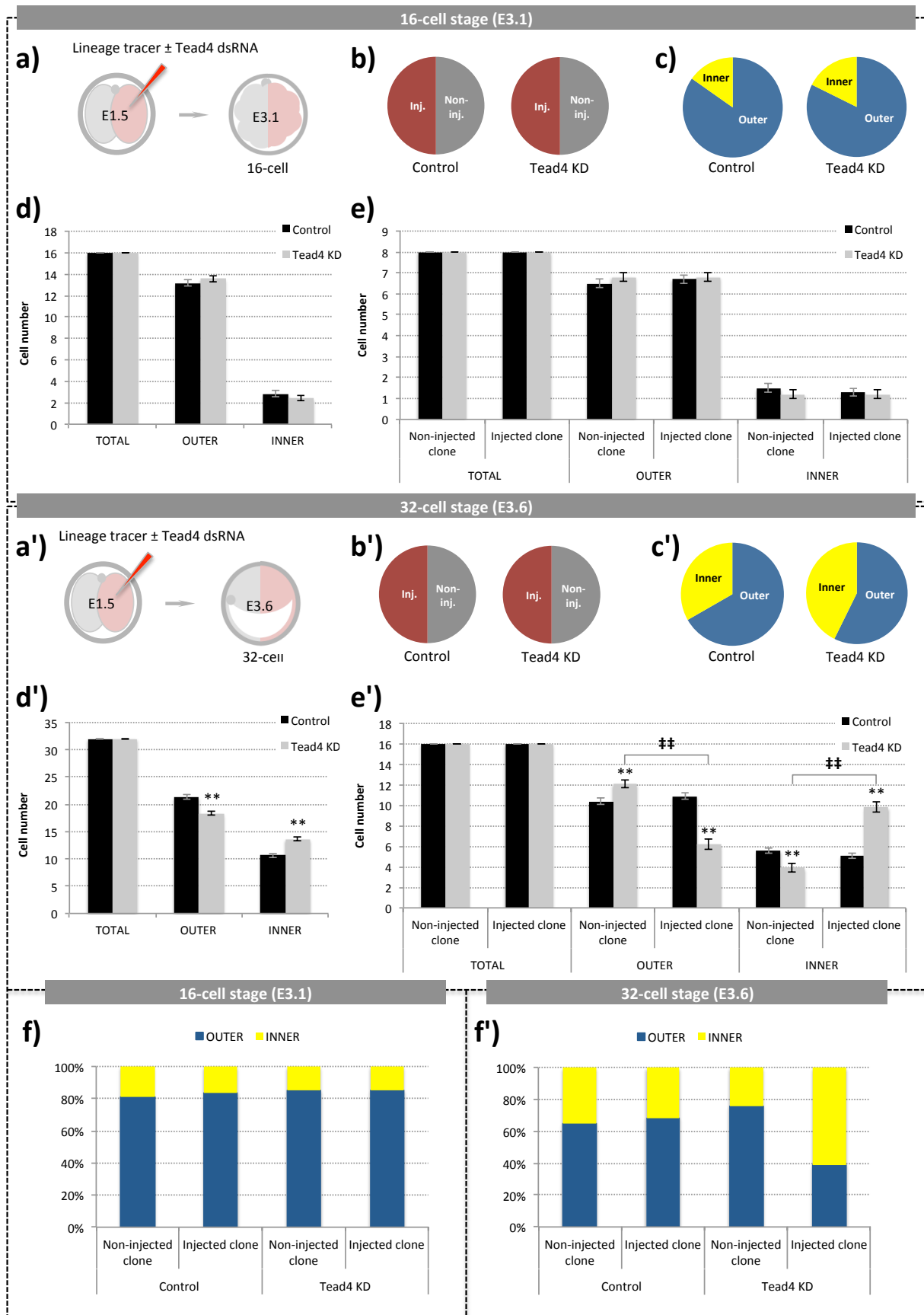


Figure 4.12 (legend overleaf)

Figure 4.12 The allocation of TE-inhibited cell clones towards the ICM commences after 16-cell stage. a,a') A schematic representation of the experimental strategy to clonally down-regulate *Tead4* expression in half of the embryo and examine cell allocation at 16-cell (E3.1) stage/ 32-cell (E3.6) stage. **b,b')** Average total cell percentage contribution of microinjected and non-microinjected cell clones in control and clonal *Tead4*-KD 16-cell (E3.1) stage/ 32-cell (E3.6) stage embryos. **c,c')** Relative averaged percentage contribution of outer and inner cell population in control and *Tead4*-KD 16-cell (E3.1) stage/ 32-cell (E3.6) stage embryos. **d,d')** Averaged total cell number for each cell population (outer and inner) in control and *Tead4*-KD 16-cell (E3.1) stage/ 32-cell (E3.6) stage embryos. **e,e')** Average number of cells from either non-microinjected or microinjected cell clones contributing to total, outer or inner cell population in control and *Tead4*-KD 16-cell (E3.1) stage/ 32-cell (E3.6) stage embryos. In d,d') and e,e') error bars represent s.e.m; ** and ‡ denote statistically significant differences between equivalent cell clones of control and *Tead4*-KD embryos, or between cell clones within control and clonal *Tead4*-KD embryo groups, respectively (confidence intervals of $p < 0.005$, 2-tailed student t-tests). **f,f')** Percentage contribution of non-microinjected and microinjected cell clones of control and *Tead4*-KD embryos to outer and inner cell population of 16-cell (E3.1) stage/ 32-cell (E3.6) stage embryos. Overall, control embryos $n = 29$ and 23 for the 16- and 32-cell stage, respectively; $n = 32$ and 9 for the equivalent *Tead4*-KD embryos.

These findings are therefore entirely in agreement with the observations made on clonal *Tead4*-KD embryos at late blastocyst (E4.5) stage and once again serve to illustrate the remarkable regulative nature of pre-implantation mouse embryo development.

Taken altogether, these results demonstrate that the ICM size of clonal *Tead4*-KD embryos remains unaffected at 16-cell (E3.1) stage (after the first wave of cell internalisation), however becomes supraphysiological by 32-cell (E3.6) stage as the excessive allocation of TE-inhibited cells towards the ICM commences during the second wave of cell internalisation, that under unperturbed developmental conditions is normally biased to contribute ICM progenitors of the PrE (Morris *et al.*, 2010) but as described in the above data (Fig. 4.3) is not the case in clonal *Tead4*-KD embryos.

4.1.5.2 Apical-abscission mediated internalisation of outer-residing TE-inhibited cells

As previously described, outer-residing TE-inhibited cells of 32-cell (E3.6) stage clonal *Tead4*-KD embryos exhibited atypical rounded non-TE like morphology associated with the enhanced apical polarity (see figure 4.7b). However, detailed analysis of a given dataset additionally revealed what was speculated to be the remnants of these cells - enucleated micro-cells enriched in apical polarity proteins residing on the embryo surface. This observation raised the possibility that starting from 32-cell stage onwards, outer-residing TE-inhibited cells might become capable of internalising by divesting themselves of the apical domain and that the failure to do so would subsequently result in the observed apoptotic cell death (see supplementary figure S2).

To test if this hypothesis was correct, *Tead4*-dsRNA was co-microinjected with PAK1-PBD-EYFP (a reporter of Rac1 activity) encoding mRNA, the embryos were *in vitro* cultured until they have

reached 32-cell (E3.5) stage at which point their developmental progress was monitored within the following 12 hours using time-lapse confocal microscopy. It is of note that the reporter of Rac1 activity, PAK1-PBD-EYFP, used in this experiment to visualise dynamic changes in the contractility of the apical membrane domain, has previously been shown to asymmetrically localise and accumulate to the cortical region of the animal pole of MII oocytes, in the proximity of the meiotic spindle prior to second meiotic polar body extrusion, thereby marking the region of the plasma-membrane actively involved in the extrusion of the polar body (Halet and Carroll, 2007). Similarly, the apical polarity factor Pard6b, has been reported to localise at the same region in MII oocyte (Vinot *et al.*, 2004). Thus it was reasoned that PAK1-PBD-EYFP would be similarly co-localised with the observed enrichment of apical polarity factors in the atypically rounded outer-residing TE-inhibited cells of *Tead4*-KD embryos but more importantly that this would provide a means to visualise the dynamic changes in the apical membrane domain to test the hypothesis.

As shown in figure 4.13b, time-lapse confocal microscopy revealed that PAK1-PBD-EYFP did accumulate at the apical membrane domain of outer-residing TE-inhibited cells. More importantly, it was possible to confirm that the outer-residing TE-inhibited cells of 32-cell stage clonal *Tead4*-KD embryos were indeed capable of internalising after the abscission of their apical membrane domain. Consistently, this process resulted in a creation of micro-cells that remained residing on the embryo surface and in addition exhibited increased levels of PAK1-PBD-EYFP fluorescent signal. These findings therefore confirmed the stated hypothesis and provided an insight into the possible mechanism that might act to allow blastomeres to adjust their position within the pre-implantation embryo in accordance to the cell fate they have been forced to acquire. Importantly, and in the context of recent reports (Samarage *et al.*, 2015; Le Maître *et al.*, 2016), these data also highlight a potential role for *Tead4* in regulating mechanisms of cellular contractility that have been shown to be required during blastomere internalisation in pre-implantation mouse embryos.

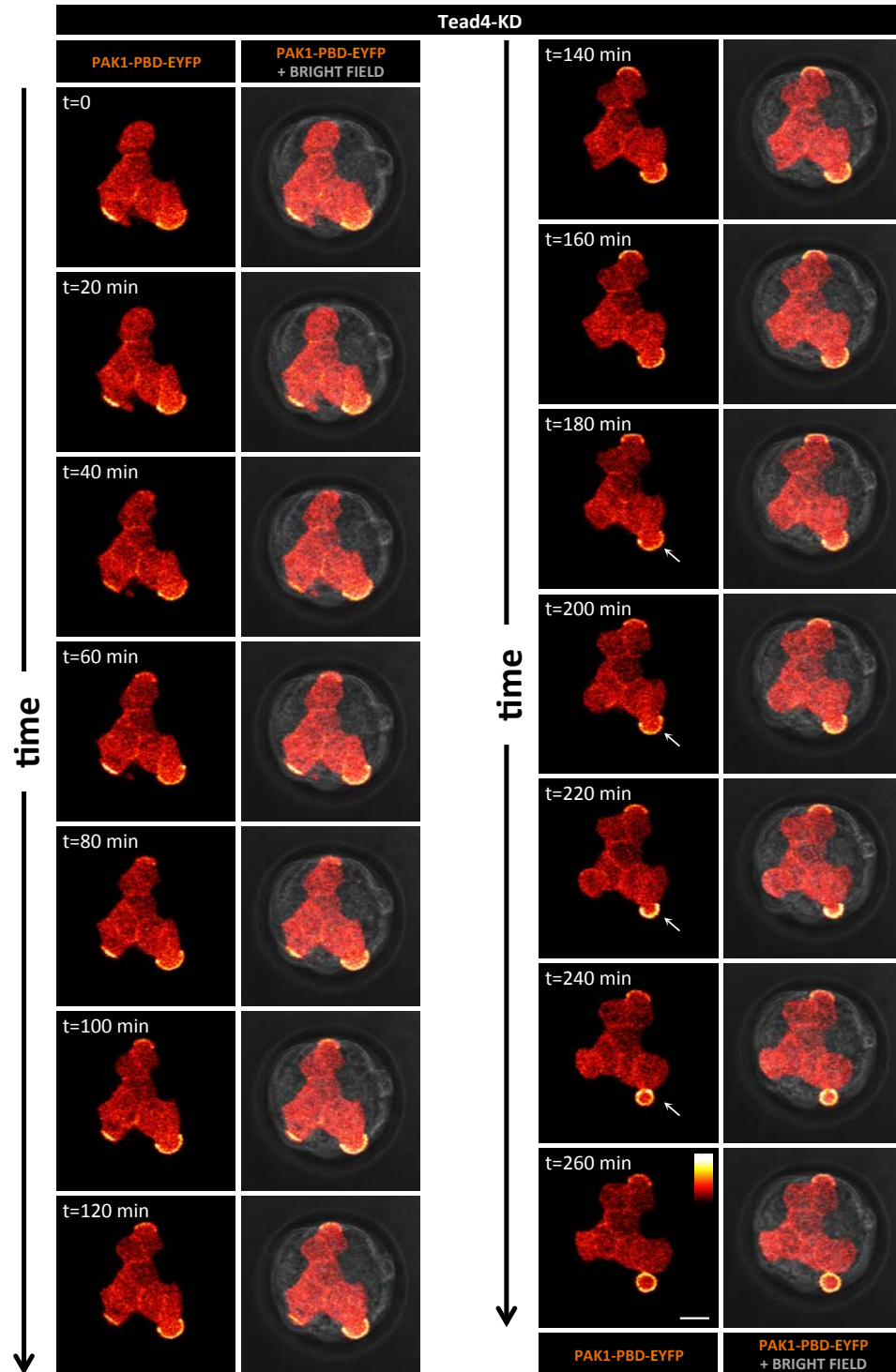
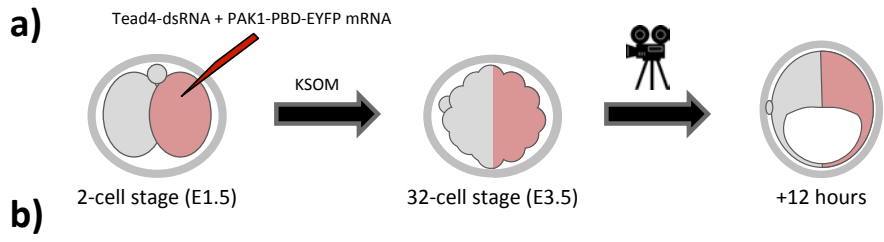


Figure 4.13 (legend overleaf)

Figure 4.13 Time-lapse confocal microscopy reveals the apical-abscission mediated internalisation of outer-residing TE-inhibited cells from 32-cell/ late morula (E3.5) stage. **a)** A schematic representation of the experimental strategy to clonally down-regulate *Tead4* and concomitantly overexpress PAK1-PDB-EYFP mRNA in half of the embryo and observe, via time-lapse confocal microscopy, apical-abscission mediated cell internalisation of outer-residing TE-inhibited cells from 32-cell/ late morula (E3.5) stage. **b)** A series of single optical z-section time-lapse images of *Tead4*-dsRNA + PAK1-PDB-EYFP mRNA microinjected 32-cell stage embryo. Arrows denote outer-residing TE-inhibited cell that internalises via apical-abscission. Fluorescent signal obtained from PAK1-PDB-EYFP is represented in the orange ('fall') spectral intensity palette. Scale bars = 20µm.

Collectively, the data presented in part I of the current result section demonstrate a significantly biased tendency of variously sized TE-inhibited cell clones towards populating the EPI over the PrE lineage at late blastocyst (E4.5) stage. This tendency of TE-inhibited cell clone to preferentially populate EPI cell lineage was not associated with the precocious and/or increased expression of EPI lineage marker *Nanog* or the reduced capacity of cells to polarise. Instead, it was associated with a decreased expression of PrE lineage markers *Fgfr2*, *Dab2* and *Lrp2* and thus likely reflects the reduced capacity of TE-inhibited ICM-residing cells to respond to PrE differentiative cues. As such, these results highlight the importance of TE-differentiating cues and ancestral cell history on the acquisition of second cell fate and thus provide additional support for the existence of an integrated cell-fate decision process.

4.2 PART II - THE INFLUENCE OF ROCK1/2 ON AMOT LOCALISATION AND THE HIPPO SIGNALLING PATHWAY DURING TROPHECTODERM AND INNER CELL MASS SEGREGATION

Rho-associated protein kinase (Rock1/2, there are two isoforms) is a serine-threonine kinase that acts downstream of the small GTPase RhoA and regulates a wide range of different cellular phenomena. Rock1/2 is known to be involved in regulating the actin cytoskeleton organisation, cell adhesion and motility, proliferation and apoptosis, remodelling of the extracellular matrix and smooth muscle cell contraction (reviewed in Hartmann *et al.*, 2015). Two recently published independent studies, utilising the specific small chemical compound inhibitor of Rock1/2, Y-27632, reported somewhat conflicting phenotypes regarding its role and significance during pre-implantation mouse embryo development (Duan *et al.*, 2014; Kono *et al.*, 2014). Specifically, the study conducted by Kono and colleagues reported that chemical inhibition of Rock1/2 activity, during *in vitro* culture from the 2-cell stage, results in embryonic arrest at the 32-cell (E3.5)/ late morula stage and is associated with improper cell polarity establishment and aberrant Hippo signalling activation in outer cells (Kono *et al.*, 2014). In contrast, the findings of Duan and colleagues observed an earlier phenotype, again associated with Rock1/2 inhibition during *in vitro* culture from the 2-cell

stage, that resulted in arrested embryonic development at the 8-cell stage (Duan *et al.*, 2014). It was therefore decided to independently and comprehensively assess the effects of Rock1/2 inhibition on pre-implantation mouse embryo development in the presented study, in an attempt to both aid the resolution of the conflicting data and to provide added insight into any identified/ confirmed phenotypes. These aims were manifest in the ultimate goal to test whether the effects of Rock1/2 inhibition on the Hippo signalling pathway were mediated via the Hippo signalling pathway component, Amot (something that previous studies failed to report), as well as to characterise in more depth Rock1/2 inhibition associated phenotype at earlier developmental time-points.

4.2.1 Rock1/2 inhibition prevents blastocoel formation in pre-implantation mouse embryo

In their effort to examine the role of Rock1/2 during pre-implantation mouse embryo development, Kono and colleagues used a 20µM concentration of Rock1/2 inhibitor, Y-27632 (Kono *et al.*, 2014) in contrast to the 100µM concentration used by Duan and colleagues (Duan *et al.*, 2014). Such a discrepancy in the concentration of Rock1/2 inhibitor used between two studies could have potentially provided an explanation for the observation different phenotypes. Thus, it was first decided to determine an effective working concentration of Y-27632/ Rock1/2 inhibitor. Accordingly, groups of 2-cell stage mouse embryos were *in vitro* cultured in amino acid supplemented KSOM media (KSOM+AA, see materials and methods) containing Y-27632 diluted to 20µM, 50µM or 100µM concentrations (or equivalent volumes of DMSO as solvent/ vehicle controls) until a stage equivalent to the late blastocyst (E4.5). As presented in figure 4.14b, all DMSO vehicle control treated embryos developed with normal morphology, as represented by hatching late blastocysts. However, embryos cultured in 50µM and 100µM Y-27632/ Rock1/2 inhibitor failed to form viable blastocoels and exhibited evidence of extensive cell death, although they clearly comprised >8 blastomeres. Conversely, >80% of the embryos from the 20µM Y-27632 treated group appeared to develop normally, forming morphologically recognisable blastocysts. Thus, given that the embryos in the 50µM Y-27632 treated group represented those in which a clearly penetrant developmental phenotype was observed using the lowest concentration of Rock1/2 inhibitor, it was decided to use this concentration in all subsequent experiments.

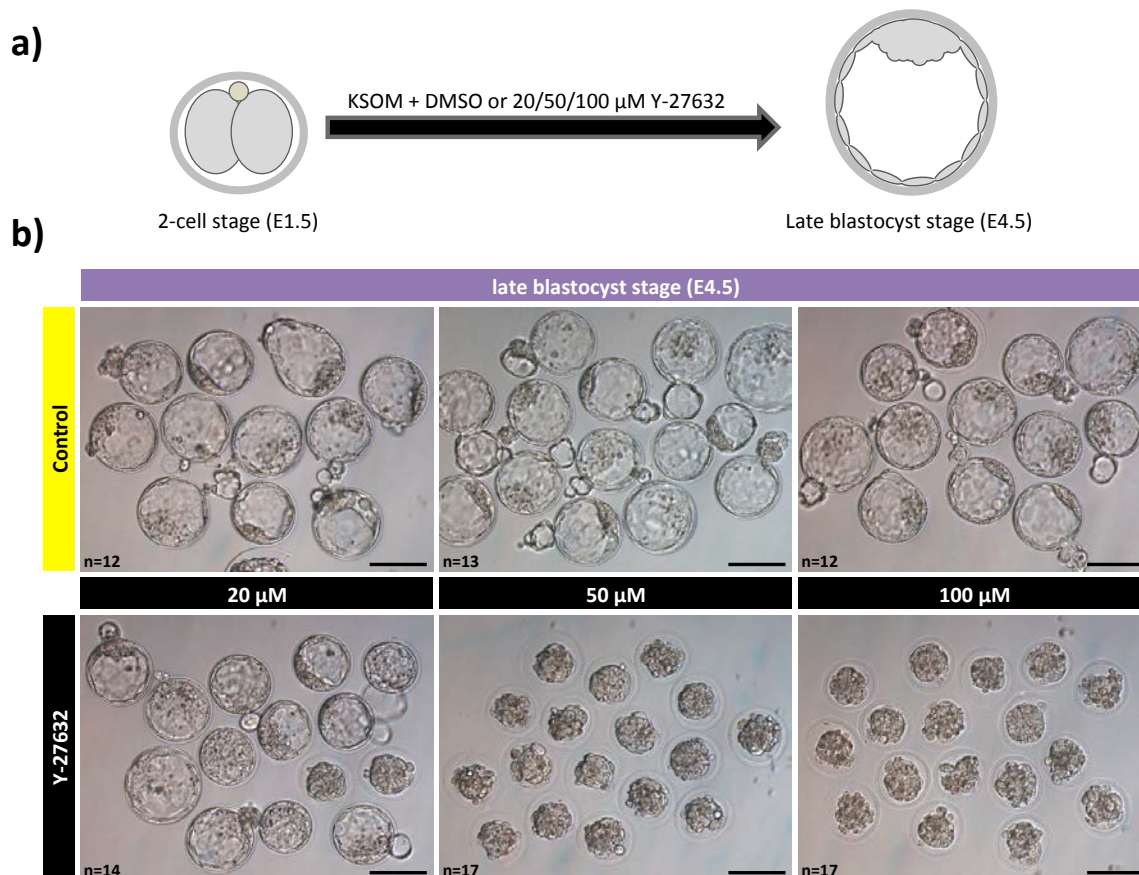


Figure 4.14 Determining an effective working concentration of Y-27632/ Rock1/2 inhibitor. a) Schematic representation of the experimental strategy to assay *in vitro* development of pre-implantation mouse embryos in three different concentrations of Y-27632/ Rock1/2 inhibitor (+DMSO vehicle controls). b) Representative bright-field micrographs of inhibitor- and vehicle-treated embryos at the end of the *in vitro* culture period. Lower panels depict embryos cultured in increasing concentrations of Rock1/2 inhibitor (black label), with appropriate DMSO vehicle control embryos displayed in corresponding upper panels (yellow label). Note the titration effect of Rock1/2-inhibition and pronounced cell death in 50 μ M and 100 μ M treated embryos. Scale bars = 100 μ m.

Next, it was decided to examine the developmental progress of Rock1/2-inhibited embryos throughout several different stages of pre-implantation development in order to determine whether the observed embryonic death was associated with stage-specific developmental arrest or alternatively was a consequence of gradually increasing developmental delay. Firstly, 2-cell (E1.5) stage embryos were recovered into KSOM+AA media containing either 50 μ M Rock1/2 inhibitor or an equivalent amount of control DMSO solvent and *in vitro* cultured and morphologically inspected at three different developmental time points; the 8-cell (E2.5), 32-cell/ late morula (E3.5) or early blastocyst (E3.75) stages. A third group of untreated embryos was similarly processed and served as a control for both the *in vitro* culture conditions and the general developmental quality of the recovered embryos.

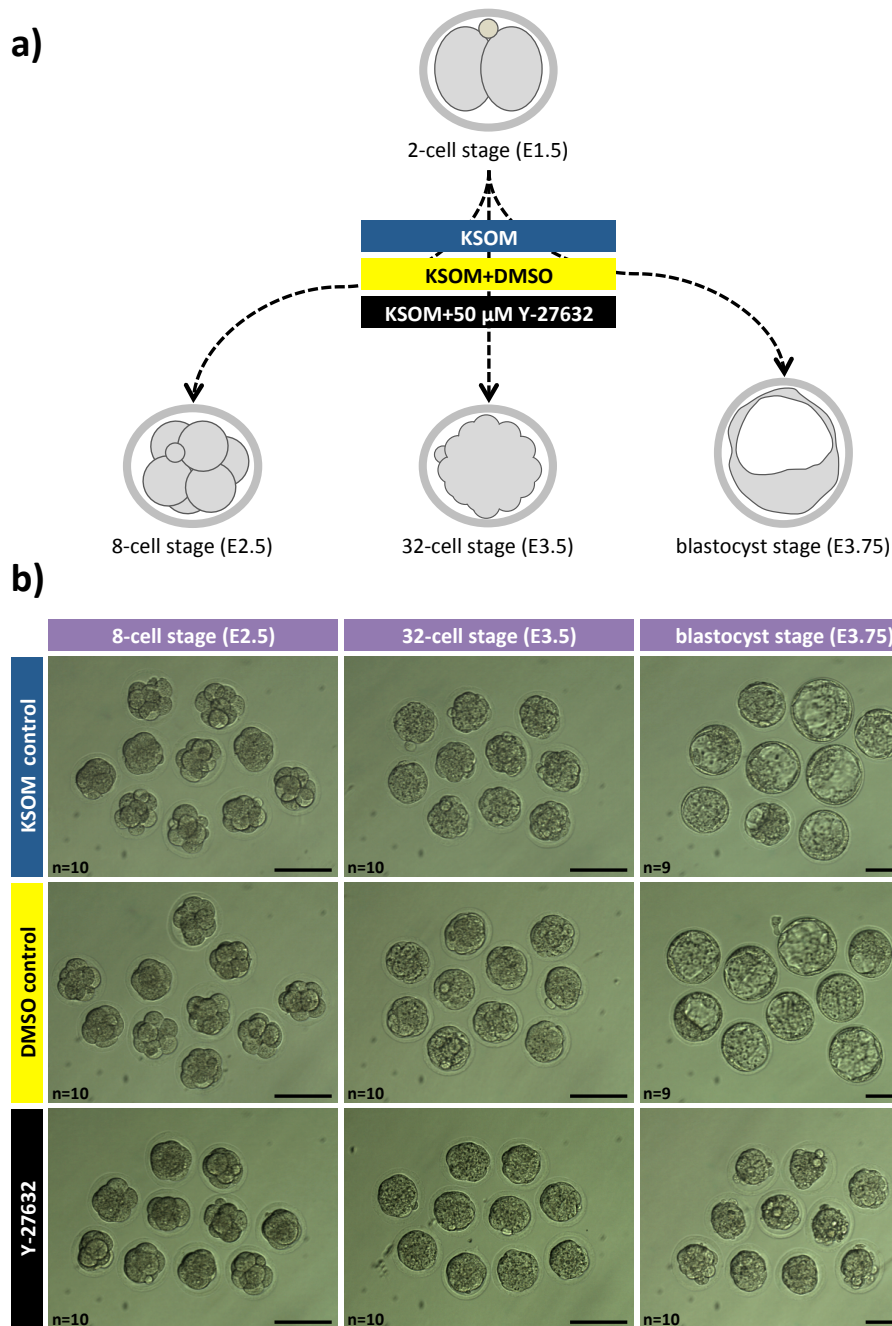


Figure 4.15 Rock1/2-inhibited embryos equivalently develop in pace with controls until the 32-cell (E3.5)/ late morula stage but subsequently fail to cavitate. **a)** Schematic representation of the experimental strategy to compare the *in vitro* development of Rock1/2-inhibited embryos with *in vitro* culture and DMSO vehicle control embryo groups at three different developmental time points. **b)** Phase contrast micrographs of live pre-implantation mouse embryos *in vitro* cultured from the 2-cell (E1.5) stage in the presence of KSOM+AA growth media alone (upper row, blue label; *i.e.* culture/ embryo quality sentinels) or in the presence of DMSO vehicle control (yellow label) or 50 μ M Y-27632/ Rock1/2 inhibitor (black label) to the indicated developmental stage. Scale bars = 100 μ m and 'n' numbers are indicated in individual micrograph panels. Note, embryos from all groups develop in tandem with each other until the 32-cell (E3.5) stage, when Y-27632 treated embryos fail to cavitate and show morphological evidence of cell death.

As shown in figure 4.15, all three groups of embryos equivalently developed in pace with each other until the 32-cell/ late morula (E3.5) stage, however while both the culture and vehicle control groups of embryos normally cavitated and formed blastocysts by E3.75, the Rock1/2-inhibited embryos failed to form a blastocoel. Moreover, in the Rock1/2-inhibited group, some embryos had begun to exhibit evidence of cell death at this stage. Importantly, the direct comparison of the embryonic development between the culture and DMSO vehicle control groups revealed no apparent morphological differences, suggesting DMSO (at the concentration used, to control a 50 μ M dose of Y-27632) has no adverse effects on embryonic development; thus confirming the appropriateness of using DMSO vehicle control alone in all the subsequently described experiments.

To further reaffirm the conclusion that the general developmental progress/ cell division of Rock1/2-inhibited embryos remain unaffected until after the 32-cell/ late morula (E3.5) stage, it was decided to compare the average total cell number of Rock1/2-inhibited and DMSO vehicle control treated embryo groups at several different stages until this stage. Therefore, both 50 μ M Rock1/2 inhibitor treated and vehicle embryo groups were *in vitro* cultured from the 2-cell (E1.5) stage until either the 8-cell (E2.5), 16-cell (E3.0) or 32-cell stages (E3.5), fixed, stained with DAPI to assess the total number of nuclei (as a correlate of cell number) and imaged using confocal microscopy. As shown in figure 4.16b, no statistically significant differences in the average total cell number between Rock1/2-inhibited and vehicle control embryos was observed at any of the three stages examined (see supplementary table ST17 for individual embryo data). This observation thus further confirms that Rock1/2-inhibited embryos develop in equivalent pace with control embryos until 32-cell (E3.5) stage, therefore permitting the unbiased comparison between experimental and control embryos of equivalent stage, up until this developmental time point.

Overall, these findings demonstrate that Rock1/2 activity is indispensable for appropriate mouse pre-implantation embryo development, as Rock1/2-inhibited embryos incapable of forming blastocoels, fail to morphologically develop beyond the late morula stage and eventually die.

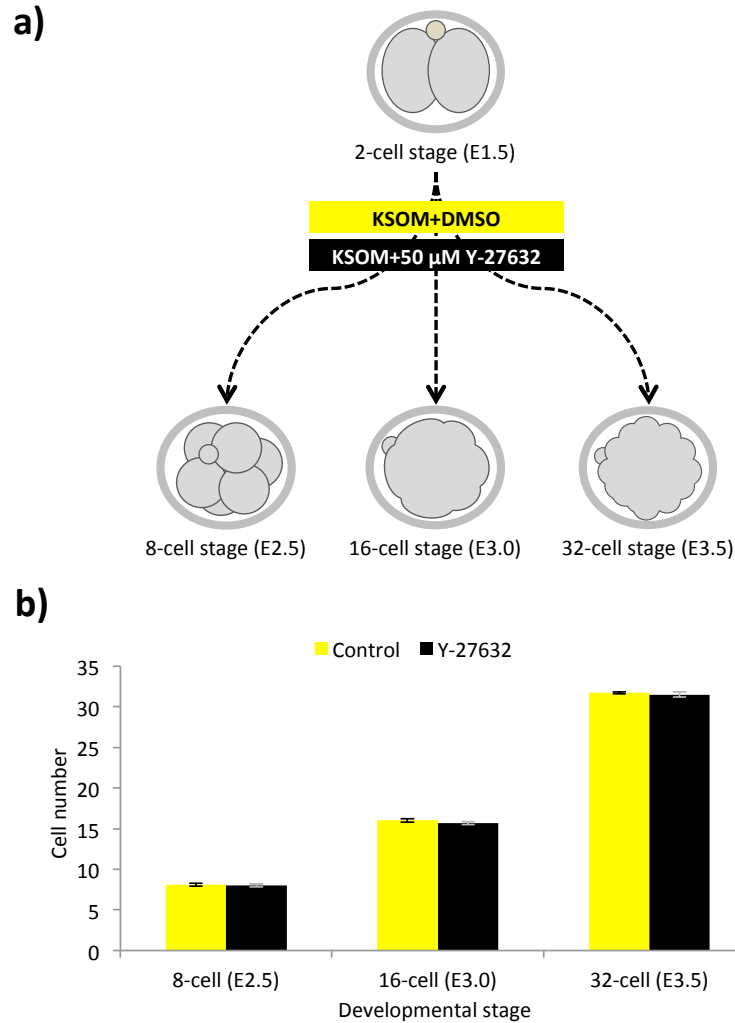


Figure 4.16 Averaged total embryo cell number in Rock1/2-inhibited (Y-27632 treated) and control (DMSO treated) groups, *in vitro* cultured from the 2-cell (E1.5) stage to the 8- (E2.5), 16- (E3.0) or 32-cell (E3.5) stages. a) Schematic representation of the control/ Rock1/2-inhibition experimental treatments of *in vitro* cultured 2-cell (E1.5) pre-implantation mouse embryos fixed at the indicated developmental time points, before total cell number was determined. **b)** Total cell number for each control and experimental group at each of the stated developmental stages. Values expressed as mean \pm s.e.m. There were no significant differences (using a 2-tailed student t-test $p < 0.05$ cut off) between control and experimental groups, within each developmental time-point studied. For control embryos, $n = 24, 26$ and 22 for the E2.5, E3.0 and E3.5 stages, respectively; $n = 29, 21$ and 22 for the equivalent Rock1/2-inhibited embryos.

4.2.2 Rock1/2 inhibition is associated with defective cell polarity establishment and improper tight junction formation

The next task was to characterise the observed Rock1/2 inhibition associated phenotype at the molecular level. Thus, embryos were *in vitro* cultured from the 2-cell (E1.5) stage until the 32-cell/ late morula (E3.5) stage in 50 μ M Y-27632/ Rock1/2 inhibitor or DMSO vehicle control containing KSOM+AA, fixed and immuno-fluorescently stained for cytoskeletal (F-actin and α -Tubulin), apical-

basolateral polarity (pERM, Prkcz/i, Pard6b and Scrib), adherens (Cdh1) and tight junction (Tjp2; Tight junction protein 2/ Zona occludens 2) marker protein expression and imaged by confocal microscopy. This analysis revealed no detectable difference in the expression or distribution of α -Tubulin between control and Rock1/2-inhibited embryos, suggesting the microtubule network remained intact after Rock1/2 inhibition (Fig. 4.17b). In addition, an initial inspection of individual confocal microscopy z-sections stained for F-actin also appeared to detail a lack of difference between control and Rock1/2-inhibited embryos, with F-actin appearing characteristically cortical in its distribution in both groups; however after examining the acquired embryo confocal z-stacks as projections, the absence of otherwise normally accumulated F-actin from the plasma-membrane at presumptive tight junction regions became evident in the outer-cells of Rock1/2-inhibited embryos (Fig. 4.17b). This suggests that actin polymerisation at tight junction associated regions might be uniquely sensitive to regulation by active Rock1/2 and thus, given the observed developmental block at late morula stage, might be particularly important/required for successful blastocyst formation. Further analysis revealed severe apical-basolateral polarity defects in Rock1/2-inhibited embryos. Specifically, in contrast to normally being accumulated only on the apical domain, Pard6b and Prkcz/i apical polarity markers were uniformly distributed throughout the plasma membrane of all outer cells and both factors were atypically enriched on the plasma membranes of inner cells, compared to the control embryo group (Fig. 4.17b). Similarly, the staining pattern observed using the anti-pERM antibody detailed atypical localisation of phospho-Ezrin (pEzr) to the basolateral plasma membrane domain of outer cells; plus pERM signal was also ectopically present at some inner-cell to inner-cell contact regions. Moreover, upon careful examination of projected confocal microscopy z-sections, it was observed that pERM was not homogeneously distributed throughout the entire apical domain, as in control embryos, but was rather concentrated into disc-like structures at pole extremities (referred herein as 'apical-discs' – see projected z-stack image in Fig. 4.17b). The appearance of such apical-disc like structures was much less profound in the case of two previously examined apical polarity markers, Pard6b and Prkcz/i (data not shown). Conversely, the basolateral polarity marker, Scrib was found to be ectopically present and substantially accumulated at the apical plasma membrane domain of outer cells in Rock1/2-inhibited embryos (see figure 4.17b and quantified data in supplementary figure S5). Such Rock1/2-dependent mis-localisation of Scrib was observed in every Y-27632 treated embryo assayed, with 84.6% of outer cells showing evidence of ectopic and apically localised Scrib. In contrast, the apparent expression level and distribution of the adherens junction marker, Cdh1, was unaffected by Rock1/2-inhibition at 32-cell/ late morula (E3.5) stage, suggesting cell-adhesion was not disrupted (Fig. 4.17b). Importantly, the distribution of the mature tight junction marker, Tjp2, revealed profound defects in tight-junction formation at this stage (Fig. 4.17b – see projected images).

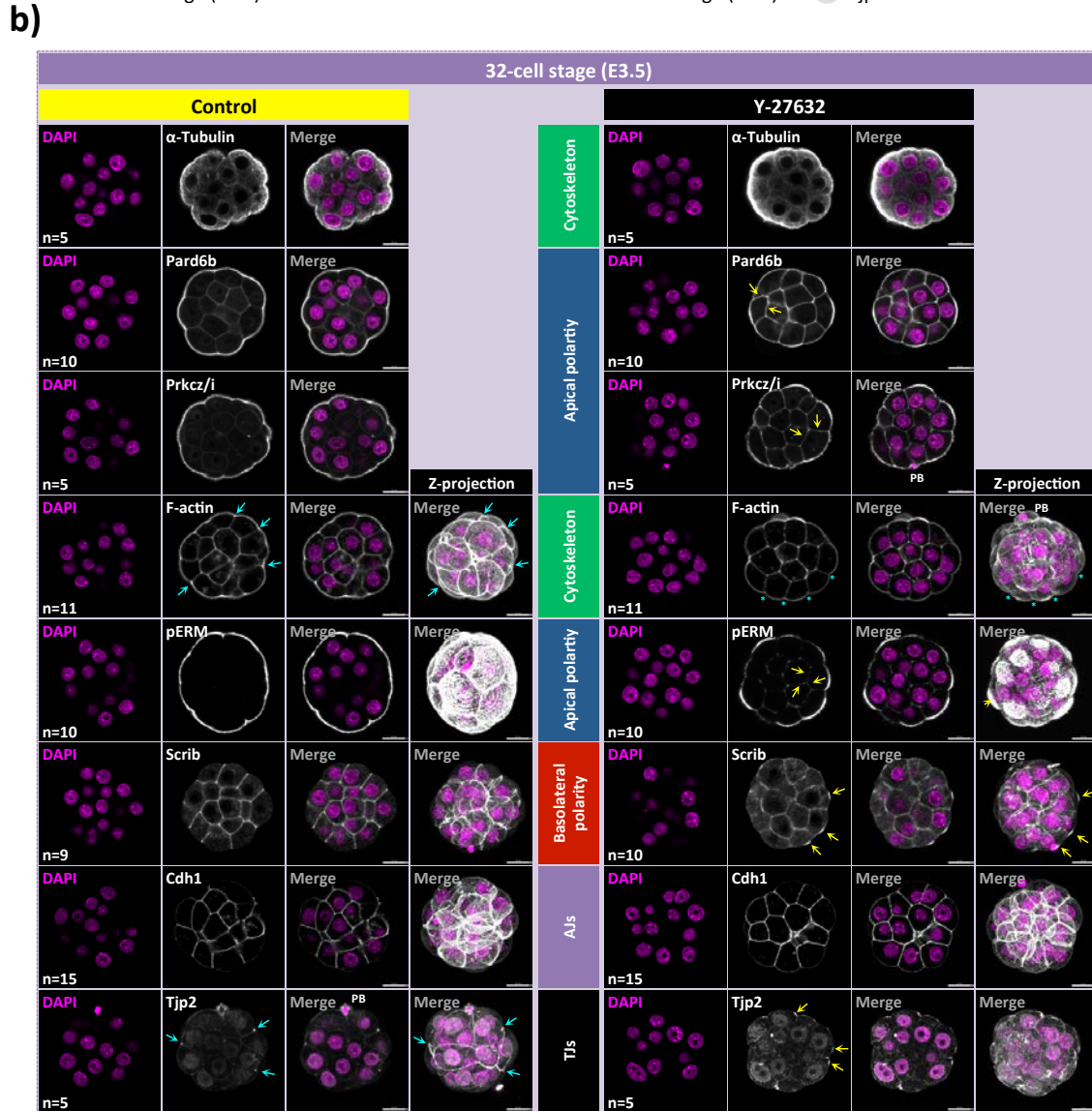


Figure 4.17 Rock1/2-inhibition is associated with defective apical-basolateral polarity and tight-junction formation. a) Schematic representation of the experimental strategy to assay the sub-cellular expression and localisation of the stated cytoskeletal, apical-basolateral polarity-associated or junctional proteins in control or Y-27632-treated (50μM)/ Rock1/2-inhibited embryos at the 32-cell stage. **b)** Representative single z-section confocal micrographs, plus selected projected images, of embryos immunofluorescently stained for the stated proteins (grey-scale) and DNA (DAPI counter-stain, magenta). Note, 'AJs' and 'TJs' relate to images immunostained for 'adherens-' and 'tight-' junction markers, respectively. 'PB' denotes the second meiotic polar body. In Rock1/2-inhibited embryos, yellow arrows highlight atypical marker protein localisation, versus controls. The yellow arrow-head in the pERM immunostained projection denotes atypically enriched 'apical-disc' formation in Rock1/2-inhibited embryos. Blue arrows in the control group denote tight-junction associated F-actin and Tjp2 and blue asterisks mark lack of tight-junction localised F-actin in Rock1/2-inhibited embryos. Scale bars = 20μm.

The lack of matured tight junctions may provide an explanation for the lack of F-actin accumulation at the same sub-cellular region and the observed polarisation failure of otherwise normally discrete apically or basolaterally localised polarity protein markers (*i.e.* Pard6b, Prkcz/i and Scrib). Additionally, it provides a compelling reason for the failure of Rock1/2-inhibited embryos to form a blastocoel, owing to a potential lack of epithelial integrity in the TE. Finally, the mis-localisation of detected pERM proteins, particularly in the observed apical-discs, suggests that unlike other apically enriched polarity factors, pEzr sub-cellular localisation might be regulated by an alternative but nonetheless Rock1/2-sensitive mechanism.

Taken together, these findings demonstrate that Rock1/2 inhibition is associated with severe defects cell polarity establishment, improper tight junction formation and lack of F-actin accumulation in the presumptive tight junction regions and are therefore largely in agreement, yet also develop and expand upon, the data previously published by Kono and colleagues (Kono *et al.*, 2014).

4.2.3 Rock1/2 inhibition effects on Hippo signalling pathway activation are mediated via Amot

Although, it has previously been demonstrated that both Rho-GTPase- and Rock1/2-inhibition prevent the outer-cells of late morula stage embryos to accumulate nuclear Yap1 due to ectopic activation of the Hippo signalling pathway effector kinase Lats2 (Kono *et al.*, 2014), the exact upstream mechanism by which any potential Rock1/2-dependent regulation of Lats1/2 activity operates was not investigated. Therefore, it was decided to examine whether the effects of Rock1/2 inhibition on Hippo signalling pathway activation were mediated via Amot. As described above (Fig. 4.17), the outer-cells of 32-cell/ late morula (E3.5) stage Rock1/2-inhibited embryos displayed mis-localisation of apical polarity factors to the basolateral regions. Since it has previously been reported that interfering with appropriate cell polarity establishment, either via the experimental introduction and expression of dominant-negative mutant constructs of Prkci or inhibiting endogenous *Pard6b* expression using shRNA (short hairpin RNA)-mediated RNAi, results in Amot mis-localisation to the adherens junctions of outer cells and consequent aberrant Hippo signalling pathway activation (Hirate *et al.*, 2013), by the 32-cell/ late (E3.5) morula stage, it was accordingly hypothesised that Amot itself maybe similarly mis-localised in Rock1/2-inhibited embryos.

4.2.3.1 Rock1/2 inhibition induces Amot mis-localisation in outer cells of late morula stage embryos and ectopic Hippo signalling pathway activation

Therefore, it was decided to test if Amot protein distribution would become altered in Rock1/2-inhibited embryos. Accordingly, 2-cell (E1.5) stage recovered embryos were *in vitro* cultured in the presence of 50 μ M Rock1/2 inhibitor, or the appropriate amount of DMSO vehicle control, until the 32-cell/ late morula (E3.5) stage and the sub-cellular expression and localisation Amot, in combination with either Yap1, as a read-out of Lats1/2 activity, or Ctnnb1 (β -catenin – at adherens junctions), as a marker of outer-cell basolateral membranes, assayed by immuno-fluorescent confocal-based microscopy (Fig. 4.18). As hypothesised, the typical localisation observed in vehicle control treated embryos, whereby Amot protein was detectable all around the plasma membranes of inner-cells but confined to the apical, cell-contact free, surfaces in outer-cells (Fig. 4.18b) was disrupted in Rock1/2-inhibited embryos. Specifically, that after Rock1/2 inhibition the Amot signal was atypically found on outer-cell lateral regions and co-localised with the adherens junction maker Ctnnb1 (*n.b.* microscopy resolution did not permit the assessment of outer-cell basal membrane localisation due to proximal signal from adjacent inner-cells; *n.b.* some outer-cells also exhibited atypical apical localisation of Ctnnb1). Moreover, such ectopic outer-cell Amot mis-localisation was associated with atypical cytoplasmic Yap1 localisation (on average 69.4% of outer cells in Rock1/2-inhibited versus 6.3% in DMSO vehicle control groups – see figure 4.18c and supplementary tables ST18), thus confirming aberrant Hippo signalling pathway activation in the outer cells of Rock1/2 inhibited embryos.

Interestingly, Rock1/2-inhibited embryos also exhibited overall increased levels of Amot protein expression (note that DMSO- and Rock1/2-inhibitor-treated embryo micrographs were obtained with the same confocal microscopy settings – Fig. 4.18b). This raised the possibility that Rock1/2 inhibition might be associated with an increase in the expression level of Amot mRNA. Thus, the experimental strategy of *in vitro* culturing 2-cell (E1.5) stage embryos in the presence of Rock1/2 inhibitor until 32-cell/ late morula (E3.5) stage was repeated and Amot transcript levels were assayed by Q-RTPCR analysis. However, no difference in Amot mRNA expression level between Rock1/2-inhibited and vehicle control embryos was observed (Fig. 4.18d), suggesting the existence of post-translational regulatory mechanisms that are responsible for the observed elevated Amot protein levels.

Taken together, these data reveal a role for Rock1/2 in not only regulating appropriate apical-basolateral polarisation but also in ensuring Amot protein is excluded from the outer-cell basolateral domains enriched in adherens junctions, under normal developmental conditions.

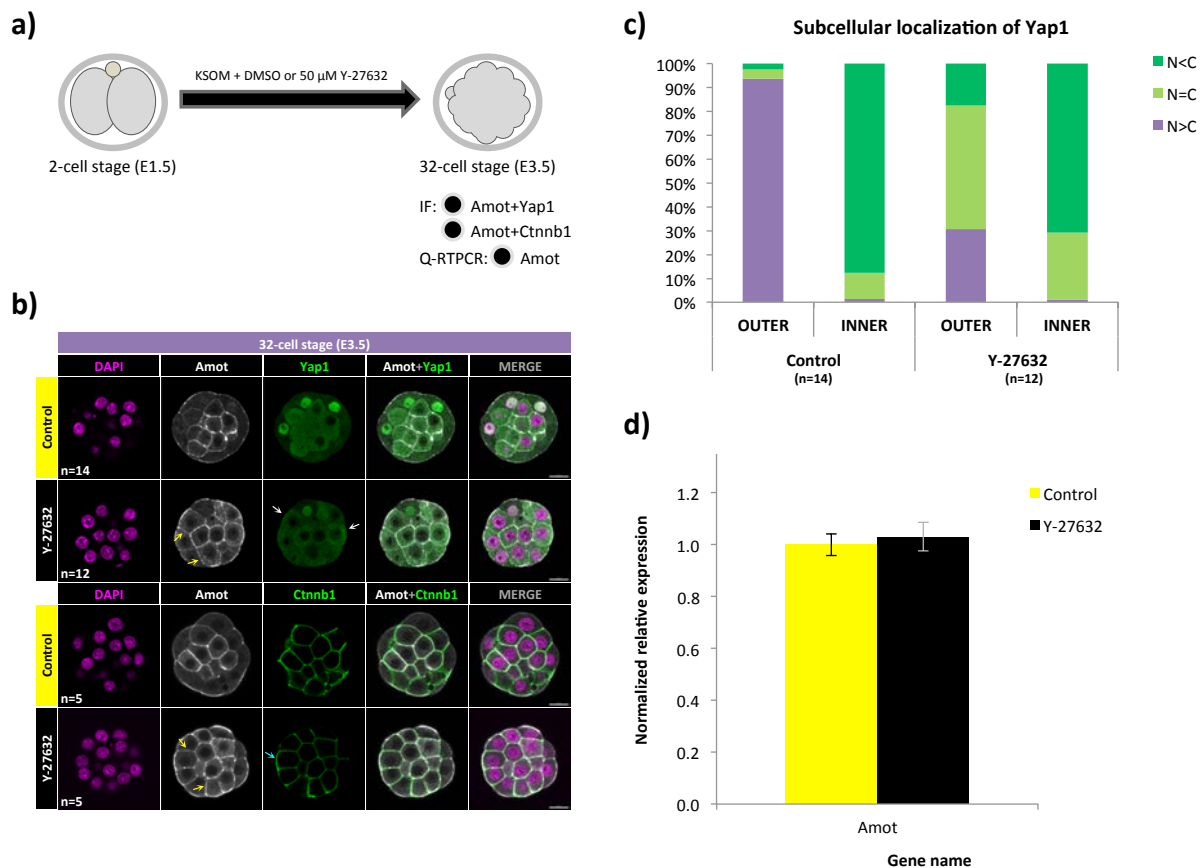


Figure 4.18 Enhanced and mis-localised outer-cell Amot expression in Rock1/2-inhibited embryos is related to activation of the Hippo signalling pathway. **a)** Schematic representation of the experimental strategy to assay Amot protein expression and localisation in combination with either Yap1 or Ctnnb1, as well as Amot mRNA level in 32-cell stage control or Y-27632-treated (50 μ M)/ Rock1/2-inhibited embryos. **b)** Representative single z-section confocal micrographs of control and Rock1/2-inhibited embryos, double-immuno-fluorescently stained for Amot (grey-scale) and either Yap1 or Ctnnb1 (green), with DAPI DNA counter-stain (magenta). Yellow, white and blue arrows highlight atypical protein localisation in Rock1/2-inhibited embryos, versus controls, for Amot (outer-cell lateral domains), Yap1 (outer-cell cytoplasmic localisation) and Ctnnb1 (outer-cell apical domain enrichment), respectively. *n.b.*, enhanced overall Amot expression in outer-cells of Rock1/2-inhibited embryos versus controls. Scale bars = 20 μ m. **c)** Graphical representation of the averaged percentages of outer- and inner-cells exhibiting nuclear Yap1 signal less than cytoplasmic signal (N<C), nuclear Yap1 signal greater than cytoplasmic signal (N>C) or approximately equal signals (N=C), from control (n=14) or Rock1/2-inhibited (n=12) embryos. **d)** Q-RT-PCR analysis revealing unaltered Amot mRNA expression levels after Rock1/2-inhibition. Amot mRNA expression levels were normalised to the composite of both H2afz and Tbp transcript expression levels. Error bars represent s.e.m.; performed in triplicate.

4.2.3.2 Experimental down-regulation of Amot prevents Rock1/2 inhibitor from exerting an effect on Hippo signalling pathway

The next aim was to directly test if the observed Amot protein mis-localisation to the adherens junctions of outer cells was functionally relevant. It was hypothesised that if Amot and its associated mis-localisation were not required for Rock1/2-mediated activation of outer-cell Lats1/2, RNAi-mediated depletion of Amot protein would not be able to block aberrant Lats1/2 activation and outer-cells would continue to express cytoplasmic Yap1. However, if the converse was true and Amot was the mediator of Rock1/2-inhibited Lats1/2 activation, outer-cell Yap1 localisation would be nuclear upon Amot depletion, despite continued Rock1/2-inhibition. Therefore, 2-cell (E1.5) stage embryos were microinjected in both blastomeres with either control GFP- or Amot-specific double stranded RNA (denoted GFP-dsRNA or Amot-dsRNA, respectively) plus RDBs (as an injection marker) and *in vitro* cultured until the 32-cell/ late morula (E3.5) stage in media supplemented with either 50µM Y-27632/ Rock1/2 inhibitor or DMSO vehicle (as a control), prior to assaying for a combination of either Amot and Yap1 or Amot and Pard6b protein expression/ localisation by immunofluorescence base confocal microscopy. As observed in non-microinjected embryos (Fig. 4.18b), Rock1/2-inhibition in GFP-dsRNA microinjected control embryos induced mis-localisation of both Amot and Pard6b to outer-cell basolateral regions and consequently resulted in cytoplasmic Yap1 localisation (Fig. 4.19b), indicative of inappropriate Hippo signalling pathway activation and thus demonstrating the effectiveness of Y-27632/ Rock1/2 inhibitor on microinjected embryos. The efficacy of the RNAi approach to specifically target Amot expression was confirmed by a severe reduction in the amount of detectable Amot protein in both Amot-dsRNA microinjected vehicle control treated and Rock1/2-inhibited embryos (Fig. 4.19b). Importantly, in the confirmed absence of Amot, Y-27632/ Rock1/2 inhibitor was no longer capable of exerting its effect on redistributing Yap1 sub-cellular localisation in outer cells from the nucleus to the cytoplasm; indicating aberrant activation of the Hippo signalling was unable to occur. Thus, despite the fact that the apical polarity factor Pard6b clearly exhibited ectopic basolateral accumulation, demonstrating a breakdown in apical-basolateral cell polarity establishment, Yap1 was found to be nuclear localised in all cells of Amot-dsRNA microinjected Rock1/2-inhibited embryos.

Therefore, these data confirm that Amot acts upstream of Yap1 and downstream of cell polarity and furthermore demonstrate that the Rock1/2 inhibition mediated effects on Hippo signalling pathway were entirely mediated via Amot and its mis-localisation to adherens junctions in outer cells.

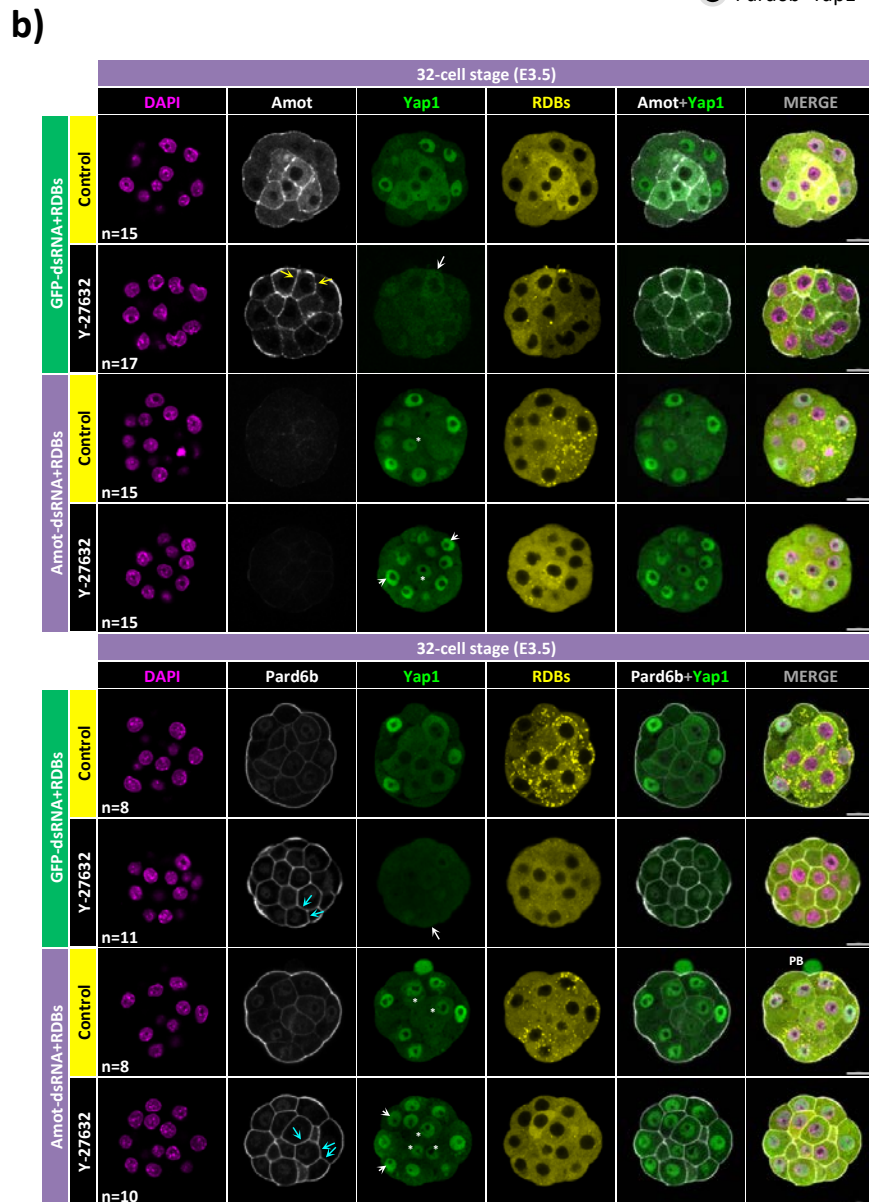
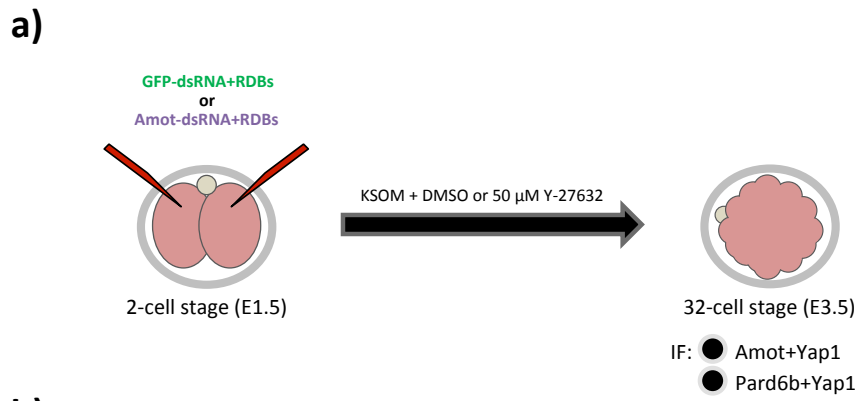


Figure 4.19 (legend overleaf)

Figure 4.19 The Rock1/2-inhibition induced ectopic activation of Hippo signalling in outer-cells is mediated by Amot. **a)** Experimental strategy to knockdown Amot protein expression in developing pre-implantation control (DMSO) or Rock1/2-inhibited (Y-27632, 50 μ M) embryos, using control (GFP-dsRNA) or Amot-specific (Amot-dsRNA) RNAi. **b)** Representative single z-section confocal micrographs of GFP-dsRNA or Amot-dsRNA microinjected, DMSO control or Rock1/2-inhibitor (Y-27632) treated embryos, double-immuno-fluorescently stained for Amot (grey-scale) and Yap1 (green), upper panels, or Pard6b (grey-scale) and Yap1 (green), lower panels. DNA DAPI counter-stain and RDBs (microinjection marker) signal, pseudo-coloured magenta and yellow, respectively. Relating to Rock1/2-inhibited GFP-dsRNA microinjected embryos, yellow and blue arrows denote atypical basolateral expression of Amot and Pard6b, versus DMSO vehicle treated embryos. White arrows highlight outer-cells no longer exhibiting nuclear enriched Yap1 thus confirming the dependency of appropriate apical polarisation and Hippo signalling suppression on Rock1/2 activity in outer-cells. Regarding Amot-dsRNA microinjected embryos, white asterisks and arrow-heads highlight nuclear enriched Yap1 that is present in both inner- and outer-cells, respectively, irrespective of Rock1/2-inhibition status (contrast with GFP-dsRNA microinjected embryos). Moreover, blue arrows again mark atypical Pard6b basolateral expression in outer-cells, only after Rock1/2-inhibition. Therefore confirming Rock1/2-activity mediated effects on Hippo signalling act through the regulation of apical-basolateral polarisation (assayed by Pard6b localisation) and then via the Amot protein (as depletion of Amot is able to block Rock1/2-inhibitor mediated activation of the Hippo signalling pathway, in outer-cells, assayed by Yap1 localisation, despite apical-basolateral polarity defects). 'PB' denotes second meiotic polar body. Scale bars = 20 μ m. Experimental and control embryo 'n' numbers are provide in each relevant panel (left-most).

4.2.4 Rock1/2 inhibition effects on tight junction formation, cell polarity and Hippo signalling pathway are unlikely to be the consequence of aberrant actin polymerisation (UNPUBLISHED RESULTS)

The involvement of Rock1/2 in controlling the dynamics of actin polymerisation has previously been described in the literature in several different contexts (reviewed in Street and Bryan, 2011). Thus, the described observation that F-actin failed to accumulate at the presumptive tight junction regions of outer cells in Rock1/2-inhibited embryos (Fig. 4.17b), left open the possibility that actin polymerisation may have been affected by Y-27632/ Rock1/2 inhibition and thus could potentially provide the underlying cause for the observed failures in tight junction formation and Prkcz/i and Pard6b apical polarity. Therefore, it was decided to investigate whether aberrant actin polymerisation *per se*, might play a role in mediating the detailed Rock1/2-inhibition mediated effects on tight junction formation, cell polarity establishment and Hippo signalling pathway activation. It was hypothesised that, if this was the case, embryo treatment with an inhibitor of actin polymerisation, for example cytochalasin D, would at least partially mimic the effects of Y-27632/ Rock1/2 inhibitor. Thus, 2-cell (E1.5) stage recovered embryos were *in vitro* cultured in KSOM+AA media up until two hours before reaching 32-cell (E3.5) stage, at which point they were transferred into either KSOM+AA containing 0.5 μ g/ml cytochalasin D or fresh KSOM+AA medium (as a control) and returned to culture for the following two hours, until they have reached the 32-cell (E3.5) stage.

Embryos were subsequently fixed and assayed by confocal microscopy for cytoskeletal (F-actin), adherens junction (Cdh1), tight junctions (Tjp1), cell polarity (pERM, Pard6b, Prkcz/i and Scrib) and Hippo signalling pathway component (Amot and Yap1) protein expression. The effectiveness of the cytochalasin D treatment was confirmed by the observed severely disrupted and seemingly random mis-localisation of the F-actin network (Fig. 4.20b). Interestingly, the ordinarily observed localisation of Amot was similarly disrupted and co-localised very well with the remnants of the mis-localised F-actin; supporting the assertion that the two normally physically interact with each other as previously reported in HEK293 cells (Human embryonic kidney cells 293) (Hirate *et al.*, 2013). Importantly, the observed distribution of Cdh1 protein revealed that the integrity of adherens junctions was completely disrupted after cytochalasin D treatment; typified by Cdh1 accumulations at the apical plasma-membrane domain and near complete exclusion from the lateral domains of outer cells, following cytochalasin D treatment. As a consequence, the blastomeres of cytochalasin D treated embryos were shown to be incapable of activating the Hippo signalling pathway, as evidenced by the ubiquitous nuclear localisation of Yap1 in all cells (Fig. 4.20c). Nevertheless, the polarised distribution of both apical and basolateral factors was preserved in the outer cells of cytochalasin D treated embryos, although the apical polarity markers appeared to have spread across the lateral membrane domains of outer cells, perhaps indicative of the presence of displaced but functional tight junctions, or simply unusually enlarged apical domains. The examination of Tjp1 distribution further supported this view as Tjp1 had been found accumulated at presumptive apical-basal membrane domain border regions (Fig. 4.20c).

Taken together, these results strongly suggest that the observed and detailed Rock1/2 inhibition effects on tight junction formation, cell polarity establishment and Hippo signalling pathway are unlikely to be the consequence of aberrant actin polymerisation, as the treatment with cytochalasin D induces largely opposing effects.

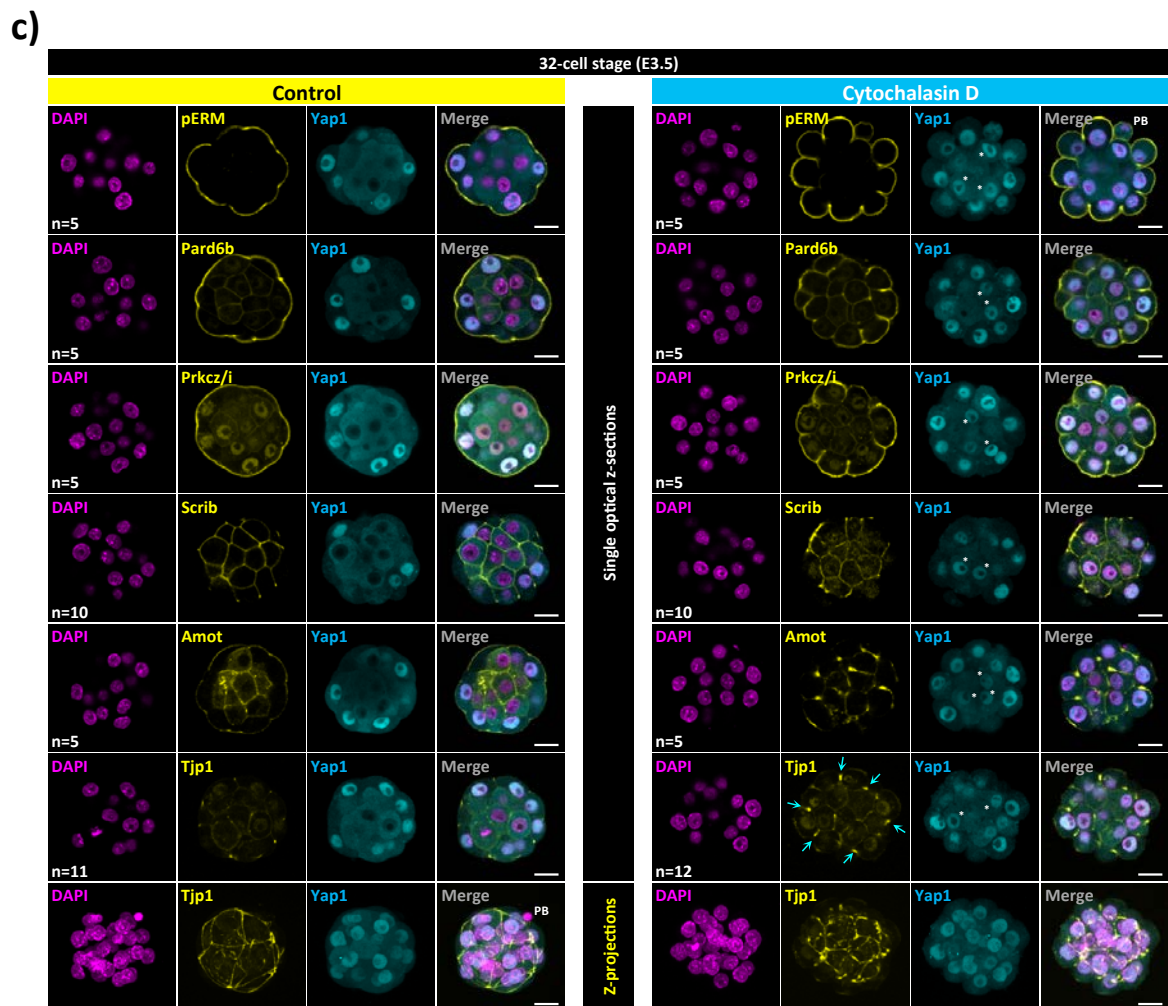
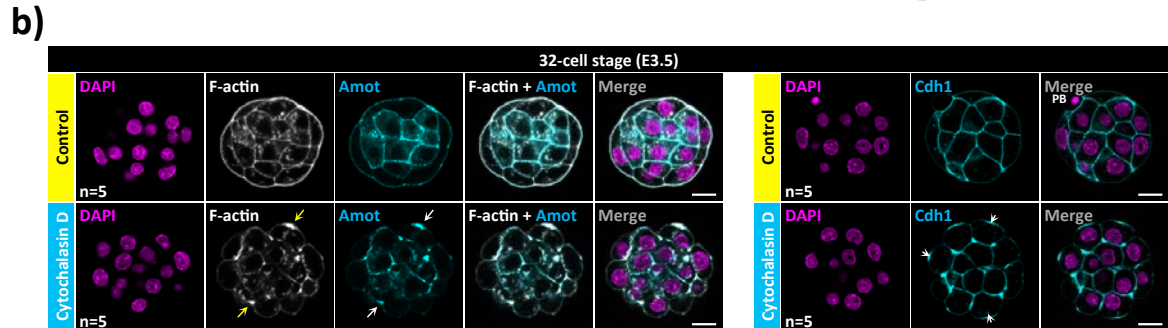
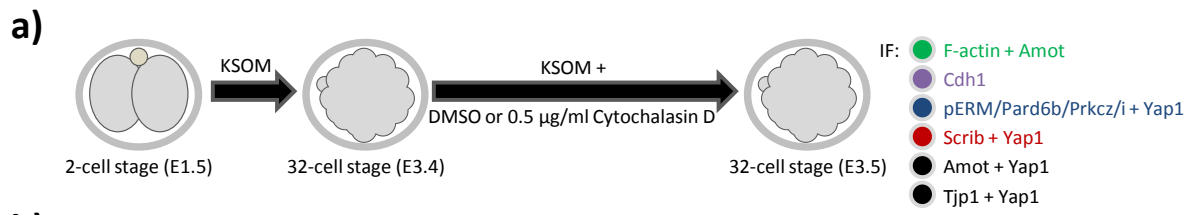


Figure 4.20 (legend overleaf)

Figure 4.20 Cytochalasin D treatment disrupts adherens junctions and consequently prevents Hippo signalling pathway activation. **a)** Schematic representation of the experimental strategy to inhibit actin polymerisation two hours prior to 32-cell (E3.5) stage and examine sub-cellular localisation of the stated cytoskeletal, apical-basolateral polarity-associated, junctional proteins or Hippo signalling pathway components in control or cytochalasin D treated (0.5 µg/ml) embryos after two hours. **b)** Representative single z-section confocal micrographs of control or cytochalasin D treated embryos stained for either adherens junction protein marker Cdh1 (cyan) or a combination of cytoskeletal F-actin (grey-scale) and Hippo signalling pathway component Amot (cyan); shown are projected confocal microscope acquired z-sections. Yellow and white arrows denote atypical localisation of F-actin and Amot proteins, respectively. White arrow-heads highlight apically accumulated and mis-localised Cdh1. **c)** Representative single z-section confocal micrographs, plus selected projected images, of control or cytochalasin D treated embryos immuno-fluorescently stained for stated proteins (yellow) in combination with Hippo signalling pathway component Yap1 (cyan). In cytochalasin D treated embryo images, cyan arrows denote accumulated Tjp1 protein indicative of displaced but present tight junctions, while white asterisks highlight ectopic nuclear localised Yap1 in inner cells indicative of an inactive Hippo signalling pathway. In **b)** and **c)**, DNA was counter-stained with DAPI (magenta). In merged images, 'PB' denotes the second meiotic polar body. Scale bars = 20µm.

4.2.5 Rock1/2 inhibition effects are already evident at the molecular level in 16-cell stage embryos

The apparent morphological and developmental defects observed in Rock1/2-inhibited embryos are only first visible after the 32-cell/ late morula (E3.5) stage. Nevertheless, the defects in cellular polarity and aberrant Hippo signalling pathway activation, associated with Rock1/2-inhibition, are observed at this stage, indicating that at molecular level, the consequences of Rock1/2 inhibition might be detectable at even earlier developmental time points. Thus, it was next decided to test if the Rock1/2 inhibition effects were also observable at the 16-cell (E3.0) stage. Accordingly, 2-cell (E1.5) stage embryos were *in vitro* cultured in KSOM+AA media containing either 50µM Y-27632/ Rock1/2 inhibitor or the equivalent volume of DMSO vehicle control, until the 16-cell (E3.0) stage, fixed and assayed for cytoskeletal (F-actin), apical-basolateral polarity (pERM, Prkcz/i, Pard6b and Scrib) and Hippo signalling pathway components (Amot and Yap1) protein expression, by confocal microscopy based immuno-fluorescence staining. Upon examining projected confocal z-stack images of 16-cell (E3.0) stage embryos a severe reduction in pERM levels after Rock1/2 inhibition was revealed (Fig. 4.21b) and although apical disc-like localisation of pERM was also observable in the accompanying vehicle control embryos, (suggesting the existence of pERM enriched apical-discs may reflect a normal distribution during the unperturbed development at the 16-cell stage) the extent to which it spread throughout the apical membrane domain was much greater than that observed in either 16-cell or 32-cell stage Rock1/2-inhibited embryos. In addition, the accumulation of F-actin observed at the tight-junction proximal regions of the plasma-membrane in vehicle control treated 16-cell (E3.0) stage embryos was absent in the Rock1/2-inhibited embryos at the same developmental stage (Fig. 4.21b).

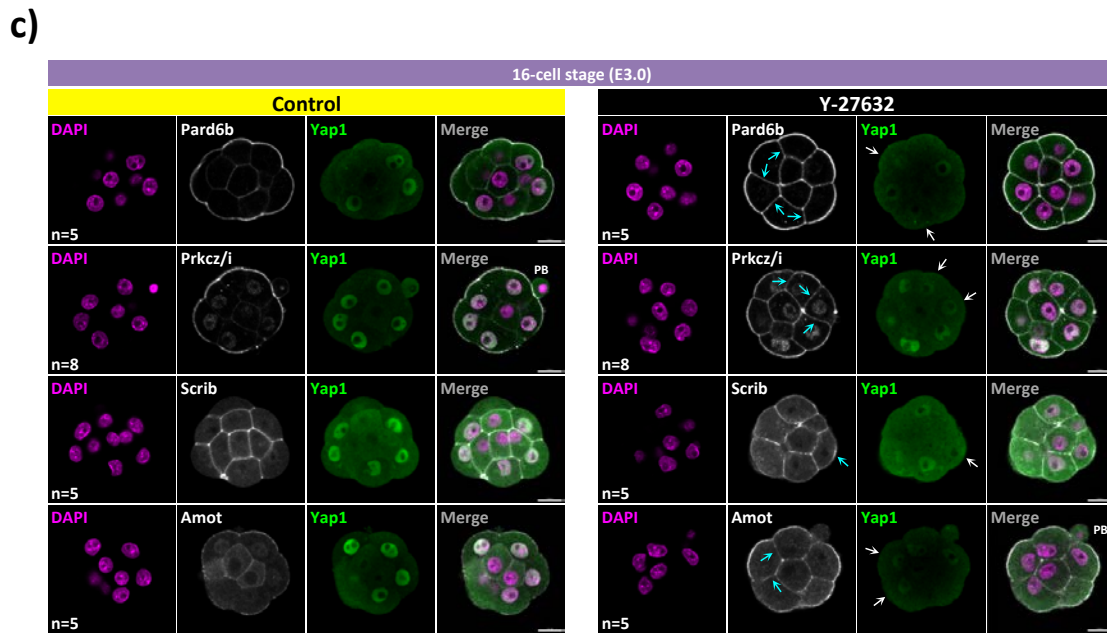
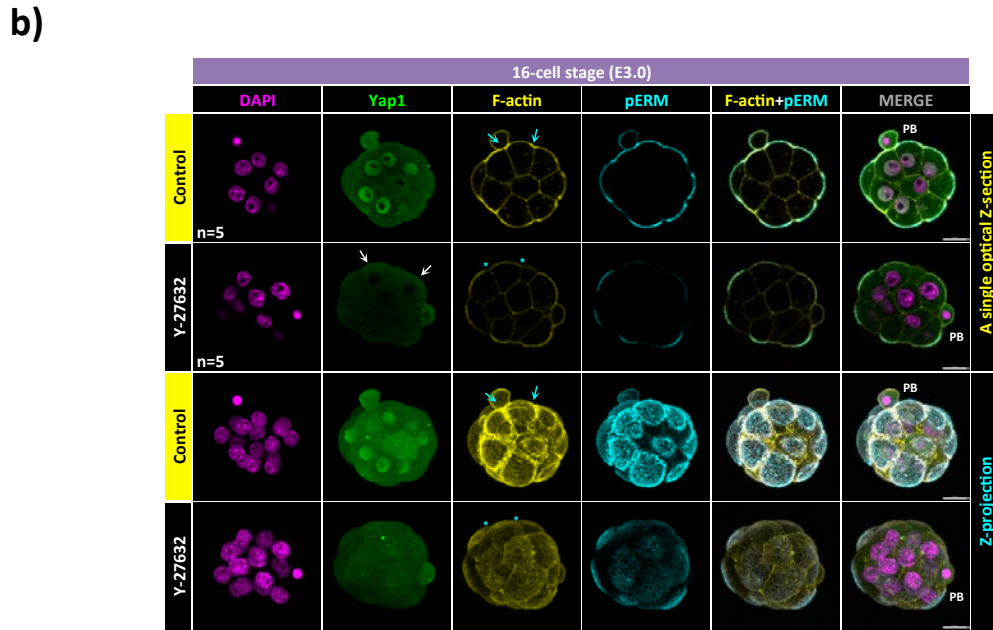
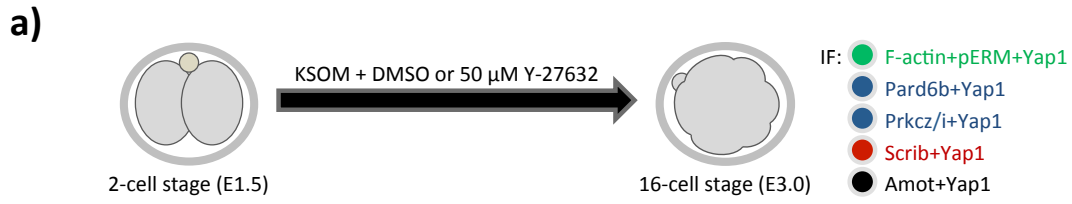


Figure 4.21 (legend overleaf)

Figure 4.21 Rock1/2-inhibition (from the 2-cell stage) is also associated with atypical cytoskeleton, apical-basolateral polarity and Hippo signalling related protein localisation at the 16-cell stage embryos. **a)** Schematic representation of the experimental strategy to assay sub-cellular localisation and expression of the stated cytoskeletal, apical-basolateral polarity-associated or Hippo signalling related proteins in control (DMSO) or Y-27632-treated (50 μ M)/ Rock1/2-inhibited 2-cell stage embryos *in vitro* cultured to the 16-cell stage. **b)** Representative single z-section confocal micrographs (plus accompanying projected images, as stated) of control and Rock1/2-inhibited embryos immuno-fluorescently stained for Yap1, F-actin and pERM (pseudo-coloured green, yellow and cyan, respectively) and DNA (DAPI counter-stain, magenta). White arrows denote loss of outer-cell nuclear localised Yap1 immuno-fluorescent staining after Rock1/2-inhibition. Blue arrows mark tight-junction proximal regions in control embryos enriched in F-actin and blue asterisks equivalent regions in Rock1/2-inhibited embryos without enriched F-actin. **c)** As in **b)** but combining Yap1 immuno-fluorescent staining (green) with either Pard6b, Prkcz/i, Scrib or Amot (represented in grey-scale). White arrows denote loss/reduced outer-cell nuclear localised Yap1 immuno-fluorescent staining after Rock1/2-inhibition. Blue arrows mark aberrant outer-cell basolateral localisation of the classical apical-polarity factors Pard6b and Prkcz/i, the atypical apical localisation of the basolateral polarity-factor Scrib or unusual lateral localisation of Amot in outer-cells. In both **b)** and **c)** 'PB' denotes the second meiotic polar body. Scale bars = 20 μ m.

In accordance to the previously described findings at the 32-cell/ late morula (E3.5) stage, both Pard6b and Prkcz/i apical polarity markers were also uniformly distributed throughout the plasma membrane of outer cells while the basolateral marker Scrib was ectopically present at the apical plasma membrane domain of Rock1/2-inhibited embryos; thus further revealing defects in the establishment of apical-basolateral polarity, but at the 16-cell (E3.0) stage (Fig. 4.21c). Consistently, Amot was similarly mis-localised to the adherens junctions in the lateral regions of outer-residing cells at the 16-cell (E3.0) stage, however the degree to which Yap1 was ectopically localised to the cytoplasm was less apparent than observed by the 32-cell/ late morula (E3.5) stage but nevertheless still evident at this earlier developmental stage (Fig. 4.21c).

Taken together, these results demonstrate that the effects of Rock1/2 inhibition from the 2-cell (E1.5) stage are already apparent at 16-cell (E3.0) stage and that these are similar in nature to those observations made at the at 32-cell/ late morula (E3.5) stage (Fig. 4.17b); *i.e.* Rock1/2 inhibition being associated with an aberrant sub-cellular localisation of cytoskeletal F-actin, defective cell polarity and mis-localisation of Hippo signalling components associated with ectopic outer-cell activation of the pathway.

4.2.6 Rock1/2 activity is indispensable for the appropriate polarisation of 8-cell stage blastomeres (UNPUBLISHED RESULTS)

It was next decided to investigate whether the effects of Rock1/2 inhibition on cell polarity establishment would be detectable at 8-cell stage, the developmental time point when blastomeres of the mouse pre-implantation embryo first polarise. Therefore, 2-cell (E1.5) stage embryos were *in vitro* cultured in KSOM+AA media containing either 50 μ M Y-27632/ Rock1/2 inhibitor or an equivalent volume of DMSO vehicle until the mid- to late-8-cell (E2.75) stage, fixed and assayed for the expression of apical cell polarity (pERM and Prkcz/i) or early tight-junction (Tjp1) protein markers, in combination with cytoskeletal (F-actin) and Hippo signalling pathway (Yap1) components, by immuno-fluorescence based confocal microscopy. As shown in figure 4.22, Rock1/2-inhibited embryos exhibited a severe reduction in pERM levels at the apical plasma-membrane domain that was in addition to an incomplete exclusion from the basolateral domain. Moreover, typical accumulation of Prkcz/i protein at the apical plasma-membrane domain (normally indicative of appropriate cell polarisation and present in vehicle control embryos) was not detectable in Rock1/2-inhibited 8-cell stage embryos. Instead, Prkcz/i remained uniformly distributed throughout the plasma-membrane thus confirming that cell polarity establishment was defective. In addition, the early tight junction marker Tjp1 was evenly distributed throughout plasma-membrane in both control and Rock1/2-inhibited embryos, suggesting the initiation of tight junction formation at the examined developmental time point had not yet started. Interestingly, no obvious alterations in F-actin localisation were observed in Rock1/2-inhibited embryos at the 8-cell stage, but this could be related to the relatively immature state of the tight junctions (as defects in tight junction associated F-actin are the only F-actin defects observed consequent to Rock1/2 inhibition at later assayed developmental stages). Similarly, a comparison of control and Rock1/2-inhibited 8-cell stage embryos also reveals no differences in Yap1 nuclear localisation at this stage, indicating a lack of Hippo pathway activation despite the described cellular polarity defects.

These results collectively demonstrate that Rock1/2 activity is indispensable for the appropriate and timely polarisation of 8-cell stage blastomeres. Furthermore, defects in cell polarity induced by Y-27632/ Rock1/2 inhibition precede the onset of tight junction formation and are therefore unlikely to be the consequence of defective tight-junction formation but rather imply a more direct involvement of Rock1/2 in cell polarity establishment.

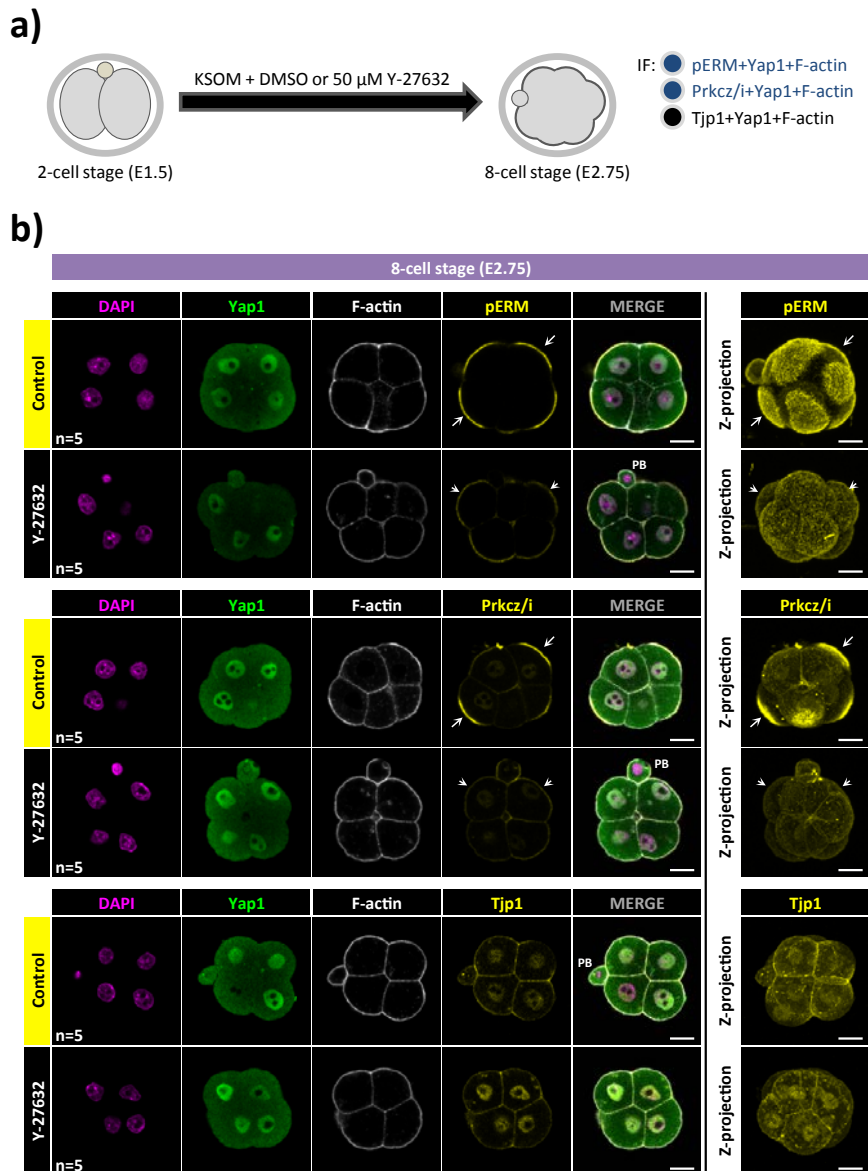


Figure 4.22 Rock1/2 inhibition effects on cell polarity establishment are observable as early as the late-8-cell stage (the developmental stage at which cellular polarisation ordinarily occurs). **a)** Schematic representation of the experimental strategy to assay the sub-cellular localisation of apical polarity- (Prkc*/i*, pERM) or tight junction- (Tjp1) associated factors in combination with cytoskeletal (F-actin) and Hippo signalling related (Yap1) proteins in control (DMSO) or Y-27632-treated (50 μ M)/ Rock1/2-inhibited embryos, *in vitro* cultured from the 2-cell (E1.5) to late-8-cell (E2.75) stage. **b)** Representative single z-section confocal micrographs (plus accompanying projected images, as stated) of control and Rock1/2-inhibited embryos stained for either Prkc*/i*, pERM or Tjp1 (yellow) in combination with F-actin (grey-scale) and Yap1 (green). DNA was counter-stained with DAPI (magenta). Arrows highlight cells in vehicle control embryos with the appropriate establishment of apical cell polarity while arrow-heads denote defective/ absence of cell polarity establishment in Rock1/2-inhibited embryos. 'PB' in merged images denotes the second meiotic polar body. Scale bars = 20 μ m.

4.2.7 Rock1/2 activity is required for cell/ blastomere internalisation processes, possibly via regulation of myosin light chain-2 phosphorylation (UNPUBLISHED RESULTS)

As previously demonstrated, it is possible, via experimental perturbations of the appropriate cell polarity establishment, to alter the number of inner cells that would ordinarily be generated in the two waves of cell internalisation consequent/ subsequent to the fourth and the fifth cell cleavage divisions (Dard, Le, *et al.*, 2009; Plusa, Frankenberg, *et al.*, 2005). Since Rock1/2 inhibition is associated with defective cell polarity establishment it was decided to examine whether the number of generated inner cells (and hence by default outer cells) had been affected as a consequence of the Rock1/2 inhibitor treatment. Thus, a re-analysis of the above described datasets was undertaken to determine the number of inner and outer cells in each individual embryo, *in vitro* cultured from the 2-cell (E1.5) stage to the 16-cell (E3.0) or 32-cell (E3.5) stages in the presence of either DMSO vehicle or Rock1/2 inhibitor (see figure 4.16; see also supplementary tables ST19). Although the total number of cells remained unaffected by Rock1/2 inhibitor, a statistically significant decrease in the number of inner cells generated in Rock1/2-inhibited embryos, when compared to vehicle control embryos, was observed at both the assayed stages examined. Accordingly, the number of outer cells in Rock1/2-inhibited embryos was also significantly increased (Fig. 4.23b). Hence, these observations strongly suggest that Rock1/2 activity is required for the cell internalisation process and the generation of ICM progenitor cells that will ultimately give rise to the EPI and PrE cell lineages.

Cell internalisation during pre-implantation mouse embryo development appears to be driven by a process of apical constriction that arises as a consequence of subtle differences in the tensile forces between neighbouring blastomeres produced by the actomyosin cortical network. An important role for Myh9, a non-muscle myosin IIa heavy chain, in regulating the apical constriction in the mouse pre-implantation embryo has recently been documented (Samarage *et al.*, 2015; Maitre *et al.*, 2016). Since Rock1/2 is known to be involved in the regulation of myosin light chain phosphorylation in human cell culture systems (Kosako *et al.*, 2000), the antibody that specifically recognises phosphorylated form (at serine 19) of smooth muscle myosin light chain 2 (represented by several different isoforms, hereinafter commonly referred to as Mlc2), was employed to assay the level of phospho(Ser19)-Mlc2 (pMlc2) in mouse pre-implantation embryos after Rock1/2 inhibition. Consequently, 2-cell (E1.5) stage embryos were *in vitro* cultured until the 16-cell (E3.0) or 32-cell stages (E3.5) in the presence of 50 μ M Rock1/2 inhibitor (or an equivalent volume of DMSO vehicle) in KSOM+AA media, fixed and immuno-fluorescently stained for pMlc2.

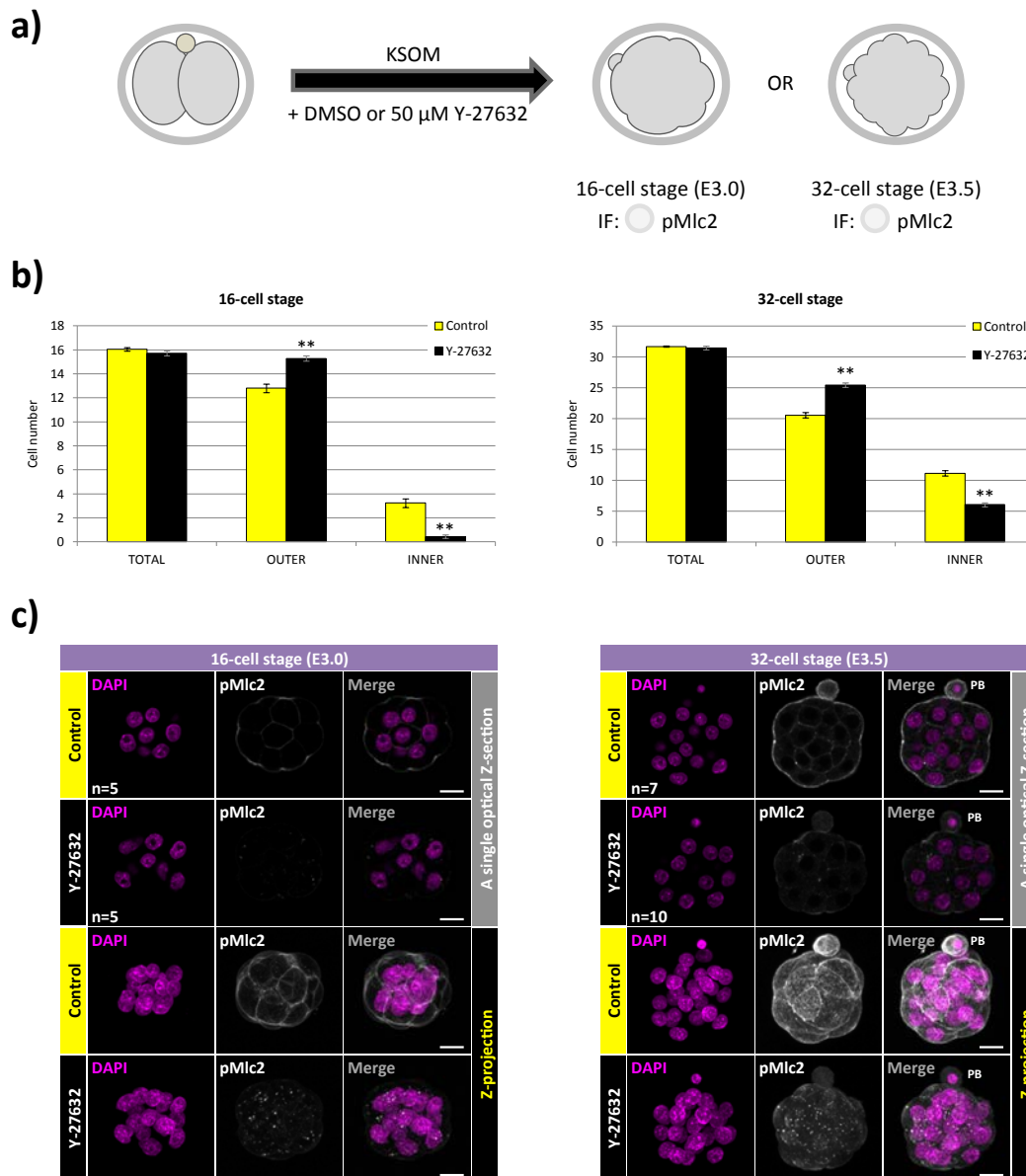


Figure 4.23 Rock1/2 inhibition is accompanied by a reduction in myosin light chain-2 phosphorylation (pMlc2) and decreased cell internalisation. **a)** Schematic representation of the experimental strategy to assay the averaged total, outer and inner cell number and phosphorylation level of myosin light chain-2 (pMlc2) protein in 16-cell (E3.0) and 32-cell (E3.5) stage vehicle control or Y-27632-treated (50 μ M)/ Rock1/2-inhibited embryos. **b)** Graphical representation of the averaged total, outer and inner cell number in 16-cell (E3.0) and 32-cell (E3.5) stage control or Rock1/2-inhibited embryos. For control embryos, n=26 and 22 for the E3.0 and E3.5 stages, respectively; n=21 and 22 for the equivalent Rock1/2-inhibited embryos. Error bars represent s.e.m.; ** denotes a statistically significant difference between control and Rock1/2-inhibited embryos ($p < 0.005$, 2-tailed student t-tests). **c)** Representative single z-section confocal micrographs and projected images of 16-cell (E3.0) and 32-cell (E3.5) stage vehicle control and Rock1/2-inhibited embryos immuno-fluorescently stained with pMlc2 (Ser19)-specific antibody (grey-scale). DNA was counter-stained with DAPI (magenta). 'PB' in merged images denotes the second meiotic polar body. Note, the images for control and Rock1/2 inhibited embryos were captured using the same confocal microscopy settings on either 16-cell (E3.0) or 32-cell (E3.5) embryos samples prepared and imaged on the same day. Scale bars = 20 μ m.

As shown in the figure 4.23c, it was found that the levels of pMlc2 were indeed significantly reduced in Rock1/2-inhibited embryos when compared to control embryos at both the 16- and 32-cell stage. Collectively, these data demonstrate that Rock1/2 is actively involved in the process of cell internalisation possibly via regulation of Mlc2 phosphorylation.

Taken together, data presented in part II of the current results section demonstrate that Rock1/2 activity is indispensable for the late morula to early blastocyst transition during pre-implantation mouse embryo development, as Rock1/2 inhibition prevented blastocoel formation. At the molecular level, this phenotype is associated with defects in the establishment of cell polarity, tight junction formation and F-actin distribution. In addition, in the absence of Rock1/2 activity, Amot is mis-localised to the adherens junctions of outer cells and ectopically activates the Hippo signalling pathway, consequently resulting in cytoplasmic Yap1 subcellular localisation. Rock1/2 inhibition is also accompanied by reduced pMlc2 levels that may have, in part, a role in preventing blastomeres from appropriately regulating their spatial position, and hence fate, within the embryo. Therefore, results collectively emphasize the importance of Rock1/2 activity in regulating several key aspects of pre-implantation mouse embryo development.

5. DISCUSSION

5.1 DISCUSSION - PART I

The underlying intention of the relevant presented section of thesis data was to examine the importance of cell history during the acquisition of the second cell fate during mouse pre-implantation embryo development. Therefore, variously sized cell clones that were unable to initiate TE differentiation were created within the developing mouse embryo and their potential to populate the EPI and PrE lineages within the ICM assayed by the late blastocyst (E4.5) stage. It was reasoned that such prevention of the initiation of TE differentiation would mimic the effects of the early removal of ICM progenitors from such differentiative cues that normally occurs as a result of their internalisation after the fourth cleavage division; therefore permitting an analysis to examine if such TE-inhibited clones would, after internalisation, be predisposed to form the pluripotent EPI, rather than differentiating PrE cell lineage, in a manner supportive of the data demonstrating such a bias in ICM founder cells generated during the fourth cleavage/ first differentiative/asymmetric round of division (Morris *et al.*, 2010). In each of the three experimental strategies employed this was found to be the case, as the ICM cells derived from the TE-inhibited clone preferentially contributed to the EPI versus the PrE cell lineage. If during early pre-implantation mouse embryo development, the TE differentiation status (or extent of differentiation) of ancestral ICM progenitor cells was unimportant, the ICM-residing TE-inhibited clones would be expected to segregate equally between the EPI and PrE lineages, in the manner similar to that observed for the marked clone in control microinjection embryo groups; however this was not the case. These data therefore indicate that the level of TE-differentiation ancestral cells of ICM progenitors are exposed to is functionally relevant, in respect to their ultimate fate in the ICM, but is certainly not deterministic as the TE-inhibited cell clones were still able contributed to the PrE lineage, albeit less efficiently. It is therefore concluded that the presented data are consistent with the existence of an integrated cell-fate process, whereby differing levels of exposure to TE differentiative cues, bias subsequent ICM founder cells to preferentially occupy either EPI or PrE cell lineages, as determined by the relative developmental timing an outer cell division gives rise to an internalised progeny cell (*i.e.* as a result of either the earlier fourth or later fifth cell cleavage division).

However, a relatively simple alternative explanation for the observed biased contribution of TE-inhibited cell clones towards the EPI lineage could be that the inactivation of the Hippo signalling pathway, and hence the potentiation of transcriptionally active Tead4, within the ICM is directly required for PrE formation (*i.e.* Tead4, associated with nuclear Yap1 functionally potentiates selected

ICM cells to differentiate to PrE and that be experimentally removing Tead4 expression this potential mechanism is blocked). However, this scenario is very improbable, as during the extensive experiments reported here, ICM cells displaying nuclear localised Yap1 (that would be indicative of an inactive Hippo signalling pathway and transcriptionally active Tead4) were never observed at any of developmental stages examined; although there is precedent for Yap1 localisation within the 'matured' PrE monolayer of late mouse blastocyst (E4.5) stage embryos in the literature (Frankenberg *et al.*, 2013). However, in the same publication the anti-Yap1 immuno-fluorescence signal is reported to be observed in the nuclei of all cells at the early/ late morula and early/ mid blastocyst stages, in a manner atypical to that reported in the entire wider mouse pre-implantation embryo-related literature and moreover the commercially obtained anti-sera used is no longer available. It remains possible the reported nuclear Yap1 immuno-fluorescent signal, in the morphologically segregated PrE layer (Frankenberg *et al.*, 2013), may reflect a role for inactivation of Hippo signalling in the maintenance of PrE/ endoderm function/ integrity in developmentally more advanced blastocysts around or beyond the peri-implantation stage, but the data presented here and in the wider literature argue against its role during the emergence of PrE identity (*i.e.* specification) during blastocyst ICM maturation. Additionally, several previous studies have demonstrated that experimentally induced inactivation of the Hippo signalling pathway within ICM results in the ectopic expression of the TE-lineage marker *Cdx2* in the blastocyst ICM (Cockburn *et al.*, 2013; Hirate *et al.*, 2013; Leung and Zernicka-Goetz, 2013; Lorthongpanich *et al.*, 2013). Therefore, it seems highly probable that the Hippo signalling pathway normally remains inactive within the ICM cells throughout the entirety of the pre-implantation stages of unperturbed mouse embryo development (and specifically during the lineage segregation that occurs during ICM maturation) as similar expression of *Cdx2* in the ICM has not been observable herein or data reported. Hence, it seem highly improbable that the observed results we report are explainable by interfering with endogenous ICM cell-fate mechanisms requiring Hippo signalling inactivation and *Tead4* expression to generate the PrE lineage. However, the findings could still be theoretically interpreted as demonstrating a direct PrE promoting requirement within the ICM for Tead4 that is independent of Yap1. However, this also seems unlikely for a number of reasons. For example, ES cell differentiation in *Tead4*^{-/-} embryoid bodies does lead to the expression of multiple cell lineage marker genes that include the primitive endoderm markers *Gata6* and *Sox17* (Nishioka *et al.*, 2008), suggesting *Tead4* itself is dispensable for PrE formation *per se*, at least in this *in vitro* experimental paradigm. Moreover, the fact that in the present data, PrE cells are observable within the TE-inhibited clones, albeit at much reduced relative frequency, corroborates this assertion. Furthermore, ES cells can be successfully derived and propagated from *Tead4*^{-/-} embryos (Nishioka *et al.*, 2008), suggesting *Tead4* is neither required to maintain pluripotent EPI lineage and also indicating that it is therefore not

required to act in a non-cell autonomous manner to support PrE formation. Collectively, all of the existing evidence argues against any direct and functional cell-fate role for Tead4 protein within the ICM of pre-implantation stage mouse embryos. Therefore, the observations that TE-inhibited cell clones are statistically less probable to contribute to mature PrE, are best explained by the inability of their ancestors to initiate TE differentiation and/ or respond to TE differentiative cues, rather than a lack of functionally relevant Tead4 protein within the ICM-residing cells of such clones.

Given previous reports that state PrE cells require the activity of *Prkcz/i* to re-polarise and maintain their position on the surface of the ICM in order to mature (Saiz *et al.*, 2013) and the fact that a TE-lineage marker protein, *Cdx2*, has been proposed to be involved in transcriptional regulation of *Prkcz/i* (Jedrusik *et al.*, 2008), defects in apical-basolateral polarisation that may have explained why TE-inhibited cell clones would be disadvantaged to populate PrE cell lineage were assayed for. However, it was not possible to detect any reductions in the protein levels of *Prkcz/i* or any other polarity associated factors, at any of the morula and blastocyst stages studied, suggesting this could not have been the mechanism by which *Tead4*-KD cells within the ICM preferentially acquired EPI cell fate. These observations are in accord with data relating to the characterisation of apical-basolateral polarisation in *Tead4*^{-/-} genetic null embryos (Nishioka *et al.*, 2008). Nonetheless, an unexpected observation detailing increases in the extent of apical polarisation in morphologically-rounded TE-inhibited clone cells that remained on the outside of the embryo at the 32-cell/ early blastocyst (E3.6) stage, was made. Whilst the presented analyses suggests that most of these cells are eradicated by apoptosis (supplementary figure S2 and supplementary tables ST5, ST6 and ST7), it was possible to observe incidences of fluorescently labelled enucleated micro-cells, enriched in apical polarity proteins on the surface of 32-cell (E3.6) and >64-cell (E4.5) stage embryos, that seem to have been formed by a process in which such cell clones regulate their development by divesting themselves of their apical domain (see figure 4.13); thus making themselves apolar and susceptible to ICM internalisation, in a manner akin to that already described for the outer-residing apolar 16-cell stage blastomeres (Anani *et al.*, 2014). Hence, this could partially explain how the cells within the *Tead4*-KD clones allocate to preferentially contribute to the ICM over the TE cell lineage. Nevertheless, the observed increase in apical polarisation, and potential ICM internalisation if the cell escapes apoptosis, does not provide an explanation for the biased potential of ICM-resident TE-inhibited cell clone to preferentially contribute to the EPI over PrE lineage.

A chromatin immuno-precipitation-based analysis of genomic *Tead4* transcription factor binding sites in trophoblastic stem (TS) cells, has previously revealed the recruitment of *Tead4* protein to the promoter proximal regions of several well documented PrE lineage marker genes, including *Fgfr2*, *Dab2* and *Lrp2* (Home *et al.*, 2012); thus demonstrating that TE-related factors and

prolonged exposure to TE differentiation cues harbour the direct potential to regulate the expression of genes required for the separation of EPI and PrE cell fates. In addition, the existence of molecular heterogeneity in *Fgf4* and *Fgfr2* gene mRNA expression between ICM founder cells generated as a result of the successive fourth and fifth cleavage divisions, whereby the first population of potentially epiblast biased inner cells (Morris *et al.*, 2010) is characterised by higher *Fgf4* and lower *Fgfr2* mRNA expression levels in contrast to the second PrE biased population (Morris *et al.*, 2010) that have relatively elevated levels of *Fgfr2* expression, has previously been documented (Krupa *et al.*, 2014). This is particularly important given the fact that increased responsiveness to Fgf signalling directs cells to differentiate towards the PrE cell lineage (Yamanaka *et al.*, 2010). The herein described observation that *Fgfr2* expression is attenuated in embryos following global TE-inhibition/ *Tead4*-KD is consistent with these data and supports the notion that prolonged exposure to TE differentiative cues primes cells to yield ICM progeny biased to populate the PrE, by becoming more responsive to PrE-promoting *Fgf4* signalling (Frankenberg *et al.*, 2011; Morris *et al.*, 2013; Nichols *et al.*, 2009; Yamanaka *et al.*, 2010). Moreover, the lack of *Fgfr2* protein plasma membrane association at the interface between some adjacent ICM cells in control embryos and between the ICM cells of the *Tead4*-dsRNA microinjected clone of *Tead4*-KD clone embryos at the 32-cell (E3.5) stage, strongly indicates that one of the reasons why TE-inhibited clones are less able to ultimately differentiate to PrE arises from a reduced ability to receive, a *Fgf4*-based, PrE promoting signal. The reason for the observed enhanced nuclear localisation of *Fgfr2* protein, that also correlates with the reduced plasma membrane association, within the *Tead4*-KD cell clone is however less clear; although it should be noted from the literature that there is precedent elsewhere for the nuclear localisation of *Fgfr2* (Bagheri-Fam *et al.*, 2008; Martin *et al.*, 2011; Schmahl *et al.*, 2004). The fact that in control microinjected embryos, some ICM cells exhibit nuclear localised *Fgfr2* expression (*i.e.* the pattern is heterogeneous between cells of the ICM), that appears to be associated with reduced plasma membrane association, whilst other cells do not, invites the notion that nuclear localisation could be a mechanism to prevent plasma membrane *Fgfr2* localisation and hence unwanted activation by *Fgf4*. It may also represent some hitherto unrecognised proteolytic cleavage event, potentially related to receptor ligand interactions, that results in nuclear import of an intra-cellular receptor fragment that contains the epitope recognised by the anti-sera used.

Interestingly, the presented data also reveals that *Dab2* protein, described in the literature as PrE lineage marker (Moore *et al.*, 2013; Yang *et al.*, 2002, 2007), is also abundantly present in TE cells throughout pre-implantation mouse embryo development. Although the reason for the observed discrepancy in *Dab2* protein expression pattern between previous studies and that presented here is unclear, it is unlikely to be accounted for by the non-specific detection of *Dab2* protein in the present

study as this signal is readily depleted after Dab2-specific dsRNA mediated RNAi knockdown of *Dab2* expression. However, different methodology employed, potentially related to sample fixation, to obtain these results might account for the observed discrepancies. Importantly, this study demonstrates that the *Dab2* gene is under the transcriptional regulation of Tead4, thereby providing an explanation for the observed presence of Dab2 protein expression in the TE lineage. The fact that Tead4 regulates the expression of *Dab2* could also help explain the presence of heterogeneity in Dab2 protein levels within the population of ICM founder cells at 32-cell (E3.6) stage, as differential quantities of Dab2 mRNA could be inherited by cells internalised following the fourth or fifth cleavage divisions, due to the uneven extent to which their ancestral mother cells were exposed to TE-differentiating cues. Moreover, the observation that heterogeneity in Dab2 expression is lost within the ICM cells of *Tead4*-KD cell clone at this same stage further supports this idea (*i.e.* no ICM cells of any *Tead4*-KD cell clone were found to express Dab2 protein, whilst inter-cell heterogeneity was readily observed in the non-microinjected clone). Interestingly, as embryo developmental progression continues towards the late blastocyst (E4.5) stage, the expression level of Dab2 protein was found to increase in TE cells whilst in Dab2-expressing ICM cells it initially remained unchanged, again indicating that Tead4 activity might be entirely responsible for the Dab2 protein expression up until the early/ mid-blastocyst stage transition. However, the fact that Dab2 protein expression within the ICM was eventually observed to increase to levels equivalent to that of the TE, at the late blastocyst (E4.5) stage, suggests a point after this developmental window of blastocyst maturation that PrE factors become involved in the regulation of *Dab2* gene expression, as previously reported (Morrisey *et al.*, 2000). Importantly, it is reported herein that by the time embryo reaches the late blastocyst (E4.5) stage, Dab2 protein expressing ICM cells are preferentially found on the blastocoel-facing surface of the ICM; demonstrating a strong correlation between Dab2 presence and superficial cell position. Indeed, previous studies have shown that the *Dab2* gene is indispensable for appropriate PrE formation, as in its absence embryos fail to properly organise an ICM surface PrE epithelial layer (Moore *et al.*, 2013; Yang *et al.*, 2002, 2007). Nevertheless, it is important to note that *Dab2*-deficient embryos exhibit the expression of late PrE markers in their ICM cells, suggesting that individual blastomeres are still capable of differentiating to/ specifying PrE. Accordingly, it has been proposed that the underlying reason why Dab2-deficient embryos display disorganised PrE epithelial structure might be due to improper cell positioning/ sorting (Yang *et al.*, 2007). The data presented herein, relating to clonal down-regulation of *Dab2*, are in agreement with these findings, as cells within *Dab2*-KD clone are able to express the late PrE lineage marker, *Gata4*, (albeit to a significantly lesser proportion than non-injected cell clone). Therefore, it is possible that the decreased contribution, albeit very mild, of the *Dab2*-KD cell clone towards PrE is due to the inability of Dab2-deficient cells to migrate/ sort towards the surface of the ICM, and as a result they eventually

become outcompeted for the superficial position by other cells outwith the clone that then populate this PrE niche. However, in this scenario, the *Dab2*-deficient cells that initially reside on the ICM surface would be able to adopt PrE cell fate (by not having any requirement for active sorting), perhaps explaining the very mild PrE-deficient phenotype observed upon clonal *Dab2* down-regulation. This is supported by previous ICM cell tracking analyses that show that the majority (75%) of eventual PrE cells (or their ancestors) are found at the ICM surface when blastocoel formation initiates (Morris *et al.*, 2010; Meilhac *et al.*, 2009). If true, this could also help to explain why the *Tead4*-KD cell clone (that also lacks *Dab2* expression) would be biased to contribute towards the EPI and away from PrE cell lineage, as it would not be able to sort to, and remain at, the prospective PrE layer. As *Dab2* protein expression is only ordinarily detected from 32-cell stage onwards (the time point when the first cell-fate decision has already been taken), it is not surprising that the clonal down-regulation of *Dab2* in half of the embryo, reported here, fails to direct blastomeres to allocate towards the ICM and away from the TE lineage, in a manner that would be reminiscent of *Tead4* down-regulation. However, this fact only implies that the absence of *Dab2* protein has no functional influence on the resolution of the first cell-fate decision and does not demonstrate that the presence of *Dab2* mRNA at stages prior to 32-cell (and its potential inheritance) is irrelevant for the appropriate undertaking of the second cell-fate decision. Taken together, the clonal inhibition of TE differentiation is not only correlated with EPI biased contribution in the ICM but is also associated with reduced expression of PrE-related genes. This is consistent with the integrated cell-fate model, given that ICM founder cells derived from ancestral cells exposed to prolonged TE differentiative cues (such as those outer-residing cells of 16-cell stage embryos) are reported to be biased towards PrE (Morris *et al.*, 2010). Accordingly, herein it is proposed that such cells become primed, by virtue of their developmental history and exposure to TE differentiative cues, to first receive PrE promoting signals and then to differentiate to the PrE lineage, albeit in a non-rigid manner that is open to regulative developmental flexibility.

As a result of the presented data, it could be argued that the observed biased contribution of TE-inhibited cell clones towards EPI maybe explained by atypically elevated and physiologically irrelevant levels of EPI lineage marker expression within the cell clone? The absence of the ectopic induction and/or increased protein expression of the EPI marker *Nanog* in *Tead4*-KD cell clone argues against this possibility. However, a relatively recent genetic study has shown that restricted expression of the pluripotency-related transcription factor *Sox2* to inner cells from the 16-cell stage is under the control of *Tead4* in a Hippo signalling pathway dependant manner (Wicklow *et al.*, 2014). Specifically, and in contrast to the activation of *Cdx2* (Nishioka *et al.*, 2009), the inactive Hippo signalling pathway in outer-cells allows *Tead4* mediated repression of *Sox2* (be it direct or indirect).

Conversely, in inner cells, the activation of Hippo signalling prevents Tead4 from repressing Sox2 expression, resulting in the consequent expression of *Fgf4* from EPI progenitor cells. The Fgf4 mediated signalling further induces gene expression profiles compatible with the appropriate derivation of the PrE in a non cell-autonomous manner, whereas the continued Sox2 expression within the EPI cells reinforces their pluripotency (Wicklow *et al.*, 2014). This report is therefore consistent with the existence of the integrated cell-fate model as it highlights the important and functional consequence of the early removal of cells from TE-promoting differentiative environments for subsequent ICM cell fate derivation. That is, to generate EPI and PrE progenitors in both cell autonomous and non cell-autonomous manners, respectively. It is also compatible with the data presented herein, suggesting that a possible reason why a significant EPI cell fate biases in TE-inhibited clones is observed, maybe partly due to increased Sox2 expression, caused by the *Tead4*-KD, contributing to their pluripotency. It is also probable that such enhanced Sox2 expression, under the proposed experimental paradigm, could also cause increased extra-cellular Fgf4 levels that in turn signal to the ICM cells outwith the TE-inhibited clone (*i.e.* the non-microinjected cells) to differentiate; thus accounting for their biased contribution towards PrE. Whilst the idea of elevated Sox2 expression levels in the *Tead4*-KD cell clone is appealing and complementary with the findings presented herein, it was not possible, despite the best efforts invested, to independently verify this potential mechanism in the current study; this was primarily due to the unreliable detection of Sox2 protein expression prior to the late blastocyst (E4.5) stage (possibly as a consequence of technical limitations), that prevented a thorough assessment of Sox2 protein expression levels in 16- and 32-cell stage clonal *Tead4*-KD embryos. Nonetheless, in the context of the integrated cell-fate model, such evidence would indicate that cells that remain exposed to prolonged or heightened TE differentiative environments are not only more likely to be able to receive and respond to PrE differentiative cues in the ICM but are also less likely to originate them. Conversely, cells that are removed from such environments relatively early are more likely to remain pluripotent and initiate PrE differentiative signalling.

A previous study investigating the ICM lineage contribution of varying ratios of marked inner cells, in reconstituted chimeric 16-cell stage embryos, has shown that the initial number of founder ICM cells has a profound effect on their ultimate fate (Krupa *et al.*, 2014). When 16-cell stage chimeras with lower numbers of initial ICM cells (*e.g.* 3) were generated, they were biased to contribute to the EPI in manner reminiscent of that previously reported for cells internalised as a result of the fourth cleavage in *in vitro* cultured embryos (that were incidentally also characterised as having a similar number of inner cells at the 16-cell stage) (Morris *et al.*, 2010). The chimeras also exhibited a biased contribution to the PrE of cells internalised following the fifth cleavage division,

again reminiscent of the previous study. However, when the 16-cell stage chimeras were made with larger numbers of initial ICM cells (*e.g.* 4 or 5), the previously observed biases were no longer observed, and the number of cells internalised after the fifth cleavage was relatively reduced (Krupa *et al.*, 2014). The authors speculated that this could be due to the increased number of inner-residing 16-cell stage blastomeres causing respectively elevated levels of extra-cellular Fgf4, when compared with chimeras with fewer cells, that in turn recruit cells that may have otherwise contributed to the EPI, into differentiating to PrE. Indeed, this speculation now seems justified given the recent evidence demonstrating Fgf4 signalling in derived inner cells is regulated via Sox2 in a Hippo signalling dependent manner (Wicklow *et al.*, 2014). Moreover, it is also consistent with experimentally verified mathematically-based modelling that indicates the formation of the initial 'salt and pepper' expression pattern of EPI (Nanog) and PrE (Gata6) markers in the ICM (Chazaud *et al.*, 2006), requires inter-cell heterogeneity in receptor tyrosine kinase/ Fgf4 pathway activation, that would be subject to fluctuation depending upon the number of inner cells (Bessonnard *et al.*, 2014). From the data presented here (Fig. 4.3-4.5), it can be observed that when the size of the generated ICM resident TE-inhibited/ *Tead4*-KD clones was largest, this was also accompanied by the greatest percentage contribution of the non-TE-inhibited ICM clones to the PrE (50.3%). However, following the generation of consecutively smaller TE-inhibited ICM cell clones, this observed PrE contribution within the non-TE-inhibited ICM clones was progressively smaller (40.9% and 34.2%, in 1 in 4 cell microinjected embryos and 1 + 8 cell chimeras, respectively). In the context of the above stated reports (Bessonnard *et al.*, 2014; Krupa *et al.*, 2014; Wicklow *et al.*, 2014), these results provide indirect evidence that larger TE-inhibited clones are indeed likely to generate greater levels of PrE promoting extra-cellular Fgf4 within the ICM than the smaller clones. Moreover, given, that Sox2 is reported to regulate the level of Fgf4 signalling and its expression is inhibited by *Tead4* (Wicklow *et al.*, 2014), the transcription factor whose expression was impaired to generate the TE-inhibited clones in the employed experimental strategy, this proposed mechanism seems eminently possible. Thus, as has previously been suggested (Bessonnard *et al.*, 2014; Krupa *et al.*, 2014), the presented data also confirm the importance of the number of generated ICM cells, and not just their developmental origin, as being important in biasing subsequent lineage segregation. One further and important discussion point relating to the presented data is that in all the three experimental strategies employed to generate TE-inhibited clones of varying size, cells deriving from these clones were always observed contributing to the PrE, albeit at a reduced frequency when compared to control clones. Inhibition of TE cell fate was not therefore an impermeable block to subsequent PrE differentiation but rather a mechanism that biased ultimate cell fate away from the PrE. In the light of the above discussions, it remains possible that the anticipated and elevated levels of Fgf4 within the ICMs that contain TE-inhibited clones may not only signal to the non-dysregulated cells (*i.e.* non-

microinjected cell clones) to differentiate to PrE, but were also sufficient to act upon cells within the TE-inhibited clone itself. Presumably such recruitment of TE-inhibited clones into a PrE differentiation pathway would require much higher local concentrations of Fgf4 ligand to be effective, as compared to the non-dysregulated cells within the ICM (especially given the presented data relating Fgfr2 down-regulation/ plasma membrane localisation – Fig. 4.8). However, given that the fluorescently marked TE-inhibited clones within the ICM are most often compacted and share many cell-to-cell contacts with each other, (when compared to the comparatively dispersed nature of ICM-residing microinjection control clones), it is possible that such elevated levels could exist within the compacted TE-inhibited clone; theoretically passing a threshold limit that would recruit a TE-inhibited cell into differentiating into PrE. Another possibility could be that the ICM cells within the TE-inhibited clone that ultimately form PrE, initiate this differentiation via an unrelated and entirely stochastic mechanism. That is to state, inherent fluctuations in their own gene expression, possibly influenced by inter-cellular signals from their neighbouring cells, predisposes their fate towards a profile required for PrE differentiation, that can be self-reinforcing and thus commit the cell to differentiate. Indeed, such stochastic mechanisms, of inherent inter-cell gene expression heterogeneity, have been put forward as the primary means by which ICM cells achieve the required lineage specific gene expressions (Ohnishi *et al.*, 2014). Whilst herein the argument is that the presented data are indicative of a significant bias in ICM cell fate based on cell history, and specifically on the degree of TE inducing differentiation ICM ancestral cells are exposed to, it is by no means dismissed that important inputs arising from such described stochastic mechanisms can also contribute to appropriate ICM lineage separation. Indeed, the defining feature of early mammalian embryo development is its highly regulative nature, by definition indicating the existence of more than a single definitive cell-fate mechanism and the existence of complementary and overlapping pathways that must work together to guide, rather than restrict, the appropriate cell-fate decisions required during pre-implantation embryo development (Bruce, 2013).

Herein the results of experiments designed to functionally test the integrated cell-fate model of pre-implantation mouse embryo development have been described. Accordingly, the early exit of inner cells generated as a result of the fourth cleavage division away from TE-differentiative cues has been modelled by generating clones of varying size in which TE differentiation has been inhibited. The results indicate that once internalised such, fluorescently marked, TE-inhibited clones do not have equal potential to contribute to either the EPI or PrE, as is seen in control embryos, but are significantly biased to populate the EPI over the PrE lineage. Thus, the data indicate that the level of TE-differentiation exposure that the ancestral cells of ICM founders experience is able to bias their ultimate cell fate. Moreover, this bias is consistent with that describing EPI bias in ICM founder cells

internalised after the fourth cleavage division (Morris *et al.*, 2010); the first possible developmental opportunity that such blastomeres can be both sequestered from TE-inductive cues and exposed to pluripotency-promoting regulation by the induction of sufficiently active Hippo signalling in the derived inner cells (Nishioka *et al.*, 2009; Cockburn *et al.*, 2013; Hirate *et al.*, 2013; Leung and Zernicka-Goetz, 2013; Anani *et al.*, 2014; Wicklow *et al.*, 2014). It has also been shown that inhibition of TE cell fate is associated with reduced expression and altered localisation of PrE specific gene products, thus indicating that ICM founders that are generated later in development (*i.e.* as a result of the fifth cleavage division) are likely to be more molecularly equipped to respond to PrE differentiative cues, by virtue of their parental cells' relatively longer exposure to TE differentiative cues. As such the conclusion of the presented data are compatible with the existence of an integrated cell-fate model of lineage segregation during pre-implantation embryogenesis, whereby TE, EPI and PrE fates all begin their segregation at the fourth cleavage division and are guided by relative exposure of founding cells in each lineage to TE-differentiative cues. However, and in keeping with the remarkable regulative capacity of the developing pre-implantation embryo, such mechanisms act to guide rather than dictate cell fate and as such can be modulated and adapted by factors such as the number of generated inner cells or the induction of self-reinforcing stochastic mechanism of gene expression.

5.2 DISCUSSION - PART II

The second part of this thesis focused on investigating the role of Rock1/2 during pre-implantation mouse embryo development and providing the resolution for the conflicting reports present in the literature (Duan *et al.*, 2014; Kono *et al.*, 2014). As previously mentioned, Kono and colleagues had reported that chemical inhibition of Rock1/2 activity from 2-cell stage prevented blastocyst formation resulting in late morula stage developmental arrest (Kono *et al.*, 2014). In contrast, Duan and colleagues observed compaction defects and 8-cell stage developmental arrest after Rock1/2 inhibition (Duan *et al.*, 2014). An obvious discrepancy that could have accounted for different outcomes of Rock1/2 inhibition was the concentration of inhibitor used in these two previous studies. Therefore the titration experiments presented herein, using both of the previously used 20 μ M and 100 μ M plus an intermediate 50 μ M concentration of the Rock1/2 inhibitor, seemed necessary to determine the lowest effective working concentration of Rock1/2 inhibitor and avoid unnecessarily eliciting any potential non-specific/ off-target effects. Even though, a great majority of embryos managed to develop into morphologically recognisable blastocysts in the presence of 20 μ M Rock1/2 inhibitor, culturing the embryos *in vitro* in the presence of an intermediate 50 μ M working concentration of Rock1/2 inhibitor prevented blastocoel formation and embryonic progress beyond

the late morula stage thus faithfully recapitulating the phenotype observed by Kono and colleagues (Kono *et al.*, 2014). A possible underlying reason why a higher dose of Rock1/2 inhibitor was required in our experiments in order to observe the previously described phenotype could have originated from differences in utilised mouse strains. In that case, it could be argued that if the effects of Rock1/2 inhibition were dose dependent, 100µM concentration of Rock1/2 inhibitor in our study would not have been sufficient to match the effects produced by the same concentration in the study of Duan and colleagues (Duan *et al.*, 2014). Nevertheless, judged by the morphological appearance of E4.5 embryos *in vitro* cultured in the presence of 100µM Rock1/2 inhibitor it appears that the embryos are still capable of reaching late morula stage before they arrest and subsequently die, suggesting that doubling the concentration of the inhibitor does not seem to produce more severe effects than those already observed for the 50µM Rock1/2 inhibitor. Therefore, the conclusion of the presented experiments is that the more severe Rock1/2-inhibition associated phenotype observed by Duan and colleagues is probably best explained by suboptimal culturing conditions, as previously suggested (Kono *et al.*, 2014). Importantly, it has previously been reported that double genetic *Rock1^{-/-}: Rock2^{-/-}* zygotic null mice exhibit embryonic lethality between E3.5-E9.5 (Kamijo *et al.*, 2011), however the exact timing of embryonic death was not examined. Although these observations are consistent with our findings, the presence of maternally inherited Rock1 and Rock2 (Kono *et al.*, 2014) could have been sufficient to prevent the observation of an earlier phenotype. Overall, the findings of the presented experiments support the view that Rock1/2 activity becomes indispensable for appropriate mouse pre-implantation embryo development at a stage prior to blastocyst formation; *i.e.* during the transition from the late morula to early blastocyst stages.

The inability of Rock1/2-inhibited embryos to develop beyond the late morula stage and cavitate is likely a reflection of the inadequate establishment of a functional epithelium/ TE. Indeed, at the molecular level, Rock1/2 inhibition has previously been found to be associated with defective cell polarity, improper tight junction formation and ectopic outer cell Hippo signalling pathway activation that were together indicative of perturbed TE lineage formation (Kono *et al.*, 2014). Indeed the findings presented here faithfully recapitulate and provide additional support to these observations. However, in contrast to the observations made by Kono and colleagues, it was not possible to detect any alterations in Cdh1 protein distribution (that would be indicative of improper adherens junction formation) in Rock1/2-inhibited embryos. However and irrespective of whether Cdh1 localisation was affected or not, adherens junctions must have remained functional after the provided Rock1/2 inhibition, in both studies, in order to permit the ectopic activation of the Hippo signalling pathway in outer cells. In addition, the data described herein also reveals the novel observation of a specific lack of tight-junction region associated F-actin following Rock1/2 inhibition.

This might suggest that actin polymerisation is uniquely sensitive to regulation by active Rock1/2 at such tight-junction associated regions and given the observed developmental block maybe particularly important/required for successful blastocyst formation (*n.b.* actin polymerisation in other subcellular regions of the cortex appeared unaffected, as assayed by fluorescently conjugated phalloidin staining). Interestingly, a complete breakdown in F-actin formation coupled with a significant decrease in the phosphorylation levels of Limk1/2 (LIM-domain containing protein kinase 1 and 2), using the higher 100 μ M Rock1/2 inhibitor dose, has been reported elsewhere (Duan *et al.*, 2014). Limk1/2 is known to be involved in regulating actin dynamics in different contexts, including its requirement to stabilise F-actin by phosphorylating and thus inactivating members of the cofilin protein family; actin-binding proteins that promote actin depolymerisation (Cuberos *et al.*, 2015). Accordingly, it has been proposed that Rock1/2 may be involved in regulating actin dynamics in the pre-implantation mouse embryo, via its regulation of Limk1/2 phosphorylation/ activity (Duan *et al.*, 2014). However, the significance of this observation would have to be confirmed by examining embryos at a developmental time-point other than the reported 2-cell stage. Nevertheless, the effects that are observed herein, after the treatment of embryos with cytochalasin D, an inhibitor of actin polymerisation, do not support this model. Namely, the inhibition of actin polymerisation after cytochalasin D treatment results in a severe disruption of adherens junctions that consequently prevents (rather than potentiating) the activation of the Hippo signalling pathway and inevitably resulted in nuclear Yap1 localisation in all cells of the 32-cell stage embryo; although notably, the induced defects in F-actin localisation were much more pronounced than observed in Rock1/2 inhibitor treated embryos. Therefore, although these data have to be cautiously interpreted, as cytochalasin D represents a very potent mycotoxin and the effect of Rock1/2 inhibition could be more subtle and specific, the compound observations suggest that the probable reason why the F-actin is not accumulated at tight junction regions is due to the inappropriate establishment of tight junction formation (and their absence in Rock1/2-inhibited embryos,) rather than a reflection of aberrant actin polymerisation *per se*.

Although the observed apical cell polarity defects reported here are largely in accord with those of a previously described study (Kono *et al.*, 2014), careful inspection of outer-cell apical polarity factor localisation, utilising projected confocal microscopy z-sections, uniquely revealed that pERM immuno-reactivity is not homogeneously distributed throughout the entire apical domain of 32-cell stage Rock1/2-inhibited embryos, as in control, but rather concentrated into disc-like structures at pole extremities (termed 'apical-discs'). Such pERM-enriched apical-discs are also observed in Rock1/2-inhibited embryos assayed at the 16-cell stage. However, it is noteworthy that although DMSO-treated control embryos at the 8- and 16-cell stage also exhibited pERM enriched

apical-discs, these were much larger than those observed at either the 16- or 32-cell stage after Rock1/2-inhibition; suggesting that their presence in Rock1/2-inhibited embryos is unlikely to be the consequence of delayed embryonic development (the fact that the average total cell numbers between vehicle control and Rock1/2-inhibited embryos at 8-, 16- and 32-cell stage were found to be statistically equal strongly supports this claim). Moreover, the apical-discs observed in control embryos were normally found surrounded by F-actin that was not present in the Rock1/2-inhibited embryo conditions, in what could be termed the putative tight-junction proximal region. Therefore, it is plausible that the mechanisms governing the apical localisation of ERM proteins (with particular functional reference to phospho-Ezrin) are independent of those responsible for the classical apical-polarity factors (*e.g.* Prkcz/i and Pard6b), but that Rock1/2 activity is nonetheless required to spread their initial apical-disc localisation throughout the entire apical domain, in a temporally regulated and possibly actin-dependent manner. In addition, it is tempting to speculate that the presence of such apical discs in undisturbed embryos at the 8- and 16-cell stages might be a reflection of the presence of immature and/or not fully functional tight junctions. Nevertheless, the functional significance of apical-disc formation remains to be determined, however it is interesting that the observed apical discs resemble structures reported in Cofilin-1 depleted embryos, detailing restriction of microvilli to the most apical regions of outer-cells (Ma *et al.*, 2009).

Given a previous report that Rock1/2 inhibition, from the 2-cell stage, induces ectopic Hippo signalling pathway activation in the outer cells of 32-cell/ late morula (E3.5) stage embryos, as a consequence of aberrant activation of Lats2 kinase (Kono *et al.*, 2014), the involvement of the Hippo signalling pathway activator Amot, in the similar phenotype reported here, was investigated. As reported, the data initially confirmed that Amot becomes mis-localised to outer-cell baso-lateral regions enriched in adherens junctions, consequent to Rock1/2 inhibition, (and that this is responsible for the ectopic activation of the Hippo signalling pathway in these cells, as confirmed using Amot-specific dsRNA construct). It is most likely that the observed altered distribution of Amot protein in the outer cells of Rock1/2-inhibited embryos is the consequence of improper cell polarity establishment, as it has previously been demonstrated that either the activity or the presence of Prkcz/i and Pard6b apical polarity factors, respectively, is required for restricting the Amot protein to the apical membrane domain (Hirate *et al.*, 2013). Although, it was observed herein that in Rock1/2-inhibited embryos, both Prkcz/i and Pard6b were evenly distributed throughout the entire plasma membrane of outer cells, the proteins themselves were still present; emphasizing the fact that the presence of functional, and crucially apically restricted, apical polarity complexes are required to sequester the Amot protein away from adherens junctions and thus prevent aberrant outer-cell Hippo signalling activation. Importantly, the herein presented data also demonstrate that Amot is

entirely responsible for mediating the effects of Rock1/2 inhibition on Hippo signalling pathway activity, as RNAi mediated depletion of Amot in the whole embryo prevented Rock1/2 inhibitor from exerting its effects on Hippo signalling; resulting in nuclear Yap1 localisation in all cells of the late morula stage embryo, irrespective of the existence of the induced apical-basolateral polarity defects. These data agree with the previously reported assertion that cellular polarity acts functionally upstream of Hippo-signalling (Hirate *et al.*, 2013), given that the apical polarity factor Pard6b, remains mis-localised to the basolateral membrane domain of outer cells in Rock1/2-inhibited embryos even in the absence of RNAi-depleted Amot protein.

Nevertheless, it has recently been proposed that an as yet unidentified mechanism(s), may be working in parallel with the apical cell polarity protein complex to regulate Yap1 subcellular localisation at developmental time-points prior to the 32-cell/ late morula (E3.5) stage (Hirate *et al.*, 2015). Consistently, the presented data reveal that Yap1 subcellular localisation is much less profoundly affected by Rock1/2-inhibition at the 16-cell stage, despite the severely disrupted distribution of apical polarity complex proteins (Prkcz/i and Pard6b) and the accompanying mis-localisation of Amot protein to adherens junction in outer cells of Rock1/2-inhibited embryos. However, it is possible that this observation may simply reflect the fact that the levels of mis-localised Amot protein are, at this developmental time-point, insufficiently high to robustly activate the Hippo signalling pathway and thus completely exclude Yap1 from the nucleus of 16-cell stage blastomeres. Interestingly, at the 8-cell stage, a developmental time-point when Amot protein becomes weakly detectable in the pre-implantation embryo (Hirate *et al.*, 2013), Rock1/2 inhibitor had no effect on Yap1 localisation despite the fact that the establishment of cell polarity was perturbed. The efforts described here to precisely determine the timing at which Rock1/2 activity is first required to sustain appropriate development, reveal that Rock1/2-inhibited embryos are incapable of appropriately establishing cell polarity from the onset; as the accumulation of Prkcz/i at the apical plasma membrane domain required Rock1/2 activity already at the 8-cell stage. Given the previous report that RNAi mediated depletion of Prkci affects tight junction formation (Dard, Le, *et al.*, 2009), it is possible that the failure in tight junction formation after Rock1/2 inhibition observed here, may be a consequence of inappropriate cell polarity establishment. Indeed the presented observation that cell polarity defects in Rock1/2-inhibited embryos precede tight junction formation is consistent with this notion. It therefore appears that the majority of the observed effects of Rock1/2 inhibition may have commonly originated from the inappropriate establishment of cellular polarity. Existing molecular evidence from other model systems, suggests that Rho-kinase (ROCK) may potentially be directly implicated in regulating the formation of the apical polarity complex through the direct phosphorylation of PAR-3 (Nakayama *et al.*, 2008). In turn, aPKC has also been

reported to phosphorylate ROCK, thereby suppressing its junctional localisation and allowing cells to retain a normally shaped apical domain (Ishiuchi and Takeichi, 2011). However, neither of these correlations can adequately explain the observed Rock1/2-inhibition associated effects reported herein. Therefore, further investigation is required to reveal the mechanism(s) by which Rock1/2 regulates the onset and maintenance of cell polarity and thus cell fate in the mouse pre-implantation embryo.

The observed decrease in the number of inner cells in Rock1/2-inhibited embryos at both the 16- and 32-cell stages, mirrored by the equally increased number of outer cells, strongly suggests an important role for Rock1/2 in regulating the process of relative cell positioning, during mouse pre-implantation development. It has previously been demonstrated that either interfering with the activity of, or preventing the expression of, the apical polarity factors Prkci and Pard3 can have an impact on relative blastomere positioning within the embryo (Dard, Le, *et al.*, 2009; Plusa, Frankenberg, *et al.*, 2005). However, while clonal overexpression of a dominant-negative mutant form of Prkci or RNAi mediated down-regulation of Pard3 have been shown to result in increased internalisation of dysregulated cells clones, either due to the increased frequency of asymmetric cell divisions and/ or an inability to maintain an outside position (Plusa, Frankenberg, *et al.*, 2005), the global siRNA mediated knock-down of Prkci across all cells of the embryo has been shown to result in an overall decrease in the number of inner cell generated by the 16-cell stage (Dard, Le, *et al.*, 2009). As opposing as these results may initially appear, they may nevertheless be reconciled by the differences in the experimental approaches employed and as a consequence highlight the importance of inter-cell heterogeneities in the extent of cell polarity that in turn influence the outcome of relative cell positioning; *i.e.* by accentuating the existing inter-blastomere heterogeneity via the clonal approach, cell internalisation is potentiated; whereas by minimising such heterogeneity by effecting global down-regulation of polarity, internalisation is restricted. Indeed, a recent early mouse embryo study has demonstrated the existence of endogenous heterogeneities in inter-blastomere cortical tension (generated by the actomyosin network); that are in turn responsible for driving a process of apical constriction that allows cells to autonomously internalise (Samarage *et al.*, 2015). The authors highlight a key role for Myh9 in regulating this process, by demonstrating that the experimental down-regulation of *Myh9* expression prevents blastomeres from undergoing apical constriction and consequent internalisation (Samarage *et al.*, 2015). Consistently, another recent study has elegantly demonstrated that individual blastomeres deficient in maternal *Myh9* are also incapable of positioning themselves inside the embryo when aggregated in chimeras with wild-type embryos (Maitre *et al.*, 2016). Furthermore, this second study proposes that the observed and required differences in actomyosin contractility between blastomeres originate as a consequence of

the asymmetric partitioning of the apical domain during (outer) cell division; whereby a daughter cell that inherits less of the apical domain will exhibit an increased contractility and would preferentially internalise. (Maitre *et al.*, 2016). Consistently, the authors also show that increased contractility of outer-residing apolar cells correlates with the presence of higher levels of cortical ppMlc2 (bi-phosphorylated (Thr18/Ser19) myosin light chain 2); suggesting that apically localised polarity factors might normally be required to oppose the action of ppMlc2 or act to prevent its phosphorylation, thereby suppressing cell contractility and its ability to internalise. In agreement with this, blastomeres of Prkcz/i-deficient embryos fail to exclude ppMlc2 from the apical plasma membrane domain (Maitre *et al.*, 2016), suggesting that Prkcz/i itself might be responsible for antagonising actomyosin mediated cell contractility. Hence, the ultimate position of a blastomere within the embryo is likely to depend on a balance between the extent of apical polarisation and actomyosin contractility. Taking such reported findings and the fact that both apical polarity and pMlc2 levels are reported here to be severely affected after Rock1/2 inhibition together, it is perhaps unsurprising that Rock1/2-inhibited embryos exhibit a robust spatial cell allocation phenotype. Nevertheless, the exact mechanism(s) (*i.e.* cell internalisation, cell division orientation or a combination of both) that regulate relative cell positioning in the embryo, and whether these equally apply during the derivation of the 16-cell and 32-cell stage embryo, remains unclear. Based on existing evidence the herein observed significant reduction in pMlc2 levels in Rock1/2-inhibited embryos, and the decreased number of inner cells, is consistent with a failure of blastomeres to undergo apical constriction and thus internalise. However, it is less clear what impact a complete breakdown of intra-cellular (outer) cell polarity (again as is reported herein after the Rock1/2 inhibition) would have on the cell positioning in this context; despite the above described correlation between global knock-down of the apical polarity factor Prkci and apical mis-localisation of pMlc2 (Dard *et al.*, 2009). In addition, it has recently been demonstrated that Prkcz/i is both indispensable for regulating the inner positioning of cells via either the above described mechanism of cell internalisation or classical asymmetric cell division (Hirate *et al.*, 2015). It is therefore possible that the absence of apical cell polarity, and potentially a lack of Prkcz/i activity, could have also been responsible for the generation of increased numbers of outer cells in Rock1/2-inhibited embryos. In summary, both the observed decreased levels of pMlc2 and the failure to establish appropriate intra-cellular polarity might be responsible for driving the cell allocation phenotypes described herein in Rock1/2-inhibited embryos. It will be of great interest and importance to conduct future research to address how each of these molecular events are interrelated and cooperate to regulate the relative spatial positioning and fate of cells within the developing preimplantation mouse embryo.

Overall, the results presented in the second part of this thesis have both thoroughly re-examined the role of Rock1/2 during pre-implantation mouse embryo development and provided hitherto unreported insight into its central role during the establishment of cellular polarity, cell positioning and ultimately cell fate. The findings demonstrate that, in the absence of Rock1/2 activity, embryos are unable to exit from the late morula stage and become early blastocysts; probably as a consequence of compromised epithelial integrity of the emerging. However, the requirement for Rock1/2 activity upon proper pre-implantation embryo development is already evident (and reported here for the first time) at the molecular level as early as the 8-cell stage, as Rock1/2 inhibition prevents the appropriate establishment of cell polarity. Importantly, impairments in the appropriate establishment of cell polarity induced by Rock1/2 inhibition most probably account for several other outer-cell observed defects; including the failure to form tight junctions with associated F-actin accumulation and the mis-localisation of Amot to basolateral regions enriched in adherens junctions that results in ectopic activation of the Hippo signalling pathway. In addition, the presented results demonstrate that Amot is the sole mediator of the observed Rock1/2-inhibition mediated effects on dysregulated Hippo signalling, that ultimately dictate the first cell-fate decision (segregation of TE versus ICM). Finally, defects in cell polarity coupled with reduced levels of pMlc2 could also provide an explanation for the decreased number of inner cells observed in Rock1/2-inhibited embryos. However, exactly how Rock1/2 regulates the establishment of cell polarity, in relation to the above described phenotypes, currently remains open to question and further investigation, meriting much research that will significantly contribute to a better understanding of pre-implantation mouse embryo development.

6. CONCLUSIONS

The importance of cell history on the acquisition of the second cell fate during pre-implantation mouse embryo development has been a matter of a profound debate. The opposing “stochastic” and “time-inside time-outside” models have each been proposed to explain how the initial differences between the population of ICM founder cells are generated and thus drive the segregation of the pluripotent EPI and differentiating PrE cell lineages. While the stochastic model proposes that transcriptional noise, that then becomes amplified via theoretical feed-back mechanisms during the characteristically long cell cycles of preimplantation mammalian development, generates the required initial differences, the “time-inside time-outside” model places the emphasis on the importance of ancestral cell history in originating these differences (*i.e.* the relevance of the extent of differentiating cues to which the ancestors of ICM founder cells have been exposed to). In an attempt to resolve this ongoing debate, the experiments described within the first part of this thesis have been designed with the intention to functionally test the time-inside time-outside model. On the basis of the results presented, it can be concluded that the extent of differentiative cues ancestral cells are exposed to during the first cell-fate decision is relevant for the acquisition of subsequent ICM cell fate; with experimentally TE-inhibited/ *Tead4*-KD cell clones exhibiting significantly biased contribution, once internalised, towards the EPI lineage and away from the PrE cell lineage. Importantly, the biased contribution of TE-inhibited cell clones towards an EPI ICM fate cannot be accounted for by an increased expression of the pluripotency related transcription factor and EPI-specific marker *Nanog*, nor the decreased expression of cell polarity protein factors or ectopic activation of the Hippo signalling pathway. Rather, the observed biased contribution of TE-inhibited cell clones within the ICM away from the PrE is associated with decreased expression of PrE lineage marker genes (*i.e.* *Fgfr2*, *Dab2* and *Lrp2*) and an observed deficiency in the plasma membrane distribution of *Fgfr2* protein (required to receive *Fgf4* mediated extra-cellular cues that are known to promote PrE differentiation – Yamanaka *et al.*, 2010). Therefore, the observed bias most probably reflects a diminished responsiveness of ICM cells, derived from the TE-inhibited cell clone, to PrE differentiating signals and/ or their decreased motility (*i.e.* their ability to reach the ICM surface during the necessary cell sorting of EPI and PrE progenitors known to occur during blastocyst maturation - Meilhac *et al.*, 2009; Plusa *et al.*, 2008). Hence, the presented data support the time-inside time-outside mode, whereby the relative timing of ICM founder cell internalisation (*i.e.* either after the first or second rounds of potential differentiative/ asymmetric cell division, or internalisation) and hence the extent to which cells are subject to TE differentiating cues, predisposes their internalised progeny towards either a pluripotency associated EPI or differentiating PrE fate in the ICM. However, the data do not exclude the possibility of co-

existing stochastically mediated mechanisms of ICM cell fate that may also contribute to appropriate ICM cell fate resolution, in a manner that potentially adds extra plasticity to this remarkably regulative developmental system. Future investigations will therefore be required to fully appreciate the mechanisms involved and indeed the extent to which cell history informs ICM cell fate derivation.

The second part of this thesis sheds new light on the role of the RhoA effector kinases Rock1/2 during pre-implantation mouse embryo development; in the context of previously reported literature (Duan *et al.*, 2014; Kono *et al.*, 2014). According to the presented results, it can be concluded that Rock1/2 activity is evidently dispensable for the process of 8-cell stage embryo compaction, yet is indispensable for blastocoel formation and is therefore required to permit embryos to develop beyond the late morula stage. Nevertheless, the findings also demonstrate that Rock1/2 certainly acts prior to this developmental stage, by regulating the germane establishment of appropriate intra-cellular apical-basolateral cell polarity (beginning at its onset at the late 8-cell stage), thereby allowing the opposing modulation of Hippo signalling pathway activity in the spatially distinct populations of cells that as a consequence under-pins the first cell-fate decision. Importantly, the presented results clearly show that Amot is the sole mediator of Rock1/2 regulatory input to the activity on Hippo signalling pathway. Interestingly, Rock1/2 activity is also indispensable for the correct formation of tight junctions and the appropriate distribution of F-actin and although this is most probably due to the requirement of Rock1/2 activity during cell polarity establishment, it appears distinct from Hippo signalling regulation. However, further investigations are undoubtedly required to comprehensively and unequivocally test such informed speculation. Additionally, Rock1/2 is involved in control of relative spatial cell positioning within the developing embryo, possibly via regulating both the establishment of cell polarity and actomyosin contractility; thus identifying an additional role that is functionally upstream of differential Hippo signalling regulation and indeed could be argued as its pre-requisite. Given the presented importance of Rock1/2 activity in regulating several key aspects of pre-implantation mouse embryo development it will be of the great interest during future investigations to uncover the mechanisms working both upstream of small GTPase RhoA (and its related genes) and its downstream effector Rock1/2, as well as to more thoroughly define those factors functioning as downstream effectors of Rock1/2 regulation, that ultimately influence cell fate.

Overall, the results presented in this thesis provide new insights into the mechanisms governing each of the cell-fate decisions of pre-implantation mouse embryo development; with detailed mechanistic emphasis placed on how Rock1/2 regulates the activity of the Hippo signalling pathway and the consequences for the classically described first cell-fate decision. In addition, the presented results further highlight how the conveying and interpretation of differentiation related

signals required to appropriately instruct development in this classical first cell-fate decision are also functionally relevant in the subsequent and germane cell-fate derivation processes occurring in the ICM during blastocyst maturation.

REFERENCES

- Ajduk A., Shivhare S.B., Zernicka-Goetz (2014) The basal position of nuclei is one pre-requisite for asymmetric cell divisions in the early mouse embryo. *Developmental Biology*, 392(2): 133-140.
- Aksoy I., Jauch R., Chen J., Dyla M., Divakar U., Bogu G.K., Teo R., Ng C.K.L., Herath W., Hutchins A.P., Robson P., Kolatkar P.R., Stanton L.W. (2013) Oct4 switches partnering from Sox2 to Sox17 to reinterpret the enhancer code and specify endoderm. *The EMBO Journal*, 32(7): 938-953.
- Alarcon V. (2010) Cell polarity regulator PARD6B is essential for trophectoderm formation in the preimplantation mouse embryo. *Biology of Reproduction*, 83(3): 347-358.
- Alarcon V.B., Marikawa Y. (2003) Deviation of the blastocyst axis from the first cleavage plane does not affect the quality of mouse postimplantation development. *Biology of Reproduction*, 69(4): 1208–1212.
- Anani S., Bhat S., Honma-Yamanaka N., Krawchuk D., Yamanaka Y. (2014) Initiation of Hippo signaling is linked to polarity rather than to cell position in the pre-implantation mouse embryo. *Development*, 141(14): 2813-2824.
- Antczak M., Van Blerkom J. (1997) Oocyte influences on early development: the regulatory proteins leptin and STAT3 are polarized in mouse and human oocytes and differentially distributed within the cells of the preimplantation embryo. *Molecular Human Reproduction*, 3(12): 1067–1086.
- Arman E., Haffner-Krausz R., Chen Y., Heath J. K., Lonai P. (1998) Targeted disruption of fibroblast growth factor (FGF) receptor 2 suggests a role for FGF signaling in pregastrulation mammalian development. *Proceedings of the National Academy of Sciences of the United States of America*, 95(9): 5082-5087.
- Artus J., Cohen-Tannoudji M. (2008) Cell cycle regulation during early mouse embryogenesis. *Molecular and Cellular Endocrinology*, 282(1-2): 78-86.
- Artus J., Panthier J-J., Hadjantonakis A-K. (2010) A role for PDGF signaling in expansion of the extra-embryonic endoderm lineage of the mouse blastocyst. *Development*, 137(20): 3361-3372.
- Artus J., Piliszek A., Hadjantonakis A-K. (2011) The primitive endoderm lineage of the mouse blastocyst: Sequential transcription factor activation and regulation of differentiation by Sox17. *Developmental Biology*, 350(2): 393-404.

- Bagheri-Fam S., Sim H., Bernard P., Jayakody I., Taketo M.M., Scherer G., Harley V.R. (2008) Loss of Fgfr2 leads to partial XY sex reversal. *Developmental Biology*, 314(1): 71-83.
- Bergsmedh A., Donohoe M.E., Hughes R.-A., Hadjantonakis A.-K. (2011) Understanding the molecular circuitry of cell lineage specification in the early mouse embryo. *Genes*, 2(3): 420-448.
- Bessonard S., De Mot L., Gonze D., Barriol M., Dennis C., Goldbeter A., Dupont G., Chazaud C. (2014) Gata6, Nanog and Erk signaling control cell fate in the inner cell mass through a tristable regulatory network. *Development*, 141(19): 3637-3648.
- Bischoff M., Parfitt D-E., Zernicka-Goetz M. (2008) Formation of the embryonic-abembryonic axis of the mouse blastocyst: relationship between orientation of early cleavage division and pattern of symmetric/asymmetric divisions. *Development*, 135(5): 953-962.
- Bornens M. (2008) Organelle positioning and cell polarity. *Nature Reviews Molecular Cell Biology*, 9(11): 874-886.
- Bruce A.W. (2013) Generating different genetic expression patterns in the early embryo: insights from the mouse model. *Reproductive Biomedicine Online*, 27(6): 586-592.
- Bruce A.W., Zernicka-Goetz M. (2010) Developmental control of the early mammalian embryo: competition among heterogeneous cells that biases cell fate. *Current Opinion in Genetics and Development*, 20(5): 485-491.
- Bryant D.M., Mostov K.E. (2008) From cells to organs: building polarized tissue. *Nature Reviews Molecular Cell Biology*, 9(11): 887-901.
- Cai K.Q., Capo-Chichi C.D., Rula M.E., Yang D.H., Xu X.X. (2008) Dynamic GATA6 expression in primitive endoderm formation and maturation in early mouse embryogenesis. *Developmental Dynamics*, 237(10): 2820-2829.
- Chambers I., Colby D., Robertson M., Nichols J., Lee S., Tweedie S., Smith A (2003) Functional expression cloning of Nanog, a pluripotency sustaining factor in embryonic stem cells. *Cell*, 113(5): 643-655.
- Chazaud C., Yamanaka Y., Pawson T., Rossant J. (2006) Early lineage segregation between epiblast and primitive endoderm in mouse blastocyst through the Grb2-MAPK pathway. *Developmental Cell*, 10(5): 615-624.
- Chen L., Wang D., Wu Z., Ma L., Daley G.Q. (2010) Molecular basis of the first cell fate determination in mouse embryogenesis. *Cell Research*, 20(9): 982-993.

- Cheng A. M., Saxton T. M., Sakai R., Kulkarni S., Mbamalu G., Vogel W., Tortorice C. G., Cardiff R. D., Cross J. C., Muller W. J., Pawson T. (1998) Mammalian Grb2 regulates multiple steps in embryonic development and malignant transformation. *Cell*, 95(6): 793-803.
- Clayton L., Hall A., Johnson M.H. (1999) A role for Rho-like GTPases in the polarization of mouse eight-cell blastomeres. *Developmental Biology*, 205(2): 322-331.
- Clayton L., Stinchcombe S.V., Johnson M.H. (1993) Cell surface localization and stability of uvomorulin during early mouse development. *Zygote*, 1(4): 333-344.
- Cockburn K., Biechele S., Garner J., Rossant J. (2013) The Hippo pathway member Nf2 is required for inner cell mass specification. *Current Biology*, 23(13): 1195-1201.
- Cockburn K., Rossant J. (2010) Making the blastocyst: lesson from the mouse. *The Journal of Clinical Investigation*, 120(4): 995-1003.
- Cuberos H., Vallee B., Vourc'h P., Tastet J., Andres C.R., Benedetti H. (2015) Roles of LIM kinases in central nervous system function and dysfunction. *FEBS Letters*, 589(24): 3795-3806.
- Dard N., Breuer M., Maro B., Louvet-Vallee S. (2008) Morphogenesis of the mammalian blastocyst. *Molecular and Cellular Endocrinology*, 282(1-2): 70-77.
- Dard N., Le T., Maro B., Louvet-Vallee (2009) Inactivation of aPKC λ reveals context dependent allocation of cell lineages in preimplantation mouse embryos. *PLOS One*, 4(9): e7117.
- Dard N., Louvet-Valee S., Maro B. (2009) Orientation of mitotic spindles during the 8- to 16-cell stage transition in mouse embryos. *Plos ONE*, 4(12): e8171.
- Dard N., Louvet-Vallee S., Santa-Maria A., Maro B. (2004) Phosphorylation of ezrin on threonine T567 plays a crucial role during compaction in the mouse early embryo. *Developmental Biology*, 271(1): 87-97.
- De Vries W.N., Evsikov A.V., Haac B.E., Fancher K.S., Holbrook A.E., Kemler R., Solter D., Knowles B.B. (2004) Maternal beta-catenin and E-cadherin in mouse development. *Development*, 131(18): 4435-4445.
- Duan X., Chen K-L., Zhang Y., Cui X-S., Kim N-H., Sun S-C (2014) ROCK inhibition prevents early mouse embryo development. *Histochemistry and Cell Biology*, 142(2): 227-233.
- Ducibella T., Ukena T., Karnovsky M., Anderson E. (1977) Changes in cell surface and cortical cytoplasmic organization during early embryogenesis in the preimplantation mouse embryo. *The Journal of Cell Biology*, 74(1): 153-167.

- Eckert J., McCallum A., Mears A., Rumsby M.G., Cameron I.T., Fleming T.P. (2004) Specific PKC isoforms regulate blastocoel formation during mouse preimplantation development. *Developmental Biology*, 274(2): 384-401.
- Enders A.C., Given R.L., Schlafke S. (1978) Differentiation and migration of endoderm in the rat and mouse at implantation. *Anatomical Record*, 190(1): 65-77.
- Feldman B., Poueymirou W., Papaioannou V. E., DeChiara T. M., Goldfarb M. (1995) Requirement of FGF-4 for postimplantation mouse development. *Science*, 267(5195): 246-249.
- Frankenberg S., Gerbe F., Bessonard S., Belville C., Pouchin P., Bardot O., Chazaud C. (2011) Primitive endoderm differentiates via a three-step mechanism involving Nanog and RTK signaling. *Developmental Cell*, 21(6): 1005-1013.
- Frankenberg S., Shaw G., Freyer C., Pask A.J., Renfree M.B. (2013) Early cell lineage specification in a marsupial: a case for diverse mechanisms among mammals. *Development*, 140(5): 965-975.
- Frum T., Halbisen M.A., Wang C., Amiri H., Robson P., Ralston A. (2013) Oct4 cell-autonomously promotes primitive endoderm development in the mouse blastocyst. *Developmental Cell*, 25(6): 610-622.
- Gardner R.L., Rossant J. (1979) Investigation of the fate of 4-5 days post-coitum mouse inner cell mass cells by blastocyst injection. *Journal of Embryology and Experimental Morphology*, 52: 141-152.
- Gardner R.L. (1997) The early blastocyst is bilaterally symmetrical and its axis of symmetry is aligned with the animal-vegetal axis of the zygote in the mouse. *Development*, 124(2): 289-301.
- Gardner R.L. (1999) Scrambled or bisected mouse eggs and the basis of patterning in mammals. *BioEssays*, 21(4): 271-274.
- Gardner R.L. (2001) Specification of embryonic axes begins before cleavage in normal mouse development. *Development*, 128(6): 839-847.
- Gerbe F., Cox B., Rossant J., Chazaud C. (2008) Dynamic expression of Lrp2 pathway members reveals progressive epithelial differentiation of primitive endoderm in mouse blastocyst. *Developmental Biology*, 313(2): 594-602.
- Goolam M., Scialdone A., Graham S.J.L., Macaulay I.C., Jedrusik A., Hupalowska A., Voet T., Marioni J.C., Zernicka-Goetz Magdalena (2016) Heterogeneity in Oct4 and Sox2 targets biases cell fate in 4-cell mouse embryos. *Cell*, 165(1): 61-74.

- Gray D., Plusa B., Piotrowska K., Na J., Tom B., Glover D.M., Zernicka-Goetz M. (2004) First cleavage of the mouse embryo responds to change in egg shape at fertilization. *Current Biology*, 14(5): 397-405.
- Guo G., Huss M., Tong G.Q., Wang C., Sun L.L., Clarke N.D., Robson P. (2010) Resolution of cell fate decisions revealed by single-cell gene expression analysis from zygote to blastocyst. *Developmental Cell*, 18(4): 675-685.
- Halet G., Carroll J. (2007) Rac activity is polarized and regulates meiotic spindle stability and anchoring in mammalian oocytes. *Developmental Cell*, 12(2): 309-317.
- Hanna J.H., Saha K., Jaenisch R. (2010) Pluripotency and cellular reprogramming: facts, hypotheses, unresolved issues. *Cell*, 143(4): 508–525.
- Hartmann S., Ridley A.J., Lutz S. (2015) The function of Rho-associated kinases ROCK1 and ROCK2 in the pathogenesis of cardiovascular disease. *Frontiers in Pharmacology*, 6: 276.
- Hiiragi T., Solter D. (2004) First cleavage plane of the mouse egg is not predetermined but defined by the topology of the two apposing pronuclei. *Nature*, 430(6997): 360–364.
- Hirate Y., Hirahara S., Inoue K., Kiyonari H., Niwa H., Sasaki H. (2015) Par-aPKC-dependent and -independent mechanisms cooperatively control cell polarity, Hippo signaling, and cell positioning in 16-cell stage mouse embryos. *Development, Growth and Differentiation*, 57(8): 544-556.
- Hirate Y., Hirahara S., Inoue K., Suzuki A., Alarcon V.B., Akimoto K., Hirai T., Hara T., Adachi M., Chida K., Ohno S., Marikawa Y., Nakao K., Shimono A., Sasaki H. (2013) Polarity-dependent distribution of Angiomotin localizes Hippo signaling in preimplantation embryos. *Current Biology*, 23(13): 1181-1194.
- Home P., Ray S., Dutta D., Bronshteyn I., Larson M., Paul S. (2009) GATA3 is selectively expressed in the trophectoderm of peri-implantation embryo and directly regulates *Cdx2* gene expression. *Journal of Biological Chemistry*, 284(42): 28729-28737.
- Home P., Saha B., Ray S., Dutta D., Gunewardena S., Yoo B., Pal A., Vivian J.L., Larson M., Petroff M., Gallagher P.G., Schulz V.P., White K.L., Golos T.G., Behr B., Paul S. (2012) Altered subcellular localization of transcription factor TEAD4 regulates first mammalian cell lineage commitment. *Proceedings of the National Academy of Sciences of the United States of America*, 109(19): 7362-7367.

- Hyafil F., Morello D., Babinet C., Jacob F. (1980) A cell surface glycoprotein involved in the compaction of embryonal carcinoma cells and cleavage stage embryos. *Cell*, 21(3): 927–934.
- Iden S., Collard J.G. (2008) Crosstalk between small GTPases and polarity proteins in cell polarization. *Nature Reviews Molecular Cell Biology*, 9(11): 846-859.
- Ishiuchi T., Takeichi M. (2011) Willin and Par3 cooperatively regulate epithelial apical constriction through aPKC-mediated ROCK phosphorylation. *Nature Cell Biology*, 13(7): 860-866.
- Jedrusik A., Parfitt D-E., Guo G., Skamagi M., Grabarek J.B., Johnson M.H., Robson P., Zernicka-Goetz M. (2008) Role of Cdx2 and cell polarity in cell allocation and specification of trophoblast and inner cell mass in the mouse embryo. *Genes and Development*, 22(19): 2692-2706.
- Johnson M.H. (2009) From mouse egg to mouse embryo: polarities, axes and tissues. *Annual Review of Cell and Developmental Biology*, 25: 483-512.
- Johnson M.H., McConnell J.M.L. (2004) Lineage allocation and cell polarity during mouse embryogenesis. *Seminars in Cell and Developmental Biology*, 15(5): 583-597.
- Johnson M.H., Ziomek C.A. (1981a) Induction of polarity in mouse 8-cell blastomeres: specificity, geometry, and stability. *The Journal of Cell Biology*, 91(1): 303-308.
- Johnson M.H., Ziomek C.A. (1981b) The foundation of two distinct cell lineages within the mouse morula. *Cell*, 24(1): 71-80.
- Kamijo H., Matsumura Y., Thumkeo D., Koike S., Masu M., Shimizu Y., Ishizaki T., Narumiya S. (2011) Impaired vascular remodelling in the yolk sac of embryos deficient in ROCK-I and ROCK-II. *Genes to Cells*, 16(10): 1012-21.
- Kang M., Piliszek A., Artus J., Hadjantonakis A-K. (2013) FGF4 is required for lineage restriction and salt-and-paper distribution of primitive endoderm factors but not their initial expression in the mouse. *Development*, 140(2): 267-279.
- Kawagishi R., Tahara M., Sawada K., Ikebuchi Y., Morishige K., Sakata M., Tasaka K., Murata Y. (2004) Rho-kinase is involved in mouse blastocyst cavity formation. *Biochemical and Biophysical Research Communications*, 319(2): 643-648.
- Kelly S.J. (1977) Studies of the developmental potential of 4- and 8-cell stage mouse blastomeres. *Journal of Experimental Zoology*, 200(3): 365–376.

- Kidder G.M., McLachlin J.R. (1985) Timing of transcription and protein synthesis underlying morphogenesis in preimplantation mouse embryos. *Developmental Biology*, 112(2): 265–275.
- Kirschstein R., Skirboll L.R. (2001) Stem cells: scientific progress and future directions. *National Institutes of Health, Department of Health and Human Services*. Available at: <http://wtcc.org/SCE/fullrptstem.pdf>.
- Kono K., Tamashiro D.A.A., Alarcon V.B. (2014) Inhibition of RHO-ROCK signaling enhances ICM and suppresses TE characteristics through activation of Hippo signaling in the mouse blastocyst. *Developmental Biology*, 394(1): 142-155.
- Kosako H., Yoshida T., Matsumura F., Ishizaki T., Narumiya S., Inagaki M. (2000) Rho-kinase/ROCK is involved in cytokinesis through the phosphorylation of myosin light chain and not ezrin/radixin/moesin proteins at the cleavage furrow. *Oncogene*, 19(52): 6059-6064.
- Krawchuk D., Honma-Yamanaka N., Anani S., Yamanaka Y. (2013) FGF4 is a limiting factor controlling the proportions of primitive endoderm and epiblast in the ICM of the mouse blastocyst. *Developmental Biology*, 384(1): 65-71.
- Krupa M., Mazur E., Szczepanska K., Filimonow K., Maleszewski M., Suwinska A. (2014) Allocation of inner cells to epiblast vs primitive endoderm in the mouse embryo is biased but not determined by the round of asymmetric divisions (8→16- and 16→32-cells). *Developmental Biology*, 385(1): 136-148.
- Lanner F., Rossant J. (2010) The role of FGF/Erk signaling in pluripotent cells. *Development*, 137: 3351-3360.
- Larue L., Ohsugi M., Hirchenhain J., Kemler R. (1994) E-cadherin null mutant embryos fail to form a trophectoderm epithelium. *Proceedings of the National Academy of Sciences of the United States of America*, 91(17): 8263–8267.
- Lavial F., Bessonard S., Ohnishi Y., Tsumura A., Chandrashekar A., Fenwick M.A., Tomaz R.A., Hosokawa H., Nakayama T., Chambers I., Hiiragi T., Chazaud C., Azuara V. (2012) Bmi1 facilitates primitive endoderm formation by stabilizing Gata6 during early mouse development. *Genes and Development*, 26(13): 1445-1458.
- Le Bin G.C., Munoz-Descalzo S., Kurowski A., Leitch H., Lou X., Mansfield W., Etienne-Dumeau C., Grabole N., Mulas C., Niwa H., Hadjantonakis A-K., Nichols J. (2014) Oct4 is required for lineage priming in the developing inner cell mass of the mouse blastocyst. *Development*, 141(5): 1001-1010.

- Leung C.Y., Zernicka-Goetz M. (2013) Angiotensin prevents pluripotent lineage differentiation in mouse embryos via Hippo pathway-dependent and -independent mechanisms. *Nature Communication*, 4: 2251.
- Levy J.B., Johnson M.H., Goodall H., Maro B. (1986) The timing of compaction: control of a major developmental transition in mouse early embryogenesis. *Journal of Embryology and Experimental Morphology*, 95: 213–237.
- Liu H., Wu Z., Shi X., Li W., Liu C., Wang D., Ye X., Liu L., Na J., Cheng H., Chen L. (2013) Atypical PKC, regulated by Rho GTPases and Mek/Erk phosphorylates Ezrin during eight-cell embryo compaction. *Developmental Biology*, 375(1): 13-22.
- Livak K.J., Schmittgen T.D. (2001) Analysis of relative gene expression data using real-time quantitative PCR and the $2^{-\Delta\Delta Ct}$ method. *Methods*, 25(4): 402-408.
- Lorthongpanich C., Messerschmidt D.M., Chan S.W., Hong W., Knowles B.B., Solter D. (2013) Temporal reduction of LATS kinases in the early preimplantation embryo prevents ICM lineage differentiation. *Genes and Development*, 27(13): 1441-1446.
- Lu C.C., Brennan J., Robertson E.J. (2001) From fertilization to gastrulation: axis formation in the mouse embryo. *Current Opinion in Genetics and Development*, 11(4): 384-392.
- Ma M., Zhou L., Guo X., Lv Z., Yu Y., Ding C., Zhang P., Bi Y., Xie J., Wang L., Lin M., Zhou Z., Huo R., Sha J., Zhou Q. (2009) Decreased cofilin 1 expression is important for compaction during early mouse embryo development. *Biochimica et Biophysica Acta*, 1793(12): 1804-1810.
- Maitre J-L., Turlier H., Illukkumbura R., Eismann B., Niwayama R., Nedelec F., Hiiragi T. (2016) Asymmetric division of contractile domains couples cell positioning and fate specification. *Nature*, 536(7616): 344-348.
- Mansour A.A., Hanna J.H. (2013) Oct4 shuffles Sox patterns to direct cell fate. *The EMBO Journal*, 32(7): 917-919.
- Marikawa Y., Alarcon V.B. (2009) Establishment of trophectoderm and inner cell mass lineages in the mouse embryo. *Molecular Reproduction and Development*, 76(11): 1019-1032.
- Marikawa Y., Alarcon V.B. (2012) Creation of trophectoderm, the first epithelium in mouse preimplantation development. *Results and Problems in Cell Differentiation*, 55: 165-184.
- Martin A.J., Grant A., Ashfield A.M., Palmer C.N., Baker L., Quinlan P.R., Purdie C.A., Thompson A.M., Jordan L.B., Berg J.N. (2011) FGFR2 protein expression in breast cancer: nuclear localization and correlation with patient genotype. *BMC Research Notes*, 4:72.

- Meilhac S.M., Adams R.J., Morris S.A., Danckaert A., Le Garrec J-F., Zernicka-Goetz M. (2009) Active cell movements coupled to positional induction are involved in lineage segregation in the mouse blastocyst. *Developmental Biology*, 331(2): 210-221.
- Mellman I., Nelson W.J. (2008) Coordinated protein sorting, targeting and distribution in polarized cells. *Nature Reviews Molecular Cell Biology*, 9(11): 833-845.
- Mihajlović A.I., Bruce A.W. (2016) Rho-associated protein kinase regulates subcellular localisation of Angiomotin and Hippo-signalling during preimplantation mouse embryo development. *Reproductive Biomedicine Online*, 33(3): 381-390.
- Mihajlović A.I., Thamodaran V., Bruce A.W. (2015) The first two cell-fate decisions of preimplantation mouse embryo development are not functionally independent. *Scientific Reports*, 5: 15034.
- Mitsui K., Tokuzawa Y., Itoh H., Segawa K., Murakami M., Takahashi K., Maruyama M., Maeda M., Yamanaka S. (2003) The homeoprotein Nanog is required for maintenance of pluripotency in mouse epiblast and ES cells. *Cell*, 113(5): 631-642.
- Moore R., Cai K.Q., Tao W., Smith E.R., Xu X-X. (2013) Differential requirement for Dab2 in the development of embryonic and extra-embryonic tissues. *BMC Developmental Biology*, 13: 39.
- Morin-Kesincki E.M., Boone B.N., Howell M., Stonebraker J.R., Teed J., Alb J.G., Manguson T.R., O'Neal W., Milgram S.L. (2006) Defects in yolk sac vasculogenesis, chorioallantoic fusion, and embryonic axis elongation in mice with targeted disruption of Yap65. *Molecular and Cellular Biology*, 26(1): 77-87.
- Morris S.A. (2011) Cell fate in the early mouse embryo: sorting out the influence of developmental history on lineage choice. *Reproductive Biomedicine Online*, 22(6): 521-524.
- Morris S.A., Graham S.J.L., Jedrusik A., Zernicka-Goetz M. (2013) The differential response to Fgf signaling in cells internalized at different times influences lineage segregation in preimplantation mouse embryos. *Open Biology*, 3(11): 130104.
- Morris S.A., Guo Y., Zernicka-Goetz M. (2012) Developmental plasticity is bound by pluripotency and the Fgf and Wnt signaling pathways. *Cell Reports*, 2(4): 756-765.
- Morris S.A., Teo R. T. Y., Li H., Robson P., Glover D. M., Zernicka-Goetz M. (2010) Origin and formation of the first two distinct cell types of the inner cell mass in the mouse embryo. *Proceedings of the National Academy of Sciences of the United States of America*, 107(14): 6364-6369.

- Morrisey E.E., Musco S., Chen M.Y., Lu M.M., Leiden J.M., Parmacek M.S. (2000) The gene encoding the mitogen-responsive phosphoprotein Dab2 is differentially regulated by GATA-6 and GATA-4 in the visceral endoderm. *The Journal of Biological Chemistry*, 275(26): 19949-19954.
- Motosugi N., Bauer T., Polanski Z., Solter D., Hiiragi T. (2005) Polarity of the mouse embryo is established at blastocyst and is not prepatterned. *Genes and Development*, 19(9): 1081-1092.
- Nakayama M., Goto T.M., Sugimoto M., Nishimura T., Shinagawa T., Ohno S., Amano M., Kaibuchi K. (2008) Rho-kinase phosphorylates PAR-3 and disrupts PAR complex formation. *Developmental Cell*, 14(2): 205-215.
- Narumiya S., Ishizaki T., Ufhata M. (2000) Use and properties of ROCK-specific inhibitor Y-27632. *Methods in Enzymology*, 325: 273-284.
- Natale D.R., Watson A.J. (2002) Rac-1 and IQGAP are potential regulators of E-cadherin-catenin interactions during murine preimplantation development. *Gene Expression Patterns*, 2(1-2): 17-22.
- Niakan K.K., Ji H., Maehr R., Vokes S.A., Rodolfa K.T., Sherwood R.I., Yamaki M., Dimos J.T., Chen A.E., Melton D.A., McMahon A.P., Eggan K. (2010) Sox17 promotes differentiation in mouse embryonic stem cells by directly regulating extraembryonic gene expression and indirectly antagonizing self-renewal. *Genes and Development*, 24(3): 312-326.
- Nichols J., Silva J., Roode M., Smith A. (2009) Suppression of Erk signaling promotes ground state pluripotency in the mouse embryo. *Development*, 136(19): 3215-3222.
- Nichols J., Zevnik B., Anastassiadis K., Niwa H., Klewe-Nebenius D., Chambers I., Scholer H., Smith A. (1998) Formation of pluripotent stem cells in the mammalian embryo depends on the POU transcription factor Oct4. *Cell*, 95(3): 379-391.
- Nishioka N., Inoue K., Adachi K., Kiyonari H., Ota M., Ralston A., Yabuta N., Hirahara S., Stephenson R.O., Ogonuki N., Makita R., Kurihara H., Morin-Kensicki E.M., Nojima H., Rossant J., Nakao K., Niwa H., Sasaki H. (2009) The Hippo signaling pathway components Lats and Yap pattern Tead4 activity to distinguish mouse trophectoderm from inner cell mass. *Developmental Cell*, 16(3): 398-410.
- Nishioka N., Yamamoto S., Kiyonari H., Sato H., Sawada A., Ota M., Nakao K., Sasaki H. (2008) Tead4 is required for specification of trophectoderm in pre-implantation mouse embryos. *Mechanisms of Development*, 125(3-4): 270-283.

- Niwa H., Toyooka Y., Shimosato D., Strumpf D., Takahashi K., Yagi R., Rossant J. (2005) Interaction between Oct3/4 and Cdx2 determines trophectoderm differentiation. *Cell*, 123(5): 917-929.
- Ohnishi Y., Huber W., Tsumura A., Kang M., Xenopoulos P., Kurimoto K., Oles A.K., Arauzo-Bravo M.J., Saitou M., Hadjantonakis A-K., Hiiragi T. (2014) Cell-to-cell expression variability followed by signal reinforcement progressively segregates early mouse lineages. *Nature Cell Biology*, 16(1): 27-37.
- Pauken C.M., Capco D.G. (1999) Regulation of cell adhesion during embryonic compaction of mammalian embryos: roles for PKC and beta-catenin. *Molecular Reproduction and Development*, 54(2): 135-144.
- Piotrowska K., Wianny F., Pedersen R.A., Zernicka-Goetz M. (2001) Blastomeres arising from the first cleavage divisions have distinguishable fates in normal mouse development. *Development*, 128(19): 3739-3748.
- Piotrowska-Nitsche K., Perea-Gomez A., Haraguchi S., Zernicka-Goetz M. (2005) Four-cell stage mouse blastomeres have different developmental properties. *Development*, 132(3): 479-490.
- Piotrowska-Nitsche K., Zernicka-Goetz M. (2005) Spatial arrangement of individual 4-cell stage blastomeres and the order in which they are generated correlate with blastocyst pattern in the mouse embryo. *Mechanisms of Development*, 122(4): 487-500.
- Plachta N., Bollenbach T., Pease S., Fraser S.E., Pantazis P. (2011) Oct4 kinetics predict cell lineage patterning in the early mammalian embryo. *Nature Cell Biology*, 13(2): 117-123.
- Plusa B., Frankenberg S., Chalmers A., Hadjantonakis A-K., Moore C.A., Papalopulu N., Papaioannou V.E., Glover D.M., Zernicka-Goetz M. (2005) Downregulation of Par3 and aPKC function directs cells towards the ICM in the preimplantation mouse embryo. *Journal of Cell Science*, 118(3): 505-515.
- Plusa B., Hadjantonakis A-K., Gray D., Piotrowska-Nitsche K., Jedrusik A., Papaioannou V.E., Glover D.M., Zernicka-Goetz M. (2005) The first cleavage of the mouse zygote predicts the blastocyst axis. *Nature*, 434(7031): 391-395.
- Plusa B., Piliszek A., Frankenberg S., Artus J., Hadjantonakis A-K. (2008) Distinct sequential cell behaviours direct primitive endoderm formation in the mouse blastocyst. *Development*, 135(18): 3081-3091.

- Ralston A., Cox B.J., Nishioka N., Sasaki H., Chea E., Rugg-Gunn P., Guo G., Robson P., Draper J.S., Rossant J. (2010) Gata3 regulates trophoblast development downstream of Tead4 and in parallel to Cdx2. *Development*, 137(3): 395-403.
- Ralston A., Rossant J. (2008) Cdx2 acts downstream of cell polarization to cell-autonomously promote trophectoderm fate in the early mouse embryo. *Developmental Biology*, 313(2): 614-629.
- Rayon T., Menchero S., Nieto A., Xenopoulos P., Crespo M., Cockburn K., Canon S., Sasaki H., Hadjantonakis A.-K., de la Pompa J.L., Rossant J., Manzanares M. (2014) Notch and Hippo converge on Cdx2 to specify the trophectoderm lineage in the mouse blastocyst. *Developmental Cell*, 30(4): 410-422.
- Riethmacher D., Brinkmann V., Birchmeier C. (1995) A targeted mutation in the mouse E-cadherin gene results in defective preimplantation development. *Proceedings of the National Academy of Sciences of the United States of America*, 92(3): 855–859.
- Rossant J. (1976) Postimplantation development of blastomeres isolated from 4- and 8-cell mouse eggs. *Journal of Embryology and Experimental Morphology*, 36(2): 283-290.
- Saiz N., Grabarek J.B., Sabherwal N., Papalopulu N., Plusa B. (2013) Atypical protein kinase C couples cell sorting with primitive endoderm maturation in the mouse blastocyst. *Development*, 140(21): 4311-4322.
- Saiz N., Plusa B. (2013) Early cell fate decisions in the mouse embryo. *Reproduction*, 145(3): R65-R80.
- Samarage C.R., White M.D., Alvarez Y.D., Fierro-Gonzalez J.C., Henon Y., Jesudason E.C., Bissiere S., Fouras A., Plachta N. (2015) Cortical tension allocates the first inner cells of the mammalian embryo. *Developmental Cell*, 34(4): 435-447.
- Sasaki H. (2015) Position- and polarity-dependent Hippo signaling regulates cell fates in preimplantation mouse embryos. *Seminars in Cell and Developmental Biology*, 47-48: 80-87.
- Schmahl J., Kim Y., Colvin J.S., Ornitz D.M., Capel B. (2004) Fgf9 induces proliferation and nuclear localization of FGFR2 in Sertoli precursors during male sex determination. *Development*, 131(15): 3627-3636.
- Schrode N., Xenopoulos P., Piliszek A., Frankenberg S., Plusa B., Hadjantonakis A.-K. (2013) Anatomy of a blastocyst: Cell behaviors driving cell fate choice and morphogenesis in the early mouse embryo. *Genesis*, 51(4): 219-233.

- Skamagi M., Wicher K.B., Jedrusik A., Ganguly S., Zernicka-Goetz M. (2013) Asymmetric localization of *Cdx2* mRNA during the first cell-fate decision in early mouse development. *Cell Reports*, 3(2): 442-457.
- Street C.A., Bryan B.A. (2011) Rho kinase proteins - pleiotropic modulators of cell survival and apoptosis. *Anticancer Research*, 31(11): 3645-3657.
- Strumpf D., Mao C-A., Yamanaka Y., Ralston A., Chawengsaksophak K., Beck F., Rossant J. (2005) *Cdx2* is required for correct cell fate specification and differentiation of trophectoderm in the mouse blastocyst. *Development*, 132(9): 2093-2102.
- Suwinska A., Czolowska R., Ozdzinski W., Tarkowski A.K. (2008) Blastomeres of the mouse embryo lose totipotency after the fifth cleavage division: Expression of *Cdx2* and *Oct4* and developmental potential of inner and outer blastomeres of 16- and 32-cell embryos. *Developmental Biology*, 322(1): 133-144.
- Tabansky I., Lenarcic A., Draft R.W., Loulier K., Keskin D.B., Rosains J., Rivera-Feliciano J., Lichtman J.W., Livet J., Stern J.N.H., Sanes J.R., Eggan K. (2013) Developmental bias in cleavage-stage mouse blastomeres. *Current Biology*, 23(1): 21-31.
- Tao H., Inoue K., Kiyonari H., Bassuk A.G., Axelrod J.D., Sasaki H., Aizawa S., Ueno N. (2012) Nuclear localization of *Prickle2* is required to establish cell polarity during early mouse embryogenesis. *Developmental Biology*, 364(2): 138-148.
- Tarkowski A.K. (1959) Experiments on the development of isolated blastomeres of mouse eggs. *Nature*, 184: 1286-1287.
- Tarkowski A.K. (1961) Mouse chimaeras developed from fused eggs. *Nature*, 190: 857-860.
- Tarkowski A.K., Wroblewska J. (1967) Development of blastomeres of mouse eggs isolated at the 4- and 8-cell stage. *Journal of Embryology and Experimental Morphology*, 18(1): 155-180.
- Thamodaran V., Bruce A.W. (2016) p38 (Mapk14/11) occupies a regulatory node governing entry into primitive endoderm differentiation during preimplantation mouse embryo development. *Open Biology*, 6(9): 160190.
- Torres-Padilla M.E., Parfitt D.E., Kouzarides T., Zernicka-Goetz M. (2007) Histone arginine methylation regulates pluripotency in the early mouse embryo. *Nature*, 445(7124): 214-218.

- Vestweber D., Gossler A., Boller K., Kemler R. (1987) Expression and distribution of cell adhesion molecule uvomorulin in mouse preimplantation embryos. *Developmental Biology*, 124(2): 451-456.
- Vestweber D., Kemler R. (1984) Rabbit antiserum against a purified surface glycoprotein decompacts mouse preimplantation embryos and reacts with specific adult tissues. *Experimental Cell Research*, 152(1): 169–178.
- Vinot S., Le T., Maro B., Louvet-Vallee (2004) Two PAR6 proteins become asymmetrically localized during establishment of polarity in mouse oocytes. *Current Biology*, 14(6): 520-525.
- Vinot S., Le T., Ohno S., Pawson T., Maro B., Louvet-Vallee S. (2005) Asymmetric distribution of PAR proteins in the mouse embryo begins at the 8-cell stage during compaction. *Developmental Biology*, 282(2): 307-319.
- Wang K., Sengupta S., Magnani L., Wilson C.A., Henry R.W., Knott J.G. (2010) Brg1 is required for Cdx2-mediated repression of Oct4 expression in mouse blastocyst. *Plos ONE*, 5(5): e10622.
- Watanabe T., Biggins J.S., Tannan N.B., Srinivas S. (2014) Limited predictive value of blastomere angle of division in trophectoderm and inner cell mass specification. *Development*, 141(11): 2279-2288.
- Watson A.J., Natale D.R., Barcroft L.C. (2004) Molecular regulation of blastocyst formation. *Animal Reproduction Science*, 82–83: 583–592.
- White M.D., Angiolini J.F., Alvarez Y.D., Kaur G., Zhao Z.W., Mocskos E., Bruno L., Bissiere S., Levi V., Plachta N. (2016) Long-lived binding of Sox2 to DNA predicts cell fate in the four-cell mouse embryo. *Cell*, 165(1): 75-87.
- Wicklow E., Blij S., Frum T., Hirate Y., Lang R.A., Sasaki H., Ralston A. (2014) Hippo pathway members restrict Sox2 to the inner cell mass where it promotes ICM fates in the mouse blastocyst. *PLOS Genetics*, 10(10): e1004618.
- Wu Q., Bruce A.W., Jedrusik A., Elis P.D., Andrews R.M., Langford C.F., Glover D.M., Zernicka-Goetz M. (2009) CARM1 is required in embryonic stem cells to maintain pluripotency and resist differentiation. *Stem Cells*, 27(11): 2637-2645.
- Yagi R., Kohn M.J., Karavanova I., Kaneko K.J., Vullhorst D., DePamphilis M.L. Buonanno A. (2007) Transcription factor TEAD4 specifies the trophectoderm lineage at the beginning of mammalian development. *Development*, 134(21): 3827-3836.

- Yamanaka Y., Lanner F., Rossant J. (2010) FGF signal-dependent segregation of primitive endoderm and epiblast in the mouse blastocyst. *Development*, 137(5): 715-724.
- Yamanaka Y., Ralston A., Stephenson R.O., Rossant J. (2006) Cell and molecular regulation of the mouse blastocyst. *Developmental Dynamics*, 235(9): 2301–2314.
- Yang D-H., Cai K.Q., Roland I.H., Smith E.R., Xu X-X. (2007) Disabled-2 is an epithelial surface positioning gene. *The Journal of Biological Chemistry*, 282(17): 13114-13122.
- Yang D-H., Smith E.R., Roland I.H., Sheng Z., He J., Martin W.D., Hamilton T.C., Lambeth J.D., Xu X-X. (2002) Disabled-2 is essential for endodermal cell positioning and structure formation during mouse embryogenesis. *Developmental Biology*, 251(1): 27-44.
- Yuan H., Corbi N., Basilico C., Dailey L. (1995). Developmental-specific activity of the FGF-4 enhancer requires the synergistic action of Sox2 and Oct-3. *Genes and Development*, 9(21): 2635-2645.
- Zernicka-Goetz M. (1998) Fertile offspring derived from mammalian eggs lacking either animal or vegetal poles. *Development*, 125(23): 4803-4808.
- Zernicka-Goetz M. (2004) First cell fate decisions and spatial patterning in the early mouse embryo. *Seminars in Cell and Developmental Biology*, 15(5): 563-572.
- Zernicka-Goetz M., Morris S.A., Bruce A.W. (2009) Making firm decision: multifaceted regulation of cell fate in the early mouse embryo. *Nature Reviews Genetics*, 10(7): 467-477.
- Zernicka-Goetz M., Pines J., McLean Hunter S., Dixon J.P., Siemering K.R., Haseloff J., Evans M.J. (1997) Following cell fate in the living mouse embryo. *Development*, 124(6): 1133-1137.
- Zernicka-Goetz M., Pines J., Ryan K., Siemering K.R., Haseloff J., Evans M.J., Gurdon J.B. (1996) An indelible lineage marker for *Xenopus* using a mutated green fluorescent protein. *Development*, 122(12): 3719-3724.
- Ziomek C.A., Johnson M.H. (1980) Cell surface interaction induces polarization of mouse 8-cell blastomeres at compaction. *Cell*, 21(3): 935-942.

APPENDICES

APPENDIX A. SUPPLEMENTARY TABLES

Supplementary table ST1. Quantified cell lineage segregation in individual late blastocyst stage (E4.5) embryos *in vitro* cultured from the 2-cell stage (E1.5)

UNPERTURBED <i>IN VITRO</i> CONTROL EMBRYOS (2-CELL to E4.5)					
#	TOTAL NUMBER OF CELLS				
	EMBRYO	TE	EPI	ICM PrE	TOTAL
1	80	63	13	4	17
2	88	67	12	9	21
3	83	60	19	4	23
4	73	63	4	6	10
5	82	58	12	12	24
6	96	74	10	12	22
7	115	89	19	7	26
8	113	91	11	11	22
9	97	77	10	10	20
10	96	68	21	7	28
11	113	75	23	15	38
12	103	78	15	10	25
13	98	76	14	8	22
14	128	104	14	10	24
15	83	62	12	9	21
16	86	70	12	4	16
TOTAL	1534	1175	221	138	359
AVERAGE	95.9	73.4	13.8	8.6	22.4
SEM	3.8	3.1	1.2	0.8	1.5

Supplementary tables ST2. Quantified cell lineage segregation in individual late blastocyst stage (E4.5) embryos *in vitro* cultured from the 2-cell stage (E1.5) after microinjection in a single cell with fluorescent RDB ± Tead4-dsRNA (immunostained for Cdx2 and Gata4)

Control (1in2, IF: Cdx2/ Gata4)															
#	TOTAL NUMBER OF CELLS					NON-INJECTED CLONE					INJECTED CLONE				
	EMBRYO	TE	EPI	ICM	TOTAL	NON-INJECTED	INJECTED	OUTER	Gata4 -	Gata4 +	TOTAL	OUTER	Gata4 -	Gata4 +	TOTAL
1	76	61	11	4	15	25	51	16	6	3	9	45	5	1	6
2	89	76	7	6	13	46	43	37	5	4	9	39	2	2	4
3	80	56	20	4	24	54	26	36	16	2	18	20	4	2	6
4	86	60	21	5	26	37	49	24	12	1	13	36	9	4	13
5	80	58	15	7	22	42	38	34	5	3	8	24	10	4	14
6	81	52	14	15	29	49	32	29	12	8	20	23	2	7	9
7	79	63	11	5	16	43	36	34	6	3	9	29	5	2	7
8	83	54	22	7	29	46	37	23	18	5	23	31	4	2	6
9	100	79	12	9	21	49	51	42	4	3	7	37	8	6	14
10	87	65	14	8	22	36	51	32	1	3	4	33	13	5	18
11	107	83	17	7	24	70	37	55	11	4	15	28	6	3	9
12	106	78	19	9	28	52	54	38	8	6	14	40	11	3	14
13	78	51	20	7	27	43	35	30	10	3	13	21	10	4	14
14	92	73	12	7	19	31	61	26	4	1	5	47	8	6	14
15	85	65	12	8	20	37	48	27	6	4	10	38	6	4	10
16	96	70	21	5	26	50	46	35	12	3	15	35	9	2	11
17	71	47	19	5	24	40	31	27	8	5	13	20	11	0	11
18	90	74	6	10	16	59	31	46	4	9	13	28	2	1	3
19	94	72	7	15	22	42	52	34	0	8	8	38	7	7	14
20	112	92	10	10	20	72	40	57	9	6	15	35	1	4	5
21	89	59	23	7	30	44	45	31	11	2	13	28	12	5	17
22	89	70	12	7	19	34	55	28	4	2	6	42	8	5	13
23	75	58	12	5	17	39	36	32	5	2	7	26	7	3	10
24	96	82	9	5	14	44	52	41	3	0	3	41	6	5	11
TOTAL	2121	1598	346	177	523	1084	1037	814	180	90	270	784	166	87	253
AVERAGE	88.4	66.6	14.4	7.4	21.8	45.2	43.2	33.9	7.5	3.8	11.3	32.7	6.9	3.6	10.5
SEM	2.2	2.4	1.1	0.6	1.0	2.2	1.9	1.9	0.9	0.5	1.0	1.6	0.7	0.4	0.8
Stat. sig. (inter-clone) *p<0.05, **p<0.005 p-value (2-tailed students t-test)							5.07E-01					6.23E-01	6.15E-01	8.39E-01	5.97E-01

Tead4 KD (1in2, IF: Cdx2/ Gata4)															
#	TOTAL NUMBER OF CELLS					NON-INJECTED CLONE					INJECTED CLONE				
	EMBRYO	TE	EPI	ICM	TOTAL	NON-INJECTED	INJECTED	OUTER	Gata4 -	Gata4 +	TOTAL	OUTER	Gata4 -	Gata4 +	TOTAL
1	70	44	20	6	26	49	21	42	1	6	7	2	19	0	19
2	76	46	26	4	30	48	28	40	7	1	8	6	19	3	22
3	72	48	19	5	24	43	29	40	0	3	3	8	19	2	21
4	82	49	27	6	33	49	33	40	5	4	9	9	22	2	24
5	104	64	33	7	40	45	59	37	4	4	8	27	29	3	32
6	72	41	27	4	31	32	40	19	10	3	13	22	17	1	18
7	77	44	29	4	33	42	35	29	9	4	13	15	20	0	20
8	90	50	22	18	40	46	44	42	1	3	4	8	21	15	36
9	71	42	25	4	29	32	39	28	3	1	4	14	22	3	25
10	78	58	12	8	20	45	33	43	1	1	2	15	11	7	18
11	80	51	17	12	29	44	36	39	1	4	5	12	16	8	24
12	91	69	16	6	22	61	30	60	0	1	1	9	16	5	21
13	79	52	17	10	27	51	28	38	5	8	13	14	12	2	14
14	86	64	12	10	22	58	28	55	0	3	3	9	12	7	19
15	96	61	29	6	35	54	42	51	1	2	3	10	28	4	32
16	88	62	20	6	26	56	32	51	4	1	5	11	16	5	21
17	71	42	20	9	29	40	31	37	2	1	3	5	18	8	26
18	94	65	25	4	29	66	28	56	7	3	10	9	18	1	19
19	67	39	23	5	28	39	28	32	4	3	7	7	19	2	21
20	67	43	17	7	24	40	27	35	1	4	5	8	16	3	19
21	91	57	17	17	34	49	42	43	0	6	6	14	17	11	28
22	89	52	32	5	37	50	39	41	5	4	9	11	27	1	28
23	92	61	20	11	31	57	35	47	3	7	10	14	17	4	21
24	88	57	18	13	31	61	27	45	9	7	16	12	9	6	15
TOTAL	1971	1261	523	187	710	1157	814	990	83	84	167	271	440	103	543
AVERAGE	82.1	52.5	21.8	7.8	29.6	48.2	33.9	41.3	3.5	3.5	7.0	11.3	18.3	4.3	22.6
SEM	2.1	1.8	1.2	0.8	1.1	1.8	1.6	1.9	0.6	0.4	0.8	1.1	1.0	0.7	1.1
Stat. sig. (exp. vs. con embryo) *p<0.05, **p<0.005 p-value (2-tailed students t-test)	*	**	**		**		**	*	**		**	**	**		**
Stat. sig. (inter-clone) *p<0.05, **p<0.005 p-value (2-tailed students t-test)							**					**	**		**

Supplementary tables ST3. Quantified cell lineage segregation in individual late blastocyst stage (E4.5) embryos *in vitro* cultured from the 2-cell stage (E1.5) after microinjection in a single cell with fluorescent RDB ± Tead4-dsRNA (immunostained for Cdx2 and Sox17)

Control (1in2, IF: Cdx2/ Sox17)															
#	TOTAL NUMBER OF CELLS					NON-INJECTED CLONE					INJECTED CLONE				
	EMBRYO	TE	EPI	ICM PrE	TOTAL	NON- INJECTED	INJECTED	OUTER	Sox17 -	INNER Sox17 +	TOTAL	OUTER	Sox17 -	INNER Sox17 +	TOTAL
1	89	71	8	10	18	48	41	37	6	5	11	34	2	5	7
2	107	83	14	10	24	44	63	36	3	5	8	47	11	5	16
3	96	78	12	6	18	30	66	23	4	3	7	55	8	3	11
4	86	69	4	13	17	38	48	29	4	5	9	40	0	8	8
5	100	81	10	9	19	39	61	33	2	4	6	48	8	5	13
6	113	101	4	8	12	58	55	53	1	4	5	48	3	4	7
7	113	85	23	5	28	55	58	45	8	2	10	40	15	3	18
8	113	91	11	11	22	60	53	44	9	7	16	47	2	4	6
9	82	66	12	4	16	56	26	51	5	0	5	15	7	4	11
10	105	82	12	11	23	54	51	44	5	5	10	38	7	6	13
11	98	72	14	12	26	51	47	33	8	10	18	39	6	2	8
12	95	69	22	4	26	40	55	31	8	1	9	38	14	3	17
13	99	85	2	12	14	50	49	46	1	3	4	39	1	9	10
TOTAL	1296	1033	148	115	263	623	673	505	64	54	118	528	84	61	145
AVERAGE	99.7	79.5	11.4	8.8	20.2	47.9	51.8	38.8	4.9	4.2	9.1	40.6	6.5	4.7	11.2
SEM	2.2	2.1	1.3	0.7	1.1	1.9	2.2	1.9	0.6	0.5	0.9	2.1	1.0	0.4	0.9
Stat. sig. (inter-clone) ‡p<0.05, ††p<0.005															
p-value (2-tailed students t-test)							3.26E-01					6.34E-01	3.30E-01	5.59E-01	2.07E-01

Tead4 KD (1in2, IF: Cdx2/ Sox17)															
#	TOTAL NUMBER OF CELLS					NON-INJECTED CLONE					INJECTED CLONE				
	EMBRYO	TE	EPI	ICM PrE	TOTAL	NON- INJECTED	INJECTED	OUTER	Sox17 -	INNER Sox17 +	TOTAL	OUTER	Sox17 -	INNER Sox17 +	TOTAL
1	95	65	26	4	30	51	44	49	1	1	2	16	25	3	28
2	91	66	16	9	25	55	36	52	2	1	3	14	14	8	22
3	91	64	20	7	27	59	32	49	4	6	10	15	16	1	17
4	73	48	19	6	25	43	30	40	1	2	3	8	18	4	22
5	84	56	21	7	28	48	36	43	3	2	5	13	18	5	23
6	84	56	22	6	28	59	25	52	4	3	7	4	18	3	21
7	82	57	21	4	25	53	29	45	5	3	8	12	16	1	17
8	70	52	10	8	18	45	25	41	0	4	4	11	10	4	14
9	71	47	18	6	24	41	30	35	2	4	6	12	16	2	18
TOTAL	741	511	173	57	230	454	287	406	22	26	48	105	151	31	182
AVERAGE	82.3	56.8	19.2	6.3	25.6	50.4	31.9	45.1	2.4	2.9	5.3	11.7	16.8	3.4	20.2
SEM	2.2	1.7	1.0	0.4	0.8	1.6	1.4	1.4	0.4	0.4	0.6	0.9	0.9	0.5	1.0
Stat. sig. (exp. vs. con embryo) *p<0.05, **p<0.005	**	**	**	*	*		**		*		*	**	**		**
p-value (2-tailed students t-test)	5.90E-04	4.58E-06	2.65E-03	2.54E-02	7.62E-03	4.61E-01	1.70E-05	6.27E-02	1.63E-02	1.73E-01	1.79E-02	2.60E-08	2.72E-05	1.93E-01	9.32E-05
Stat. sig. (inter-clone) ‡p<0.05, ††p<0.005							††					††	††		††
p-value (2-tailed students t-test)							1.33E-05					1.30E-09	9.80E-07	5.49E-01	4.23E-07

Supplementary tables ST5. Incidence of apoptotic cells within individual late blastocyst stage (E4.5) embryos *in vitro* cultured from the 2-cell stage (E1.5) after microinjection in a single cell with fluorescent RDB ± Tead4-dsRNA (immunostained for Cdx2 and Gata4)

Control (1in2, IF: Cdx2/ Gata4) apoptotic cells										
#	TOTAL NUMBER OF CELLS					NON-INJECTED CLONE		INJECTED CLONE		
	EMBRYO	TE	ICM	NON-INJECTED	INJECTED	OUTER	ICM	OUTER	ICM	
1	5	2	3	0	5	0	0	2	3	
2	7	4	3	2	5	1	1	3	2	
3	5	3	2	2	3	2	0	1	2	
4	5	0	5	0	5	0	0	0	5	
5	4	0	4	0	4	0	0	0	4	
6	5	1	4	3	2	0	3	1	1	
7	5	1	4	3	2	0	3	1	1	
8	3	2	1	1	2	1	0	1	1	
9	9	4	5	3	6	3	0	1	5	
10	1	1	0	1	0	1	0	0	0	
11	4	2	2	4	0	2	2	0	0	
12	6	3	3	4	2	3	1	0	2	
13	2	2	0	0	2	0	0	2	0	
14	7	5	2	2	5	2	0	3	2	
15	4	1	3	1	3	0	1	1	2	
16	7	3	4	3	4	1	2	2	2	
17	8	3	5	4	4	1	3	2	2	
18	4	1	3	2	2	0	2	1	1	
19	3	1	2	1	2	0	1	1	1	
20	4	2	2	1	3	0	1	2	1	
21	5	4	1	2	3	1	1	3	0	
22	4	0	4	3	1	0	3	0	1	
23	2	2	0	1	1	1	0	1	0	
24	3	2	1	2	1	2	0	0	1	
TOTAL	112	49	63	45	67	21	24	28	39	
AVERAGE	4.7	2.0	2.6	1.9	2.8	0.9	1.0	1.2	1.6	
SEM	0.4	0.3	0.3	0.3	0.3	0.2	0.2	0.2	0.3	
Stat. sig. (inter-clone) †p<0.05, ††p<0.005					‡					
p-value (2-tailed students t-test)					3.92E-02			3.17E-01	1.03E-01	

Tead4 KD (1in2, IF: Cdx2/ Gata4) apoptotic cells										
#	TOTAL NUMBER OF CELLS					NON-INJECTED CLONE		INJECTED CLONE		
	EMBRYO	TE	ICM	NON-INJECTED	INJECTED	OUTER	ICM	OUTER	ICM	
1	4	1	3	1	3	0	1	1	2	
2	8	6	2	0	8	0	0	6	2	
3	7	4	3	3	4	3	0	1	3	
4	14	8	6	4	10	2	2	6	4	
5	15	10	5	1	14	1	0	9	5	
6	12	9	3	5	7	4	1	5	2	
7	7	1	6	2	5	1	1	0	5	
8	13	7	6	4	9	2	2	5	4	
9	15	12	3	0	15	0	0	12	3	
10	11	8	3	1	10	1	0	7	3	
11	10	3	7	5	5	1	4	2	3	
12	4	3	1	1	3	1	0	2	1	
13	10	5	5	6	4	3	3	2	2	
14	17	6	11	4	13	1	3	5	8	
15	5	3	2	0	5	0	0	3	2	
16	8	5	3	1	7	0	1	5	2	
17	3	1	2	1	2	0	1	1	1	
18	9	5	4	4	5	2	2	3	2	
19	8	7	1	1	7	1	0	6	1	
20	4	1	3	2	2	0	2	1	1	
21	10	6	4	2	8	1	1	5	3	
22	13	8	5	4	9	3	1	5	4	
23	4	4	0	1	3	1	0	3	0	
24	6	4	2	2	4	1	1	3	1	
TOTAL	217	127	90	55	162	29	26	98	64	
AVERAGE	9.0	5.3	3.8	2.3	6.8	1.2	1.1	4.1	2.7	
SEM	0.8	0.6	0.5	0.4	0.8	0.2	0.2	0.6	0.4	
Stat. sig. (exp. vs. con embryo) *p<0.05, **p<0.005	**	**			**			**	*	
p-value (2-tailed students t-test)	3.84E-05	3.03E-05	5.97E-02	3.59E-01	3.91E-05	2.86E-01	8.01E-01	5.03E-05	2.86E-02	
Stat. sig. (inter-clone) †p<0.05, ††p<0.005					††			††	††	
p-value (2-tailed students t-test)					7.40E-06			6.67E-05	5.88E-04	

Supplementary tables ST6. Incidence of apoptotic cells within individual late blastocyst stage (E4.5) embryos *in vitro* cultured from the 2-cell stage (E1.5) after microinjection in a single cell with fluorescent RDB ± Tead4-dsRNA (immunostained for Cdx2 and Sox17)

Control (1in2, IF: Cdx2/ Sox17) apoptotic cells										
#	TOTAL NUMBER OF CELLS					NON-INJECTED CLONE		INJECTED CLONE		
	EMBRYO	TE	ICM	NON-INJECTED	INJECTED	OUTER	ICM	OUTER	ICM	
1	4	3	1	2	2	1	1	2	0	
2	0	2	2	0	2	0	0	0	2	
3	9	3	6	4	5	2	2	1	4	
4	4	2	2	1	3	0	1	2	1	
5	2	2	0	0	2	0	0	2	0	
6	4	2	2	1	3	0	1	2	1	
7	3	3	0	2	1	2	0	1	0	
8	4	2	2	2	2	1	1	1	1	
9	10	6	4	5	5	3	2	3	2	
10	7	3	4	2	5	1	1	2	3	
11	6	3	3	4	2	2	2	1	1	
12	12	6	6	8	4	3	5	3	1	
13	3	0	3	0	3	0	0	0	3	
TOTAL	70	35	35	31	39	15	16	20	19	
AVERAGE	5.4	2.7	2.7	2.4	3.0	1.2	1.2	1.5	1.5	
SEM	0.9	0.5	0.5	0.6	0.4	0.3	0.4	0.3	0.4	
Stat. sig. (inter-clone) †p<0.05, ‡‡p<0.005										
p-value (2-tailed students t-test)					4.20E-01			3.64E-01	6.59E-01	

Tead4 KD (1in2, IF: Cdx2/ Sox17) apoptotic cells										
#	TOTAL NUMBER OF CELLS					NON-INJECTED CLONE		INJECTED CLONE		
	EMBRYO	TE	ICM	NON-INJECTED	INJECTED	OUTER	ICM	OUTER	ICM	
1	7	5	2	1	6	1	0	4	2	
2	3	2	1	0	3	0	0	2	1	
3	7	5	2	0	7	0	0	5	2	
4	5	4	1	1	4	1	0	3	1	
5	10	5	5	5	5	1	4	4	1	
6	7	7	0	1	6	1	0	6	0	
7	9	7	2	2	7	2	0	5	2	
8	4	4	0	0	4	0	0	4	0	
9	3	1	2	0	3	0	0	1	2	
TOTAL	55	40	15	10	45	6	4	34	11	
AVERAGE	6.1	4.4	1.7	1.1	5.0	0.7	0.4	3.8	1.2	
SEM	0.8	0.7	0.5	0.5	0.5	0.2	0.4	0.5	0.3	
Stat. sig. (exp. vs. con embryo) *p<0.05, **p<0.005					**			**		
p-value (2-tailed students t-test)	5.59E-01	5.19E-02	1.78E-01	1.46E-01	7.20E-03	2.32E-01	1.95E-01	2.40E-03	5.99E-01	
Stat. sig. (inter-clone) †p<0.05, ‡‡p<0.005					‡‡			‡‡		
p-value (2-tailed students t-test)					9.50E-05			2.00E-04	1.61E-01	

Supplementary tables ST7. Incidence of apoptotic cells within individual late blastocyst stage (E4.5) embryos *in vitro* cultured from the 2-cell stage (E1.5) after microinjection in a single cell with fluorescent RDB ± Tead4-dsRNA (immunostained for Gata4 and Nanog)

Control (1in2, IF: Gata4/ Nanog) apoptotic cells									
#	TOTAL NUMBER OF CELLS					NON-INJECTED CLONE		INJECTED CLONE	
	EMBRYO	TE	ICM	NON-INJECTED	INJECTED	OUTER	ICM	OUTER	ICM
1	7	3	4	2	5	1	1	2	3
2	4	1	3	2	2	0	2	1	1
3	2	0	2	1	1	0	1	0	1
4	6	4	2	3	3	2	1	2	1
5	2	1	1	1	1	0	1	1	0
6	5	1	4	3	2	1	2	0	2
7	6	3	3	5	1	2	3	1	0
8	6	5	1	5	1	5	0	0	1
9	6	1	5	3	3	1	2	0	3
10	4	2	2	2	2	1	1	1	1
11	6	2	4	4	2	1	3	1	1
12	5	2	3	2	3	1	1	1	2
13	8	4	4	5	3	3	2	1	2
14	2	1	1	1	1	0	1	1	0
15	6	3	3	5	1	3	2	0	1
16	2	0	2	1	1	0	1	0	1
17	4	1	3	2	2	0	2	1	1
18	6	3	3	3	3	1	2	2	1
19	3	0	3	1	2	0	1	0	2
20	5	1	4	2	3	0	2	1	2
21	6	2	4	5	1	2	3	0	1
22	0	0	0	0	0	0	0	0	0
23	4	4	0	3	1	3	0	1	0
24	2	1	1	1	1	1	0	0	1
25	11	6	5	7	4	2	5	4	0
TOTAL	11	6	5	7	4	2	5	4	0
AVERAGE	4.7	2.0	2.7	2.8	2.0	1.2	1.6	0.8	1.1
SEM	0.5	0.3	0.3	0.4	0.2	0.3	0.2	0.2	0.2
Stat. sig. (inter-clone) †p<0.05, ‡†p<0.005									
p-value (2-tailed students t-test)					6.57E-02			2.66E-01	1.38E-01

Tead4 KD (1in2, IF: Gata4/ Nanog) apoptotic cells									
#	TOTAL NUMBER OF CELLS					NON-INJECTED CLONE		INJECTED CLONE	
	EMBRYO	TE	ICM	NON-INJECTED	INJECTED	OUTER	ICM	OUTER	ICM
1	10	6	4	2	8	1	1	5	3
2	12	8	4	3	9	1	2	7	2
3	21	11	10	8	13	3	5	8	5
4	12	5	7	1	11	1	0	4	7
5	9	5	4	1	8	0	1	5	3
6	15	7	8	3	12	2	1	5	7
7	9	5	4	3	6	1	2	4	2
8	4	0	4	1	3	0	1	0	3
9	11	3	8	5	6	2	3	1	5
10	8	7	1	3	5	2	1	5	0
11	16	9	7	7	9	3	4	6	3
12	12	4	8	6	6	0	6	4	2
13	9	3	6	5	4	0	5	3	1
14	12	8	4	5	7	3	2	5	2
15	16	6	10	11	5	3	8	3	2
16	13	10	3	5	8	3	2	7	1
17	7	5	2	1	6	0	1	5	1
18	14	9	5	3	11	2	1	7	4
19	14	7	7	2	12	1	1	6	6
20	14	6	8	6	8	2	4	4	4
21	14	4	10	4	10	1	3	3	7
22	22	8	14	8	14	2	6	6	8
23	13	6	7	6	7	1	5	5	2
TOTAL	13	6	7	6	7	1	5	5	2
AVERAGE	12.5	6.2	6.3	4.3	8.2	1.5	2.8	4.7	3.5
SEM	0.8	0.5	0.6	0.5	0.6	0.2	0.4	0.4	0.5
Stat. sig. (exp. vs. con embryo) *p<0.05, **p<0.005	**	**	**	*	**		*	**	**
p-value (2-tailed students t-test)	2.81E-09	7.33E-08	1.27E-05	2.32E-02	3.40E-10	4.21E-01	1.70E-02	4.97E-10	6.97E-05
Stat. sig. (inter-clone) †p<0.05, ‡†p<0.005					**			**	
p-value (2-tailed students t-test)					2.83E-05			3.06E-08	3.23E-01

Supplementary tables ST8. Quantified cell lineage segregation in individual late blastocyst stage (E4.5) embryos *in vitro* cultured from the 2-cell stage (E1.5) after microinjection in a single cell with fluorescent RDB tracer alone or RDB and GFP-dsRNA (immuno-stained for Cdx2 and Gata4)

RDB (1in2, IF: Cdx2/Gata4)															
#	EMBRYO	TOTAL NUMBER OF CELLS					NON-INJECTED CLONE					INJECTED CLONE			
		TE	EPI	ICM	PVE	TOTAL	NON-INJECTED	INJECTED	OUTER	Gata4	INNER	TOTAL	OUTER	INNER	
1	94	74	13	7	20	49	45	39	7	3	10	35	6	4	
2	108	73	29	6	35	45	63	30	12	3	15	43	17	3	
3	96	70	12	4	16	37	49	33	3	1	4	37	9	2	
4	110	83	14	13	27	50	60	35	8	7	15	48	6	12	
5	108	82	14	12	26	67	41	50	10	7	17	32	4	5	
6	92	72	13	7	20	41	51	34	3	4	7	38	10	3	
7	89	72	6	11	17	43	46	38	2	3	5	34	4	8	
8	108	80	14	14	28	57	51	41	7	9	16	39	7	5	
9	89	68	12	9	21	38	51	29	6	3	9	39	6	6	
10	79	58	13	8	21	47	32	32	11	4	15	26	2	4	
11	120	78	26	16	42	69	51	42	17	10	27	36	9	6	
12	92	69	18	5	23	39	53	29	9	1	10	40	9	4	
13	77	57	7	13	20	37	40	27	4	6	10	30	3	7	
14	89	76	5	8	13	45	44	44	1	0	1	32	4	8	
15	94	64	17	13	30	40	54	27	9	4	13	37	8	9	
16	94	73	12	9	21	54	40	39	10	5	15	34	2	4	
17	90	70	12	8	20	48	42	40	6	2	8	30	6	6	
18	75	51	20	4	24	36	39	27	9	0	9	24	11	4	
19	84	60	15	9	24	50	34	37	8	5	13	23	7	4	
20	85	60	16	9	25	44	41	32	7	5	12	28	9	4	
21	88	58	20	10	30	41	47	26	10	5	15	32	10	5	
22	97	64	25	8	33	40	57	25	13	2	15	39	12	6	
23	104	80	17	7	24	55	49	45	9	1	10	35	8	6	
24	98	74	19	5	24	54	44	40	10	4	14	34	9	1	
25	97	63	25	9	34	55	42	31	18	6	24	32	7	3	
26	97	85	7	5	12	42	55	37	3	2	5	48	4	3	
27	114	81	24	9	33	41	73	29	3	9	12	52	21	0	
28	112	83	17	12	29	62	50	43	10	9	19	40	7	3	
29	111	88	11	12	23	58	53	44	5	9	14	44	6	3	
30	99	82	12	5	17	48	51	40	5	3	8	42	7	2	
TOTAL	2880	2148	465	267	732	1432	1448	1065	235	130	367	1083	230	135	
AVERAGE	96.0	71.6	15.5	8.9	24.4	47.7	48.3	35.5	7.8	4.4	12.2	36.1	7.7	4.5	
SEM	2.1	1.8	1.1	0.6	1.2	1.6	1.6	1.2	0.7	0.5	1.0	1.3	0.7	0.4	
Stat. sig. (inter-clone) #p<0.05, ##p<0.005															
p-value (2-tailed students t-test)							8.14E-01					7.34E-01	8.74E-01	8.77E-01	9.56E-01

GFP-dsRNA+RDB (1in2, IF: Cdx2/Gata4)															
#	EMBRYO	TOTAL NUMBER OF CELLS					NON-INJECTED CLONE					INJECTED CLONE			
		TE	EPI	ICM	PVE	TOTAL	NON-INJECTED	INJECTED	OUTER	Gata4	INNER	TOTAL	OUTER	INNER	
1	93	67	12	14	26	48	45	35	8	5	13	32	4	9	
2	99	66	27	6	33	49	50	33	16	0	16	33	11	6	
3	82	62	11	9	20	42	40	32	6	4	10	30	5	5	
4	97	74	19	4	23	50	47	33	16	1	17	41	3	3	
5	93	64	23	6	29	49	44	33	15	1	16	31	8	5	
6	102	81	12	9	21	49	53	41	4	4	8	40	8	5	
7	106	79	14	13	27	50	56	34	7	9	16	45	7	4	
8	95	78	8	9	17	49	46	42	2	5	7	36	6	4	
9	109	82	16	11	27	53	56	42	5	6	11	40	11	5	
10	102	74	13	15	28	48	54	40	1	7	8	34	12	8	
11	98	81	8	9	17	39	59	28	7	4	11	53	1	5	
12	95	74	12	9	21	44	51	34	7	3	10	40	5	6	
13	100	72	16	12	28	44	46	41	10	3	13	31	6	9	
14	82	64	11	7	18	41	41	34	6	1	7	30	5	6	
15	99	79	14	6	20	49	50	42	5	2	7	37	9	4	
16	102	86	8	8	16	53	49	43	6	4	10	43	2	4	
17	87	62	16	9	25	49	38	37	11	1	12	25	5	8	
18	103	75	23	5	28	50	53	34	13	3	16	41	10	2	
19	83	63	16	4	20	35	48	26	5	4	9	37	11	0	
20	88	59	25	4	29	53	35	44	9	0	9	15	16	4	
21	90	68	12	10	22	45	45	34	4	7	11	34	8	3	
22	81	67	10	4	14	35	46	31	2	2	4	36	8	2	
23	86	66	15	5	20	42	44	33	7	2	9	33	8	3	
24	116	88	23	5	28	63	53	49	12	2	14	39	11	3	
25	88	59	20	9	29	43	45	27	11	5	16	32	9	4	
26	106	76	19	11	30	49	57	38	7	4	11	38	12	7	
27	91	64	16	11	27	48	43	31	11	6	17	33	5	5	
28	97	72	19	6	25	47	50	44	2	1	3	28	17	5	
29	84	54	26	4	30	43	41	28	12	3	15	26	14	1	
30	91	62	24	5	29	51	40	34	13	4	17	28	11	1	
31	104	78	20	6	28	50	54	41	5	4	9	37	15	2	
32	99	76	14	9	23	51	48	36	12	3	15	40	2	6	
33	99	75	13	11	24	52	47	37	9	6	15	38	4	5	
34	101	79	17	5	22	52	49	41	8	3	11	38	9	2	
35	102	80	18	4	22	54	48	42	9	3	12	38	9	1	
36	86	60	15	11	26	45	41	30	5	10	15	30	10	1	
37	96	72	18	6	24	40	56	23	13	4	17	49	5	2	
TOTAL	3532	2638	603	291	894	1764	1768	1327	301	136	437	1311	302	155	
AVERAGE	95.5	71.3	16.3	7.9	24.2	47.7	47.8	35.9	8.1	3.7	11.8	35.4	8.2	4.2	
SEM	1.4	1.4	0.8	0.5	0.8	0.9	0.9	0.7	0.4	0.6	0.6	1.1	0.6	0.4	
Stat. sig. (comp. vs. non-embryo) #p<0.05, ##p<0.005															
p-value (2-tailed students t-test)	8.31E-01	8.93E-01	5.69E-01	1.86E-01	8.71E-01	9.76E-01	7.93E-01	8.16E-01	7.63E-01	2.66E-01	7.25E-01	6.96E-01	6.15E-01	5.60E-01	8.42E-01
Stat. sig. (inter-clone) #p<0.05, ##p<0.005															
p-value (2-tailed students t-test)							9.35E-01					7.74E-01	9.77E-01	3.39E-01	5.50E-01

Supplementary tables ST9. Incidence of apoptotic cells within individual late blastocyst stage (E4.5) embryos *in vitro* cultured from the 2-cell stage (E1.5) after microinjection in a single cell with fluorescent RDB tracer alone or RDB and GFP-dsRNA (immuno-stained for Cdx2 and Gata4)

RDB (1in2, IF: Cdx2/ Gata4) apoptotic cells										
#	TOTAL NUMBER OF CELLS					NON-INJECTED CLONE		INJECTED CLONE		
	EMBRYO	TE	ICM	NON-INJECTED	INJECTED	OUTER	ICM	OUTER	ICM	
1	4	2	2	1	3	0	1	2	1	
2	3	1	2	2	1	1	1	0	1	
3	11	6	5	6	5	3	3	3	2	
4	7	4	3	3	4	2	1	2	2	
5	5	1	4	3	2	1	2	0	2	
6	4	3	1	1	3	1	0	2	1	
7	9	2	7	5	4	1	4	1	3	
8	6	2	4	4	2	2	2	0	2	
9	9	2	7	3	6	0	3	2	4	
10	12	4	8	8	4	3	5	1	3	
11	5	1	4	4	1	1	3	0	1	
12	6	5	1	5	1	4	1	1	0	
13	12	4	8	4	8	1	3	3	5	
14	11	4	7	5	6	1	4	3	3	
15	6	4	2	3	3	3	0	1	2	
16	4	1	3	4	0	1	3	0	0	
17	5	2	3	4	1	2	2	0	1	
18	11	6	5	7	4	4	3	2	2	
19	6	0	6	3	3	0	3	0	3	
20	9	6	3	3	6	2	1	4	2	
21	12	3	9	4	8	0	4	3	5	
22	5	2	3	0	5	0	0	2	3	
23	5	4	1	0	5	0	0	4	1	
24	13	7	6	7	6	4	3	3	3	
25	6	0	6	2	4	0	2	0	4	
26	10	5	5	6	4	4	2	1	3	
27	7	3	4	4	3	3	1	0	3	
28	3	0	3	2	1	0	2	0	1	
29	7	4	3	5	2	3	2	1	1	
30	3	2	1	2	1	2	0	0	1	
TOTAL	216	90	126	110	106	49	61	41	65	
AVERAGE	7.2	3.0	4.2	3.7	3.5	1.6	2.0	1.4	2.2	
SEM	0.6	0.4	0.4	0.4	0.4	0.3	0.3	0.2	0.2	
Stat. sig. (inter-clone) *p<0.05, **p<0.005										
p-value (2-tailed students t-test)					8.03E-01			4.52E-01	7.03E-01	

GFP-dsRNA+RDB (1in2, IF: Cdx2/ Gata4) apoptotic cells										
#	TOTAL NUMBER OF CELLS					NON-INJECTED CLONE		INJECTED CLONE		
	EMBRYO	TE	ICM	NON-INJECTED	INJECTED	OUTER	ICM	OUTER	ICM	
1	11	4	7	6	5	3	3	1	4	
2	8	1	7	5	3	1	4	0	3	
3	17	6	11	8	9	3	5	3	6	
4	3	3	0	0	3	0	0	3	0	
5	9	4	5	4	5	2	2	2	3	
6	7	2	5	3	4	1	2	1	3	
7	8	0	8	7	1	0	7	0	1	
8	6	3	3	3	3	0	3	3	0	
9	4	0	4	2	2	0	2	0	2	
10	7	2	5	6	1	2	4	0	1	
11	11	4	7	7	4	3	4	1	3	
12	11	2	9	6	5	1	5	1	4	
13	6	1	5	1	5	0	1	1	4	
14	5	3	2	2	3	2	0	1	2	
15	6	5	1	6	0	5	1	0	0	
16	8	4	4	3	5	1	2	3	2	
17	9	3	6	5	4	2	3	1	3	
18	7	1	6	4	3	1	3	0	3	
19	4	2	2	1	3	0	1	2	1	
20	20	12	8	8	12	7	1	5	7	
21	8	3	5	5	3	1	4	2	1	
22	10	6	4	7	3	3	4	3	0	
23	5	1	4	3	2	1	2	0	2	
24	8	5	3	7	1	5	2	0	1	
25	4	1	3	3	1	1	2	0	1	
26	7	3	4	4	3	2	2	1	2	
27	13	7	6	6	7	3	3	4	3	
28	15	6	9	7	8	5	2	1	7	
29	3	0	3	2	1	0	2	0	1	
30	3	1	2	3	0	1	2	0	0	
31	1	0	1	1	0	0	1	0	0	
32	9	1	8	3	6	0	3	1	5	
33	9	6	3	4	5	2	2	4	1	
34	5	2	3	3	2	1	2	1	1	
35	7	2	5	3	4	1	2	1	3	
36	8	6	2	3	5	2	1	4	1	
37	8	6	2	4	4	3	1	3	1	
TOTAL	290	118	172	155	135	65	90	53	82	
AVERAGE	7.8	3.2	4.6	4.2	3.6	1.8	2.4	1.4	2.2	
SEM	0.6	0.4	0.4	0.4	0.4	0.3	0.2	0.2	0.3	
Stat. sig. (exp. vs. con embryo) *p<0.05, **p<0.005										
p-value (2-tailed students t-test)	4.59E-01	7.30E-01	4.53E-01	3.04E-01	8.41E-01	7.45E-01	2.56E-01	8.47E-01	9.00E-01	
Stat. sig. (inter-clone) *p<0.05, **p<0.005										
p-value (2-tailed students t-test)					3.26E-01			3.78E-01	5.84E-01	

Supplementary tables ST10. Quantified cell lineage segregation in individual late blastocyst stage (E4.5) embryos *in vitro* from the 4-cell stage (E2.0) after microinjection in a single cell with fluorescent RDB tracer alone or RDB and GFP-dsRNA (immuno-stained for Cdx2 and Gata4)

Control (1in4, IF: Cdx2/Gata4)															
#	TOTAL NUMBER OF CELLS					NON-INJECTED CLONE				INJECTED CLONE					
	EMBRYO	TE	EPI	ICM PrE	TOTAL	NON-INJECTED	INJECTED	OUTER	Gata4 -	Gata4 +	TOTAL	OUTER	Gata4 -	Gata4 +	TOTAL
1	86	65	11	10	21	62	24	49	8	5	13	16	3	5	8
2	94	70	19	5	24	70	24	49	16	5	21	21	3	0	3
3	104	83	14	7	21	88	16	74	10	4	14	9	4	3	7
4	97	75	17	5	22	78	19	61	13	4	17	14	4	1	5
5	101	76	16	9	25	73	28	58	10	5	15	18	6	4	10
6	97	71	17	9	26	70	27	53	12	5	17	18	5	4	9
7	99	68	24	7	31	72	27	46	19	7	26	22	5	0	5
8	101	82	10	9	19	75	26	56	10	9	19	26	0	0	0
9	95	75	13	7	20	68	27	53	11	4	15	22	2	3	5
10	98	70	19	9	28	71	27	50	12	9	21	20	7	0	7
11	103	83	7	13	20	71	32	56	3	12	15	27	4	1	5
12	105	78	17	10	27	77	28	57	15	5	20	21	2	5	7
13	84	59	17	8	25	51	33	38	11	2	13	21	6	6	12
14	105	76	17	12	29	76	29	58	8	10	18	18	9	2	11
15	101	77	20	4	24	79	22	62	14	3	17	15	6	1	7
16	80	61	12	7	19	54	26	39	9	6	15	22	3	1	4
17	115	97	11	7	18	83	32	67	9	7	16	30	2	0	2
18	108	88	14	6	20	76	32	60	12	4	16	28	2	2	4
19	111	91	12	8	20	81	30	67	6	8	14	24	6	0	6
TOTAL	1884	1445	287	152	439	1375	509	1053	208	114	322	392	79	38	117
AVERAGE	99.2	76.1	15.1	8.0	23.1	72.4	26.8	55.4	10.9	6.0	16.9	20.6	4.2	2.0	6.2
SEM	2.0	2.3	0.9	0.5	0.9	2.1	1.0	2.1	0.8	0.6	0.8	1.2	0.5	0.5	0.7

Tead4 KD (1in4, IF: Cdx2/Gata4)															
#	TOTAL NUMBER OF CELLS					NON-INJECTED CLONE				INJECTED CLONE					
	EMBRYO	TE	EPI	ICM PrE	TOTAL	NON-INJECTED	INJECTED	OUTER	Gata4 -	Gata4 +	TOTAL	OUTER	Gata4 -	Gata4 +	TOTAL
1	104	72	25	7	32	77	27	65	7	5	12	7	18	2	20
2	78	47	18	13	31	58	20	38	11	9	20	9	7	4	11
3	87	62	16	9	25	69	18	53	9	7	16	9	7	2	9
4	95	66	15	14	29	69	26	60	4	5	9	6	11	9	20
5	75	50	20	5	25	59	16	45	10	4	14	5	10	1	11
6	82	61	12	9	21	59	23	53	3	3	6	8	9	6	15
7	100	71	19	10	29	75	25	55	12	8	20	16	7	2	9
8	97	61	22	14	36	81	16	55	14	12	26	6	8	2	10
9	92	68	13	11	24	67	25	59	4	4	8	9	9	7	16
10	75	44	27	4	31	56	19	43	9	4	13	1	18	0	18
11	105	83	12	10	22	84	21	73	6	5	11	10	6	5	11
12	96	69	20	7	27	71	25	58	8	5	13	11	12	2	14
13	84	58	20	6	26	67	17	57	8	2	10	1	12	4	16
14	89	65	14	10	24	70	19	53	9	8	17	12	5	2	7
15	102	76	14	12	26	76	26	55	11	10	21	21	3	2	5
16	88	57	20	11	31	65	23	53	7	5	12	4	13	6	19
17	98	73	19	6	25	80	18	68	7	5	12	5	12	1	13
18	95	62	26	7	33	70	25	52	12	6	18	10	14	1	15
19	108	76	14	18	32	86	22	61	9	16	25	15	5	2	7
20	78	47	27	4	31	55	23	42	13	0	13	5	14	4	18
21	80	55	19	6	25	59	21	46	10	3	13	9	9	3	12
22	87	55	25	7	32	67	20	49	13	5	18	6	12	2	14
23	78	57	13	8	21	53	25	41	9	3	12	16	4	5	9
24	75	56	14	5	19	59	16	49	6	4	10	7	8	1	9
25	91	71	11	9	20	69	22	58	5	6	11	13	6	3	9
26	89	60	14	15	29	66	23	42	11	13	24	18	3	2	5
27	105	69	25	11	36	81	24	62	10	9	19	7	15	2	17
28	110	78	23	9	32	95	15	70	18	7	25	8	5	2	7
29	108	81	16	11	27	89	19	69	10	10	20	12	6	1	7
TOTAL	2651	1850	533	268	801	2032	619	1584	265	183	448	266	268	85	353
AVERAGE	91.4	63.8	18.4	9.2	27.6	70.1	21.3	54.6	9.1	6.3	15.4	9.2	9.2	2.9	12.2
SEM	2.1	1.9	0.9	0.6	0.9	2.0	0.7	1.7	0.6	0.7	1.0	0.9	0.8	0.4	0.8
Stat. sig. (exp. vs. con embryo)	*	**	*		**		**					**	**		**
*p<0.05, **p<0.005															
p-value (2-tailed students t-test)	1.02E-02	2.00E-04	1.72E-02	1.43E-01	7.00E-04	4.33E-01	1.00E-04	7.70E-01	8.95E-02	7.27E-01	2.44E-01	3.45E-09	1.81E-06	1.29E-01	1.72E-06

Supplementary tables ST11. Incidence of apoptotic cells within individual late blastocyst stage (E4.5) embryos *in vitro* cultured from the 4-cell stage (E2.0) after microinjection in a single cell, with fluorescent RDB tracer alone or RDB and GFP-dsRNA (immuno-stained for Cdx2 and Gata4)

Control (1in4, IF: Cdx2/ Gata4) apoptotic cells									
#	TOTAL NUMBER OF CELLS					NON-INJECTED CLONE		INJECTED CLONE	
	EMBRYO	TE	ICM	NON-INJECTED	INJECTED	OUTER	ICM	OUTER	ICM
1	2	1	1	1	1	0	1	1	0
2	4	1	3	2	2	0	2	1	1
3	2	2	0	1	1	1	0	1	0
4	5	2	3	4	1	2	2	0	1
5	4	4	0	2	2	2	0	2	0
6	5	2	3	3	2	2	1	0	2
7	9	4	5	7	2	3	4	1	1
8	4	2	2	3	1	2	1	0	1
9	6	2	4	4	2	1	3	1	1
10	4	2	2	3	1	2	1	0	1
11	10	9	1	10	0	9	1	0	0
12	2	1	1	2	0	1	1	0	0
13	1	1	0	1	0	1	0	0	0
14	4	0	4	1	3	0	1	0	3
15	2	2	0	2	0	2	0	0	0
16	5	0	5	3	2	0	3	0	2
17	3	1	2	3	0	1	2	0	0
18	0	0	0	0	0	0	0	0	0
19	4	2	2	3	1	2	1	0	1
TOTAL	76	38	38	55	21	31	24	7	14
AVERAGE	4.0	2.0	2.0	2.9	1.1	1.6	1.3	0.4	0.7
SEM	0.6	0.5	0.4	0.5	0.2	0.5	0.3	0.1	0.2

Tead4 KD (1in4, IF: Cdx2/Gata4) apoptotic cells									
#	TOTAL NUMBER OF CELLS					NON-INJECTED CLONE		INJECTED CLONE	
	EMBRYO	TE	ICM	NON-INJECTED	INJECTED	OUTER	ICM	OUTER	ICM
1	3	0	3	2	1	0	2	0	1
2	9	6	3	5	4	3	2	3	1
3	5	4	1	3	2	3	0	1	1
4	7	1	6	4	3	1	3	0	3
5	6	2	4	5	1	1	4	1	0
6	12	8	4	10	2	7	3	1	1
7	2	2	0	1	1	1	0	1	0
8	7	3	4	4	3	2	2	1	2
9	8	5	3	6	2	5	1	0	2
10	2	0	2	1	1	0	1	0	1
11	4	3	1	3	1	3	0	0	1
12	4	1	3	2	2	1	1	0	2
13	18	10	8	13	5	10	3	0	5
14	8	6	2	4	4	3	1	3	1
15	6	3	3	4	2	1	3	2	0
16	7	5	2	3	4	3	0	2	2
17	5	3	2	0	5	0	0	3	2
18	5	2	3	0	5	0	0	2	3
19	4	3	1	1	3	1	0	2	1
20	7	4	3	4	3	3	1	1	2
21	5	5	0	4	1	4	0	1	0
22	9	5	4	7	2	4	3	1	1
23	2	2	0	0	2	0	0	2	0
24	9	6	3	6	3	4	2	2	1
25	5	2	3	2	3	1	1	1	2
26	3	0	3	2	1	0	2	0	1
27	6	1	5	3	3	0	3	1	2
28	3	1	2	2	1	1	1	0	1
29	3	3	0	1	2	1	0	2	0
TOTAL	174	96	78	102	72	63	39	33	39
AVERAGE	6.0	3.3	2.7	3.5	2.5	2.2	1.3	1.1	1.3
SEM	0.6	0.4	0.3	0.5	0.2	0.4	0.2	0.2	0.2
Stat. sig. (exp. vs. con embryo)	*	*			**			**	*
*p<0.05, **p<0.005									
p-value (2-tailed students t-test)	2.24E-02	4.91E-02	1.88E-01	4.15E-01	1.00E-04	3.97E-01	8.18E-01	1.60E-03	4.00E-02

Supplementary tables ST12. Quantified cell lineage segregation in individual late blastocyst stage (E4.5) embryos derived from 8-cell stage (E2.5) chimeric embryos consisting of a single control (fluorescent RDB tracer alone) or *Tead4*-KD (fluorescent RDB tracer plus *Tead4*-dsRNA) cell (immuno-stained for *Cdx2* and *Gata4*)

Control (1+8, IF: <i>Cdx2</i> / <i>Gata4</i>)															
#	TOTAL NUMBER OF CELLS					NON-INJECTED CLONE			INJECTED CLONE						
	EMBRYO	TE	EPI	ICM PrE	TOTAL	NON- INJECTED	INJECTED	OUTER	INNER Gata4 - Gata4 +		TOTAL	OUTER	INNER Gata4 - Gata4 +		TOTAL
1	87	67	10	10	20	75	12	60	6	9	15	7	4	1	5
2	84	60	20	4	24	75	9	55	16	4	20	5	4	0	4
3	64	49	11	4	15	52	12	41	9	2	11	8	2	2	4
4	87	69	14	4	18	80	7	65	12	3	15	4	2	1	3
5	97	68	25	4	29	84	13	57	24	3	27	11	1	1	2
6	100	82	9	9	18	85	15	72	6	7	13	10	3	2	5
7	97	78	12	7	19	84	13	74	4	6	10	4	8	1	9
8	106	82	16	8	24	99	7	75	16	8	24	7	0	0	0
9	80	69	4	7	11	66	14	57	4	5	9	12	0	2	2
10	99	73	18	8	26	88	11	62	18	8	26	11	0	0	0
11	90	69	17	4	21	79	11	59	16	4	20	10	1	0	1
12	89	67	14	8	22	79	10	63	8	8	16	4	6	0	6
13	75	62	9	4	13	67	8	57	6	4	10	5	3	0	3
14	116	100	7	9	16	100	16	84	7	9	16	16	0	0	0
15	87	70	9	8	17	79	8	62	9	8	17	8	0	0	0
16	82	66	8	8	16	72	10	62	8	8	16	10	0	0	0
17	86	64	18	4	22	78	8	56	18	4	22	8	0	0	0
18	86	73	8	5	13	78	8	67	6	5	11	6	2	0	2
19	109	89	11	9	20	97	12	83	7	7	14	6	4	2	6
20	108	86	10	12	22	92	16	70	10	12	22	16	0	0	0
21	89	74	8	7	15	77	12	66	4	7	11	8	4	0	4
22	99	84	10	5	15	89	10	74	10	5	15	10	0	0	0
23	110	91	10	9	19	101	9	85	9	7	16	6	1	2	3
24	83	57	10	16	26	68	15	48	8	12	20	9	2	4	6
25	87	75	3	9	12	69	18	68	0	1	1	7	3	8	11
26	79	59	13	7	20	65	14	55	6	4	10	4	7	3	10
27	84	65	13	6	19	76	8	61	9	6	15	4	4	0	4
28	94	77	12	5	17	80	14	66	10	4	14	11	2	1	3
29	83	69	10	4	14	74	9	63	7	4	11	6	3	0	3
30	100	73	14	13	27	89	11	69	10	10	20	4	4	3	7
TOTAL	2737	2167	353	217	570	2397	340	1990	283	184	467	237	70	33	103
AVERAGE	91.2	72.2	11.8	7.2	19.0	79.9	11.3	64.3	9.4	6.1	15.6	7.9	2.3	1.1	3.4
SEM	2.1	2.0	0.9	0.5	0.9	2.1	0.5	1.8	0.9	0.5	1.0	0.6	0.4	0.3	0.6

Tead4 KD (1+8, IF: <i>Cdx2</i> / <i>Gata4</i>)															
#	TOTAL NUMBER OF CELLS					NON-INJECTED CLONE			INJECTED CLONE						
	EMBRYO	TE	EPI	ICM PrE	TOTAL	NON- INJECTED	INJECTED	OUTER	INNER Gata4 - Gata4 +		TOTAL	OUTER	INNER Gata4 - Gata4 +		TOTAL
1	87	58	25	4	29	79	8	58	18	3	21	0	7	1	8
2	92	71	14	7	21	85	7	66	12	7	19	5	2	0	2
3	85	62	18	5	23	69	16	54	11	4	15	8	7	1	8
4	89	73	7	9	16	79	10	70	5	4	9	3	2	5	7
5	91	74	13	4	17	83	8	70	9	4	13	4	4	0	4
6	78	58	10	10	20	70	8	56	6	8	14	2	4	2	6
7	71	58	8	5	13	64	7	57	2	5	7	1	6	0	6
8	81	62	14	5	19	70	11	62	3	5	8	0	11	0	11
9	84	61	19	4	23	76	8	60	12	4	16	1	7	0	7
10	99	75	15	9	24	92	7	71	12	9	21	4	3	0	3
11	102	77	15	10	25	90	12	68	12	10	22	9	3	0	3
12	92	74	14	4	18	85	7	71	10	4	14	3	4	0	4
13	103	84	14	5	19	87	16	79	8	0	8	5	6	5	11
14	86	69	11	6	17	78	8	69	3	6	9	0	8	0	8
15	79	52	23	4	27	71	8	50	18	3	21	2	5	1	6
16	71	49	18	4	22	64	7	46	16	2	18	3	2	2	4
17	74	52	14	8	22	66	8	52	7	7	14	0	7	1	8
TOTAL	1464	1109	252	103	355	1308	156	1059	164	85	249	50	88	18	106
AVERAGE	86.1	65.2	14.8	6.1	20.9	76.9	9.2	62.3	9.6	5.0	14.6	2.9	5.2	1.1	6.2
SEM	2.4	2.5	1.2	0.6	1.0	2.2	0.7	2.2	1.2	0.6	1.2	0.7	0.6	0.4	0.6
Stat. sig. (exp. vs. con embryo)		*	*				*					**	**		**
*p<0.05, **p<0.005															
p-value (2-tailed students t-test)	1.17E-01	3.41E-02	4.03E-02	1.38E-01	1.61E-01	3.35E-01	2.20E-02	4.83E-01	8.89E-01	1.66E-01	5.73E-01	2.14E-06	5.02E-04	9.36E-01	2.30E-03

Supplementary tables ST13. Incidence of apoptotic cells within individual late blastocyst stage (E4.5) embryos derived from 8-cell stage (E2.5) chimeric embryos consisting of a single control (fluorescent RDB tracer alone) or *Tead4*-KD (fluorescent RDB tracer plus Tead4-dsRNA) cell (immuno-stained for Cdx2 and Gata4)

Control (1+8, IF: Cdx2/ Gata4) apoptotic cells										
#	TOTAL NUMBER OF CELLS					NON-INJECTED CLONE		INJECTED CLONE		
	EMBRYO	TE	ICM	NON-INJECTED	INJECTED	OUTER	ICM	OUTER	ICM	
1	6	3	3	5	1	3	2	0	1	
2	6	3	3	3	3	1	2	2	1	
3	8	4	4	8	0	4	4	0	0	
4	8	5	3	6	2	5	1	0	2	
5	3	1	2	0	3	0	0	1	2	
6	4	3	1	4	0	3	1	0	0	
7	2	2	0	2	0	2	0	0	0	
8	2	0	2	2	0	0	2	0	0	
9	7	4	3	6	1	3	3	1	0	
10	3	2	1	2	1	1	1	1	0	
11	4	2	2	3	1	1	2	1	0	
12	2	0	2	1	1	0	1	0	1	
13	4	0	4	3	1	0	3	0	1	
14	5	0	5	5	0	0	5	0	0	
15	8	5	3	7	1	4	3	1	0	
16	8	7	1	7	1	6	1	1	0	
17	9	6	3	5	4	3	2	3	1	
18	6	3	3	4	2	2	2	1	1	
19	7	5	2	6	1	4	2	1	0	
20	7	0	7	7	0	0	7	0	0	
21	3	1	2	2	1	1	1	0	1	
22	2	1	1	0	2	0	0	1	1	
23	10	3	7	8	2	3	5	0	2	
24	7	2	5	4	3	1	3	1	2	
25	18	7	11	9	9	5	4	2	7	
26	8	5	3	6	2	5	1	0	2	
27	7	7	0	7	0	7	0	0	0	
28	5	3	2	3	2	1	2	2	0	
29	5	1	4	4	1	1	3	0	1	
30	14	3	11	9	5	3	6	0	5	
TOTAL	188	88	100	138	50	69	69	19	31	
AVERAGE	6.3	2.9	3.3	4.6	1.7	2.3	2.3	0.6	1.0	
SEM	0.6	0.4	0.5	0.5	0.3	0.4	0.3	0.1	0.3	

Tead4 KD (1+8, IF: Cdx2/ Gata4) apoptotic cells										
#	TOTAL NUMBER OF CELLS					NON-INJECTED CLONE		INJECTED CLONE		
	EMBRYO	TE	ICM	NON-INJECTED	INJECTED	OUTER	ICM	OUTER	ICM	
1	8	3	5	5	3	3	2	0	3	
2	3	2	1	3	0	2	1	0	0	
3	10	3	7	8	2	3	5	0	2	
4	7	4	3	4	3	3	1	1	2	
5	11	3	8	6	5	0	6	3	2	
6	8	3	5	1	7	1	0	2	5	
7	1	1	0	1	0	1	0	0	0	
8	6	0	6	5	1	0	5	0	1	
9	5	3	2	1	4	0	1	3	1	
10	9	6	3	8	1	6	2	0	1	
11	9	4	5	6	3	1	5	3	0	
12	12	8	4	7	5	3	4	5	0	
13	4	1	3	2	2	0	2	1	1	
14	10	3	7	9	1	3	6	0	1	
15	10	4	6	8	2	3	5	1	1	
16	8	7	1	8	0	7	1	0	0	
17	11	4	7	8	3	3	5	1	2	
TOTAL	132	59	73	90	42	39	51	20	22	
AVERAGE	7.8	3.5	4.3	5.3	2.5	2.3	3.0	1.2	1.3	
SEM	0.7	0.5	0.6	0.7	0.5	0.5	0.5	0.4	0.3	
Stat. sig. (exp. vs. con embryo) *p<0.05, **p<0.005										
p-value (2-tailed students t-test)	1.37E-01	4.08E-01	2.17E-01	4.08E-01	1.80E-01	9.92E-01	2.69E-01	1.83E-01	5.45E-01	

Supplementary tables ST14. Quantified cell lineage segregation in individual late blastocyst stage (E4.5) embryos *in vitro* cultured from the 2-cell stage (E1.5) after microinjection in a single cell with fluorescent RDB ± Dab2-dsRNA (immunostained for Gata4 and Nanog)

#	TOTAL NUMBER OF CELLS										NON-INJECTED CLONE										INJECTED CLONE									
	EMBRYO	OUTER	Nanog ⁺	Gata4 ⁺	INNER	Nanog ⁺	Gata4 ⁺	TOTAL	NON-INJECTED	INJECTED	OUTER	Nanog ⁺	Gata4 ⁺	INNER	Nanog ⁺	Gata4 ⁺	TOTAL	OUTER	Nanog ⁺	Gata4 ⁺	INNER	Nanog ⁺	Gata4 ⁺	TOTAL						
1	86	65	13	6	0	21	43	29	10	2	14	36	3	4	0	7														
2	38	77	9	6	0	43	34	2	4	0	12	43	3	4	0	9														
3	76	52	11	5	0	17	51	42	6	2	0	1	8	36	5	0	13													
4	94	76	3	1	0	13	31	41	30	1	0	1	8	36	5	0	13													
5	72	59	7	4	2	0	13	31	41	30	1	0	1	8	36	5	0	13												
6	96	72	11	11	2	0	24	47	49	36	5	6	0	11	36	6	5	2	0	13										
7	97	68	20	8	1	0	29	47	50	31	11	4	1	0	16	37	9	4	0	0	13									
8	97	81	8	8	0	0	16	53	44	45	3	5	0	8	36	5	3	0	0	0	13									
9	109	85	13	11	0	0	24	54	55	45	3	6	0	9	40	10	5	0	0	0	13									
10	107	82	11	11	0	0	24	54	55	45	3	6	0	9	40	10	5	0	0	0	13									
11	107	86	9	11	0	0	21	52	46	3	5	0	0	8	41	6	4	0	0	0	13									
12	110	80	18	12	0	0	30	53	57	40	7	6	0	13	40	11	6	0	0	0	13									
13	103	77	17	9	0	0	26	52	51	37	10	5	0	15	40	7	4	0	0	0	13									
14	94	74	14	6	0	0	20	50	44	40	7	3	0	10	34	4	3	0	0	0	13									
15	90	61	15	14	0	0	29	42	48	30	5	7	0	12	31	10	7	0	0	0	13									
16	88	70	9	8	1	0	18	40	48	36	3	1	0	4	34	6	7	1	0	0	13									
17	120	62	21	13	0	0	32	46	51	36	11	0	0	16	36	20	3	0	0	0	13									
18	97	68	10	13	0	0	23	46	47	35	2	7	0	18	33	8	6	0	0	0	13									
19	84	62	16	6	0	0	22	39	45	28	8	3	0	11	34	5	5	0	0	0	13									
20	86	68	10	8	0	0	18	47	39	34	6	7	0	13	34	4	3	0	0	0	13									
21	91	67	11	11	1	1	24	46	45	32	8	6	0	14	35	3	5	1	1	10	13									
22	103	71	18	11	0	3	32	53	50	38	8	6	0	1	15	33	10	5	0	2	17	13								
23	89	71	6	11	0	1	18	40	49	30	4	5	0	1	10	31	2	0	0	0	13									
24	82	59	12	8	3	0	23	46	36	33	6	6	0	12	26	6	2	1	0	0	13									
25	84	62	16	6	0	0	11	39	44	38	1	0	0	1	34	5	5	0	0	0	13									
26	83	72	6	5	0	0	29	45	47	30	8	6	1	0	15	33	8	5	1	0	14	13								
27	92	63	16	11	2	0	29	45	47	30	8	6	1	0	15	33	8	5	1	0	14	13								
28	75	54	15	6	0	0	21	34	41	25	7	2	0	0	9	29	8	4	0	0	12	13								
29	98	73	12	10	3	0	25	47	51	33	8	4	2	0	14	40	4	6	1	0	11	13								
30	100	74	13	12	0	1	26	48	52	38	5	5	0	0	10	36	8	7	0	1	16	13								
31	83	59	8	14	0	0	17	34	48	32	3	5	0	1	8	35	2	0	0	0	14	13								
32	83	59	8	14	0	0	17	34	48	32	3	5	0	1	8	35	2	0	0	0	14	13								
33	97	76	10	11	0	0	21	48	49	37	2	0	0	11	39	1	9	0	0	0	13	13								
34	97	76	10	11	0	0	21	48	49	37	2	0	0	11	39	1	9	0	0	0	13	13								
TOTAL	3183	2404	432	298	30	17	777	1564	1637	1154	207	147	10	6	370	1210	225	153	20	11	407	1360	1360							
AVERAGE	93.6	70.7	12.7	8.8	0.9	0.5	22.9	46.0	47.6	35.1	6.1	4.3	0.2	10.9	35.6	6.6	4.4	0.6	0.3	12.0	40.7	37.0	37.0							
SEM	1.8	1.4	0.3	0.5	0.3	0.2	1.1	1.1	0.6	0.9	0.3	0.4	0.3	0.5	0.7	0.7	0.6	0.3	0.2	0.2	0.2	0.2	0.2							
Stat. sig. (inner-clone) $p < 0.05$.																														
Stat. sig. (inner-clone) $p < 0.05$.																														
Posterior 2-tailed students t test																														

#	TOTAL NUMBER OF CELLS										NON-INJECTED CLONE										INJECTED CLONE									
	EMBRYO	OUTER	Nanog ⁺	Gata4 ⁺	INNER	Nanog ⁺	Gata4 ⁺	TOTAL	NON-INJECTED	INJECTED	OUTER	Nanog ⁺	Gata4 ⁺	INNER	Nanog ⁺	Gata4 ⁺	TOTAL	OUTER	Nanog ⁺	Gata4 ⁺	INNER	Nanog ⁺	Gata4 ⁺	TOTAL						
1	76	60	10	6	0	10	40	38	6	0	13	32	3	4	0	9														
2	76	52	8	8	0	0	16	40	38	22	10	0	0	13	22	5	0	0	0	0	13	13								
3	70	62	8	8	0	0	16	39	39	29	4	6	0	10	33	4	2	0	0	0	13	13								
4	90	65	18	5	2	0	25	48	42	31	12	4	1	0	17	34	6	1	1	0	16	16								
5	83	65	9	8	0	1	18	37	46	33	3	1	0	4	32	6	7	0	1	14	14	14								
6	88	67	14	6	1	0	21	47	41	37	7	3	0	0	10	30	7	3	1	0	11	11								
7	84	67	4	11	2	0	17	45	39	39	1	4	1	0	6	28	3	7	1	0	11	11								
8	71	62	9	9	1	3	23	49	52	37	6	4	0	2	12	23	5	2	0	1	9	9								
9	84	67	14	6	1	0	27	44	40	31	8	5	0	0	13	26	11	0	3	0	12	12								
10	84	57	19	5	3	0	27	44	40	31	8	5	0	0	13	26	11	0	3	0	12	12								
11	88	62	15	7	1	3	26	39	49	28	6	4	0	1	11	34	9	3	1	2	15	15								
12	80	60	16	4	0	0	20	36	44	22	10	4	0	1	14	38	6	0	0	0	16	16								
13	85	64	12	8	1	0	21	44	41	30	7	6	1	0	14	34	5	2	0	0	17	17								
14	111	82	17	11	0	1	29	59	52	48	6	5	0	0	11	34	11	6	0	1	18	18								
15	105	86	10	10	0	0	20	50	55	36	6	8	0	0	14	49	4	2	0	0	19	19								
16	92	76	6	6	0	0	18	46	46	35	4	4	0	1	12	40	4	2	0	0	17	17								
17	97	71	16	8	1	3	28	54	49	41	5	4	1	3	13	30	14	2	0	0	17	17								
18	86	71	6	9	0	0	15	45	41	34	5	6	0	0	11	37	11	3	0	0	14	14								
19	108	81	16	10	0	1	27	49	59	39	4	6	0	0	10	42	12	4	0	1	17	17								
20	89	74	6	9	0	0	15	49	40	39	4	6	0	0	10	35	2	3	0	0	15	15								
21	101	73	18	9	0	1	28	50	51	38	6	6	0	0	12	35	12	3	0	1	16	16								
22	105	66	16	19	4	0	39	53	52	31	10	9	3	0	22	35	6	10	1	1	17	17								
23	82	69	7	11	0	0	17	42	41	31	4	5	0	1	15	35	2	0	0	0	16	16								
24	82	69	7	11	0	0	17	42	41	31	4	5	0	1	15	35	2	0	0	0	16	16								
TOTAL	2164	1633	268	201	21	16	577	1054	1056	743	143	137	11	8	268	826	146	74	10	8	243	243								
AVERAGE	68.0	48.0	12.0	8.4	0.9	0.7	22.0	45.5	44.5	33.6	6.0	5.1	0.5	11.8	34.4	6.1	3.3	0.4	0.3	10.1	31.6	31.6								
SEM	2.4	2.0	1.0	0.7	0.2	0.2	1.3	1.2	0.6	1.1	0.3	0.2	0.2	0.8	1.2	0.6	0.3	0.1	0.1	0.3	0.3	0.3	0.3							
Stat. sig. (inner-clone) $p < 0.05$.																														
Stat. sig. (inner-clone) $p < 0.05$.																														
Posterior 2-tailed students t test																														

Supplementary tables ST15. Quantification of spatial cell lineage segregation in individual 16-cell stage (E3.1) embryos *in vitro* cultured from the 2-cell stage (E1.5) after microinjection in a single cell with fluorescent RDB ± Tead4-dsRNA

Control (1in2) 1st wave										
#	TOTAL NUMBER OF CELLS					NON-INJECTED CLONE		INJECTED CLONE		
	EMBRYO	OUTER	INNER	NON-INJECTED	INJECTED	OUTER	INNER	OUTER	INNER	
1	16	13	3	8	8	5	3	8	0	
2	16	14	2	8	8	6	2	8	0	
3	16	13	3	8	8	6	2	7	1	
4	16	13	3	8	8	6	2	7	1	
5	16	14	2	8	8	7	1	7	1	
6	16	15	1	8	8	8	0	7	1	
7	16	13	3	8	8	6	2	7	1	
8	16	13	3	8	8	6	2	7	1	
9	16	13	3	8	8	5	3	8	0	
10	16	12	4	8	8	6	2	6	2	
11	16	14	2	8	8	7	1	7	1	
12	16	13	3	8	8	6	2	7	1	
13	16	14	2	8	8	6	2	8	0	
14	16	15	1	8	8	7	1	8	0	
15	16	14	2	8	8	7	1	7	1	
16	16	13	3	8	8	7	1	6	2	
17	16	11	5	8	8	6	2	5	3	
18	16	14	2	8	8	7	1	7	1	
19	16	15	1	8	8	8	0	7	1	
20	16	14	2	8	8	7	1	7	1	
21	16	15	1	8	8	7	1	8	0	
22	16	12	4	8	8	7	1	5	3	
23	16	10	6	8	8	6	2	4	4	
24	16	14	2	8	8	7	1	7	1	
25	16	12	4	8	8	6	2	6	2	
26	16	10	6	8	8	5	3	5	3	
27	16	16	0	8	8	8	0	8	0	
28	16	13	3	8	8	8	0	5	3	
29	16	10	6	8	8	5	3	5	3	
TOTAL	464	382	82	232	232	188	44	194	38	
AVERAGE	16.0	13.2	2.8	8.0	8.0	6.5	1.5	6.7	1.3	
SEM	0.0	0.3	0.3	0.0	0.0	0.2	0.2	0.2	0.2	
Stat. sig. (inter-clone) †p<0.05, ††p<0.005										
p-value (2-tailed students t-test)								4.49E-01	4.48E-01	

Tead4 KD (1in2) 1st wave										
#	TOTAL NUMBER OF CELLS					NON-INJECTED CLONE		INJECTED CLONE		
	EMBRYO	OUTER	INNER	NON-INJECTED	INJECTED	OUTER	INNER	OUTER	INNER	
1	16	14	2	8	8	8	0	6	2	
2	16	10	6	8	8	5	3	5	3	
3	16	13	3	8	8	6	2	7	1	
4	16	11	5	8	8	5	3	6	2	
5	16	14	2	8	8	6	2	8	0	
6	16	11	5	8	8	5	3	6	2	
7	16	15	1	8	8	7	1	8	0	
8	16	13	3	8	8	6	2	7	1	
9	16	13	3	8	8	7	1	6	2	
10	16	13	3	8	8	7	1	6	2	
11	16	12	4	8	8	6	2	6	2	
12	16	16	0	8	8	8	0	8	0	
13	16	14	2	8	8	8	0	6	2	
14	16	14	2	8	8	7	1	7	1	
15	16	11	5	8	8	6	2	5	3	
16	16	13	3	8	8	7	1	6	2	
17	16	14	2	8	8	6	2	8	0	
18	16	14	2	8	8	7	1	7	1	
19	16	14	2	8	8	7	1	7	1	
20	16	16	0	8	8	8	0	8	0	
21	16	15	1	8	8	7	1	8	0	
22	16	13	3	8	8	6	2	7	1	
23	16	13	3	8	8	6	2	7	1	
24	16	16	0	8	8	8	0	8	0	
25	16	11	5	8	8	6	2	5	3	
26	16	14	2	8	8	7	1	7	1	
27	16	14	2	8	8	7	1	7	1	
28	16	16	0	8	8	8	0	8	0	
29	16	14	2	8	8	6	2	8	0	
30	16	15	1	8	8	8	0	7	1	
31	16	13	3	8	8	8	0	5	3	
32	16	15	1	8	8	8	0	7	1	
TOTAL	512	434	78	256	256	217	39	217	39	
AVERAGE	16.0	13.6	2.4	8.0	8.0	6.8	1.2	6.8	1.2	
SEM	0.0	0.3	0.3	0.0	0.0	0.2	0.2	0.2	0.2	
Stat. sig. (exp. vs. con embryo) *p<0.05, **p<0.005										
p-value (2-tailed students t-test)		3.33E-01	3.33E-01			2.21E-01	2.21E-01	7.41E-01	7.41E-01	
Stat. sig. (inter-clone) †p<0.05, ††p<0.005										
p-value (2-tailed students t-test)								1.00E+00	1.00E+00	

Supplementary tables ST16. Quantification of spatial cell lineage segregation in individual 32-cell stage (E3.6) embryos *in vitro* cultured from the 2-cell stage (E1.5) after microinjection in a single cell with fluorescent RDB ± Tead4-dsRNA

Control (1in2) 2nd wave									
#	TOTAL NUMBER OF CELLS					NON-INJECTED CLONE		INJECTED CLONE	
	EMBRYO	OUTER	INNER	NON-INJECTED	INJECTED	OUTER	INNER	OUTER	INNER
1	32	24	8	16	16	13	3	11	5
2	32	19	13	16	16	9	7	10	6
3	32	24	8	16	16	13	3	11	5
4	32	26	6	16	16	13	3	13	3
5	32	21	11	16	16	9	7	12	4
6	32	21	11	16	16	11	5	10	6
7	32	22	10	16	16	11	5	11	5
8	32	20	12	16	16	10	6	10	6
9	32	20	12	16	16	10	6	10	6
10	32	19	13	16	16	9	7	10	6
11	32	21	11	16	16	10	6	11	5
12	32	22	10	16	16	9	7	13	3
13	32	20	12	16	16	10	6	10	6
14	32	20	12	16	16	10	6	10	6
15	32	20	12	16	16	10	6	10	6
16	32	22	10	16	16	9	7	13	3
17	32	18	14	16	16	10	6	8	8
18	32	20	12	16	16	10	6	10	6
19	32	22	10	16	16	12	4	10	6
20	32	21	11	16	16	9	7	12	4
21	32	24	8	16	16	12	4	12	4
22	32	23	9	16	16	10	6	13	3
23	32	22	10	16	16	11	5	11	5
TOTAL	736	491	245	368	368	240	128	251	117
AVERAGE	32.0	21.3	10.7	16.0	16.0	10.4	5.6	10.9	5.1
SEM	0.0	0.4	0.4	0.0	0.0	0.3	0.3	0.3	0.3
Stat. sig. (inter-clone) ‡p<0.05, ††p<0.005									
p-value (2-tailed students t-test)								2.28E-01	2.88E-01

Tead4 KD (1in2) 2nd wave									
#	TOTAL NUMBER OF CELLS					NON-INJECTED CLONE		INJECTED CLONE	
	EMBRYO	OUTER	INNER	NON-INJECTED	INJECTED	OUTER	INNER	OUTER	INNER
1	32	19	13	16	16	12	4	7	9
2	32	17	15	16	16	10	6	7	9
3	32	17	15	16	16	13	3	4	12
4	32	18	14	16	16	12	4	6	10
5	32	19	13	16	16	13	3	6	10
6	32	19	13	16	16	11	5	8	8
7	32	17	15	16	16	13	3	4	12
8	32	20	12	16	16	12	4	8	8
9	32	19	13	16	16	13	3	6	10
TOTAL	288	165	123	144	144	109	35	56	88
AVERAGE	32.0	18.3	13.7	16.0	16.0	12.1	3.9	6.2	9.8
SEM	0.0	0.4	0.4	0.0	0.0	0.4	0.4	0.5	0.5
Stat. sig. (exp. vs. con embryo) *p<0.05, **p<0.005		**	**			**	**	**	**
p-value (2-tailed students t-test)		1.00E-05	1.00E-05			1.45E-03	1.45E-03	1.32E-06	1.32E-06
Stat. sig. (inter-clone) ‡p<0.05, ††p<0.005								‡‡	‡‡
p-value (2-tailed students t-test)								1.01E-07	1.01E-07

Supplementary table ST17. Total number of cells in control (DMSO treated) and Rock1/2-inhibited (Y-27632 treated) embryos *in vitro* cultured from the 2-cell (E1.5) stage until the 8-cell (E2.5), 16-cell (E3.0) or 32-cell (E3.5) stages.

TOTAL NUMBER OF CELLS						
#	Control			Y-27632		
	8-cell stage (E2.5)	16-cell stage (E3.0)	32-cell stage (E3.5)	8-cell stage (E2.5)	16-cell stage (E3.0)	32-cell stage (E3.5)
1	8	17	32	10	16	32
2	12	16	30	6	16	32
3	8	16	32	8	16	32
4	8	14	32	6	16	32
5	8	16	32	8	12	30
6	8	16	32	8	16	28
7	8	16	32	10	16	32
8	8	16	32	8	16	31
9	8	16	32	8	16	30
10	8	16	32	8	16	32
11	8	16	32	8	16	32
12	8	16	32	8	15	34
13	8	16	31	8	16	32
14	8	16	32	8	16	32
15	8	16	31	8	16	32
16	8	16	32	8	16	32
17	8	16	31	8	16	28
18	7	16	32	10	16	32
19	8	16	31	7	16	32
20	8	16	32	8	16	32
21	8	19	31	8	15	31
22	8	15	32	8		32
23	8	16		8		
24	8	16		8		
25		16		8		
26		16		8		
27				8		
28				8		
29				8		
TOTAL	195.0	417.0	697.0	233.0	330.0	692.0
AVERAGE	8.1	16.0	31.7	8.0	15.7	31.5
SEM	0.2	0.2	0.1	0.2	0.2	0.3
Stat. sig. (exp. vs. con embryo) *p<0.05, **p<0.005						
p-value (2-tailed students t-test)				7.04E-01	2.00E-01	4.78E-01

Supplementary tables ST18. Quantified subcellular Yap1 localization in control (DMSO treated) and Rock1/2-inhibited (Y-27632 treated) embryos *in vitro* cultured from the 2-cell (E1.5) stage until the 32-cell (E3.5) stage.

Control													
#	TOTAL NUMBER OF CELLS				Yap1 subcellular localization								
	EMBRYO	OUTER	INNER	MITOTIC	OUTER				INNER				
					N>C	N=C	N<C	M	N>C	N=C	N<C	M	
1	32	22	10	0	18	1	3	0	0	0	0	10	0
2	33	20	13	0	19	1	0	0	0	0	3	10	0
3	32	23	9	0	21	2	0	0	0	0	0	9	0
4	30	19	10	1	18	0	1	0	0	0	0	10	1
5	32	20	12	0	18	2	0	0	0	0	1	11	0
6	32	21	11	0	21	0	0	0	0	0	2	9	0
7	27	17	9	1	16	1	0	0	0	0	4	5	1
8	32	17	13	2	17	0	0	0	0	0	3	10	2
9	32	18	12	2	18	0	0	1	0	0	0	12	1
10	32	17	15	0	17	0	0	0	0	0	0	15	0
11	32	17	13	2	16	0	1	2	0	0	0	13	0
12	30	18	11	1	16	2	0	0	0	0	2	9	1
13	30	16	12	2	16	0	0	0	1	2	2	9	2
14	32	21	11	0	18	2	1	0	1	1	1	9	0
TOTAL	438.0	266.0	161.0	11.0	249.0	11.0	6.0	3.0	2.0	18.0	141.0	8.0	
AVERAGE	31.3	19.0	11.5	0.8	17.8	0.8	0.4	0.2	0.1	1.3	10.1	0.6	
SEM	0.4	0.6	0.5	0.2	0.4	0.2	0.2	0.2	0.1	0.4	0.6	0.2	

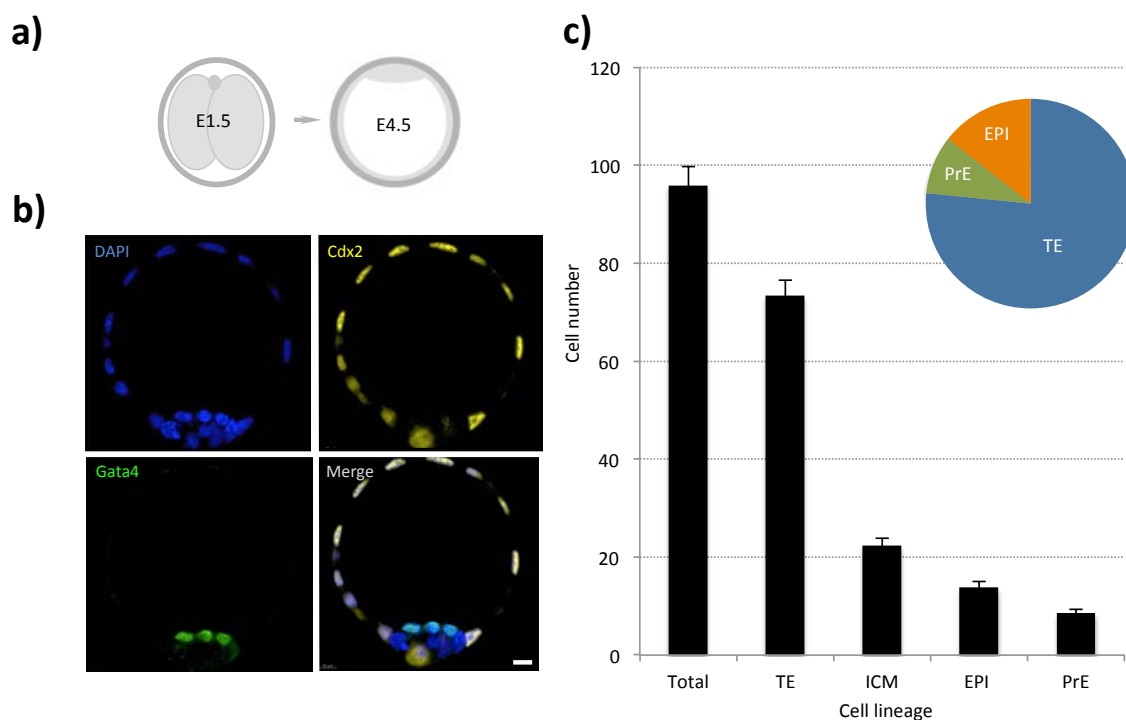
Y-27632													
#	TOTAL NUMBER OF CELLS				Yap1 subcellular localization								
	EMBRYO	OUTER	INNER	MITOTIC	OUTER				INNER				
					N>C	N=C	N<C	M	N>C	N=C	N<C	M	
1	32	24	8	0	6	11	7	0	0	0	1	7	0
2	32	23	9	0	4	8	11	0	0	0	0	9	0
3	29	22	3	4	9	12	1	3	0	0	2	1	1
4	32	28	4	0	2	21	5	0	0	0	0	4	0
5	32	24	8	0	5	10	9	0	0	0	0	8	0
6	32	24	6	2	10	11	3	1	0	0	5	1	1
7	31	23	7	1	5	13	5	1	0	0	2	5	0
8	30	20	8	2	12	6	2	1	0	0	2	6	1
9	32	24	8	0	7	16	1	0	1	2	2	5	0
10	31	26	5	0	8	16	2	0	0	4	1	0	0
11	31	22	8	1	11	10	1	1	0	0	2	6	0
12	27	18	8	1	6	10	2	1	0	0	3	5	0
TOTAL	371.0	278.0	82.0	11.0	85.0	144.0	49.0	8.0	1.0	23.0	58.0	3.0	
AVERAGE	30.9	23.2	6.8	0.9	7.1	12.0	4.1	0.7	0.1	1.9	4.8	0.3	
SEM	0.5	0.7	0.5	0.4	0.9	1.2	1.0	0.3	0.1	0.5	0.8	0.1	
Stat. sig. (exp. vs. con embryo)		**	**		**	**	**				**		
*p<0.05, **p<0.005													
p-value (2-tailed students t-test)	5.52E-01	2.37E-04	1.25E-06	7.64E-01	4.81E-09	7.26E-07	3.19E-03	1.48E-01	6.46E-01	2.91E-01	2.70E-05	1.95E-01	

Supplementary tables ST19. Total, outer and inner cell number in 16-cell (E3.0) and 32-cell (E3.5) stage, control (DMSO treated) and Rock1/2-inhibited (Y-27632 treated) embryos *in vitro* cultured from the 2-cell (E1.5) stage.

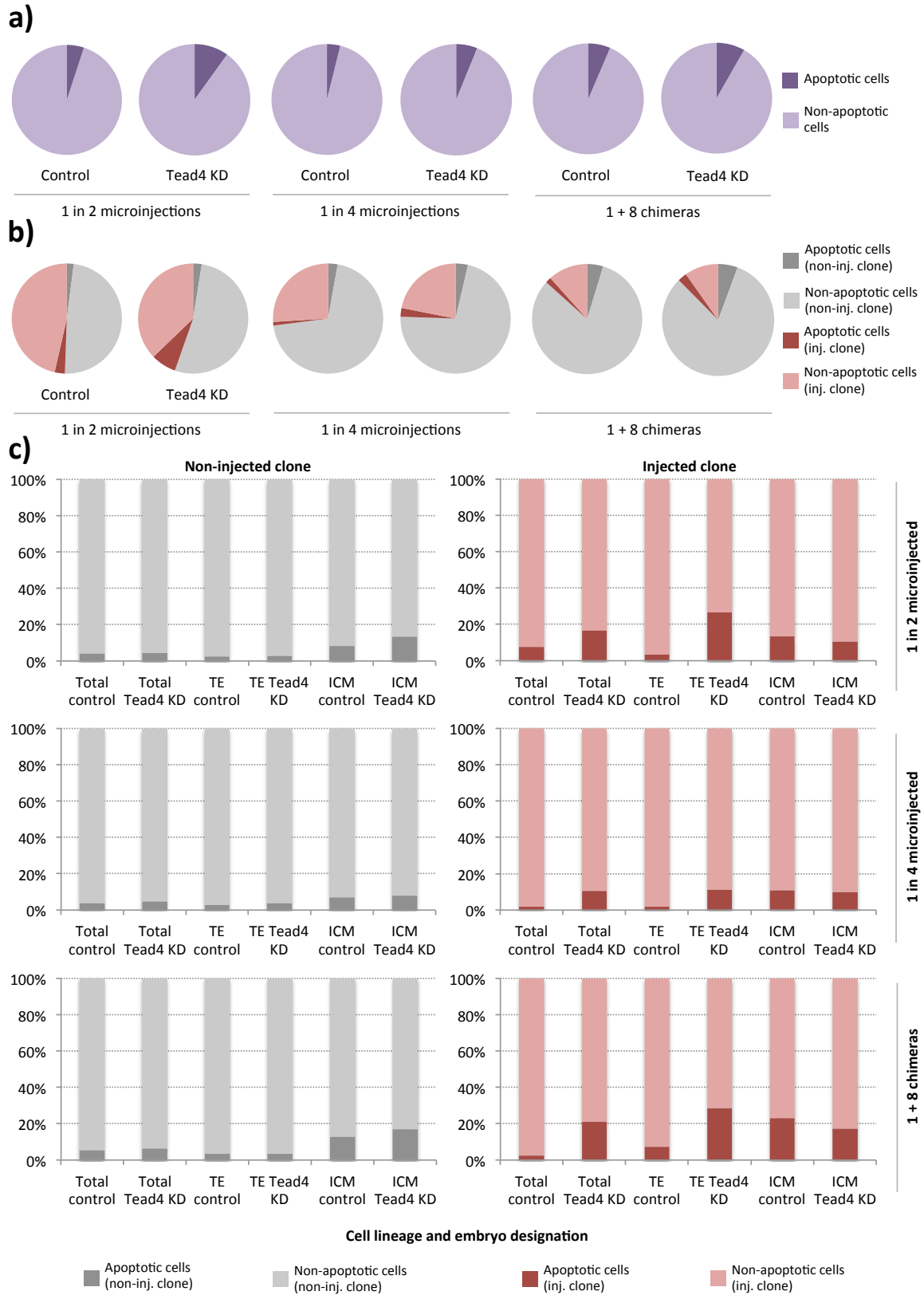
16-cell stage (E3.0)						
#	Control			Y-27632		
	TOTAL	OUTER	INNER	TOTAL	OUTER	INNER
1	17	13	4	16	16	0
2	16	9	7	16	16	0
3	16	13	3	16	16	0
4	14	13	1	16	14	2
5	16	14	2	12	12	0
6	16	13	3	16	16	0
7	16	14	2	16	15	1
8	16	11	5	16	16	0
9	16	10	6	16	15	1
10	16	13	3	16	16	0
11	16	13	3	16	15	1
12	16	15	1	15	15	0
13	16	14	2	16	15	1
14	16	15	1	16	16	0
15	16	13	3	16	15	1
16	16	12	4	16	16	0
17	16	15	1	16	15	1
18	16	14	2	16	16	0
19	16	15	1	16	15	1
20	16	11	5	16	16	0
21	19	15	4	15	15	0
22	15	9	6			
23	16	11	5			
24	16	11	5			
25	16	13	3			
26	16	14	2			
TOTAL	417.0	333.0	84.0	330.0	321.0	9.0
AVERAGE	16.0	12.8	3.2	15.7	15.3	0.4
SEM	0.2	0.4	0.4	0.2	0.2	0.1
Stat. sig. (exp. vs. con embryo) *p<0.05, **p<0.005					**	**
p-value (2-tailed students t-test)				2.00E-01	4.78E-07	1.10E-08

32-cell stage (E3.5)						
#	Control			Y-27632		
	TOTAL	OUTER	INNER	TOTAL	OUTER	INNER
1	32	21	11	32	26	6
2	30	19	11	32	25	7
3	32	19	13	32	26	6
4	32	20	12	32	24	8
5	32	20	12	30	25	5
6	32	22	10	28	22	6
7	32	23	9	32	22	10
8	32	24	8	31	25	6
9	32	21	11	30	25	5
10	32	20	12	32	26	6
11	32	23	9	32	25	7
12	32	22	10	34	28	6
13	31	20	11	32	27	5
14	32	24	8	32	26	6
15	31	22	9	32	26	6
16	32	18	14	32	26	6
17	31	20	11	28	24	4
18	32	20	12	32	24	8
19	31	19	12	32	25	7
20	32	16	16	32	27	5
21	31	18	13	31	27	4
22	32	21	11	32	28	4
TOTAL	697.0	452.0	245.0	692.0	559.0	133.0
AVERAGE	31.7	20.5	11.1	31.5	25.4	6.0
SEM	0.1	0.4	0.4	0.3	0.3	0.3
Stat. sig. (exp. vs. con embryo) *p<0.05, **p<0.005					**	**
p-value (2-tailed students t-test)				4.78E-01	5.54E-11	3.47E-12

APPENDIX B. SUPPLEMENTARY FIGURES

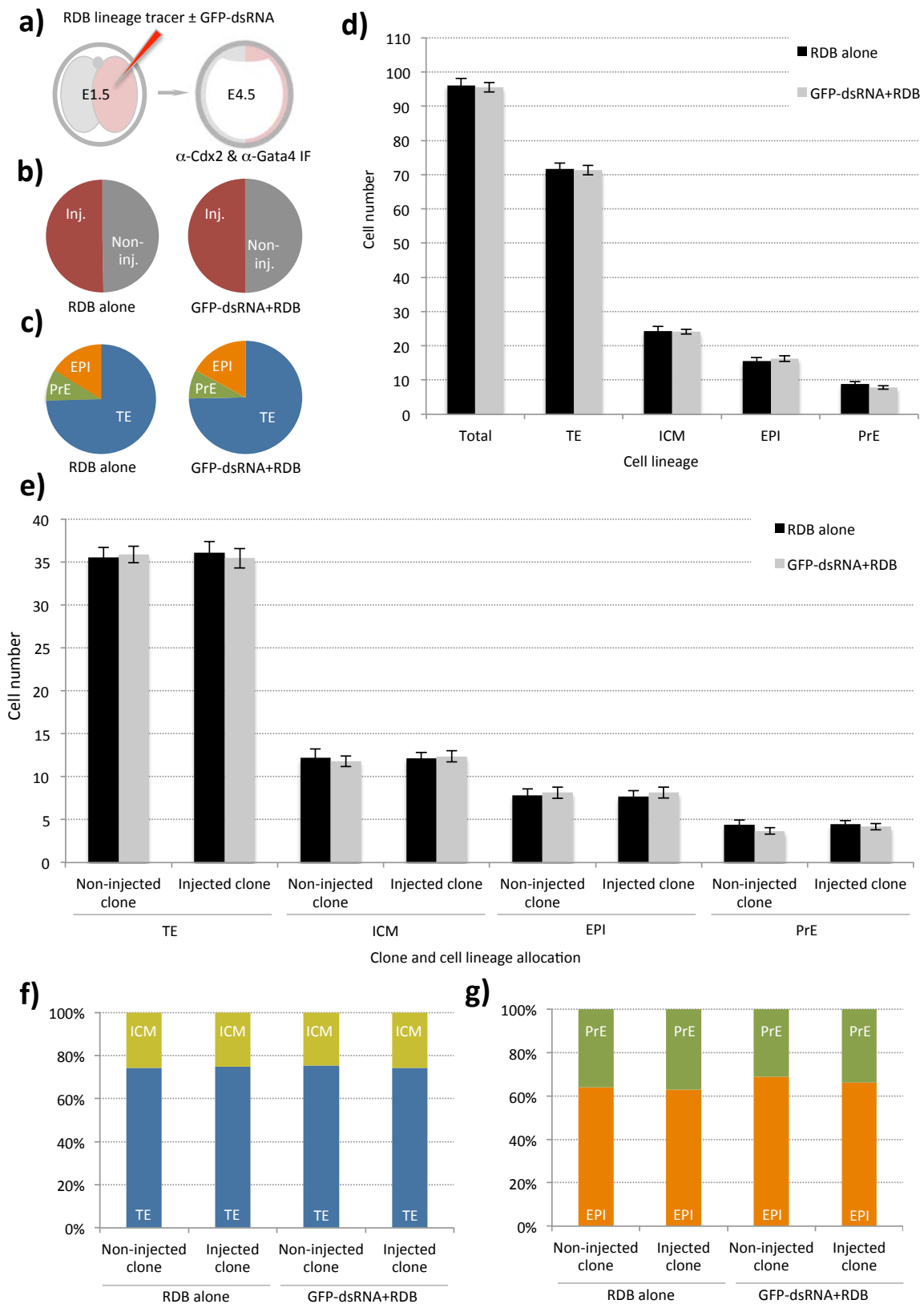


Supplementary figure S1. Relative cell lineage segregation in unperturbed pre-implantation mouse embryos *in vitro* cultured from the 2-cell (E1.5) stage until the late blastocyst stage (E4.5); establishing an experimental baseline. a) Schematic representation of the *in vitro* culture period of recovered 2-cell (E1.5) stage embryos. **b)** Representative single confocal z-plane image through the centre of a cultured E4.5 stage late blastocyst immuno-fluorescently stained for TE (Cdx2 – yellow) and PrE (Gata4 – green) lineage markers, plus DNA nuclear co-stain (DAPI – blue). Scale bars = 10µm. **c)** Bar chart reporting the average cell number contribution to each late blastocyst (E4.5) stage cell lineage of *in vitro* cultured embryos (as described in a) above). Trophectoderm (TE) and primitive endoderm (PrE) contribution was assigned by presence of specific lineage marker immuno-fluorescent staining (see b) above). Epiblast (EPI) contribution was determined by a lack of immuno-fluorescent stain for either TE or PrE marker protein within the inner-cell mass (ICM; PrE + EPI). The average total number of cells is also given (n= 16 and error bars represent s.e.m.). Inset – pie chart detailing the same data in percentage format. See supplementary table ST1 for individual embryo data.



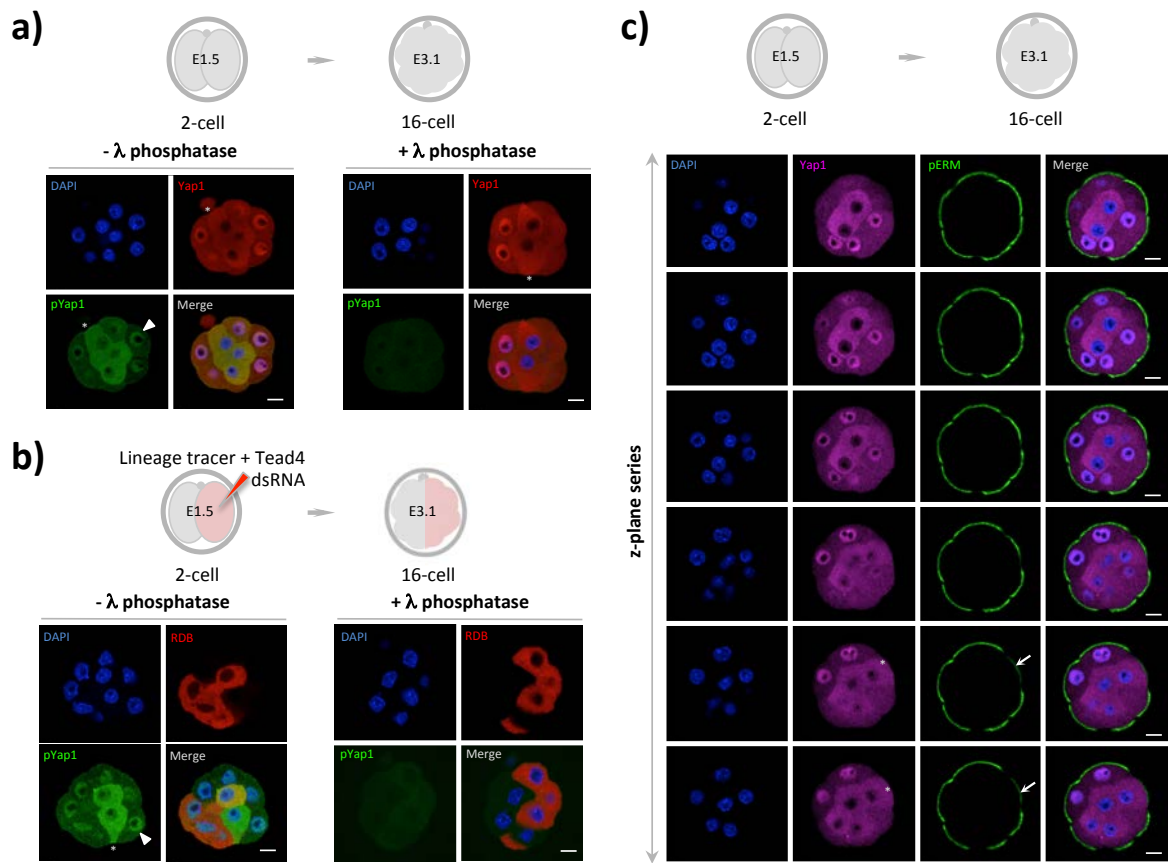
Supplementary figure S2. (legend overleaf)

Supplementary figure S2. Average percentage rates of apoptosis in control and *Tead4*-dsRNA microinjected and chimeric embryos. **a)** Pie charts detailing average rates of total apoptosis observed (by the presence of fragmented inter-phase nuclei) in either control or *Tead4*-dsRNA microinjected embryos, cultured to the late blastocyst (E4.5) stage (whereby one cell at the 2- or 4-cell stages, referred to as '1 in 2' or '1 in 4 microinjections' respectively, was microinjected – data refers to embryos described in figure 4.3 and 4.4). Pie charts describing the observed total apoptosis rates in chimeric embryos composed from unperturbed 8-cell stage embryos aggregated with either one control or one *Tead4*-KD 8-cell stage blastomere (referred to as '1 + 8 chimeras' – data refers to embryos described in figure 4.5) and then similarly cultured to the late blastocyst, are also given. **b)** Pie charts describing the data given in a) but detailing the average rates of apoptosis in the non-microinjected and microinjected cell clones (unmarked and RDB-marked clones in chimeric embryos) of the cultured late blastocysts (cell clones are distinguishable by the presence or absence of injected RDB lineage tracer). **c)** Percentage bar charts expanding the data given in a) and b) but detailing the average incidence of apoptosis within each of the late blastocyst cell lineages of both control and *Tead4* knockdown embryos, in each of the three experimental paradigms ('1 in 2' and '1 in 4' microinjections, plus '1 + 8' chimeras). For individual embryo apoptosis data, refer to supplementary tables ST5, ST11 and ST13. All data were obtained from embryo groups immuno-stained for Cdx2 and Gata4.



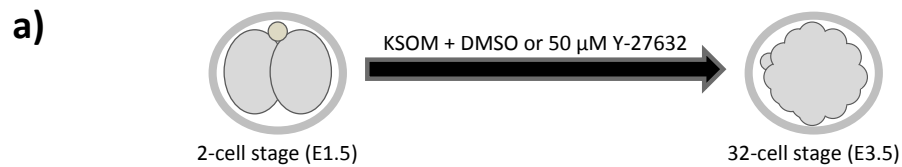
Supplementary figure S3. (legend overleaf)

Supplementary figure S3. No statistically significant difference in blastocyst lineage derivation between two groups of control embryos microinjected with either RDBs alone or RDBs + GFP-dsRNA in one cell at the 2-cell stage. **a)** Schematic of the experimental strategy to clonally mark one-half of control embryo cells with either RDBs or RDBs + GFP-dsRNA and assess cell lineage allocation in late blastocysts (E4.5) via Cdx2 (TE marker) and Gata4 (early PrE marker) immunofluorescence detection (*n.b.* inner-cells devoid of either lineage marker were classified as EPI). **b)** Average total cell percentage contribution of microinjected and non-microinjected cell clones in either group of control microinjected embryos (*i.e.* RDB alone or GFP-dsRNA+RDB). **c)** Relative averaged percentage contribution of total cell number to the late blastocyst lineages (TE, PrE and EPI) in either clonal control group of microinjected embryos. **d)** Averaged total cell number for each late blastocyst lineage (ICM = EPI + PrE) in each group of clonal control embryos. **e)** Average number of cells from either non-microinjected or microinjected cell clones contributing to late blastocyst lineages, in each group of clonal control embryos. In d) and e), error bars represent s.e.m; * / ** and ‡ / †† denote statistically significant differences between equivalent cell clones of each group of clonal control embryos, or between cell clones within each control groups itself, respectively (confidence intervals of $p < 0.05$ and $p < 0.005$, 2-tailed student t-tests); however note the lack of statistically significant difference between the two groups of clonal control embryos, thus highlighting validity of using the RDB alone control group in relation to the experiments described in the main text of this thesis report. **f)** Averaged percentage contribution of non-microinjected and microinjected cell clones, of each group of clonal control embryos, to TE or ICM of late blastocysts. **g)** Averaged percentage contribution of non-microinjected and microinjected ICM cell clones, of each group of clonal control embryos, to PrE or EPI lineages. Overall, in the RDB alone clonal control group of embryos $n = 30$ and in the GFP-dsRNA+RBD clonal control group $n = 37$ (see supplementary tables ST8 and ST9 for individual embryo cell allocation and apoptosis data, respectively).

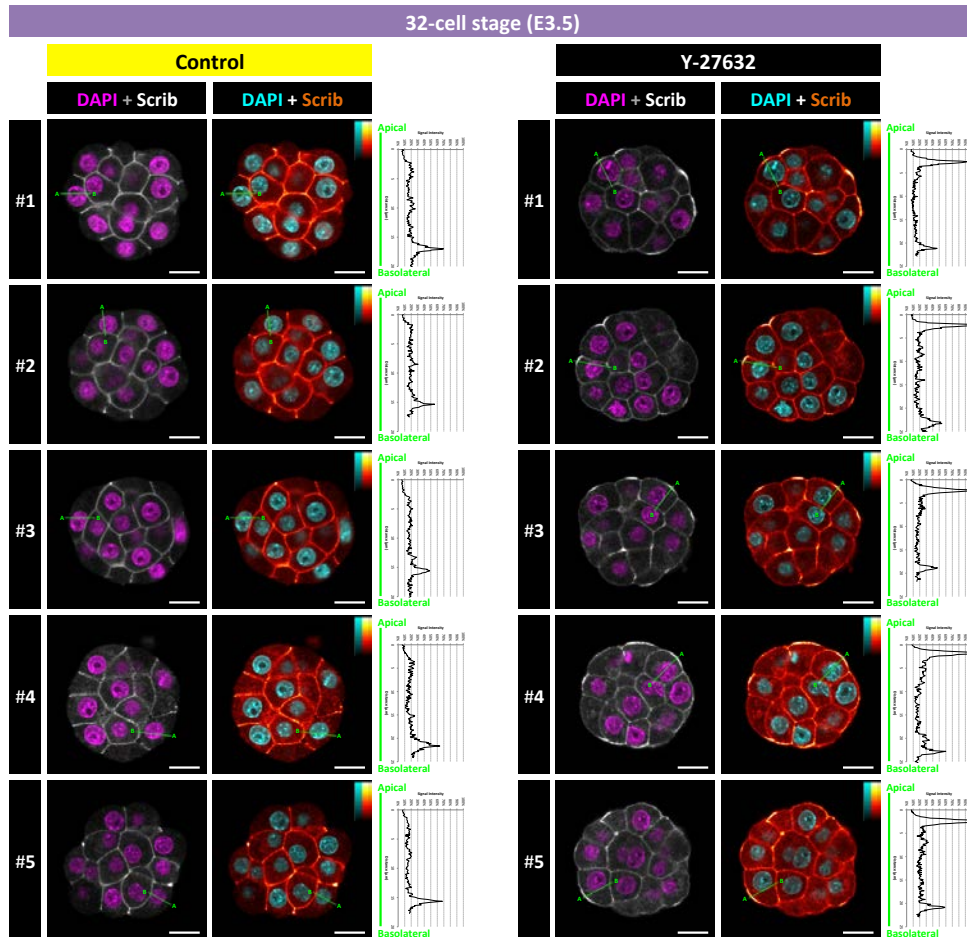


Supplementary figure S4. (legend overleaf)

Supplementary figure S4. Yap1, phospho-Yap1 and phospho-ezrin (pERM) expression and intracellular localisation within non-perturbed and Tead4-specific dsRNA microinjected (in one cell at the 2-cell stage) embryos at the mid-16-cell (E3.1) stage. **a)** Representative single confocal z-plane of mid-16-cell stage (E3.1) stage embryos, *in vitro* cultured from the 2-cell stage (E1.5) and double immuno-stained for Yap1 (red – *n.b.* anti-sera does not discriminate between phosphorylated and non-phosphorylated forms) and phosphorylated-Yap1 (green – pYap1). Note that the specificity of the anti-pYap1 anti-sera for only the phosphorylated isoform of Yap1 was confirmed by pre-incubating fixed embryos with λ phosphatase prior to immuno-staining (compare lack of signal in right panel with that in left panel). Yap1 immuno-staining (red) is enriched in the nuclei of outer-cells and the cytoplasm of inner-cells, with an occasional outer-cell displaying a cytoplasmic signal (see asterisks). pYap1 localisation is consistently cytoplasmic, with low level nuclear expression, in inner-cells (plus the occasional outer-cell – asterisk). However, it is also present within the nuclei of outer-cells, suggesting a basal level of nuclear Yap1 import that is irrespective of phosphorylation status (see arrow-head highlighted examples). **b)** Representative single confocal z-plane of mid-16-cell stage embryos, *in vitro* cultured after microinjection with RDB lineage tracer (red) plus Tead4-dsRNA in one cell at the 2-cell stage and immuno-stained for pYap1 (green). Right panel shows immuno-staining after pre-treatment with λ phosphatase and left panel without treatment. Note, pYap1 localisation is dictated by a cell's relative spatial position within the embryo (*i.e.* mainly cytoplasmic in inner-cells and nuclear in outer-cells) irrespective of whether the cell is derived from the microinjected, and hence *Tead4* KD, clone or non-microinjected clone. This result indicates that the mis-localisation of Yap1 protein (using the anti-sera that does not discriminate between phosphorylated and non-phosphorylated isoforms) observed after *Tead4* KD in mid-16-cell (E3.1) and 32-cell (E3.6) stage embryos (see figure 4.6) is not phosphorylated. **c)** Six consecutive confocal z-plane images of unperturbed 16-cell stage embryos, *in vitro* cultured from the 2-cell stage, and immuno-stained for Yap1 (pseudo-coloured magenta – *n.b.* anti-sera does not discriminate between phosphorylated and non-phosphorylated forms) and phospho-ezrin (green - using pERM antibody). Note nuclear localised Yap1 signal in the outer-cells accompanied by robust pERM immuno-staining in the apical domain. Conversely, Yap1 localisation is cytoplasmic and excluded from the nucleus in encapsulated inner-cells. However, occasionally an outer-cell exhibiting cytoplasmic Yap1 localisation (akin to that normally observed in inner-cells – see asterisk) is observed and is associated with either reduced pERM immuno-staining (as in the example given – see arrow) or a very small exposed apical domain (data not shown). In relation to all panels of the figure, DNA was counter-stained with DAPI and the scale bars = 10 μ M.



b)



Supplementary figure S5. Rock1/2-inhibition causes apical mis-localisation of the basolateral polarity factor Scrib (Scribble) to the apical pole of outer cells at the 32-cell stage (+ quantitation). a) Schematic representation of the experimental strategy to assay subcellular expression and localisation of the basolateral polarity factor Scrib (Scribble) in control or Y-27632-treated (50 μ M)/ Rock1/2-inhibited embryos at 32-cell stage. b) Individual confocal microscopy z-planes of five control (left column, yellow masthead) and five Y-27632 treated/ Rock1/2-inhibited (right column, black masthead) embryos, immuno-fluorescently stained for Scrib and DAPI counterstained for DNA and reproduced using two colour palettes; on the left Scrib and DAPI are represented in grey-scale and magenta, respectively and on the right Scrib staining is represented in the orange ('fall') spectral intensity palette and DAPI in cyan. Scale bars = 20 μ m. Quantitation of the anti-Scrib immuno-fluorescence signal along the indicated axes (shown in each micrograph as a green line), from the apical to basolateral domains ('A' to 'B') is shown to the right of each individual embryo's micrograph couplet. Note, the ectopic enrichment of Scrib in the apical domain of Y-27632 treated/ Rock1/2-inhibited embryos, in contrast to the normal basolateral localisation as seen in control embryos.

APPENDIX C. CURRICULUM VITAE



MIHAJLOVIĆ I. Aleksandar

Date of Birth: 5th April 1986. **Nationality:** Serbian
Home Address: Bezdrevská 15 **Work Address:** Branišovská 31
37005 České Budějovice 37005 České Budějovice
Czech Republic Czech Republic
Telephone No.: +420 733 430 393

Education

- 2012-present** **Ph.D. Studies in Molecular and Cellular Biology and Genetics, Faculty of Science, University of South Bohemia, Czech Republic**
Ph.D. Thesis: "*The involvement of the Hippo signalling pathway in the first two cell-fate decisions of pre-implantation mouse embryo development*", supervised by **Alexander W. Bruce Ph.D.**, Department of Molecular Biology and Genetics, Faculty of Science, University of South Bohemia
- 2010-2012** **Research Associate in Animal Physiology, Faculty of Science, University of Novi Sad, Serbia**
Research area: *Mechanisms of mitochondrial biogenesis in Leydig cells*, supervised by Prof. Dr. Silvana Andrić, Department of Biology and Ecology, Faculty of Sciences, University of Novi Sad
- 2009-2010** **MSc. in Biology at the University of Novi Sad, Serbia** (GPA 10.00/ max. 10.00)
Masters Thesis: "*Effect of testosterone on NO-cGMP signalling pathway in adult rat Leydig cells*", supervised by Prof. Dr. Silvana Andrić
- 2005-2009** **BSc. in Biology at the University of Novi Sad, Serbia** (GPA 9.92/ max. 10.00)
Bachelors Thesis: "*Hepatocarcinogenesis caused by microcystin exposure*", supervised by Prof. Dr. Zorica Svirčev, Department of Biology and Ecology, Faculty of Sciences, University of Novi Sad

Grants and Scholarships

- 2015-2016** **GAJU Grant** - individual Ph.D. student project grant funded by the Grant Agency of the University of South Bohemia (004/2015/P). Project title: "Are the first two cell differentiation events of mammalian embryogenesis integrated or totally distinct? Implications for improved IVF clinical outcomes".
- 2011** **Young Scientist Forum Grant** to attend 11th Young Scientist Forum and 36th FEBS Congress in Torino, Italy
- 2010** **EMBO Grant** to attend EMBO Practical Course: "Anatomy and Embryology of the Mouse" in Split, Croatia
- 2009-2010** Scholarship of the **University Foundation for Development of Scientific and Artistic Youth of Novi Sad**
- 2009** **Eurobank EFG** Scholarship for the Best Serbian Students
- 2006-2009** Scholarship of the **Ministry of Education and Sports of Serbia**

Laboratory Skills

Routinely performing: pre-implantation mouse embryo manipulation (embryo collection at zygotic, 2-cell, 4-cell and 8-cell stage, microinjections, immuno-fluorescent staining, confocal imaging)

Frequently performing: generation of chimeric embryos from individual 4-cell and 8-cell stage blastomeres, RQ-PCR, PCR, agarose gel electrophoresis, molecular cloning, mRNA and dsRNA preparation

Capable of performing: Leydig cell primary culture preparation, radioimmunoassay, total RNA and protein isolation, several spectrophotometric, fluorometric and colorimetric analyses.

Well acquainted with: TUNEL assay, SDS-PAGE and Western blotting, genome DNA isolation and knock-out mice genotyping

Teaching Experience

- 2012-present** Providing formal revision classes for undergraduate course “Molecular Biology and Genetics” (held by my Ph.D. supervisor A.W. Bruce)
- 2011-present** One of my responsibilities as a PhD student is to facilitate integration of undergraduate students into our laboratory by teaching them some of the techniques we employ, explaining them how to critically analyse the data and helping them to develop a sense of a teamwork.
- 2010-2012** **Seminar Assistant in Animal Physiology Course** – engaged in holding seminars for undergraduate students and evaluating their performance during the course

Scientific Events Attended

- 2016** **XXIV Cytoskeletal club**, Vranovská Ves, Czech Republic -- oral communication
- 2015** **The 3rd Portuguese Society for Developmental Biology (SPBD) Meeting (held jointly with sister societies from Britain and Spain)**, Algarve, Portugal – poster presentation
- 2015** **The 6th European Molecular Biology Organisation (EMBO) Meeting**, Birmingham, UK – poster presentation
- 2015** **Confocal Microscopy and Image Analysis Workshop**, České Budějovice, Czech Republic
- 2015** **XXIII Cytoskeletal club**, Vranovská Ves, Czech Republic
- 2014** **XXII Cytoskeletal club**, Vranovská Ves, Czech Republic
- 2013** **The 3rd International Educational Event “VITA NOVA”**, Bratislava, Slovakia
- 2013** **Oocyte and embryo retreat**, Valtice, Czech Republic - oral communication
- 2013** **Summer school - focus on microinjection and advanced imaging**, Brno, Czech Republic
- 2012** **EMBO Practical Course: “3D Developmental Imaging”**, Oeiras, Portugal
- 2011** **Serbian Society for Mitochondrial and Free Radical Physiology 1st Congress “Mitochondria and Free Radicals in Biomedicine”**, Belgrade, Serbia - oral communication
- 2011** **36th FEBS Congress “Biochemistry for Tomorrow’s Medicine” and 11th Young Scientist Forum**, Torino, Italy – poster presentation
- 2010** **International Life Sciences Students’ Conference 2010**, Nijmegen, The Netherlands – oral communication
- 2010** **EMBO Practical Course: “Anatomy and Embryology of the Mouse”**, Split, Croatia

List of Publications

Mihajlović AI, Bruce AW (2016) Rho-associated protein kinase regulates subcellular localisation of Angiomotin and Hippo-signalling during preimplantation mouse embryo development. *Reprod Biomed Online*, 33:381-390.

Mihajlović AI, Thamodaran V, Bruce AW (2015) The first two cell-fate decisions of preimplantation mouse embryo development are not functionally independent. *Sci Rep.*, 5:15034.

Stojkov-Mimic NJ, Bjelic MM, Radovic SM, **Mihajlovic AI**, Sokanovic SJ, Baburski AZ, Janjic MM, Kostic TS, Andric SA (2015) Intratesticular alpha1-adrenergic receptors mediate stress-disturbed transcription of steroidogenic stimulator NUR77 as well as steroidogenic repressors DAX1 and ARR19 in Leydig cells of adult rats. *Mol Cell Endocrinol.*, 412:309-19.

Bjelic MM, Stojkov NJ, Baburski AZ, Sokanovic SJ, **Mihajlovic AI**, Janjic MM, Kostic TS, Andric SA (2014) Molecular adaptations of testosterone-producing Leydig cells during systemic in vivo blockade of the androgen receptor. *Mol Cell Endocrinol.*, 396(1-2):10-25.

Stojkov NJ, Baburski AZ, Bjelic MM, Sokanovic SJ, **Mihajlovic AI**, Drljaca DM, Janjic MM, Kostic TS, Andric SA (2014) In vivo blockade of α 1-adrenergic receptors mitigates stress-disturbed cAMP and cGMP signaling in Leydig cells. *Mol Hum Reprod.*, 20(1):77-88.

Stojkov NJ, Janjic MM, Baburski AZ, **Mihajlovic AI**, Drljaca DM, Sokanovic SJ, Bjelic MM, Kostic TS, Andric SA (2013) Sustained in vivo blockade of α 1-adrenergic receptors prevented some of stress-triggered effects on steroidogenic machinery in Leydig cells. *Am J Physiol Endocrinol Metab.*, 305(2):E194-204.

Andric SA, Kojic Z, Bjelic MM, **Mihajlovic AI**, Baburski AZ, Sokanovic SJ, Janjic MM, Stojkov NJ, Stojilkovic SS, Kostic TS (2013) The opposite roles of glucocorticoid and α 1-adrenergic receptors in stress triggered apoptosis of rat Leydig cells. *Am J Physiol Endocrinol Metab.*, 304(1):E51-9.

Janjic MM, Stojkov NJ, Bjelic MM, **Mihajlovic AI**, Andric SA, Kostic TS (2012) Transient rise of serum testosterone level after single sildenafil treatment of adult male rats. *J Sex Med.*, 9(10):2534-43.

Stojkov NJ, Janjic MM, Bjelic MM, **Mihajlovic AI**, Kostic TS, Andric SA (2012) Repeated immobilization stress disturbed steroidogenic machinery and stimulated the expression of cAMP signaling elements and adrenergic receptors in Leydig cells. *Am J Physiol Endocrinol Metab.*, 302(10):E1239-51.

Kostic TS, Stojkov NJ, Bjelic MM, **Mihajlovic AI**, Janjic MM, Andric SA (2011) Pharmacological doses of testosterone upregulated androgen receptor and 3-Beta-hydroxysteroid dehydrogenase/delta-5-delta-4 isomerase and impaired leydig cells steroidogenesis in adult rats. *Toxicol Sci.*, 121(2):397-407.

© for non-published parts Aleksandar I. Mihajlović

mihaja00@prf.jcu.cz

The involvement of the Hippo signalling pathway in the first two cell-fate decisions of pre-implantation mouse embryo development

Ph.D. Thesis, 2017

All rights reserved
For non-commercial use only

Printed in the Czech Republic

University of South Bohemia in České Budějovice
Faculty of Science
Branišovská 1760
CZ-37005 České Budějovice, Czech Republic

Phone: +420 387 776 201
www.prf.jcu.cz, e-mail: sekret-fpr@prf.jcu.cz